SH
11
A2
53
FISH

U.S. Department
of Commerce

Volume 118
Number 1
January 2020

Fishery Bulletin

Fishery Bulletin

U.S. Department of Commerce

Wilbur L. Ross Jr.
Secretary

National Oceanic and Atmospheric Administration

Neil A. Jacobs
Acting Administrator

National Marine Fisheries Service

Chris Oliver
Assistant Administrator
for Fisheries

Fishery Bulletin (ISSN 0090-0656) is published quarterly by the Scientific Publications Office, National Marine Fisheries Service, NOAA, 7600 Sand Point Way NE, Seattle, WA 98115-0070.

Although the contents of this publication have not been copyrighted and may be reprinted entirely, reference to source is appreciated.

The Secretary of Commerce has determined that the publication of this periodical is necessary according to law for the transaction of public business of this Department. Use of funds for printing of this periodical has been approved by the Director of the Office of Management and Budget.

For Sale by the Superintendent of Documents, U.S. Government Publishing Office, Washington, DC 20401. Subscription price per year: $32.00 domestic and $44.80 foreign. Cost per single issue: $19.00 domestic and $26.60 foreign. **See back for order form.**

Scientific Editor

José I. Castro

National Marine Fisheries Service, NOAA
263 13th Avenue South
Saint Petersburg, Florida 33701

Managing Editor

Kathryn Dennis

Scientific Publications Office
National Marine Fisheries Service, NOAA
1845 Wasp Boulevard, Building 176
Honolulu, Hawaii 96818

Associate Editor

Cara Mayo

Scientific Publications Office
National Marine Fisheries Service, NOAA
7600 Sand Point Way NE
Seattle, Washington 98115-0070

Editorial Board

Henry L. Bart Jr.	Tulane University, New Orleans, Louisiana
Matthew D. Campbell	National Marine Fisheries Service, Pascagoula, Mississippi
Shannon L. Cass-Calay	National Marine Fisheries Service, Miami, Florida
William B. Driggers III	National Marine Fisheries Service, Pascagoula, Mississippi
Gretchen L. Grammer	South Australian Research and Development Institute, Adelaide, Australia
Richard Langton	National Marine Fisheries Service, Walpole, Maine (retired)
Richard S. McBride	National Marine Fisheries Service, Woods Hole, Massachusetts
Richard L. Merrick	National Marine Fisheries Service, Falmouth, Massachusetts (retired)
Richard D. Methot	National Marine Fisheries Service, Seattle, Washington
Lisa J. Natanson	National Marine Fisheries Service, Narragansett, Rhode Island
Joseph M. Quattro	University of South Carolina, Columbia, South Carolina
Mark S. Peterson	University of Southern Mississippi, Ocean Springs, Mississippi
John F. Walter III	National Marine Fisheries Service, Miami, Florida
Bruce Wright	Aleutian Pribilof Island Association, Anchorage, Alaska

***Fishery Bulletin* website: https://spo.nmfs.noaa.gov/fb.htm**

Fishery Bulletin carries original research reports on investigations in fishery science, engineering, and economics. It began as the Bulletin of the United States Fish Commission in 1881; it became the Bulletin of the Bureau of Fisheries in 1904 and the *Fishery Bulletin* of the U.S. Fish and Wildlife Service in 1941. Separates were issued as documents through volume 46; the last document was no. 1103. Beginning with volume 47 in 1931 and continuing through volume 62 in 1963, each separate appeared as a numbered bulletin. A new system began in 1963, with volume 63, in which papers are bound together in a single issue. Beginning with volume 70, number 1, January 1972, *Fishery Bulletin* became a periodical, issued quarterly. In this form, it is available by subscription from the Superintendent of Documents, U.S. Government Publishing Office, Washington, DC 20401. It is also available free in limited numbers to libraries, research institutions, and state and federal agencies and in exchange for other scientific publications.

U.S. Department of Commerce
Seattle, Washington

Volume 118
Number 1
January 2020

Fishery Bulletin

SMITHSONIAN
JUN 14 2022
LIBRARIES

Contents

Short contribution

1–7 **Kiyomi Murakumo, Rui Matsumoto, Taketeru Tomita, Yousuke Matsumoto, and Keiichi Ueda**
The power of ultrasound: observation of nearly the entire gestation and embryonic developmental process of captive reef manta rays (*Mobula alfredi*)

Articles

8–20 **Cristiana M. Bank, Kenneth Oliveira, Sandra J. Sutherland, Michael P. Armstrong, Jorge Landa, and Steven X. Cadrin**
Age validation for goosefish (*Lophius americanus*) in the northeastern United States

21–36 **Lisa J. Natanson, Megan Winton, Heather Bowlby, Warren Joyce, Bethany Deacy, Rui Coelho, and Daniela Rosa**
Updated reproductive parameters for the shortfin mako (*Isurus oxyrinchus*) in the North Atlantic Ocean with inferences of distribution by sex and reproductive stage

37–50 **Joseph J. Bizzarro, Elizabeth A. Gilbert-Horvath, E. J. Dick, Aaron M. Berger, Katherine T. Schmidt, Don Pearson, Christine Petersen, Lisa A. Kautzi, Rebecca R. Miller, John C. Field, and John Carlos Garza**
Genetic identification of blue rockfish (*Sebastes mystinus*) and deacon rockfish (*S. diaconus*) to enable life history analyses for stock assessment

51–62 **William B. Driggers III, Matthew D. Campbell, Kristin M. Hannan, Eric R. Hoffmayer, Christian M. Jones, and James A. Sulikowski**
Spatial variability in the fecundity of Atlantic sharpnose sharks (*Rhizoprionodon terraenovae*) in the northern Gulf of Mexico

---

The National Marine Fisheries Service (NMFS) does not approve, recommend, or endorse any proprietary product or proprietary material mentioned in this publication. No reference shall be made to NMFS, or to this publication furnished by NMFS, in any advertising or sales promotion that would indicate or imply that NMFS approves, recommends, or endorses any proprietary product or proprietary material mentioned herein or that has as its purpose an intent to cause directly or indirectly the advertised product to be used or purchased because of this NMFS publication.

The NMFS Scientific Publications Office is not responsible for the contents of the articles.

63–73 **Phaedra Doukakis, Ethan A. Mora, Susan Wang, Paul Reilly, Russ Bellmer, Kristine Lesyna, Travis Tanaka, Natnael Hamda, Mary L. Moser, Daniel L. Erickson, Jason Vestre, Jon McVeigh, Kevin Stockmann, Kristen Duncan, and Steven T. Lindley**

Postrelease survival of green sturgeon (*Acipenser medirostris*) encountered as bycatch in the trawl fishery that targets California halibut (*Paralichthys californicus*), estimated by using pop-up satellite archival tags

74–86 **Erin L. Markin and David H. Secor**

Growth of juvenile Atlantic sturgeon (*Acipenser oxyrinchus oxyrinchus*) in response to dual-season spawning and latitudinal thermal regimes

87–99 **Jennifer Cahalan and Craig Faunce**

Development and implementation of a fully randomized sampling design for a fishery monitoring program

101–104 **Guidelines for authors**

National Marine
Fisheries Service
NOAA

Fishery Bulletin
established in 1881

Spencer F. Baird
First U.S. Commissioner
of Fisheries and founder
of *Fishery Bulletin*

The power of ultrasound: observation of nearly the entire gestation and embryonic developmental process of captive reef manta rays (*Mobula alfredi*)

Kiyomi Murakumo (contact author)[1]
Rui Matsumoto[1,2]
Taketeru Tomita[1,2]
Yousuke Matsumoto[1]
Keiichi Ueda[2]

Email address for contact author: k-murakumo@okichura.jp

[1] Okinawa Churaumi Aquarium
Ishikawa 424
Motobu, Okinawa 905-0206, Japan

[2] Okinawa Churashima Research Center
Okinawa Churashima Foundation
Ishikawa 888
Motobu, Okinawa 905-0206, Japan

Abstract—The aim of this study was to make ultrasound observations of 2 captive reef manta rays (*Mobula alfredi*), thereby collecting the first known data regarding the embryonic development of reef manta rays throughout almost the entire gestation period. The gestation period and water temperature at parturition were ~1 year and ~27°C, both of which are consistent with observations of wild individuals. On the basis of embryonic features observed through ultrasound, 3 developmental stages were recognized: early (0–80 d after copulation), middle (80–150 d after copulation), and late (150–360 d after copulation). The middle stage was distinguished from the early stage by the presence of large, wing-shaped pectoral fins, cephalic lobes, and buccal pumping, whereas the late stage was distinguished from the middle stage by the overlapping of the right and left pectoral fins and cessation of motion of the entire body in utero. These criteria will be useful for determining the gestation stages of wild reef manta rays.

Studies on the life history of large aquatic vertebrates, including the reef manta ray (*Mobula alfredi*) and the giant manta (*M. birostris*), are extremely difficult because such species move fast and have extensive ranges in vast marine environments and because technology for studying free-roaming aquatic animals does not exist (Castro, 2016). In the aquarium, observations are also difficult, because of the slow growth of animals, which can take decades to reach maturity, and because they are difficult to maintain for such long periods. Life history traits concerned with female reproduction, gestation cycle, gestation period, and fecundity are essential for studies on the conservation and management of large aquatic vertebrates.

Knowledge of the female reproductive biology of manta rays (Mobulidae) is still limited (Couturier et al., 2012). Marshall and Bennett (2010) observed the breeding behavior (e.g., courtship display, copulation, and parturition) of wild reef manta rays and estimated the gestation period for this species, on the basis of the duration between 2 consecutive parturition events for the same individual. However, their data were based on observations of females in the field, and no internal anatomical or embryonic developments were observed. The only documented observation of an embryo of a live reef manta ray can be found in Tomita et al. (2012), who conducted ultrasound examinations of a pregnant manta ray at the Okinawa Churaumi Aquarium, located in Okinawa, Japan, and described its embryonic respiratory behavior. However, this report provided only a "snapshot" of this species' embryonic development during late-term gestation, and this species' entire gestation process, from early to late term, has not been reported.

Long-term captivity and successful breeding of reef manta rays at the Okinawa Churaumi Aquarium have provided a unique opportunity to monitor

Manuscript submitted 21 July 2019.
Manuscript accepted 18 December 2019.
Fish. Bull. 118: 1–7 (2020).
Online publication date: 24 January 2020.
doi: 10.7755/FB.118.1.1

The views and opinions expressed or implied in this article are those of the author (or authors) and do not necessarily reflect the position of the National Marine Fisheries Service, NOAA.

the entire gestation process of this species. In 2007, a reef manta ray gave birth in the Kuroshio Tank (which has a volume of 7500 m^3). This event was the first captive birth of this species (Matsumoto and Uchida, 2008), and since then, 2 females have given birth to a total of 8 more offspring at the aquarium.

To the best of our knowledge, this report is the first to define almost the entire gestation process and embryonic development of the reef manta ray. This study would not have been possible without the recent development of underwater ultrasound (Tomita et al., 2019). Some previous studies have demonstrated that ultrasound is a powerful technique for observing the embryonic condition of captive, viviparous elasmobranchs (e.g., Carrier et al., 2003; Daly et al., 2007). However, the device used in this study is unique in that it can be used by scuba divers at water depths of 10 m or more, allowing the observation of pregnant females without handling the specimens and, therefore, minimizing potential stress.

Materials and methods

Experimental animals

The 2 female reef manta rays (specimens 1 and 2) examined were originally captured by using a set net off Okinawa Island, Japan. Specimen 1 was 205 cm in disc width (DW) when captured in 1998 and had grown to 387 cm DW by 2013, whereas specimen 2 was 227 cm DW when captured in 2008 and had grown to 368 cm DW by 2015. Specimen 1 gave birth 7 times from 2007 through 2013, and specimen 2 gave birth once in 2015.

Ultrasound examinations

Ultrasound examinations were conducted in the Kuroshio Tank at the Okinawa Churaumi Aquarium, by using a FAZONE M[1] ultrasound device (Fujifilm Global, Tokyo, Japan) and a transducer in a 3.525-MHz linear array and at depths up to 24 cm. The examinations were conducted by using either 1) water-surface ultrasound (Fig. 1) or 2) underwater ultrasound (Fig. 2). For water-surface ultrasound, the ultrasound probe was attached to the tip of a PVC pipe that was ~2 m long, and the observer approached the specimens from above during feeding. When the animals swam near the surface, the transducer was placed on the skin of the dorsal surface above the uterus. For underwater ultrasound, the device was housed in a water- and pressure-resistant case (Tomita et al., 2019), and scuba divers collected ultrasound data by placing the transducer on the skin of the dorsal surface above the uterus.

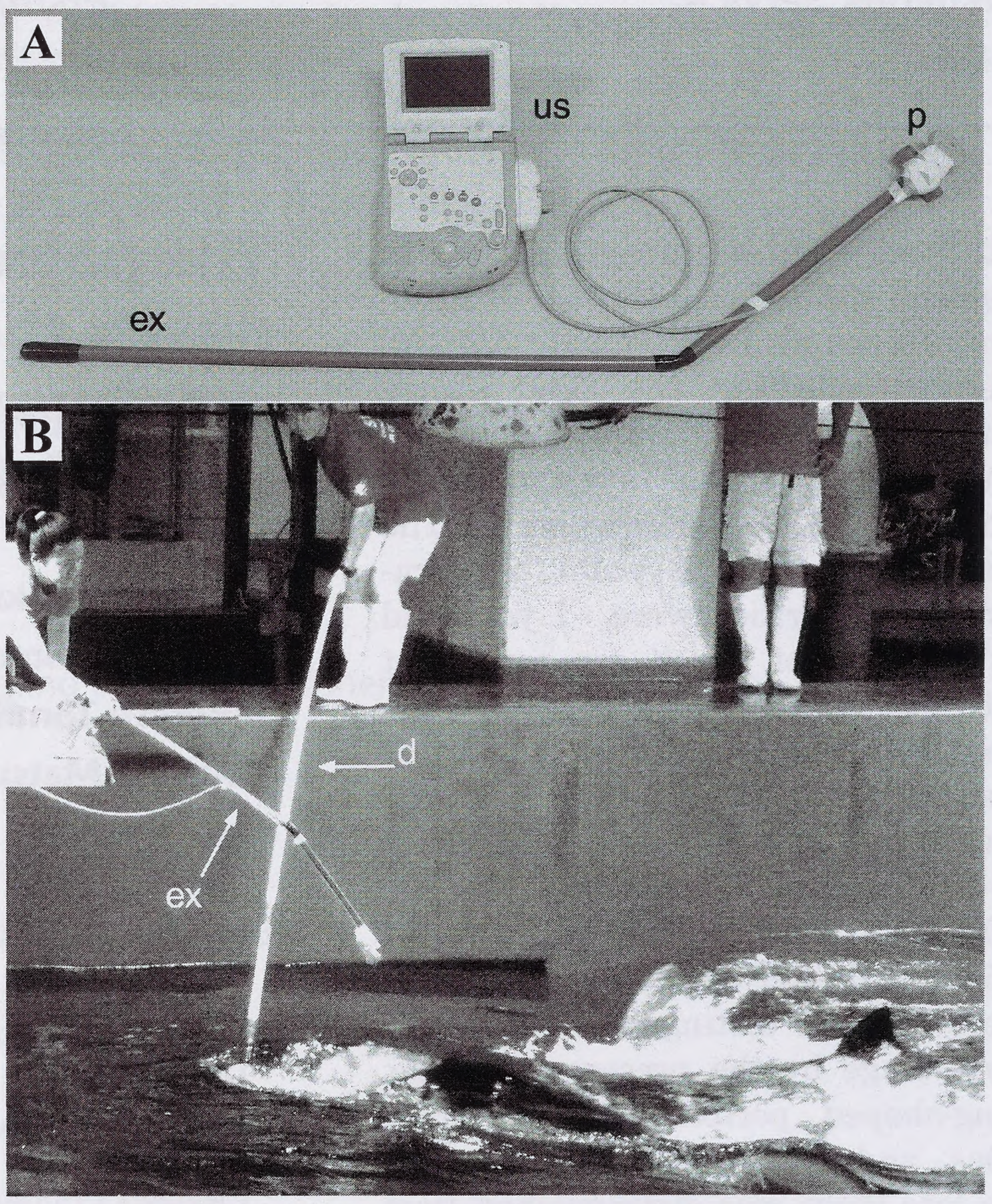

Figure 1

Photographs of the water-surface ultrasound device and technique used to make observations of the gestation and embryonic developmental process of captive reef manta rays (*Mobula alfredi*) during 2007–2015 at the Okinawa Churaumi Aquarium in Japan. (**A**) The probe (p) of the ultrasound device (us) was extended with a PVC pipe (ex). (**B**) An aquarium staff member persuades the reef manta ray to swim to the surface by serving krill with a long-handled dipper (d), while another staff member obtains ultrasound footage from above.

We conducted ultrasound experiments for 93 d, about once every month. The beginning of the ultrasound observations was timed differently for each pregnancy, starting from 12 h to 31 d after mating.

Analysis of ultrasound footage was conducted by using software designed to edit images in the DICOM file format (OsiriX, vers. 3.9.2–3.9.4, Pixmeo SARL, Geneva, Switzerland). Through analysis of footage, we confirmed the developmental condition of the embryo, such as the presence or absence of yolk sac and cephalic lobes and the size of the pectoral fins. In addition, we observed the kinematics of the embryo, confirming the presence or absence of buccal movements.

Results

We tracked a total of 7 pregnancies in 2 female reef manta rays, and 6 of these pregnancies resulted in successful births. Mating events were observed for all pregnancies. The gestation periods, calculated from the 6 pregnancy events of the 2 captive females from 2007 through 2015 with the assumption that fertilization occurred on the day

---

[1] Mention of trade names or commercial companies is for identification purposes only and does not imply endorsement by the National Marine Fisheries Service, NOAA.

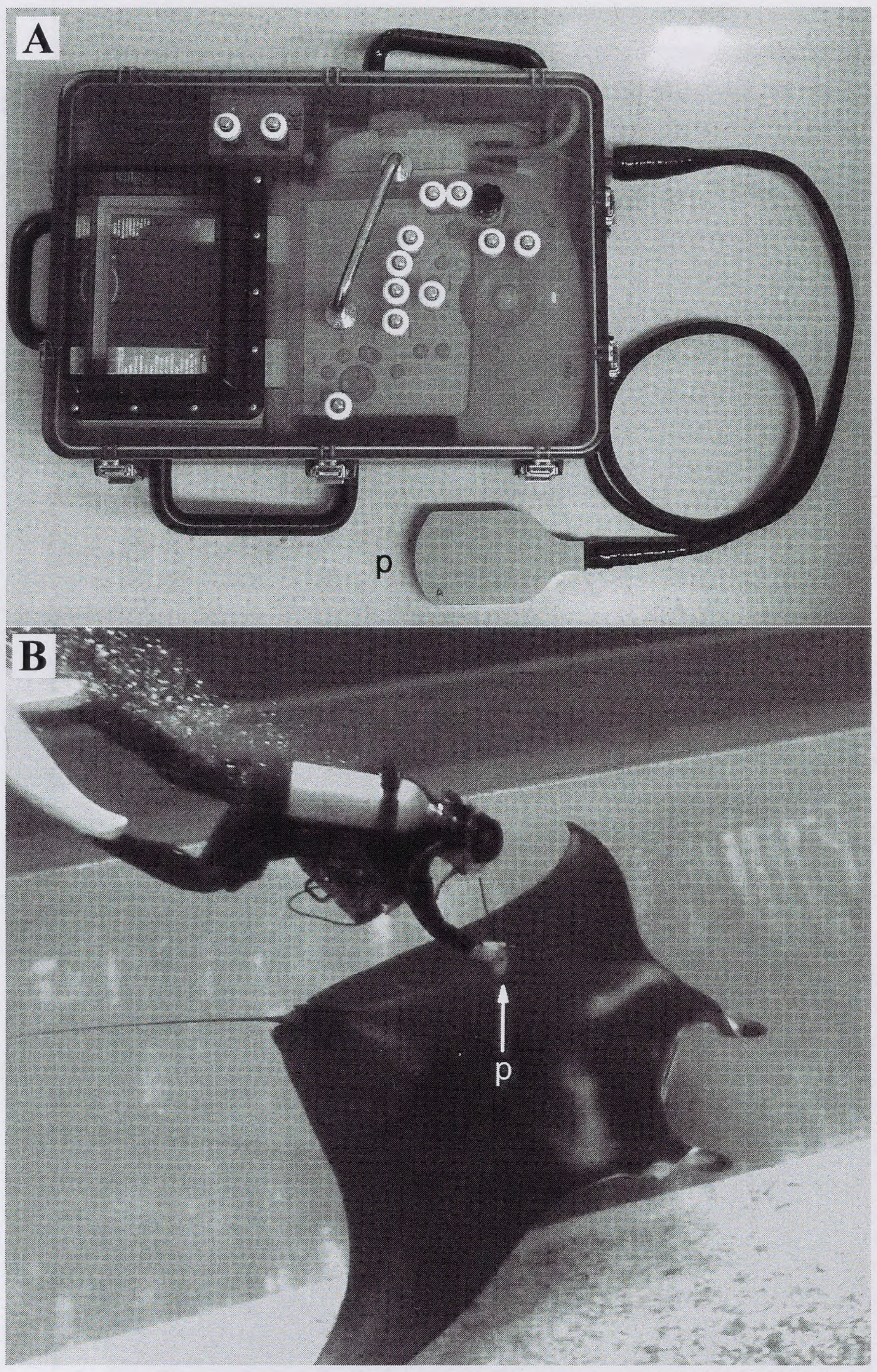

Figure 2

Photographs of the underwater ultrasound device and technique used to make observations of the gestation and embryonic developmental process of captive reef manta rays (*Mobula alfredi*) during 2007–2015 at the Okinawa Churaumi Aquarium in Japan. (**A**) The ultrasound device was housed in a pressure- and water-proof case. (**B**) A scuba diver positions the ultrasound probe (p) on the dorsal surface of a reef manta ray.

of mating, ranged from 363 to 379 d (mean: 370.5 d [standard deviation (SD) 5.7]) (Table 1). All the parturition events occurred in May and June, and the water temperature during these events ranged from 24.9°C to 27.5°C (mean: 27.0°C [SD 0.8]) (Table 1). All pregnant females observed in this study bore a single embryo. The birth size of the manta ray offspring ranged from 153.5 to 192.0 cm DW (mean: 180.3 cm [SD 14.1]) (Table 1).

The gestation process of the reef manta rays was divided into 3 stages: early (0–80 d after copulation; Fig. 3), middle (80–150 d after copulation; Fig. 4), and late (150–360 d after copulation; Fig. 5). These 3 stages were recognized in 3 pregnancies, after the underwater ultrasound was introduced in this study in 2010.

At the beginning of the early stage (0–20 d after copulation), the amount of uterine fluid was relatively small, as indicated by the diameter of the internal uterine cavity (maximum of ~10 cm; Fig. 3A). The embryo was not yet visible, and yolk could be observed. Later (~50 d after copulation), the motionless embryo could be observed in utero (Fig. 3B).

The amount of uterine fluid was greater during the middle stage than during the early stage, as indicated by the diameter of the internal uterine cavity (maximum of 30 cm). In addition, the pectoral and dorsal fins and cephalic lobes were well developed (Fig. 4B), and the yolk sac was slender, cylindrical, and easily identifiable in ultrasound images (diameter of ~2 cm) (Fig. 4C). Furthermore, the tips of the right and left pectoral fins were bent dorsally or ventrally along the curve of the uterine wall but never overlapped, and the embryo rotated its body inside the uterine cavity and exhibited buccal pumping (Fig. 4D).

During the late stage, the relative amount of uterine fluid decreased, as the size of the embryonic body increased, and a conspicuous bulge was observed on the dorsal surface of the maternal body. The uterus was greatly expanded; therefore, the entire uterine image could not be acquired by ultrasound, and uterine diameter was no longer available. The yolk sac was still present but was rarely observed in ultrasound images, possibly because of its small size, and the pectoral fins were folded dorsally, with the right and left pectoral fins largely overlapping (Fig. 5A). The embryo did not show complete body movements, such as body rotation, in utero. Internal organs (e.g., spiral intestine) were visible (Fig. 5B). However, during the last part of this stage, the embryonic head was rarely observed because the depth of the embryonic head from the maternal skin surface was >24 cm, a depth that exceeds the limit of the ultrasound used. Therefore, buccal pumping was not observed.

Discussion

This study produced the first data of the entire gestation period of a manta ray. The gestation period of 370.5 d (SD 5.7), estimated from the 6 pregnancy events of the 2 captive females, is consistent with the 1-year gestation period that has been reported for wild reef manta rays (Marshall and Bennett, 2010). It also is significantly longer than the gestation period reported for other stingrays, for example, periods of 2, 3, and 4 months in the pelagic stingray (*Pteroplatytrygon violacea*), the round stingray (*Urobatis halleri*), and the bull ray (*Aetomylaeus bovinus*), respectively (Ranzi, 1934; Babel, 1967). The results of this study also indicate that parturition occurred in the summer, at water temperatures of ~27°C, as previously reported for wild reef manta rays (Marshall and Bennett, 2010).

The results of this study reveal that buccal pumping is a good indicator for distinguishing between the early and middle developmental stages of the reef manta ray. This observation is similar to the observations of the oviparous catshark species, the small-spotted catshark (*Scyliorhinus canicula*), and the cloudy catshark (*Scyliorhinus torazame*),

Table 1

Summary information for 7 captive births of reef manta rays (*Mobula alfredi*) at Okinawa Churaumi Aquarium during 2007–2015. Averages, calculated by excluding the stillborn event on 13 May 2012, are given with standard deviations (SDs) in parentheses. Two females accounted for these birth events. Specimen 1 gave birth 6 times before dying during pregnancy on 31 May 2013. Specimen 2 gave birth once during the study period, on 1 June 2015. N/A=not available.

		Birth size				
Birth events	Sex of newborns	Disc width (cm)	Body weight (kg)	Water temperature (°C)	Gestation duration (days)	Birth status
16 June 2007	Female	192.0	68.5	26.0	374	Normal
17 June 2008	Male	182.0	N/A	27.5	368	Normal
24 June 2009	Female	192.0	70.0	27.0	372	Normal
26 June 2010	Female	182.0	66.0	27.5	367	Normal
24 June 2011	Female	180.0	60.5	27.8	363	Normal
13 May 2012	Male	158.4	49.0	24.9	329	Stillborn
1 June 2015	Female	153.5	31.5	26.0	379	Normal
Average (SD)		180.3 (14.1)	59.3 (16.0)	27.0 (0.8)	370.5 (5.7)	

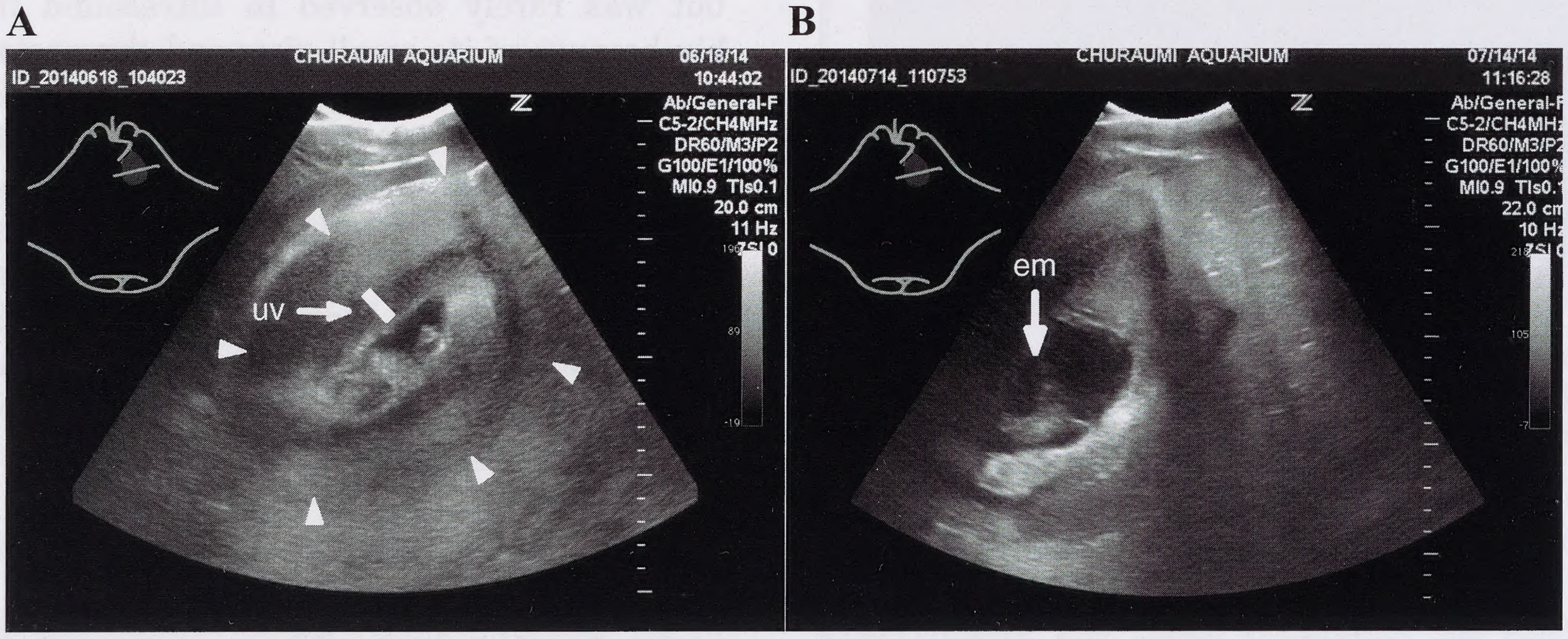

Figure 3

Ultrasound images of embryos in the early developmental stage (0–80 d after copulation) in a captive reef manta ray (*Mobula alfredi*) at the Okinawa Churaumi Aquarium in Japan: (**A**) embryo at 20 d after copulation, from ultrasound of specimen 2 on 18 June 2014, and (**B**) embryo (em) at 46 d after copulation, from ultrasound of specimen 2 on 14 July 2014. In panel A, the white arrows indicate the uterine chamber surface and the white line indicates the thick layer of uterine villi (uv). In panel B, the embryo is visible inside the uterine chamber.

in which embryos first exhibited buccal pumping during the middle gestation period, after the jaw and hyoid structure are fully developed (Diez and Davenport, 1987; Thomason et al., 1996; Tomita et al., 2014). Interestingly, in this study, we failed to observe any evidence of tail-waving movement, which is typically observed in oviparous batoids (Diez and Davenport, 1987; Thomason et al., 1996). The tail motion of oviparous batoid embryos is thought to create water flow inside the egg case and to promote the exchange of water between the inside and outside of the egg case. However, the lack of embryonic tail motion in the reef manta ray probably reflects the nonnecessity of such water replacement during viviparous reproduction.

The results of this study also indicate that the overlapping of the pectoral fins is a good indicator of the late developmental stage of the reef manta ray. According to our observations, the right and left pectoral fins are tightly folded posteriorly as the embryo grows and the tips of the right and left pectoral fins begin to overlap at 150 d after copulation. Because this change almost coincides with the

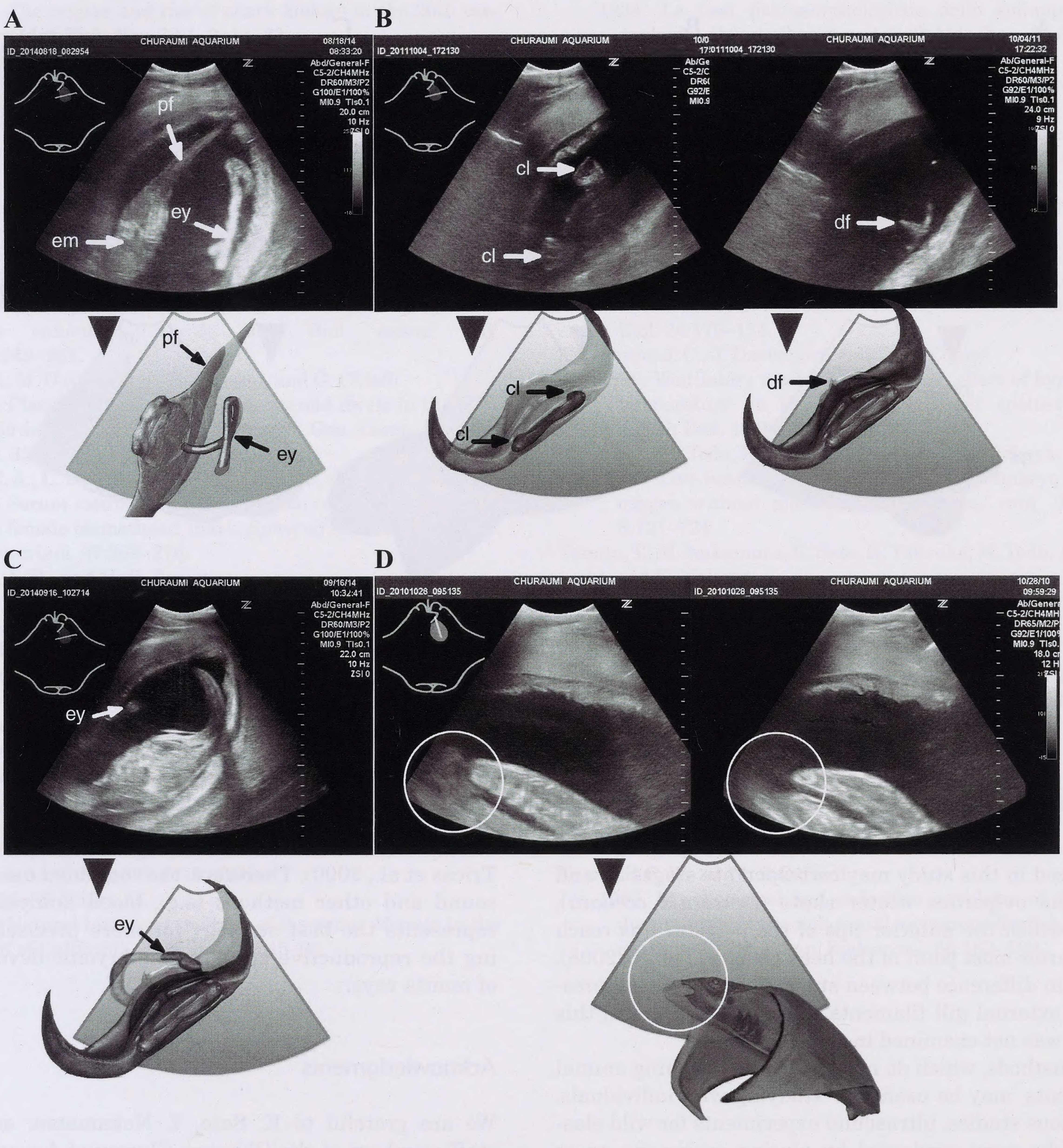

Figure 4

Ultrasound flat sections (top images) and 3-dimensional images (bottom images) of embryos in the middle developmental stage (80–150 d after copulation) in 2 captive reef manta rays (*Mobula alfredi*) at the Okinawa Churaumi Aquarium in Japan. (**A**) Both images of an embryo (em) at 81 d after copulation (in specimen 2 on 18 August 2014) show the large pectoral fin (pf) and embryonic yolk (ey). (**B**) In images of an embryo at 103 d after copulation (in specimen 1 on 4 October 2011), the right and left cephalic lobes (cl, left images) and dorsal fin (df, right images) are visible. (**C**) The images of an embryo at 110 d after copulation (in specimen 2 on 16 September 2014) show well-developed and non-overlapping pectoral fins. (**D**) In the images of an embryo at 125 d after copulation (in specimen 1 on 28 October 2010), the cyclic opening (left) and closing (right) of the mouth can be seen.

time when the pregnancy becomes obvious from external observations and because the occurrence of this overlap is relatively easy to detect by ultrasound, the feature is useful as an indicator of the late stage of pregnancy. Similar fin overlap has also been reported to occur in dead embryos of other *Mobula* species, such as the giant manta (K. Ueda and Y. Matsumoto, personal observ.) and the smoothtail mobula (*Mobula thurstoni*) (Notarbartolo-di-Sciara, 1988), indicating that the same stage criteria could be used for other *Mobula* species. Even though the developmental staging of *Mobula* species was not established in a previous study, the middle and late stages

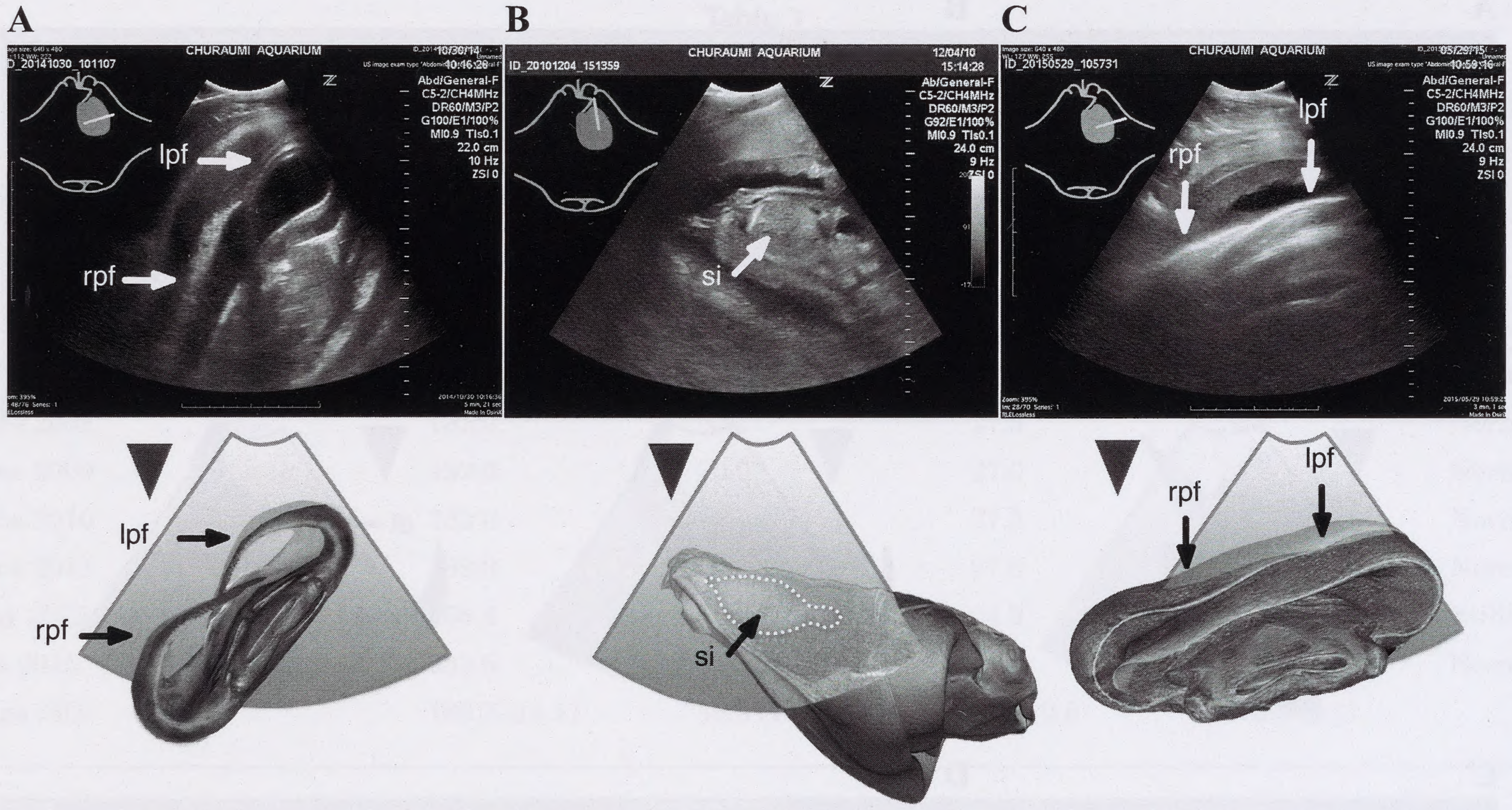

Figure 5

Ultrasound flat sections (top images) and 3-dimensional images (bottom images) of embryos in the late developmental stage (150–360 d after copulation) in 2 captive reef manta rays (*Mobula alfredi*) at the Okinawa Churaumi Aquarium in Japan. (**A**) In both images of an embryo at 154 d after copulation (in specimen 2 on 30 October 2014), the overlapping right pectoral fin (rpf) and left pectoral fin (lpf) are visible. (**B**) The images of an embryo at 162 d after copulation (in specimen 1 on 4 December 2010) provide a vertical cross section of the spiral intestine (si). (**C**) The images of an embryo at 365 d after copulation (in specimen 2 on 29 May 2015) show the rpf and lpf overlapping.

recognized in this study may correspond to stages 32 and 33 of the oviparous winter skate (*Leucoraja ocellata*), during which the anterior tips of the pectoral fins reach the anterior-most point of the head (Maxwell et al., 2008). The main difference between stage 32 and 33 is the presence of external gill filaments at stage 32; however, this feature was not examined in this study.

Our methods, which do not require constraining animal movements, may be useful for studying wild individuals. In previous studies, ultrasound experiments for wild elasmobranchs were conducted by placing specimens on or near the research vessels (e.g., Sulikowski et al., 2016). The constraints used to place specimens on or near a vessel are potentially stressful for the specimens and are almost impossible to use in studying large elasmobranchs, such as manta rays.

Despite its advantages, the use of underwater ultrasound had some limitations in our study. The main limitation was the low resolution of the ultrasound images. During early gestation, the small embryo and its movements are difficult to detect. Previous studies have shown that sex hormones can be used for detecting pregnancy in viviparous elasmobranchs. For example, concentration of plasma progesterone is generally elevated during the early stages of pregnancy and declines in the later stages (Tsang and Callard, 1987; Fasano et al., 1992; Manire et al., 1995; Snelson et al., 1997; Tricas et al., 2000). Therefore, the combined use of ultrasound and other methods (e.g., blood analysis) likely represents the best strategy for more precisely studying the reproductive cycle and embryonic development of manta rays.

Acknowledgments

We are grateful to K. Sato, Y. Nakamatsu, and other staff members at the Okinawa Churaumi Aquarium and Okinawa Churashima Research Center for their help and useful comments. This work was supported by the admission fees of the Okinawa Churaumi Aquarium.

Literature cited

Babel, J. S.
1967. Reproduction, life history, and ecology of the round stingray, *Urolophus halleri cooper*. Calif. Dep. Fish Game, Fish Bull. 137, 104 p.

Carrier, J. C., F. L. Murru, M. T. Walsh, and H. L. Pratt Jr.
2003. Assessing reproductive potential and gestation in nurse sharks (*Ginglymostoma cirratum*) using ultrasonography and endoscopy: an example of bridging the gap between field research and captive studies. Zoo Biol. 22:179–187.

Castro, J. I.
2016. The origins and rise of shark biology in the 20th century. Mar. Fish. Rev. 78(1–2):14–33.

Couturier, L. I. E., A. D. Marshall, F. R. A. Jaine, T. Kashiwagi, S. J. Pierce, K. A. Townsend, S. J. Weeks, M. B. Bennett, and A. J. Richardson.
2012. Biology, ecology and conservation of the Mobulidae. J. Fish Biol. 80:1075–1119.

Daly, J., I. Gunn, N. Kirby, R. Jones, and D. Galloway.
2007. Ultrasound examination and behavior scoring of captive broadnose sevengill sharks, *Notorynchus cepedianus* (Peron, 1807). Zoo Biol. 26:383–395.

Diez, J. M., and J. Davenport.
1987. Embryonic respiration in the dogfish (*Scyliorhinus canicula* L.). J. Mar. Biol. Assoc. U.K. 67:249–261.

Fasano, S., M. D'Antonio, R. Pierantoni, and G. Chieffi.
1992. Plasma and follicular tissue steroid levels in the elasmobranch fish, *Torpedo marmorata*. Gen. Comp. Endocrinol. 85:327–333.

Manire, C. A., L. E. L. Rasmussen, D. L. Hess, and R. E. Hueter.
1995. Serum steroid hormones and the reproductive cycle of the female bonnethead shark, *Sphyrna tiburo*. Gen. Comp. Endocrinol. 97:366–376.

Marshall, A. D., and M. B. Bennett.
2010. Reproductive ecology of the reef manta ray *Manta alfredi* in southern Mozambique. J. Fish Biol. 77:169–190.

Matsumoto, Y., and S. Uchida.
2008. Reproductive behavior of Manta rays (*Manta birostris*) in captivity. *In* Proceedings of the 7th International Aquarium Congress; Shanghai, China, 19–24 October, p. B123–B127. Shanghai Ocean Aquarium, Shanghai, China.

Maxwell, E. E., N. B. Fröbisch, and A. C. Heppleston.
2008. Variability and conservation in late chondrichthyan development: ontogeny of the winter skate (*Leucoraja ocellata*). Anat. Rec. 291:1079–1087.

Notarbartolo-di-Sciara, G.
1988. Natural history of the rays of the genus *Mobula* in the Gulf of California. Fish. Bull. 86:45–66.

Ranzi, S.
1934. Le basi fisio-morphologiche dello sviluppo embrionale dei Selaci. Part 2 and 3. Pubbl. Staz. Zool. Napoli. 13:331–437.

Snelson, F. F., Jr., L. E. L. Rasmussen, M. R. Johnson, and D. L. Hess.
1997. Serum concentrations of steroid hormones during reproduction in the Atlantic stingray, *Dasyatis sabina*. Gen. Comp. Endocrinol. 108:67–79.

Sulikowski, J. A., C. R. Wheeler, A. J. Gallagher, B. K. Prohaska, J. A. Langan, and N. Hammerschalag.
2016. Seasonal and life-stage variation in the reproductive ecology of a marine apex predator, the tiger shark *Galeocerdo cuvier*, at a protected female-dominated site. Aquat. Biol. 24:175–184.

Thomason, J. C., J. Davenport, and E. Le Comte.
1996. Ventilatory mechanisms and the effect of hypoxia and temperature on the embryonic lesser spotted dogfish. J. Fish Biol. 49:965–972.

Tomita, T., M. Toda, K. Ueda, S. Uchida, and K. Nakaya.
2012. Live-bearing manta ray: how the embryo acquires oxygen without placenta and umbilical cord. Biol. Lett. 8:721–724.

Tomita, T., M. Nakamura, K. Sato, H. Takaoka, M. Toda, J. Kawauchi, and K. Nakaya.
2014. Onset of buccal pumping in catshark embryos: how breathing develops in the egg capsule. PLoS ONE 9:e109504.

Tomita, T., K. Murakumo, K. Ueda, H. Ashida, and R. Furuyama.
2019. Locomotion is not a privilege after birth: ultrasound images of viviparous shark embryos swimming from one uterus to the other. Ethology 125:122–126.

Tricas, T. C., K. P. Maruska, and L. E. L. Rasmussen.
2000. Annual cycles of steroid hormone production, gonad development, and reproductive behavior in the Atlantic stingray. Gen. Comp. Endocrinol. 118:209–225.

Tsang, P. C. W., and I. P. Callard.
1987. Morphological and endocrine correlates of the reproductive cycle of the aplacental viviparous dogfish, *Squalus acanthias*. Gen. Comp. Endocrinol. 66:182–189.

National Marine
Fisheries Service
NOAA

Fishery Bulletin
established in 1881

Spencer F. Baird
First U.S. Commissioner
of Fisheries and founder
of *Fishery Bulletin*

Age validation for goosefish (*Lophius americanus*) in the northeastern United States

Cristiana M. Bank (contact author)[1]
Kenneth Oliveira[2]
Sandra J. Sutherland[3]
Michael P. Armstrong[4]
Jorge Landa[5]
Steven X. Cadrin[1]

Email address for contact author: cbank@vineyardwind.com

[1] School for Marine Science and Technology
University of Massachusetts Dartmouth
836 South Rodney French Boulevard
New Bedford, Massachusetts 02744

[2] Biology Department
University of Massachusetts Dartmouth
285 Old Westport Road
North Dartmouth, Massachusetts 02747

[3] Northeast Fisheries Science Center
National Marine Fisheries Service, NOAA
166 Water Street
Woods Hole, Massachusetts 02543

[4] Massachusetts Division of Marine Fisheries
30 Emerson Avenue
Gloucester, Massachusetts 01930

[5] Centro Oceanográfico de Santander
Instituto Español de Oceanografía
Promontorio de San Martín s/n
39004 Santander-Cantabria, Spain

Abstract—The goosefish (*Lophius americanus*) supports a valuable commercial fishery in the northeastern United States, but annual catch limits are relatively low because of uncertainty in assumed growth rates used for stock assessment. We evaluated the accuracy of the vertebral aging protocol and explored alternative aging methods by injecting chemical markers into individual goosefish held in the laboratory and tagged and recaptured in the field. The chemical left visible marks on vertebrae, illicia, and otoliths at the time of injection, but visibility and intensity of the marks varied among these aging structures. Times after marking ranged from 185 to 860 d for the 20 fish that were analyzed. Observed and expected counts of annuli after the chemical mark indicate that growth increments on vertebrae do not represent annuli and, therefore, cannot be used to accurately determine the age of goosefish. Identification of presumed annuli after the chemical mark was not possible for otoliths because the mark was not visible in most of the samples. Identification of presumed annuli was better for illicium samples than for vertebral samples. The growth rates of the individuals recaptured in the field provide preliminary information on annual growth of goosefish.

The goosefish (*Lophius americanus*) is an important target species in the commercial bottom fishery in the northeastern United States, with individuals caught in multiple types of fishing gears, including trawls, gill nets, and scallop dredges (Richards et al., 2008). Prior to 1980, goosefish were considered "trash fish" and discarded in favor of more desirable species, but market demand increased regionally and internationally, surpassing traditional target species, like the Atlantic cod (*Gadus morhua*) and haddock (*Melanogrammus aeglefinus*), in price and revenue (NMFS[1]). A fisheries management plan was implemented in 1999 (Haring and Maguire, 2008), but the lack of basic life history information required a precautionary approach (NEFSC, 2010; NEFSC[2]; Richards[3]). Goosefish are not overfished; however, fishermen have had a significant reduction in their total allowable catch (e.g., allowable catch for 2017–2019 was 43% below the overfishing limit; NEFMC[4])

Manuscript submitted 25 March 2019.
Manuscript accepted 3 January 2020.
Fish. Bull. 118:8–20 (2020).
Online publication date: 30 January 2020.
doi: 10.7755/FB.118.1.2

The views and opinions expressed or implied in this article are those of the author (or authors) and do not necessarily reflect the position of the National Marine Fisheries Service, NOAA.

---

[1] NMFS (National Marine Fisheries Service). 2017. Fisheries of the United States 2016. NOAA, Natl. Mar. Fish. Serv., Curr. Fish. Stat. 2016, 147 p. [Available from website.]

[2] NEFSC (Northeast Fisheries Science Center). 2013. 2013 monkfish operational assessment. Northeast Fish. Sci. Cent. Ref. Doc. 13-23, 116 p. [Available from website.]

[3] Richards, R. A. 2016. 2016 monkfish operational assessment. Northeast Fish. Sci. Cent. Ref. Doc. 16-09, 109 p. [Available from website.]

[4] NEFMC (New England Fishery Management Council). 2016. Acceptable biological catch (ABC) recommendations for monkfish for fishing years for 2017–2019, 3 p. Sci. Stat. Committ., New England Fish. Manage. Counc., Newburyport, MA. [Available from website.]

as a result of the scientific uncertainty in the latest stock assessment, which was conducted in 2010 (NEFSC, 2010). A statistical catch-at-length model that assumed growth is known was used to determine the status of the goosefish fishery for the stock assessment completed in 2010 and for the operational assessment completed in 2013 (NEFSC, 2010; NEFSC[2]). The available information on age and growth from analysis of annuli on vertebrae indicates linear growth, similar growth rates for males and females, and an absence of males older than 7 years in the goosefish population, with females living up to 14 years (Richards et al., 2008). However, the vertebral aging method for goosefish had not been validated when the stock assessment was conducted, contributing to the underlying cause of the uncertainty about growth rates for this species.

The structure preferred for age determination for *Lophius* species varies, and the interpretation of growth increments on all structures of these species is challenging (Griffiths and Hecht, 1986; Maartens et al., 1999; Walmsley et al., 2005; Landa et al., 2013). European scientists used sagittal otoliths in the first aging studies of white anglerfish (*L. piscatorius*) and black anglerfish (*L. budegassa*) (e.g., Guillou, 1978; Tsimenidis and Ondrias, 1980). However, age estimation through analysis of otoliths has proven to be difficult because of confusing secondary structures (checks) and increasing opacity with age; as a result, the illicium (first spine of the dorsal fin) has become more widely used than the otolith in growth studies of both of these species (e.g., Dupouy et al., 1986; Duarte et al., 1997; Quincoces et al.[5]). The results of the 3 international aging workshops and exchanges on species of *Lophius* in Europe, during which illicia and otoliths were compared by age readers, indicate that age estimates from analysis of illicia had better repeatability, precision, and relative bias than those from analysis of otoliths (Dupouy[6]; Duarte et al.[7]; Landa[8]). The results obtained from micro-increment analysis of otoliths from white anglerfish and black anglerfish (Wright et al., 2002; La Mesa and De Rossi, 2008) and from tag-recapture and length–frequency studies (e.g., Laurenson et al., 2005; Jónsson[9]; Landa et al., 2008) have been useful for establishing better age estimation criteria and for obtaining corroborated growth patterns based on analysis of illicia from specimens caught in European waters (Landa et al., 2013; Ofstad et al., 2013).

Illicia also have been used for aging species of *Lophius* in Africa and Japan. South African scientists first used sagittal otoliths for aging devil anglerfish (*L. vomerinus*) (Griffiths and Hecht, 1986) then switched to illicia (Maartens et al., 1999; Walmsley et al., 2005). Japanese scientists have used vertebrae for aging yellow goosefish (*L. litulon*) (Yoneda et al., 1997), although in a more recent study growth rates from age estimates based on analysis of illicia and from tag-recapture experiments were similar. The age estimates from the illicia had better reader agreement than those from the vertebrae, and the illicium was determined to be the preferred structure for the yellow goosefish (Takeya et al., 2017).

Armstrong et al. (1992) developed an age estimation method for goosefish in which presumed annual growth increments are counted on baked vertebrae. A deep, coarse-textured ridge and a narrow dark band (winter ring or growth increment) interspersed by wider, uniformly textured zones were interpreted to represent 1 year of growth. Hartley (1995) compared aging structures for goosefish and concluded that the method of Armstrong et al. (1992) worked the best because winter growth increments, also referred to as *presumed annuli*, were difficult to identify on otoliths for goosefish older than 3 years and illicia provided inconsistent age estimates. On the basis of Hartley's (1995) work, the Northeast Fisheries Science Center implemented the methods described in Armstrong et al. (1992) and vertebrae became the aging structure used for goosefish in 1996. Cullen et al.[10] compared growth estimates by using aging methods based on analysis of illicia and vertebrae from large goosefish and determined that, although analysis of both structures produced similar ages, it was more difficult to detect presumed annuli on illicia than on vertebrae.

Our objective was to validate Armstrong et al.'s (1992) vertebral aging method for goosefish and to explore the suitability of alternative structures for age estimation. Our approach was to determine if growth increments on vertebrae, otoliths, and illicia are formed annually. Chemical marking was used in laboratory and field samples to establish a known timeline after marking. By using the marked samples, we attempted to identify the structure that had the most consistent and identifiable annual growth increment for age estimation.

Materials and methods

Important factors in keeping goosefish alive in captivity were determined through trial and error during the course of this study. Field protocols and laboratory methods were adapted throughout this study to meet the research objectives by minimizing injury and stress of fish, increasing sample size, and promoting natural growth of marked specimens.

---

[5] Quincoces, I., M. Santurtún, and P. Lucio. 1998. Biological aspects of white anglerfish (*Lophius piscatorius*) in the Bay of Biscay (ICES Division VIIIa,b,d) in 1996–1997. ICES CM 1998/O:48, 29 p. [Available from website.]

[6] Dupouy, H. (ed.). 1997. International ageing workshop on European monkfish, 34 p. IFREMER, Lorient, France.

[7] Duarte, R., J. Landa, C. Morgado, A. Marçal, S. Warne, E. Barcala, E. Bilbao, J. Dimeet, H. Djurhuus, E. Jónsson, et al. 2005. Report of the anglerfish *Illicia*/otoliths ageing workshop; Lisbon, Portugal, 8–12 November 2004, 47 p. IPIMAR, Lisbon, Portugal. [Available from website.]

[8] Landa, J. (ed.). 2011. Report of the anglerfish (*Lophius piscatorius*) illicia and otoliths exchange 2011, 61 p. ICES Plann. Group Comm. Catch Discards Biol. Sampl. [Available from website.]

[9] Jónsson, E. 2007. Verification of anglerfish (*Lophius piscatorius*) age estimation through comparison of length modes of age read fish (illicia) to length modes of large year-classes appearing in the Icelandic stock. ICES CM 2007/K:03, 17 p. [Available from website.]

[10] Cullen, D. W., A. K. Johnson, A. Richards, and K. Lang. 2007. Comparing age and growth estimates for large monkfish (*Lophius americanus* V.) using *illicium* and vertebral aging methods. ICES CM 2007/K:24. [Available from website.]

Laboratory specimens

Live, undamaged goosefish were individually selected during commercial fishing trips on vessels outfitted with gill nets or otter trawls and during research scallop-dredge and bottom-trawl surveys (Howe, 1989; Winton et al., 2017). Specimens were collected over 6 years (2009–2015), during every month of the year, except September. Most specimens were collected from waters of southern New England, with a few specimens taken from the Gulf of Maine (Fig. 1), at depths of 45–65 m. Fish were transported to the laboratory in aerated live wells with minimal handling.

Goosefish were held separately in 15-m^3 circular tanks with sterilized fine-grain silica sand approximately 8 cm deep so that they could burrow and lie flat. The water supply was a semi-closed, recirculating seawater system consisting of 2 sand filters, 2 bag filters (50 and 25 µm), and an ultraviolet sterilizer for the incoming replacement water. Ultraviolet sterilizers were installed within the recirculating system that included a protein skimmer, biofiltration system, and degassing towers. Temperature was controlled by a heating system in the winter and a chiller in the summer. Water temperature was maintained to simulate seasonal changes in a range of 7–14°C, and the laboratory was under natural light following the seasonal cycle of light and dark hours.

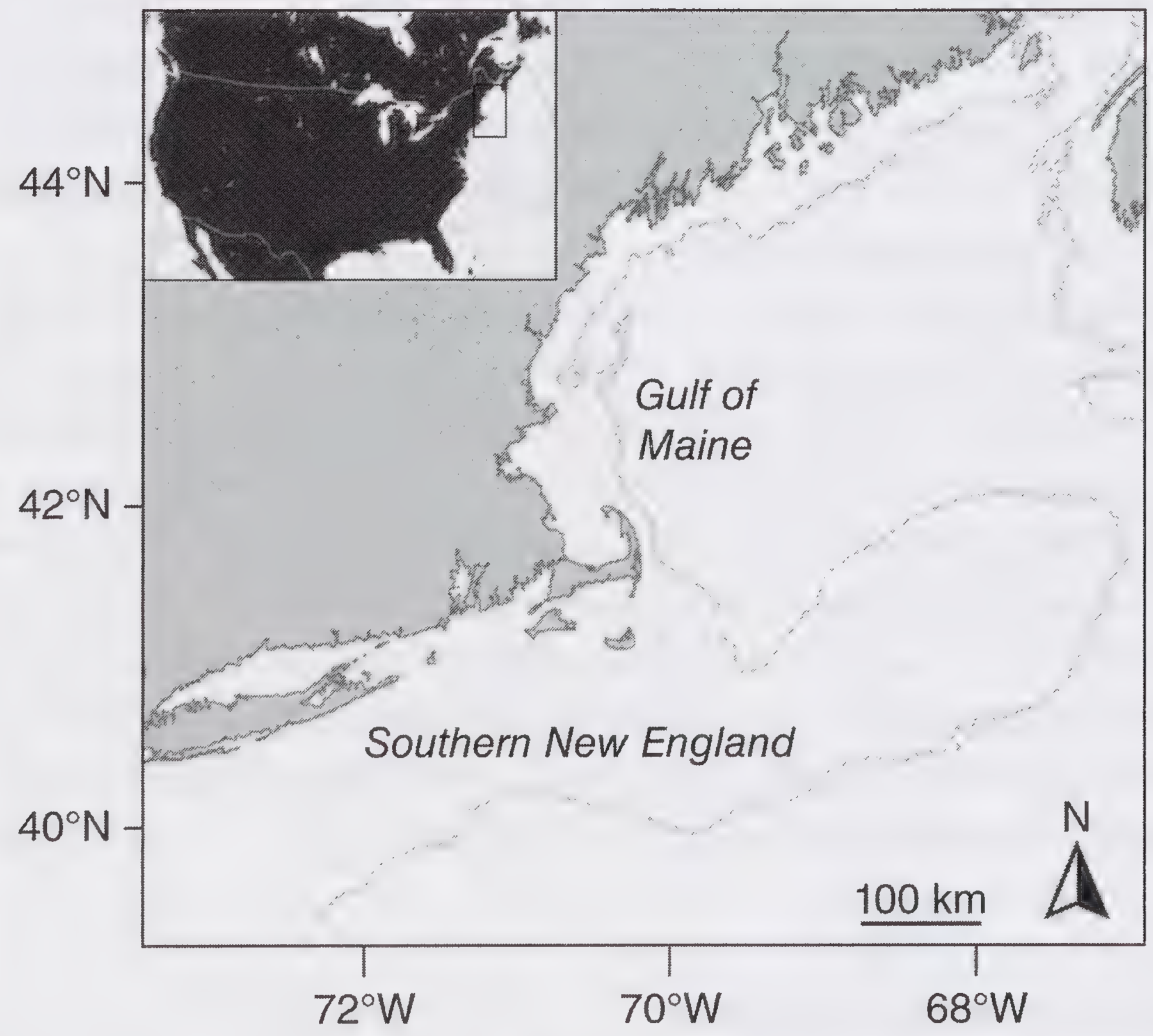

Figure 1

Map of the Gulf of Maine and southern New England, where goosefish (*Lophius americanus*) were collected as specimens for this study. Sampling occurred on commercial fishing trips and research scallop-dredge and bottom-trawl surveys between 2009 and 2015. Specimens were either transported to a laboratory or tagged and recaptured in the field.

A variety of food and feeding techniques were used throughout this study. One or 2 live fish (Cyprinodontidae; Atlantic silverside, *Menidia menidia*; or golden shiner, *Notemigonus crysoleucas*) were introduced into the tank to stimulate normal feeding behavior (Suppl. Videos 1 and 2) (online only). Dead fish (mackerel scad, *Decapterus macarellus*; Clupeidae; or Engraulidae) or longfin inshore squid (*Doryteuthis* (*Amerigo*) *pealeii*) were dangled in front of the goosefish specimens to elicit feeding strikes (Suppl. Video 3) (online only). If the first 2 methods of feeding failed, attempts were made to nudge dead prey into the corner of the mouth of the goosefish to trigger a feeding response. Feeding attempts were made every few days and increased during the summer months. Each feeding attempt was recorded, including technique and feed species used, weight of ingested food, water temperature, fish behavior, and general health of fish.

Acclimation time averaged 30 d but varied depending on the health of the fish. Behavioral indicators of acclimatization included camouflaging, burrowing into the sand, waving the illicium to attract prey, and eating. When one or more of these indicators were observed, specimens were measured and injected with oxytetracycline (MP Biomedicals[11], Irvine, CA) or fluorexon calcein (Acros Organics, Geel, Belgium) by using a 10-mL Norm-Ject Luer lock syringe (Air-Tite Products Co. Inc., Virginia Beach, VA) with a 20 G1 precision glide needle.

Initially, all injections were intramuscular and consisted of 75 mg/kg of oxytetracycline (Oliveira, 1995; Dekker[12]), but we adjusted our methods after we observed swelling, fluid-filled abscesses, and tissue necrosis at the injection site of both recaptured and laboratory specimens. Oxytetracycline was tested in 3 concentrations: 25 mg/kg, 50 mg/kg, and 75 mg/kg (McFarlane and Beamish, 1987), and the powder was mixed in a 90% saline solution until it dissolved, creating a clear yellow liquid with a pH of 1.6. As an alternative marker, fluorexon calcein was injected in 2 concentrations: 25 mg/kg and 75 mg/kg. The powder was mixed in a 90% saline solution, and approximately 1 g of sodium carbonate was added as a buffer for each gram of fluorexon calcein. The liquid became dark orange with a pH of 6.5. Injections were intraperitoneal and administered on the ventral side by pulling out the pelvic fins to create space between the skin and internal organs for insertion of the needle (Suppl. Fig. 1) (online only). Five specimens were not injected so that they could serve as controls for investigating the effects of injections.

---

[11] Mention of trade names or commercial companies is for identification purposes only and does not imply endorsement by the National Marine Fisheries Service, NOAA.

[12] Dekker, W. 1986. Age reading of European eels using tetracycline labelled otoliths. ICES CM 1986/M:16, 14 p. [Available from website.]

Field specimens

The specimens of goosefish that were used for field experiments were caught in the wild in gill nets of commercial vessels and tagged during 2009–2015. Selected specimens were kept aboard the fishing vessel in live wells to ascertain health before tagging. Only healthy fish (i.e., fish with no body damage and bright clear eyes, exhibiting active behavior) were chosen for this study. Following the protocols developed in the laboratory, each fish received a chemical injection. A centi-TD data storage tag (Star-Oddi, Garðabær, Iceland) was implanted under the skin on the dorsal side, and a visible, external tag was attached through the tail muscle to alert fishermen that the recaptured fish was worth $500 (Cadrin et al.[13]). Initially, pink T-bar tags (Hallprint Fish Tags, Hindmarsh Valley, Australia) were attached dorsally, but they were replaced with Petersen disc tags (Floy Tag Inc, Seattle, WA), attached through the tail muscle to increase tag retention, visibility, and recovery rate. Fish were returned to live wells for a short period of time to recover, and health was assessed again before releasing the fish.

Preparation of aging structures

When fish died in the laboratory or were recaptured in the wild, they were measured to the nearest millimeter, weighed to the nearest kilogram, and dissected. Sex and maturity stage was determined from macroscopic examination of gonads (Armstrong et al., 1992). Whenever possible, all 3 aging structures (illicia, sagittal otoliths, and vertebrae) were extracted, embedded in epoxy in silicone molds, and allowed to harden in the dark. Samples were sectioned with a double-bladed IsoMet Low Speed saw (model no. 11-1280-160, Buehler, Lake Bluff, IL) and mounted on glass slides. Protocols for each structure were as follows: the 10th vertebra was sectioned (0.3 mm) in the sagittal plane at the focus of the centrum; illicia were sectioned (0.31–0.58 mm) 0.5 cm above the basal bulb (Duarte et al., 1997); and one otolith of each pair was sectioned (0.18–0.20 mm) transversely through the nucleus. An Olympus BX51 microscope (Olympus, Tokyo, Japan) with an ultraviolet light attachment was used to view the chemical mark. A combination of ultraviolet light and transmitted light produced an image showing both the chemical mark and growth increments (Fig. 2). Images of the sections were taken with a CoolSNAP-Procf color digital camera (Media Cybernetics Inc., Rockville, MD).

For all specimens, the 8th vertebra was kept intact. For a subset of 7 fish, the second otolith was kept whole and hand ground to a thin lateral section by using sequentially finer-grit abrasive discs resulting in a ~1 mm flat disc. Prepared otoliths were then fixed to a glass slide by using a mounting adhesive. The exposed side of the otolith was polished by using a polishing cloth and MicroPolish II (0.3 µm) alumina powder (Buehler) in water. Whole vertebrae and laterally sectioned otoliths were viewed under a Nikon SMZ1500 microscope (Nikon Instruments Inc., Melville, NY) fitted with an ultraviolet-light attachment and Nikon Digital Sight DS-Fi1c camera. Images of the structures were taken with imaging software (NIS-Elements, Nikon Instruments Inc.) under reflected light to show the growth increments and under ultraviolet light with different filters to show the chemical mark. The images were then merged by using Adobe Photoshop (Adobe Inc., San Jose, CA), and opacity was adjusted to create a new image showing the exact locations of the chemical mark and the growth increments (Figs. 3 and 4).

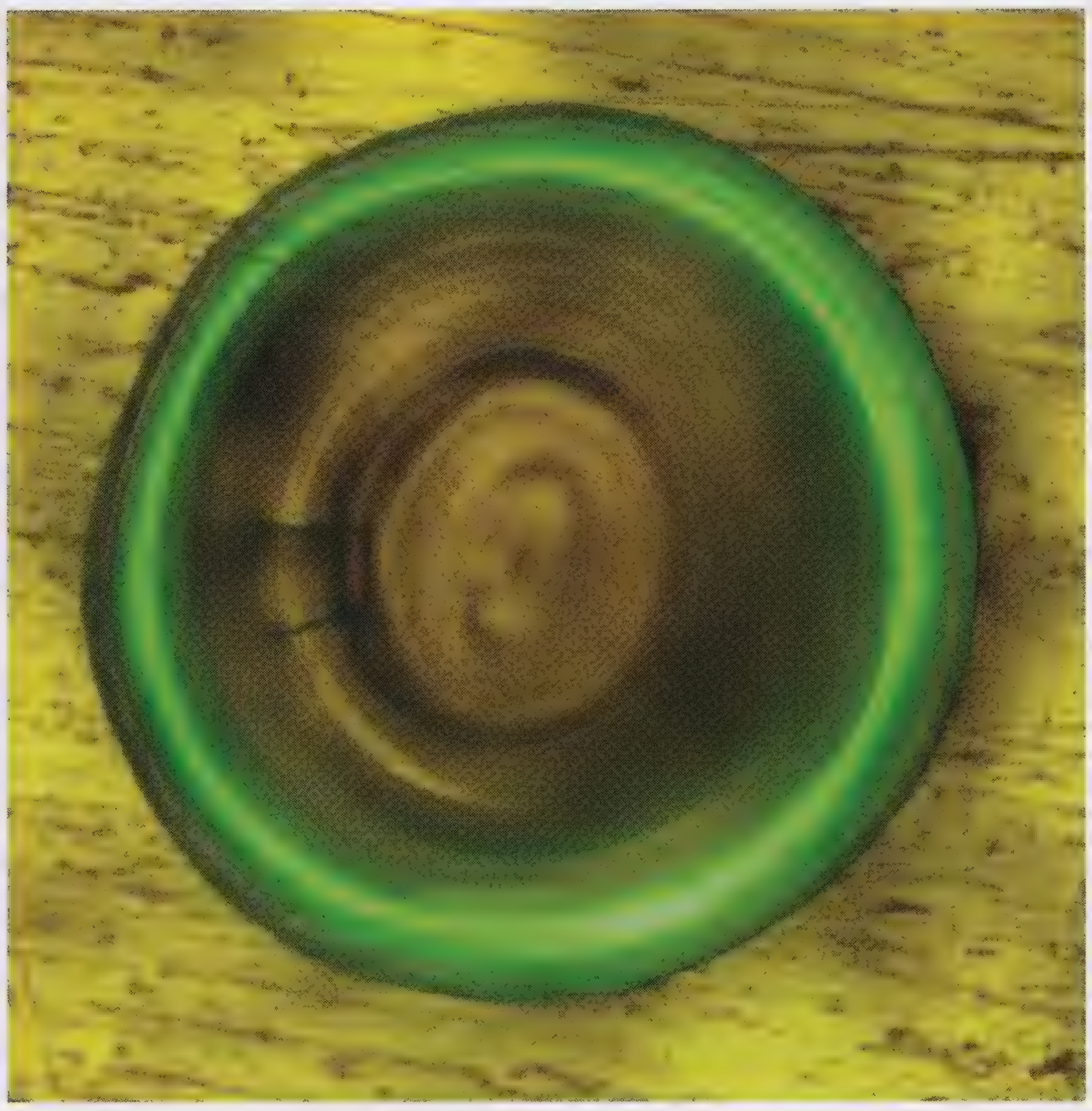

Figure 2

Image of a section of an illicium from a goosefish (*Lophius americanus*) tagged and recaptured in waters of the Gulf of Maine (fish ID 2). The illicium was sectioned (0.31–0.58 mm) 0.5 cm above the basal bulb and placed under a mixed ultraviolet and transmitted light source to show the chemical mark (25 mg/kg of fluorexon) and growth increments. This fish was tagged in October 2012 and recaptured in October 2013 after 365 d at large. Its total length was 67 cm at time of recapture.

Image analysis and validation of age estimates

Aging structures from fish that lived less than 6 months were compared to those from control fish that had no injections to determine if the chemical was incorporated into the structure. Aging structures from fish that lived more than 6 months were analyzed for mark visibility and validation of annual growth increments. Images alone cannot be used to identify presumed annuli on vertebrae because a physical ridge is associated with a growth increment (Armstrong et al., 1992). The location of the chemical mark was drawn on each 8th vertebra with a pencil, and vertebrae were baked in a drying oven at 230°C for 20–60 min (Armstrong et al., 1992). Two age readers who had experience with goosefish vertebrae viewed the 8th vertebra to identify the growth increments, to estimate the age of each fish, and to count the number of presumed annuli after the chemical mark. The readers did not know when the fish was injected, how long it lived after injection, or the size of the fish. As a condition of the Armstrong et al. (1992) protocol, readers were provided the month the fish died because aging protocols assume a birth date of 1 January.

---

[13] Cadrin, S. X., C. Bank, J. H. Grabowski, and G. D. Sherwood. 2017. Archival tagging and age validation in the mid-Atlantic. 2014 monkfish RSA. Project completion report, 51 p. Northeast Fish. Sci. Cent., Natl. Mar. Fish. Serv., NOAA, Woods Hole, MA. [Available from website.]

Eleven chemically marked illicium samples from the same fish used in the vertebral validation study were analyzed independently by the senior author and by an age reader experienced with other *Lophius* species. Illicium aging consists of identifying dark (opaque) and light (hyaline) growth increments under magnification of 50–20× with transmitted light. Each dark increment is counted and assumed to represent 1 year of growth. Aging criteria followed protocols developed by Duarte et al. (1997), with modifications and improvements suggested by Landa et al. (2013) and Ofstad et al. (2013). The first presumed annulus was located on the basis of criteria developed for white anglerfish by Wright et al. (2002), who concluded that the oval structure in the center represents a benthic growth increment and that the true first presumed annulus is a clearly identifiable growth increment beyond the oval. Each growth increment was identified, the age of the fish was estimated, and the number of presumed annuli identified after the chemical mark was documented in the images.

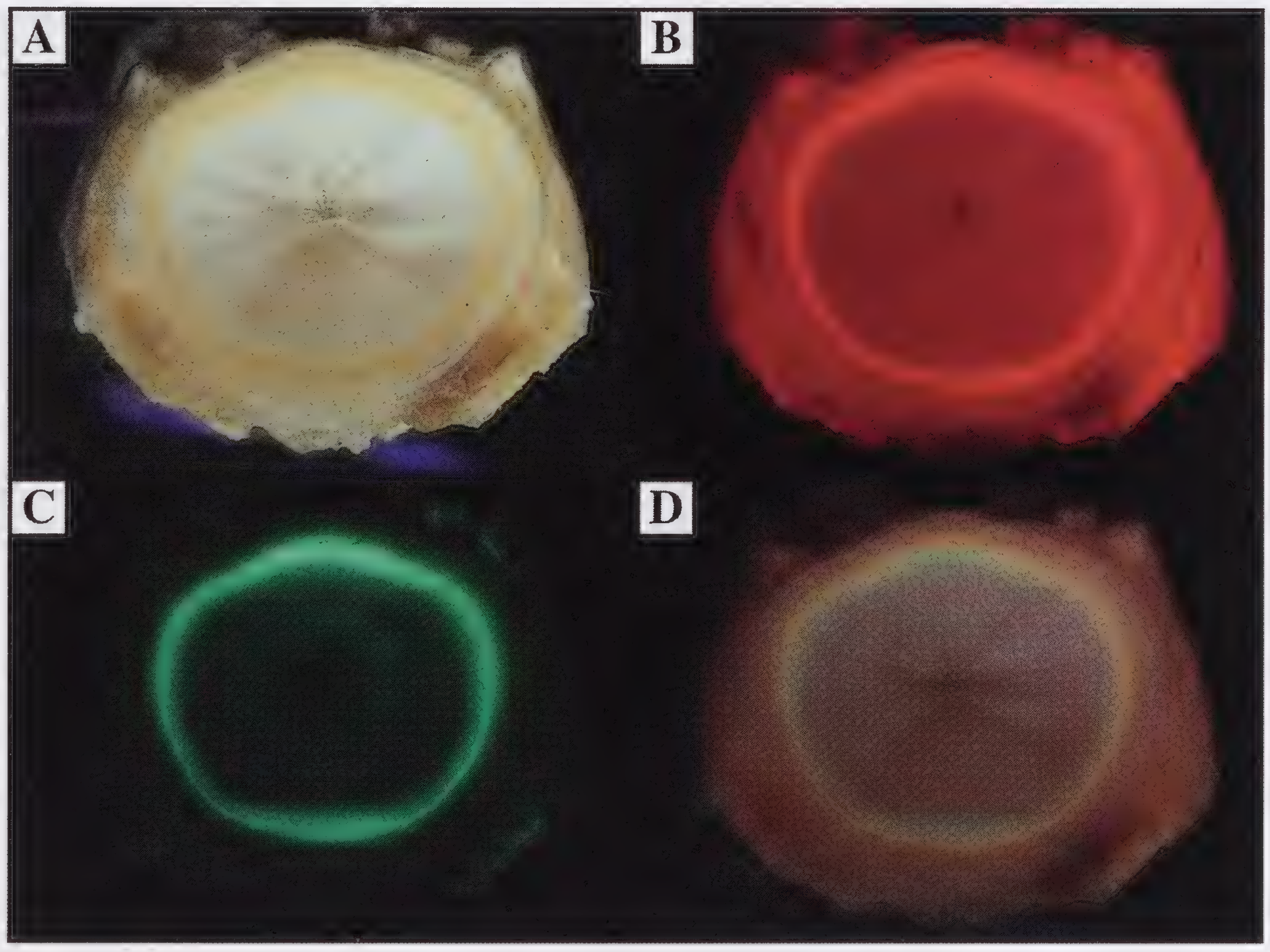

Figure 3

Images of a vertebra from a goosefish (*Lophius americanus*) (fish ID 2) under different light sources: (**A**) reflected light, (**B**) ultraviolet light with a GFP-B filter, and (**C**) ultraviolet light with a DSRed filter. (**D**) Image created by merging the images shown in the other 3 panels. This fish was caught, injected with 25 mg/kg of fluorexon, and released in waters of the Gulf of Maine in October 2012. After 365 d at large, it was recaptured in October 2013 and measured 67 cm in total length.

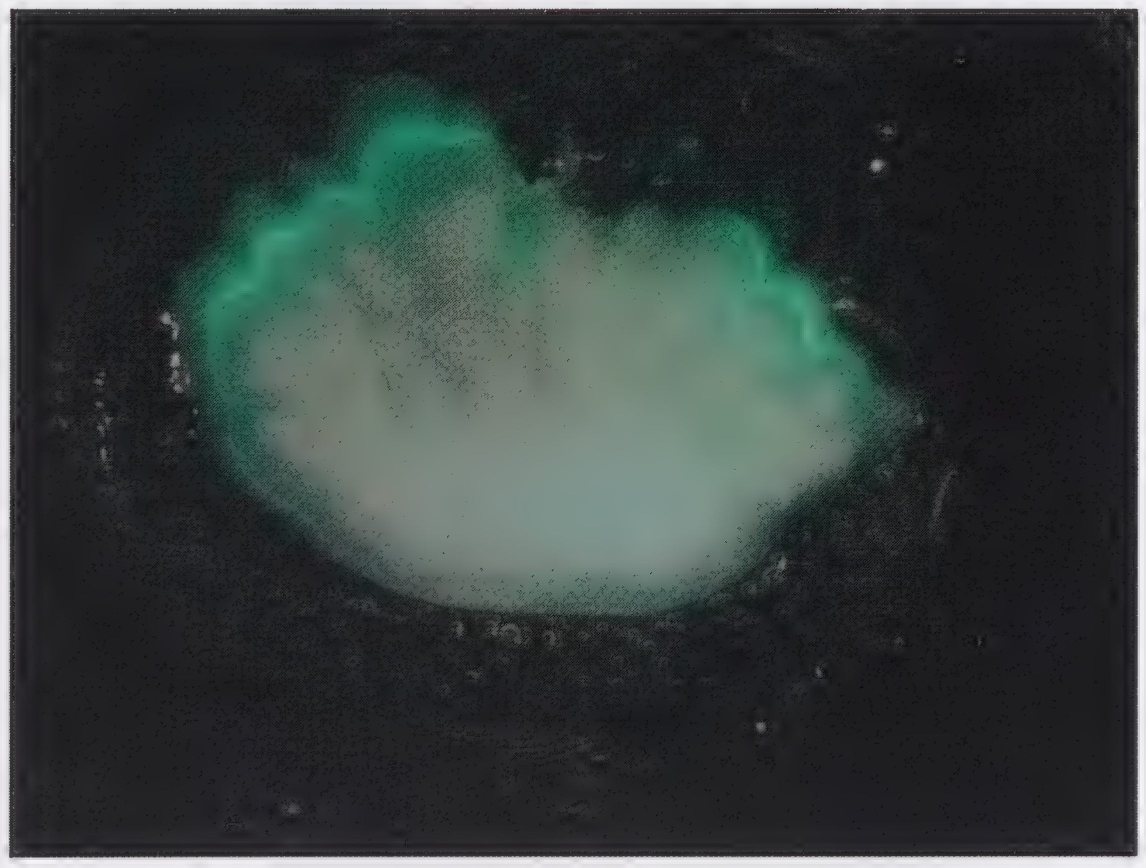

Figure 4

Image created by merging a reflected-light image with an ultraviolet-light image of a laterally sectioned otolith from a goosefish (*Lophius americanus*) caught in November 2010 in waters of southern New England and held in the laboratory (fish ID S). The mark (green line) is visible but discontinuous. This fish measured 51 cm in total length [TL] at the time of injection with 25 mg/kg of oxytetracycline. It grew 6 cm TL during 467 d in the laboratory and was 57 cm TL at time of death.

Results

Laboratory specimens

Between 2009 and 2015, 74 goosefish were transported to the laboratory, 36 specimens were injected with a chemical marker (20 fish with oxytetracycline and 16 fish with fluorexon), 5 specimens were used as controls, and the remaining 33 goosefish did not survive acclimation. Total length [TL] of all laboratory fish ranged from 15 to 69 cm, with an average of 51 cm. Of the injected laboratory fish, 10 specimens were included in the validation analysis, with times after marking of 223–860 d (Table 1) and

Table 1

Summary information for specimens of goosefish (*Lophius americanus*) used for validation of age estimates from analysis of vertebrae and illicia. Specimens, collected in waters of southern New England and the Gulf of Maine and injected with a chemical marker during 2009–2015, were held in the laboratory or tagged and recaptured in the field. Growth is from time alive after injection. All lengths and growth rates are provided in total length. Asterisks (*) indicate fish for which readers did not identify on vertebral and illicium samples the expected number of annuli after the chemical mark. Samples from some specimens were not analyzed or not available (N/A). For some other specimens, no mark was visible on the structure.

										No. of annuli after chemical mark				
											Vertebrae		Illicia	
Fish ID	Lab/field	Injection date	Death date	No. of days alive	Length at injection (cm)	Length at death (cm)	Growth (cm)	Annual growth rate (cm)	Sex	Expected	Reader 1	Reader 2	Reader 1	Reader 2
C	Lab	10/20/15	5/30/16	223	14.9	35.5	20.6	33.7	M	1	3*	1	No mark	No mark
L	Lab	3/27/14	08/03/16	860	28.9	61.2	32.3	13.7	M	2	2	2	N/A	N/A
W	Lab	5/24/12	3/18/13	298	33.0	41.0	8.0	9.8	F	1	2*	1	No mark	No mark
F	Lab	09/08/10	10/15/12	767	40.0	58.0	18.0	8.6	M	2	2	2	2	2
G	Lab	6/14/13	9/16/15	824	43.5	51.5	8.0	3.5	M	2	1*	0*	N/A	2
J	Lab	06/06/11	07/09/12	398	48.0	50.0	2.0	1.8	F	1	0*	0*	1	1
T	Lab	06/06/11	02/02/13	606	49.0	54.0	5.0	3.0	F	2	2	0*	2	1*
S	Lab	11/15/10	2/25/12	467	51.0	57.0	6.0	4.7	M	2	1*	0*	1*	1*
M	Lab	06/06/11	02/12/12	251	57.0	60.0	3.0	4.4	F	1	1	0*	1	1
O	Lab	2/13/14	12/22/14	312	63.0	60.0	−3.0	−3.5	F	1	0*	0*	N/A	N/A
7	Field	4/16/11	10/18/11	185	59.0	63.0	4.0	7.9	F	0	0	0	0	0
12	Field	05/09/15	12/17/2015	222	66.0	67.0	1.0	1.6	F	0	0	0	N/A	N/A
1	Field	11/10/09	7/16/10	248	68.0	75.5	7.5	11.0	F	1	0*	0*	1	1
10	Field	08/01/14	7/14/2015	347	70.0	77.5	7.5	7.9	F	1	1	1	N/A	N/A
11	Field	08/02/14	7/28/2015	360	75.0	79.0	4.0	4.1	F	1	0*	0*	N/A	N/A
9	Field	7/31/2014	4/20/2015	263	78.0	82.0	4.0	5.6	F	1	0*	0*	N/A	N/A
8	Field	08/02/14	3/29/2015	239	80.0	83.0	3.0	4.6	N/A	1	1	1	N/A	N/A
2	Field	10/17/12	10/17/13	365	N/A	67.0	N/A	N/A	M	1	0*	0*	1	1
4	Field	10/17/12	9/17/13	333	N/A	71.0	N/A	N/A	M	1	0*	0*	No mark	No mark
5	Field	10/17/12	04/07/14	537	N/A	76.5	N/A	N/A	F	2	2	0*	2	2

annual growth rates of −3.5–33.7 cm TL (Table 1, Fig. 5). All fish died, except for 1 specimen (fish ID L), which was sacrificed after 860 d. Food consumption increased from June through September as temperatures increased, peaking in September (12.8°C), and then decreased sharply in October, although water temperatures remained high (13.2°C). Food consumption was lowest from March through May (Fig. 6).

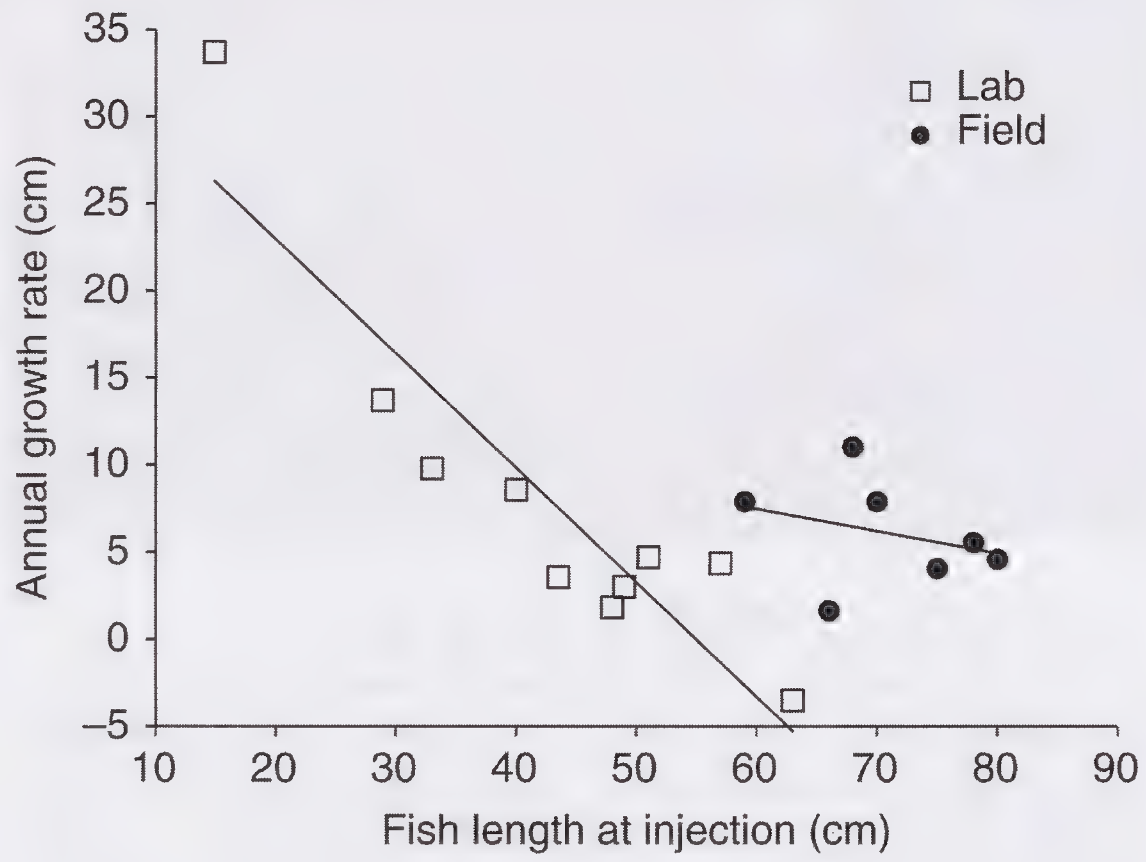

Figure 5

Relationship of annual growth rate with fish length at time of injection for goosefish (*Lophius americanus*) that were caught in waters of southern New England and the Gulf of Maine and injected with a chemical marker between 2009 and 2015. Open squares indicate growth for specimens held in the laboratory, black circles indicate growth for specimens that were tagged and recaptured in the field, and the diagonal lines indicate the trend lines. Growth and lengths are given in centimeters in total length.

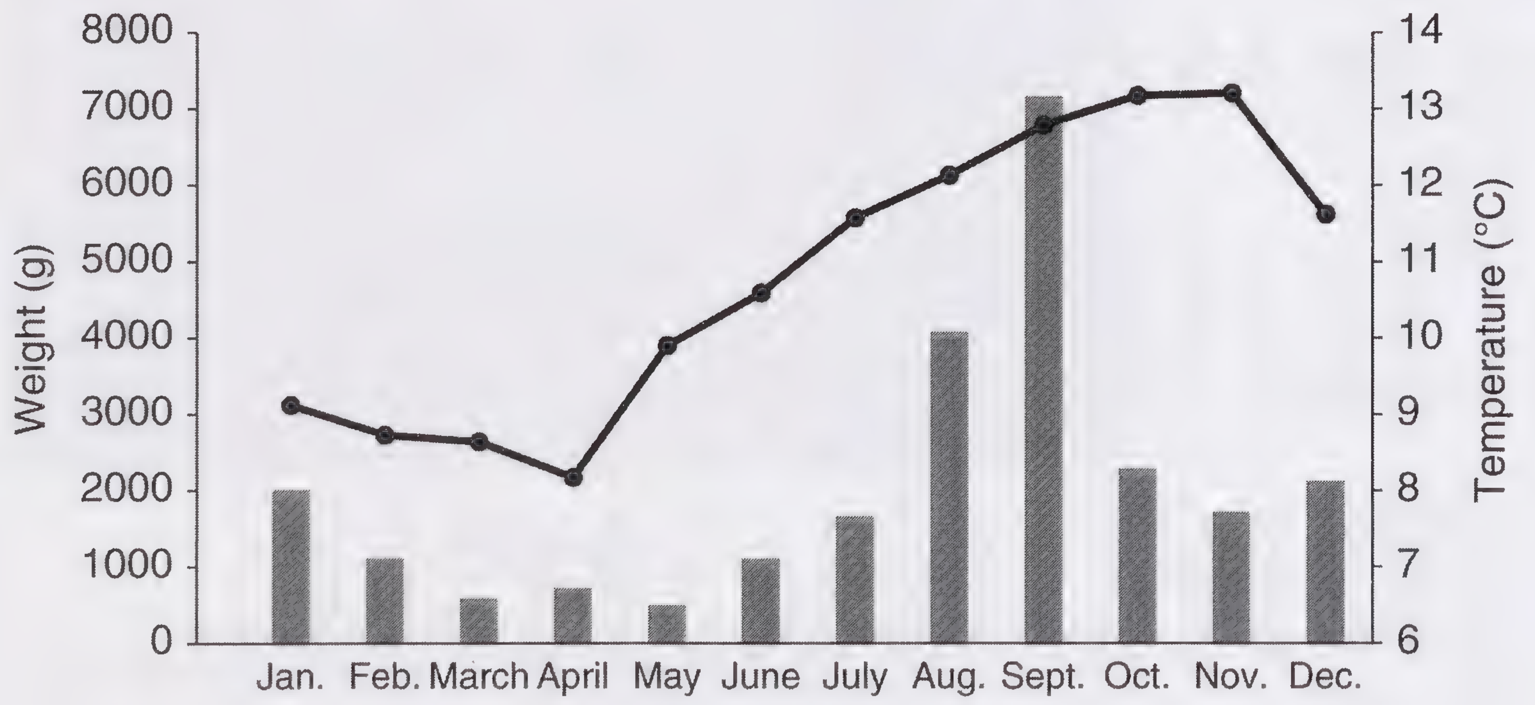

Figure 6

Monthly consumption of all prey by goosefish (*Lophius americanus*) held in the laboratory after capture in waters of southern New England and the Gulf of Maine between 2010 and 2013. Also provided are monthly average temperatures of tank water for 5 of the 10 laboratory specimens used in this study during this time frame.

Field specimens

Between 2009 and 2015, 501 goosefish were caught, injected with chemical markers, and released with data storage tags. Tagging occurred during every season, with the fewest fish released in the winter and the most fish released during the spring. A total of 169 specimens were injected with oxytetracycline, and 332 fish were injected with fluorexon. Total length at release ranged from 38 to 101 cm, with an average of 67 cm. Of the injected specimens, 38 fish were recaptured. Of the recaptured goosefish, 35 specimens had received 25 mg/kg of fluorexon, 2 fish had received 75 mg/kg of oxytetracycline, and 1 fish had received 50 mg/kg of oxytetracycline. Of those recaptured in the field, 10 specimens were included in the validation analysis, with times after marking of 185–537 d (Table 1) and annual growth rates of 1.6–11.0 cm (Table 1, Fig. 5).

Chemical marking

Fluorexon at both concentrations (25 and 75 mg/kg) produced a brighter, more visible mark than oxytetracycline, and a chemical mark was frequently visible on a vertebra or illicium without an ultraviolet light. Oxytetracycline produced a visible mark at all 3 concentrations (25, 50 and 75 mg/kg); however, 2 vertebral samples lost the intensity of the oxytetracycline mark over time and could not be used in the validation analysis. We determined that an intraperitoneal injection of 25 mg/kg of fluorexon was the most successful method for marking the aging structures (Suppl. Table) (online only).

Image analysis

Whenever possible, all 3 aging structures from laboratory and field specimens were analyzed to detect chemical marks. Some fish recaptured in the field had structures missing, and some structures were analyzed in a smaller subset. Specimens from both the field and laboratory that lived less than 6 months were grouped for analysis. These specimens did not live long enough or grow enough for a clear, distinct mark to be separate from the edge of their sampled structures. The edge of the structures from injected fish fluoresced under ultraviolet light, indicating that the chemical was incorporated into the calcified structures, whereas the edge of the structures from control fish did not. No autofluorescence was detected in otoliths from control specimens. However, the chemical mark was not seen in structures from every specimen, and the visibility and intensity of the mark varied between structures. For specimens that lived less than 6 months, the rate of detection of the chemical mark was highest (81%) for the illicia (*n*=31) and lowest (13%) for the transverse-sectioned otoliths (n=30). For vertebrae, both whole (n=28) and sectioned (n=23), the chemical mark was detected in 43% of the specimens.

Mark visibility for laboratory and field specimens that lived more than 6 months improved to 91% for the whole vertebrae (n=22). The detection rate for illicia (n=21) and sectioned vertebrae (n=14) was 86%, and the detection rate for transverse-sectioned otoliths remained the lowest at 36% (n=11) (Suppl. Table) (online only). Results improved to 43% for laterally sectioned otoliths (n=7), but the mark was not continuous and was not incorporated uniformly into the otolith (Fig. 4).

Age estimation: vertebrae

Twenty-two fish lived long enough to be included in the validation analysis with vertebrae (185–860 d post-marking), but only 20 specimens were used because 2 fish (1 specimen from the laboratory and 1 specimen from the field) did not have a mark that could be detected on the whole vertebrae at the time of analysis. Reader 1 identified the expected number of presumed annuli outside the mark for 45% of vertebral samples, and reader 2 identified the expected number of presumed annuli for 40% of samples (Table 1, Fig. 7A). The most common problem for both readers was the lack of a visible winter growth increment that should have been identifiable after the chemical mark. Six fish that lived for over 1 year and 3 fish that lived through a complete winter were expected to have at least 1 winter growth increment counted, but a clear winter growth ring was not visible in vertebrae sampled from them. Therefore, age was underestimated for 9 fish that were larger than 50 cm TL. Conversely, the age of the 2 smallest fish (36 and 41 cm TL) was overestimated by reader 1, who identified additional presumed annual growth increments when only 1 increment was expected (Table 1, Suppl. Fig. 2 (online only)).

Age estimation: illicia

Illicia from 11 of the same chemically marked fish were analyzed for age estimation and age validation after the chemical mark. Using the same age estimation criteria, both readers agreed on the location of most of the presumed annuli. Therefore, most of the ages estimated by both readers were similar (70% of agreement and disagreements of only ±1 year for 3 illicia), and the age estimated by both readers increased with fish length (Fig. 8). Both readers agreed on the position of the presumed first annulus (mean diameter: ~210 µm) in 80% of the illicia that were analyzed (Fig. 9). An oval nucleus was noted in almost

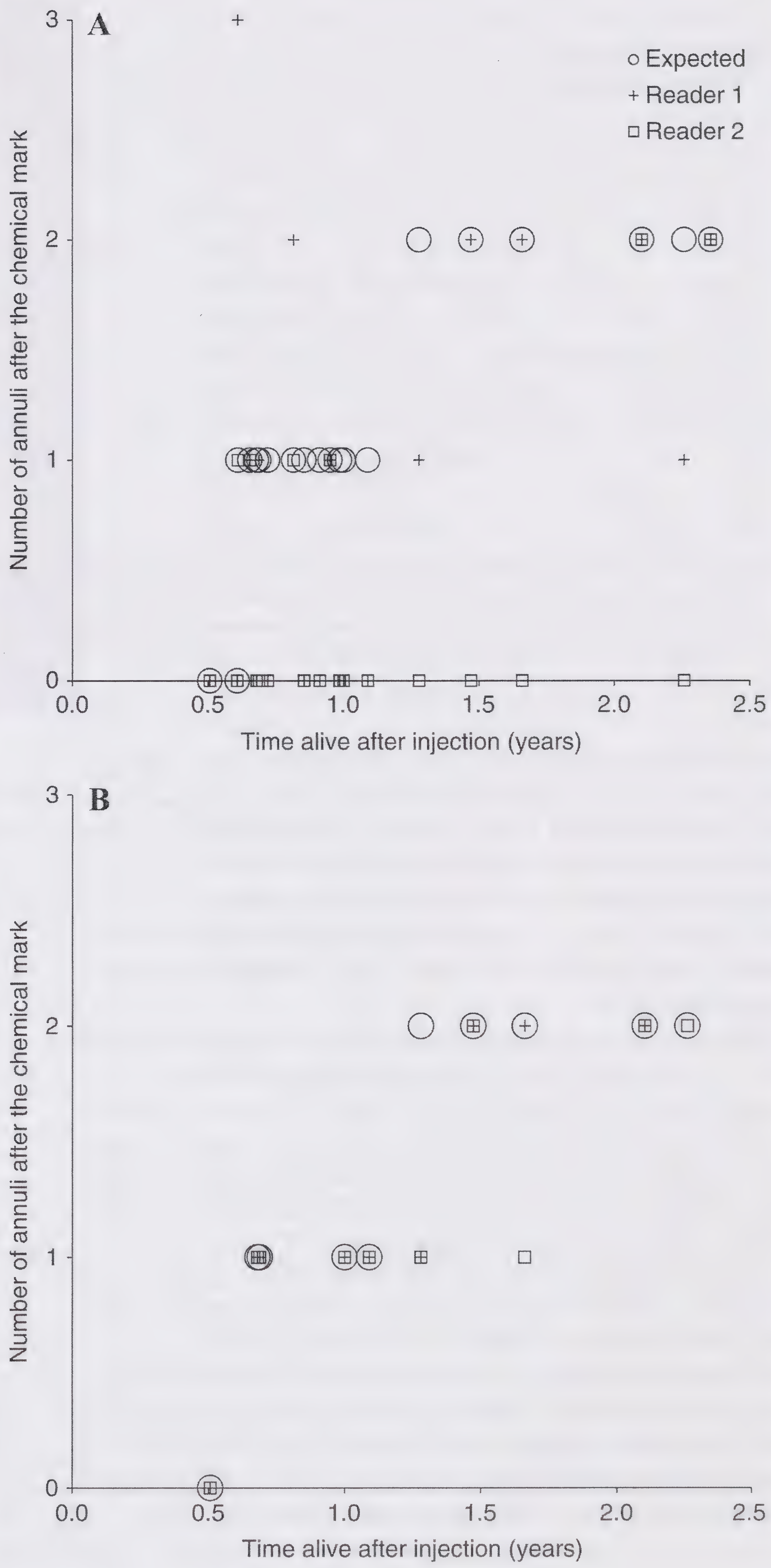

Figure 7

Relationships between the time elapsed from injection of a chemical marker to death for specimens of goosefish (*Lophius americanus*) and the numbers of annuli counted by each of 2 readers in the (**A**) vertebrae and (**B**) illicia of specimens. The number of annuli expected in that period are also included. Specimens, collected in waters of southern New England and the Gulf of Maine during 2009–2015, were injected with a chemical marker and held in the laboratory or tagged and recaptured in the field.

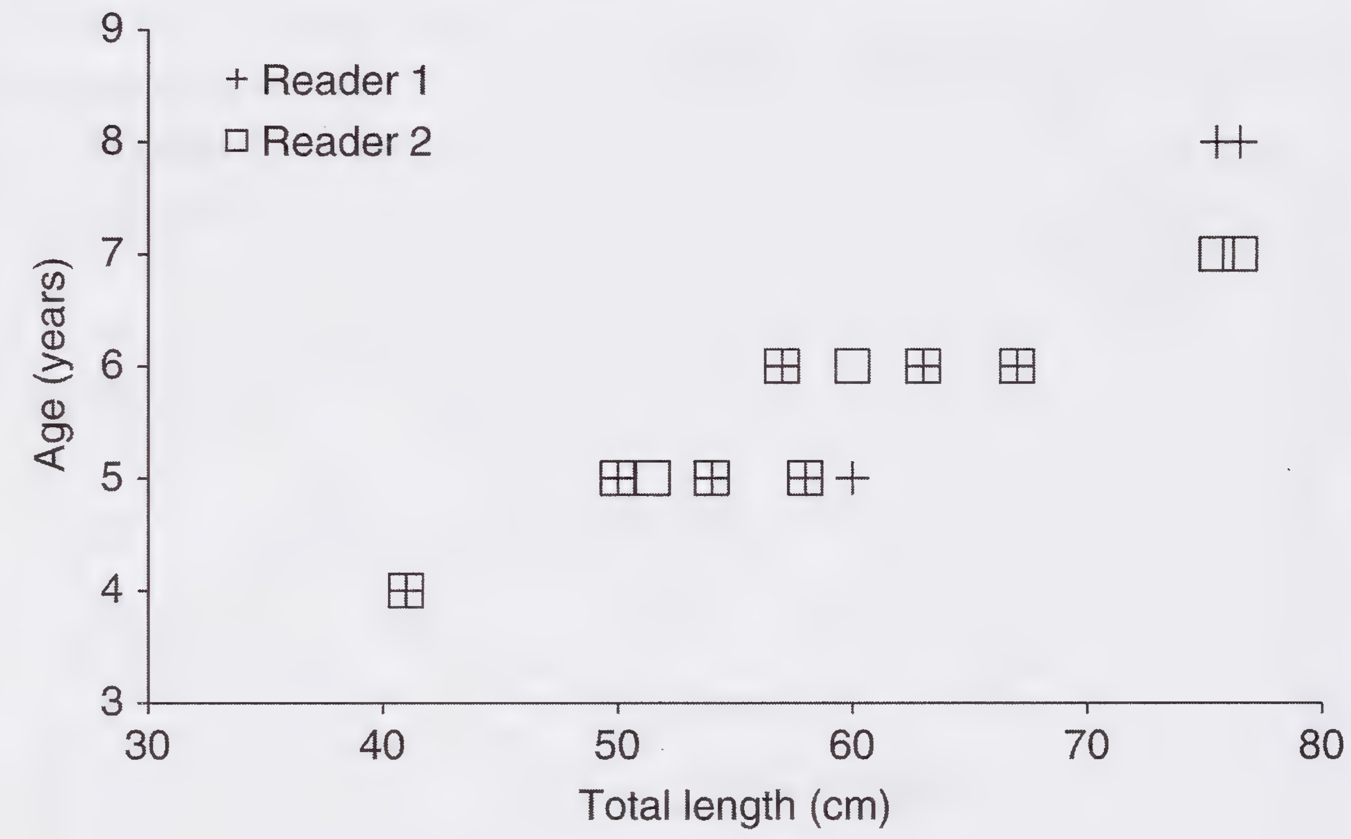

Figure 8

Relationship of estimated age, based on counts of annuli on illicia by 2 readers, and the total length of specimens of goosefish (*Lophius americanus*). Specimens were captured in waters of southern New England and the Gulf of Maine between 2009 and 2015.

all illicium samples, with a mean diameter of ~100 µm. A narrow dark increment outside the nucleus in some samples was considered to be a check, with a mean diameter of ~150 µm (Fig. 9). The chemical injections left marks in the illicia of differing intensity, from very sharp and narrow in some illicia to weaker and wider chemical marks in others (Fig. 9). The width of this mark affected the ease of interpretation.

Although the chemical mark was not clearly observed on the aging structure from 1 specimen (fish ID W), the remaining 10 fish were used for age validation. In most cases, both readers observed a number of growth increments (dark increments considered as annual) after the chemical mark that matched the number of winters elapsed (Table 1, Fig. 7B). For 3 of the fish that lived over 1 year but lacked a winter growth increment on the aged vertebra, a winter ring was seen on the analyzed illicium (Fig. 10). Therefore, reader 1 and reader 2 had an accuracy rate of 89% (9 aged illicia) and 80% (10 aged illicia), respectively (Table 1, Fig. 7B). An increasing relationship was observed between the time at large (between the chemical mark and death) and the number of presumed annuli counted by each reader in the illicia (Fig. 7B).

Discussion

Results indicate that growth increments on vertebrae do not represent annual growth and, therefore, cannot be used to accurately determine the age of goosefish. For half the fish that survived over 6 months after chemical marking, in both the laboratory and the wild, the expected number of annuli outside the chemical mark were not observed, and the difference between observed and expected number of annuli was greater than the measurement error of the technique (Table 1, Fig. 7A).

Several hypotheses explain why growth increments might not have followed an annual cycle in our study. Griffiths and Hecht (1986) and Maartens et al. (1999) hypothesized that the growth of *Lophius* species is a sporadic phenomenon rather than one of traditional seasonal growth. Armstrong et al. (1996) found a high percentage of empty stomachs for goosefish, indicating that infrequent eating could contribute to irregular growth increments. Our observations of feeding patterns in the laboratory are consistent with Armstrong's (1996) observations.

Another hypothesis to explain why annual growth increments may not form on vertebrae is the wide range of temperatures that goosefish experience during vertical movements (Rountree et al., 2008). Archival-tag data indicate that some fish in the western Gulf of Maine inhabit bottom temperatures of 6°C in the summer but vertically migrate into temperatures of 12–16°C for hours at a time before dropping back to bottom temperatures of 6°C (Bank, 2016). However, this behavior of diel vertical migration is highly variable. Therefore, the large range of temperatures experienced during a 24-h period may affect growth patterns on vertebrae.

Experimentally induced changes in behavior, resulting from the stress of tagging and injection procedure, could also disrupt a seasonal cycle of growth and alter ring formation. However, the results of various studies indicate that these effects may be minimal for other finfish species (Francis et al., 1992; Righton et al., 2006). To avoid this potential issue, we included only wild fish that were at large for 6 months or more, minimizing the effects of stress on behavior and growth. The observed annual growth rates were more variable for fish in the laboratory (−3.5–33.7 cm TL) than for those recaptured in the field (1.6–11.0 cm TL) (Fig. 5); however, our laboratory results were comparable to annual growth rates observed in a larger conventional tagging study (−2.2–31.8 cm TL; Sherwood et al.[14]). Therefore, it is unlikely that the stress of tagging fish or the rearing of fish in the laboratory influenced seasonal growth over the duration of our study. Therefore, the prominent growth increments, originally thought to represent annuli, may indicate periods of feeding, fast growth, rapid temperature changes, spawning periods, or stress, rather than annual cycles.

The failed validation of the vertebral aging method has important implications for stock assessment and management of goosefish fisheries. The pattern in this study of underestimating ages of the goosefish ≥50 cm TL and overestimating ages of small goosefish (≤41 cm) indicates

---

[14] Sherwood, G. D., J. H. Grabowski, and C. Brown. 2013. Tagging to assess monkfish movement: additional tagging to assess monkfish (*Lophius americanus*) movements and stock structure in the northeastern United States. 2009 Monkfish Research Set Aside Program. Final report, 30 p. Northeast Fish. Sci. Cent., Natl. Mar. Fish. Serv., NOAA, Woods Hole, MA. [Available from website.]

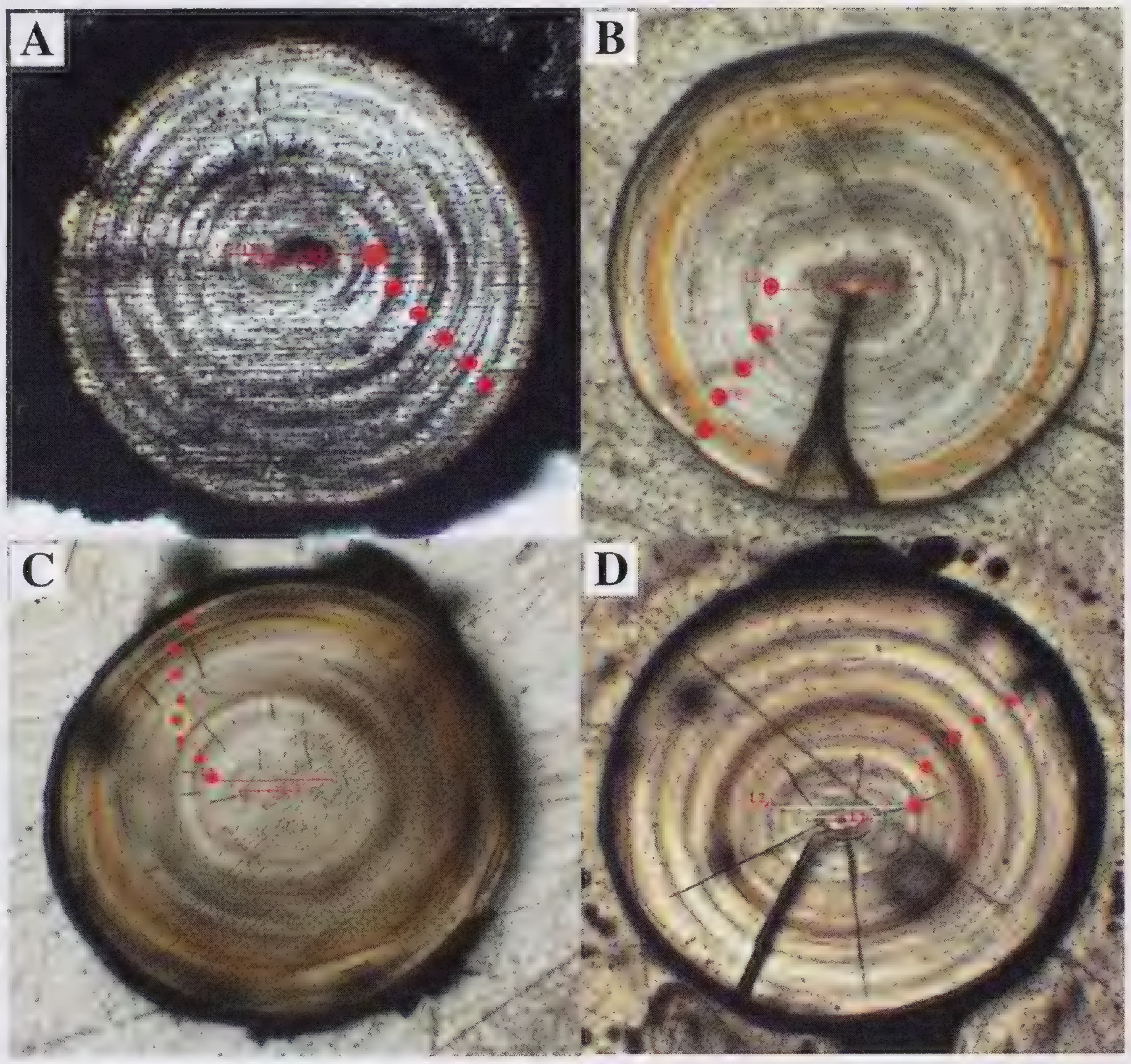

Figure 9

Images of illicia from specimens of goosefish (*Lophius americanus*) of various sizes and ages and with various times at large after tagging or times alive after injection in the laboratory. Specimens were captured in waters of southern New England and the Gulf of Maine and injected with a chemical marker during 2009–2015. The chemical mark is visible in the images as a brownish-yellow ring. Growth increments are indicated with red dots. (**A**) This specimen (fish ID 7) spent 185 d at large (April–October 2011) after an injection of 50 mg/kg of oxytetracycline and measured 63 cm in total length [TL] at death. The chemical mark is barely visible in the last wide light increment (WLI) near the edge of the illicium section. Both readers observed 6 narrow dark increments (NDIs). (**B**) This specimen (fish ID J) lived 398 d in the laboratory (June 2011–July 2012) after an injection of 25 mg/kg of fluorexon and measured 50 cm TL at death. The chemical mark is located in the penultimate WLI, and an NDI and a subsequent WDI are visible toward the edge. Both readers counted 5 NDIs. (**C**) This specimen (fish ID 5) spent 1.5 years at large (October 2012–April 2014) after an injection of 25 mg/kg of fluorexon and measured 77 cm TL at death. Both readers identified 7 NDIs, and one reader identified an additional NDI (yellow circle). Two NDIs were identified after the chemical mark toward the edge. (**D**) This specimen (fish ID F) lived for ~2 years in the laboratory (September 2010–October 2012) after an injection of 75 mg/kg of oxytetracycline and measured 58 cm TL at death. Both readers observed 5 clearly visible NDIs. Two NDIs (corresponding to 2 winters elapsed) are identified after the chemical mark toward the edge.

that the linear growth assumed in the stock assessment completed in 2010 (NEFSC, 2010; NEFSC[2]) is an artefact of aging error. In response to our results, the most recent peer review of that goosefish stock assessment concluded that the vertebral aging method is not valid and the statistical catch-at-length model should not be used as a basis for fishery management advice for this species (Richards[3]).

Chemical marking was not successful in otoliths; therefore, validation of growth increments was not possible. These results were surprising because otoliths are typically the preferred structure for age estimation in bony fish species. Otoliths are known to be metabolically inert and do not reflect physiological changes throughout the lifespan of fish (Phelps et al., 2007). Otoliths typically have limited resorption and continuous accretion of recognizable layers that result from biomineralization (calcium carbonate, mainly in the form of aragonite, is precipitated on a protein matrix of otolin; VanderKooy[15]). It is difficult to determine why the otolith did not pick up the chemical mark consistently in our study. Mohler (1997) did not have success marking bony structures in larval Atlantic salmon (*Salmo salar*) with oxytetracycline immersions, but he was successful with calcein immersions and intensity of the marks were greater for the more concentrated calcein immersions. Hernaman et al. (2000) suggested that stress may be a possible cause for the absence of a mark in otoliths from both tetracycline and calcein for a coral-dwelling goby, *Gobiodon histrio*. In our study, if the chemical was not absorbed because of stress, the mark would not be detected in all 3 of the structures we analyzed. We frequently detected marks in illicia and vertebrae but not in otoliths.

Results for accurately identifying winter growth increments after the chemical mark were better for illicium samples than for vertebral samples, but the sample size was smaller for illicia (n=9) than for vertebrae (n=20). The accuracy and agreement among readers provides a validation of this aging method and indicates the potential feasibility of using illicia for age estimation of goosefish going forward. However, the position of the first annulus has not been validated, and further studies will be required. The analysis of micro-increments in otoliths has been used satisfactorily to locate the first annulus in illicia and otoliths of both European congeners, the white anglerfish and black anglerfish (Hislop et al., 2001; Wright et al., 2002; La Mesa and De Rossi, 2008; Hernández et al., 2015), and in this study helped inform where to locate the first presumed annulus. The advances described here on the growth pattern (proving that dark increments are annuli) can help inform aging studies that use illicia for both *Lophius* species in Europe and the other 4 species of this genus for which no validation with chemical marking has been previously performed. Shifts from one aging structure (otolith or vertebra) to another, more appropriate one (mainly illicium) has taken place

---

[15] VanderKooy, S. J. (ed.). 2009. A practical handbook for determining the age of Gulf of Mexico fishes, 2nd ed. Gulf States Mar. Fish. Comm. Publ. No. 167, 157 p. [Available from website.]

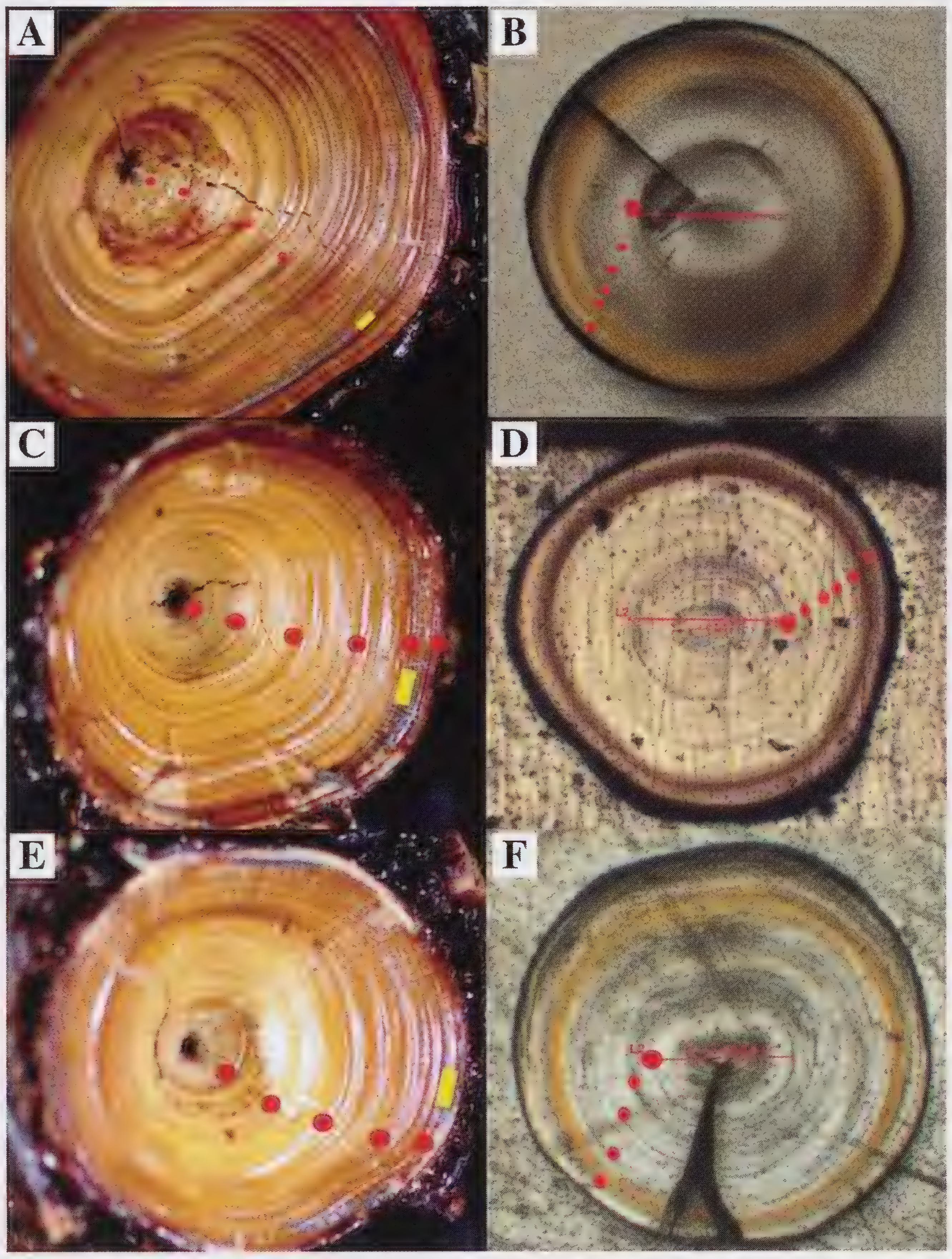

Figure 10

Images of the 8th vertebrae and illicia from 3 specimens of goosefish (*Lophius americanus*) that lived for more than 1 year and for which the expected numbers of annuli after the mark from a chemical injection were not counted on the vertebrae but were identified on the illicia. Specimens were captured in waters of southern New England and the Gulf of Maine and injected with a chemical marker during 2009–2015. Red dots indicate presumed annuli, a yellow rectangle indicates the position of the chemical mark, and red lines indicate measurements of the benthic ring and first annulus. The chemical mark is visible in each illicium as a dark or orange band. (**A**) Vertebra and (**B**) illicium of a specimen (fish ID 2) that was 67 cm in total length [TL] at death and spent 365 d at large after an injection of 25 mg/kg of fluorexon. (**C**) Vertebra and (**D**) illicium of a specimen (fish ID S) that was 57 cm TL at death and lived 467 d after an injection of 25 mg/kg of oxytetracycline. (**E**) Vertebra and (**F**) illicium of a specimen (fish ID J) that was 50 cm TL at death and lived 398 d after an injection of 25 mg/kg of fluorexon.

among studies of other *Lophius* congeners, as discussed in the “Introduction” section.

The difficulty of detecting presumed annuli in illicia from goosefish that has been reported by some authors (Hartley, 1995; Cullen et al.[10]) may be related to the specific techniques required for processing the illicium samples (e.g., recommended thickness of 0.5 mm and the precise location of the section). The wrong section thickness, for example, can make the annuli interpretation more difficult. Hartley (1995) used a section of the spine near the base of the structure and concluded that it was difficult to consistently obtain sections with prominent zones. However, that study took place before Duarte et al. (1997) described their aging protocols and techniques and advised that annual rings are best distinguished at 0.5 cm above the base of the illicium.

The maximum size obtained for goosefish (138 cm TL) (Richards et al., 2008) is intermediate with respect to those estimated for both congeners in Europe (~100 cm TL in black anglerfish and ~170–200 cm TL in white anglerfish) (Caruso, 1986; Landa et al., 2013). Annual growth rates estimated for recaptured fish in our study (about 4–8 cm TL) are comparable to those for fish of the European congers in the same size range (60–80 cm TL). Estimates are slightly lower than those of 6–8 cm TL/year and 4–10 cm TL/year for white anglerfish from tag-recapture experiments conducted in waters of the northeastern Atlantic Ocean (Landa et al., 2018, fig. 4; Ofstad et al., 2013, fig. 5B); however, black anglerfish in the Mediterranean Sea had growth rates of 4–7 cm TL/year based on length–frequency analysis for fish of similar sizes (García-Rodríguez et al., 2005; Landa and Barcala, 2017). Continuing the tag-recapture project from this study on a larger scale with either chemical or external marking, in combination with other age validation techniques that focus on juvenile fish, would help increase our understanding of the age and growth of goosefish.

In summary, the vertebral aging method for goosefish cannot be validated. Chemical marking was unsuccessful for otoliths; therefore, growth increments could not be validated. Preliminary results indicate that illicia produce a recognizable annual growth pattern, and both readers agreed on the location of most of the growth increments considered to be annual. The use of the illicium as the preferred structure for age estimation for this species should be explored further and aging protocols should be developed. Results from this study have been used to justify the rejection of the model that was employed in the last stock assessment and was based on vertebral age estimation and growth (Richards[3]). The initial growth rates estimated in this study, coupled with additional tag-recapture data, improve our understanding of the true growth of this species. With new growth estimates, and improved age estimation techniques, a validated growth pattern can be incorporated into stock assessments in the future to reduce scientific uncertainty and can lead to better management of this species.

Acknowledgments

We are indebted to the fishermen who generated funds for this research through the Monkfish Research Set-Aside Program of the National Marine Fisheries Service. We thank the captain and crew of the fishing vessels *Adventura*, *Argo*, *'Bout Time*, *C. W. Griswold*, *Finast Kind II*, *Gertrude H*, *Odyssey*, *Shamrock*, and *Shirley Ann* for allowing us to tag goosefish aboard their vessels and for supplying live specimens of goosefish for the laboratory. This research would not have been possible without their help and support. We also thank G. Sherwood, J. Grabowski, A. Richards, and L. Alade for their collaboration and support.

Literature cited

Armstrong, M. P., J. A. Musick, and J. A. Colvocoresses.
1992. Age, growth, and reproduction of the goosefish *Lophius americanus* (Pisces: Lophiiformes). Fish. Bull. 90:217–230.
1996. Food and ontogenetic shifts in feeding of the goosefish, *Lophius americanus*. J. Northw. Atl. Fish. Soc. 18:99–103.

Bank, C.
2016. Validation of age determination methods for monkfish (*Lophius americanus*). M.S. thesis, 105 p. Univ. Mass. Dartmouth, North Dartmouth, MA. [Available from website.]

Caruso, J. H.
1986. Lophiidae. *In* Fishes of the North-eastern Atlantic and the Mediterranean, vol. 3 (P.J.P. Whitehead, M.-L. Bauchot, J.-C. Hureau, J. Nielsen and E. Tortonese, eds.), p. 1362–1363. UNESCO, Paris.

Duarte, R., M. Azevedo, and P. Pereda.
1997. Study of the growth of southern black and white monkfish stocks. ICES J. Mar. Sci. 54:866–874.

Dupouy, H., R. Pajot, and B. Kergoat.
1986. Etude de la croissance des baudroies *Lophius piscatorius* et *L. budegassa*, de l'Atlantique nord-est obtenue à partir de l'illicium. Rev. Trav. Inst. Pech. Marit. 48:107–131.

Francis, R. I. C. C., L. J. Paul, and K. P. Mulligan.
1992. Ageing of adult snapper (*Pagrus auratus*) from otolith annual ring counts: validation by tagging and oxytetracycline injection. Aust. J. Mar. Freshw. Res. 43:1069–1089.

García-Rodríguez, M., P. Pereda, J. Landa, and A. Esteban.
2005. On the biology and growth of the anglerfish *Lophius budegassa* Spinola, 1807 in the Spanish Mediterranean: a preliminary approach. Fish. Res. 71:197–208.

Griffiths, M. H., and T. Hecht.
1986. A preliminary study of age and growth of the monkfish *Lophius upsicephalus* (Pisces: Lophiidae) on the Agulhas Bank, South Africa. S. Afr. J. Mar. Sci. 4:51–60.

Guillou, A.
1978. Biologie et niveau d'exploitation des stocks de langoustine, de merlu, des baudroies et de sole dans le proche Atlantique. Rev. Trav. Inst. Pech. Marit. 42:115–151.

Haring, P., and J.-J. Maguire.
2008. The monkfish fishery and its management in the northeastern USA. ICES J. Mar. Sci. 65:1370–1379.

Hartley, D.
1995. The population biology of the goosefish, *Lophius americanus*, in the Gulf of Maine. M.S. thesis, 142 p. Univ. Mass., Amherst, MA.

Hernaman, V., P. L. Munday, and M. L. Schläppy.
2000. Validation of otolith growth-increment periodicity in tropical gobies. Mar. Biol. 137:715–726.

Hernández, C., J. Landa, J. Barrado, A. Antolínez, and M. B. Santos.
2015. First estimates of age and growth of juvenile black anglerfish (*Lophius budegassa*), in the north-eastern Atlantic waters. Fish. Res. 161:269–272.

Hislop, J. R. G., A. Gallego, M. R. Heath, F. M. Kennedy, S. A. Reeves, and P. J. Wright.
2001. A synthesis of the early life history of the anglerfish, *Lophius piscatorius* (Linnaeus, 1758) in northern British waters. ICES J. Mar. Sci. 58:70–86.

Howe, A. B.
1989. State of Massachusetts inshore bottom trawl survey. *In* Proceedings of a workshop on bottom trawl surveys. Atlantic States Mar. Fish. Comm., Spec. Rep. 17; Woods Hole, MA, 1–3 November 1988 (T. R. Azarovitz, J. McGurrin, and R. Seagraves, eds.), p. 33–38. [Available from website.]

La Mesa, M., and F. De Rossi.
2008. Early life history of the black anglerfish *Lophius budegassa* Spinola, 1807 in the Mediterranean Sea using otolith microstructure. Fish. Res. 93:234–239.

Landa, J., and E. Barcala.
2017. Corroboration of fast growth rate of blackbellied angler (*Lophius budegassa*) in Spanish Mediterranean. Fish. Aquac. J. 8(4):237.

Landa, J., R. Duarte, and I. Quincoces.
2008. Growth of white anglerfish (*Lophius piscatorius*) tagged in the Northeast Atlantic, and a review of age studies on anglerfish. ICES J. Mar. Sci. 65:72–80.

Landa, J., J. Barrado, and F. Velasco.
2013. Age and growth of anglerfish (*Lophius piscatorius*) on the Porcupine Bank (west of Ireland) based on illicia age estimation. Fish. Res. 137:30–40.

Laurenson, C. H., A. Johnson, and I. G. Priede.
2005. Movements and growth of monkfish *Lophius piscatorius* tagged at the Shetland Islands, northeastern Atlantic. Fish. Res. 71:185–195.

Maartens, L., A. J. Booth, and T. Hecht.
1999. The growth of monkfish *Lophius vomerinus* in Namibian waters, with a comparison of otolith and illicia methods of aging. Fish. Res. 44:139–148.

McFarlane, G. A., and R. J. Beamish.
1987. Selection of dosages of Oxytetracycline for age validation studies. Can. J. Fish. Aquat. Sci. 44:905–909.

Mohler, J. W.
1997. Management briefs: immersion of larval Atlantic salmon in calcein solutions to induce a non-lethally detectable mark. North Am. J. Fish. Manage. 17: 751–756.

NEFSC (Northeast Fisheries Science Center).
2010. 50th Northeast regional stock assessment workshop (50th SAW) assessment report. Northeast Fish. Sci. Cent. Ref. Doc. 10-17, 844 p. [Available from website.]

Ofstad, L. H., C. Angus, T. Pedersen, and P. Steingrund.
2013. Age and growth of anglerfish (*Lophius piscatorius*) in Faroese waters. Fish. Res. 139:51–60.

Oliveira, K.
1996. Field validation of annular growth rings in the American eel, *Anguilla rostrate*, using tetracycline-marked otoliths. Fish. Bull. 94:186–189.

Phelps, Q. E., K. R. Edwards, and D. W. Willis.
2007. Precision of five structures for estimating age of common carp. North Am. J. Fish. Manage. 27:103–105.

Richards, R. A., P. C. Nitschke, and K. A. Sosebee.
2008. Population biology of monkfish *Lophius americanus*. ICES J. Mar. Sci. 65:1291–1305.

Righton, D., O. S. Kjesbu, and J. Metcalfe.
2006. A field and experimental evaluation of the effect of data storage tags on the growth of cod. J. Fish Biol. 68: 385–400.

Rountree, R. A., J. P. Gröger, and D. Martins.
2008. Large vertical movements by a goosefish, *Lophius americanus*, suggests the potential of data storage tags for behavioral studies of benthic fishes. Mar. Freshw. Behav. Physiol. 41:73–78.

Takeya, Y., T. Takatsu, T. Yamanaka, Y. Shibata, and M. Nakaya.
2017. Use of the illicium for age determination and verification of yellow goosefish *Lophius litulon* off Aomori Prefecture, northern Japan. Nippon Suisan Gakkaishi 83:9–17.

Tsimenidis, N. C., and J. C. Ondrias.
1980. Growth studies on the angler-fishes *Lophius piscatorius* L., 1758 and *Lophius budegassa* Spinola, 1807 in Greek waters. Thalassographika 3:63–94.

Walmsley, S. A., R. W. Leslie, and W. H. H. Sauer.
2005. The biology and distribution of the monkfish *Lophius vomerinus* off South Africa. Afr. J. Mar. Sci. 27:157–168.

Winton, M., C. Huntsberger, D. Rudders, G. DeCelles, K. Thompson, K. Goetting, and R. Smolowitz.
2017. Spatiotemporal patterns of flatfish bycatch in two scallop access areas on Georges Bank. J. Northw. Atl. Fish. Sci. 49:23–37.

Wright, P. J., D. A. Woodroffe, F. M. Gibb, and J. D. M. Gordon.
2002. Verification of first annulus formation in the illicia and otoliths of white anglerfish, *Lophius piscatorius* using otolith microstructure. ICES J. Mar. Sci. 59:587–593.

Yoneda, M., M. Tokimura, H. Fujita, N. Takeshita, K. Takeshita, M. Matsuyama, and S. Matsuura.
1997. Age and growth of anglerfish *Lophius litulon* in the East China Sea and the Yellow Sea. Fish. Sci. 63: 887–892.

National Marine
Fisheries Service
NOAA

Fishery Bulletin
established in 1881

Spencer F. Baird
First U.S. Commissioner
of Fisheries and founder
of *Fishery Bulletin*

Updated reproductive parameters for the shortfin mako (*Isurus oxyrinchus*) in the North Atlantic Ocean with inferences of distribution by sex and reproductive stage

Lisa J. Natanson (contact author)[1]
Megan Winton[2]
Heather Bowlby[3]
Warren Joyce[3]
Bethany Deacy[4]
Rui Coelho[5]
Daniela Rosa[5]

Email address for contact author: lisa.natanson@noaa.gov

[1] Northeast Fisheries Science Center
National Marine Fisheries Service, NOAA
28 Tarzwell Drive
Narragansett, Rhode Island 02882

[2] Atlantic White Shark Conservancy
235 Orleans Road
Chatham, Massachusetts 02650

[3] Bedford Institute of Oceanography
Fisheries and Oceans Canada
1 Challenger Drive
P.O. Box 1006
Dartmouth, Nova Scotia B2Y 4A2, Canada

[4] Riverside Technologies Inc.
for Southeast Fisheries Science Center
National Marine Fisheries Service, NOAA
3500 Delwood Beach Road
Panama City, Florida 32408

[5] Portuguese Institute for the Ocean and Atmosphere
Avienida 5 de Outubro s/n
8700-305 Olhão, Portugal

Abstract—Prompted by recent concern about the stock status of the shortfin mako (*Isurus oxyrinchus*) in the North Atlantic Ocean, we examined reproductive data from 731 individuals (351 females and 380 males) collected by 3 scientific organizations to improve estimates of size and age at maturity. Males ranged in size from 70 to 283 cm fork length (FL) and females from 71 to 338 cm FL. Females matured between 263 and 291 cm FL, with an estimated median length at maturity (L_{50}) of 280 cm FL and a median weight at maturity (WT_{50}) of 275 kg. Males matured between 173 and 187 cm FL, with an L_{50} of 182 cm FL and WT_{50} of 64 kg. Catch records from 4 international programs were also examined to investigate spatiotemporal variation in the distribution of life history stages based on updated size-at-maturity estimates and to identify potential parturition and nursery grounds. These records identified the Gulf of Mexico and the eastern North Atlantic Ocean off Portugal as birthing and nursery areas, with the most important nursery area occurring in the western North Atlantic Ocean.

The shortfin mako (*Isurus oxyrinchus*) is a large, highly migratory, coastal-pelagic shark species in the family Lamnidae that occurs in temperate and subtropical seas worldwide (Bigelow and Schroeder, 1948). In the North Atlantic Ocean, this species is considered to consist of one stock that migrates throughout the North Atlantic Basin (ICCAT[1]). Shortfin makos are commonly caught in both commercial and recreational fisheries throughout their range; although often not the target species, they are frequently retained for their meat, fins, and jaws (Casey and Kohler, 1992; Babcock and Nakano, 2008). Although the species has long been considered vulnerable to overexploitation because of its late age at maturity, low reproductive potential, and commercial value (Dulvy et al., 2008; Cortés et al., 2010), catch levels were considered sustainable (ICCAT[2]). However, the results of an electronic tagging study conducted in 2013–2015

Manuscript submitted 27 August 2019.
Manuscript accepted 8 January 2020.
Fish. Bull. 118:21–36 (2020).
Online publication date: 30 January 2020.
doi: 10.7755/FB.118.1.3

The views and opinions expressed or implied in this article are those of the author (or authors) and do not necessarily reflect the position of the National Marine Fisheries Service, NOAA.

---

[1] ICCAT (International Commission for the Conservation of Atlantic Tunas). 2017. Report of the 2017 ICCAT shortfin mako assessment meeting (Madrid, Spain 12–16 June 2017), 42 p. ICCAT, Madrid, Spain. [Available from website.]

[2] ICCAT (International Commission for the Conservation of Atlantic Tunas). 2013. 2012 shortfin mako stock assessment and ecological risk assessment meeting (Olhão, Portugal—June 11 to 18, 2012). Collect. Vol. Sci. Pap. ICCAT 69:1427–1570. [Available from website.]

indicate that fishing mortality rates in the North Atlantic Ocean may be 10 times higher than previously estimated, prompting an increase in concern about the status of the species (Byrne et al., 2017; ICCAT[1,3]) and its listing as endangered on the IUCN Red List of Threatened Species in 2019 (Rigby et al., 2019).

The recent change in the estimated status of the stock has been attributed to improvements in available data as well as in the assessment model used (ICCAT[1,4]). Shortfin mako assessments have traditionally been based on surplus production models, which pool recruitment, growth, and mortality into a single production function (Haddon, 2011). Such models have often been applied to assess the status of elasmobranchs lacking empirical estimates of vital rates and life history characteristics (Cortés, 2004), but they do not adequately depict the biology of the species. Because these models have not been adequate, the International Commission for the Conservation of Atlantic Tunas (ICCAT) has moved toward age-structured integrated approaches that incorporate estimates of important biological characteristics for the assessment of the North Atlantic Ocean stock of shortfin makos (ICCAT[1]). Although the new assessment approaches will likely provide a better representation of the stock's dynamics, they require empirical estimates of biological parameters, as well as uncertainty associated with those estimates (Patterson et al., 2001; ICCAT[4]).

Reproductive potential is a critical component to age-structured stock assessments and necessitates precise estimates of size and age at maturity, particularly for sexually dimorphic species (Quinn, 2003). However, maturity data are often lacking or unreliable for highly migratory pelagic sharks (Cortés, 1998, 2002); available estimates are often derived from sparse, opportunistic data sets (e.g., Francis and Duffy, 2005) or from samples originating in multiple ocean basins (Mollet et al., 2000). The most recent study on the reproductive biology of female shortfin makos was published in 2000 (Mollet et al., 2000), and there has never been a comprehensive study on male reproduction (although maturity estimates based on limited data are available; see Natanson et al., 2006, and Maia et al., 2007). The lack of data is largely due to difficulties in obtaining specimens representing all stages of maturity. In particular, mature females are rarely captured, either because they escape or break fishing gear (Pratt and Casey, 1983; Maia et al., 2007) or they are not in the commercial fishing grounds. Consequently, large mature females are seldom encountered by scientists, and estimates of maturity have often been based on a combination of reproductive data compiled from specimens collected in different areas.

Because life history variability arises through genetic isolation (Francis et al., 2007) as well as through differences in historical fishing pressure or environmental conditions (Tanaka et al., 1990; Bradley et al., 2017), combining data from multiple regions could be misleading and ultimately result in inappropriate management. Mollet et al. (2000) found significant differences in size at maturity between populations in the Northern and Southern Hemispheres, with females from the western North Atlantic Ocean being larger (2.98 m total length [TL], compared with 2.73 m TL for females in the southern population). Although these data and conclusions are limited because of sample availability at the time, the value for females from the western North Atlantic Ocean (298.6 cm TL, which corresponds to 275.6 cm fork length [FL]) is currently used in stock assessments (ICCAT[1]). From limited sampling, it is difficult to determine how representative each estimate is of the entire population. A better understanding of reproductive potential would further increase the reliability of projections used for management advice.

In addition to their application in stock assessments, improved estimates of life history parameters can enhance understanding of the demographic characteristics of populations. For example, combining size and maturity information with spatial data could improve understanding of the demographic structure and seasonal movement patterns of the various life stages of shortfin makos (Barreto et al., 2016). For the population in the North Atlantic Ocean, ICCAT has requested the development of spatial management measures that promote conservation, with an initial focus on identifying birthing areas to improve management advice (ICCAT[5]). For several species, the distribution of mature females has been used to infer breeding or parturition areas (Casey and Pratt, 1985; Coelho et al., 2018). The extent of overlap in the distributions of males and females may also provide insight into sex-specific selectivity or vulnerability to fisheries in specific locations or at specific times (Mucientes et al., 2009).

In this study, we updated the reproductive parameters of both male and female shortfin makos from the western North Atlantic Ocean, and we present here comprehensive estimates of median length at maturity (L_{50}) and median weight at maturity (WT_{50}) for males and females. We used the updated reproductive parameters to classify data collected in the broader North Atlantic Basin by life stage and examined potential variation in spatial and seasonal distributions by sex. We also examined locations and stages of mature females and neonates to identify possible parturition grounds and consider the distribution of young-of-the-year (YOY) shortfin makos to identify potential nursery areas.

---

[3] ICCAT (International Commission for the Conservation of Atlantic Tunas). 2017. Report of the Standing Committee on Research and Statistics (SCRS) (Madrid, Spain, 2 to 6 October 2017), 301 p. ICCAT, Madrid, Spain. [Available from website.]

[4] ICCAT (International Commission for the Conservation of Atlantic Tunas). 2019. Report of the 2019 ICCAT shortfin mako shark stock assessment meeting (Madrid, Spain 20–24 May 2019), 27 p. ICCAT, Madrid, Spain. [Available from website.]

[5] ICCAT (International Commission for the Conservation of Atlantic Tunas). 2017. Recommendation by ICCAT on the conservation of North Atlantic stock of shortfin mako caught in association with ICCAT fisheries. ICCAT Rec. 17-08, 3 p. [Available from website.]

Materials and methods

Specimens of shortfin makos were collected from research cruises, recreational fishing tournaments, commercial fishing trips, and strandings along the northeastern coast of North America between Newfoundland, Canada, and the west coast of Florida, including the Gulf of Mexico, between 1971 and 2018. A subset of the female maturity data that were analyzed in this study (n=61, 17%) was previously used to estimate median L_{50} by Mollet et al. (2000). Biologists from the Apex Predators Program and the Panama City Laboratory of the National Marine Fisheries Service (NMFS) and the Maritimes Region of Fisheries and Oceans Canada assessed maturity for 730 shortfin makos (n=675, n=20, and n=35, respectively; Suppl. Table 1 (online only)). Data collection was overseen by the senior author, and measurements were taken by experienced personnel by using a consistent sampling protocol. Full dissections (described later in the "Maturity indicators" section) were completed on the majority of specimens. However, because of time constraints at shark tournaments, it was not possible to perform a full workup of all specimens. In such instances, maturity for each sex was determined by visual examination only by using criteria based on detailed examinations as described later. Each shark was classified as mature or immature, and these data were used in calculating ogives for the analyses of median size at maturity (see the "Maturity indicators" and "Size at maturity" sections).

Morphometrics

Fork lengths were either measured directly (i.e., from the tip of the snout to the fork in the tail, over the body [OTB]) or calculated from OTB TL (i.e., from the tip of the snout to a point on the horizontal axis intersecting a perpendicular line extending downward from the tip of the upper caudal lobe to form a right angle) by using conversions from Kohler et al. (1995). In some cases, measurements were converted to straight-line FL (FL_S; these converted lengths are presented in parentheses) to facilitate comparison of lengths with those from other studies. Measurement of FL_S was taken from the tip of the nose to the fork in the tail by placing a tape measure under the shark so that the body curvature was not included in the measurement. Linear regression was used to derive a conversion from FL_S to FL_{OTB} by using data collected during this study (n=20). There was low variability around the fitted relationship (coefficient of determination [r^2]=0.996; Suppl. Fig. 1 (online only)):

$$FL_S = 0.1821 + 0.9792(FL_{OTB}) \tag{1}$$

The equation derived by Francis (2006) was used to convert between FL_S and straight-line TL (TL_S). Throughout the text, converted values are indicated by an asterisk (*). Whole weight (WT) was taken when possible and is presented in kilograms.

Maturity indicators

Maturity indicators were developed from the organ measurement data collected during detailed dissections. We used the standardized terminology for dissection measurements from Hamlett (1999) and Hamlett and Koob (1999) and followed the protocols for measuring and weighing of reproductive organs detailed by Natanson and Gervelis (2013). Although most specimens were measured fresh, samples collected by commercial fishermen were frozen at sea and thawed prior to sampling in the laboratory. Measurements from the frozen tracts were used only if they fell within the range of the fresh measurements to minimize potential biases from extreme values. Maturity status was assigned to each shark in the field on the basis of visual inspection of reproductive organs as described later in the "Results" section. For specimens that were not classified at the time of dissection, maturity stage was later determined through comparison of organ measurements with maturity criteria derived from staged individuals (see the "Results" section). Morphometric measurements of the reproductive organs of both sexes were plotted against FL to show how growth of the reproductive system changed as an individual approached maturity. Reproductive organs grow rapidly when approaching maturity; therefore, the location of the inflection in these relationships relates to L_{50}.

Initial internal examination for female maturity noted presence or absence of embryos, ovulation, and presence or absence of nutritive capsules following Jensen et al. (2002). Prior mating activity was assessed on the basis of the presence or absence of a membrane over the urogenital sinus, which was determined by passing a probe through the posterior end of the uterus into the cloaca. For males, initial maturity was obtained by examining the external claspers manually for functionality by using 3 criteria: rotation, rigidity, and the ability of the rhipidion to splay (Clark and von Schmidt, 1965). Clasper length was measured from the posterior tip to the insertion of the pelvic fin (Pratt, 1996; outer clasper length as defined by Compagno, 2001). Siphon sacs were measured as per Natanson and Gervelis (2013).

All internal measurements (in millimeters) were taken at the widest portion of the organ from the right side of the shark. These measurements included the anterior oviduct width, oviducal gland width, uterus width and length, ovary width and length, and the largest yolked follicle for females and the siphon sac length and testis diameter and length for males. When possible, the ovary or testis was weighed to the nearest gram. Trophonemata were measured to the nearest millimeter when present. For sharks that did not undergo full dissection, the internal organs were visually assessed for maturity on the basis of the criteria from Natanson and Gervelis (2013); in particular, this assessment included a characterization of the epigonal tissue around the ovaries, follicle size and color, and the general appearance of the uterus and oviducal gland for females and a characterization of clasper condition and epigonal tissue around the testis for males. Individuals that appeared to have given birth in the current year were defined as postpartum, although those that had given birth, with indications of recovery, were considered in a resting stage (Castro, 2009).

Size at maturity

Median size at maturity was estimated for both sexes by using maturity ogives fit to binomial maturity data from both dissections and visual assessments. Data from all years were combined on the basis of the results of a preliminary analysis that indicated no evidence of variation in parameters between 2 time periods (1971–1987 and 2003–2018) (senior author, unpubl. data). The probability that a given individual i was mature was modeled as the outcome of a Bernoulli random variable, where $y_i=0$ for immature and $y_i=1$ for mature individuals, respectively:

$$y_i \sim \text{Bernoulli}(p_i), \qquad (2)$$

where p_i = the probability shark i is mature.
We modeled p_i as a function of size (separately in terms of FL and weight) as follows:

$$\text{logit}(p_i) = \beta_0 + \beta_1 Size_i, \qquad (3)$$

where logit(p_i) = the logit link function.
The function constrains p_i to values between 0 and 1;

β_0 = an intercept term, and
β_1 = the effect of size in terms of either FL or weight.

Models were fit to each sex separately through maximum likelihood methods by using functions available in R (vers. 3.5.1; R Core Team, 2018). The inflection point of the relationship (where P=0.5) for either sex represents the median size at maturity (i.e., L_{50} or WT_{50}) and was calculated from the fitted model parameters as $-\beta_0/\beta_1$. By using the boot package (vers. 1.3-20) in R (Canty and Ripley, 2017), 95% confidence intervals around L_{50} and WT_{50} were bootstrapped from fits of a binomial generalized linear model to 1000 resamples of the maturity data (Harry et al., 2013). Given the well-established relationship between size and maturity and previously documented differences in size at maturity between male and female shortfin makos (Natanson et al., 2006), we did not conduct formal model selection in this study. For all models, normalized diagnostic plots of the residuals were examined visually to evaluate the appropriateness of model assumptions (Zuur et al., 2010).

Demographic structure

To investigate the spatial distribution of the population by life stage, shortfin mako catch records were obtained from 4 long-term, fishery-dependent sampling programs: 1) NMFS Cooperative Shark Tagging Program, 1962–2017; 2) NMFS Pelagic Observer Program, 1992–2017; 3) Canadian At-Sea Observer Program from the Maritimes region, 1979–2018; and 4) Portuguese Institute for the Ocean and Atmosphere onboard pelagic longliners from the Portuguese fleet, 2008–2016 (Suppl. Table 2) (online only). Data from 18,119 shortfin makos were used in distribution analyses, with the majority of samples (87%) collected from west of longitude 45°W. These data include date, size, sex, and location (Suppl. Table 2) (online only).

Females (n=9310) ranged in size from 23.0 to 325.0 cm FL_{OTB}. Only 22 of those females were classified as mature on the basis of an FL_{OTB} >291.0 cm (the length of the largest immature female observed; Tables 1 and 2). Males (n=8809) ranged in size from 25.0 to 310.0 cm, and 1174 of those males were considered mature on the basis of an FL_{OTB} >187.1 cm (the length of the largest immature male observed; Tables 1 and 3). The 5 largest males in the data set were larger than the verified size limit for male shortfin makos. Attempts to confirm the accuracy of the sizes through the original archived data were inconclusive; therefore, caution should be exercised in taking these values as a new size range for male shortfin makos. Regardless, they would be classified as mature males and, for that reason, were included in our analyses. The majority of the catch data provide lengths in FL_S; therefore, for these analyses, measurements provided as FL_{OTB} or TL_S were converted to FL_S, as described previously. In instances where TL_{OTB} or WT had been previously converted to FL_{OTB}, we assessed maturity on the basis of FL_{OTB} rather than apply a second conversion; this approach was deemed reasonable given our conservative rationale for maturity classification (see the next paragraph). All estimated FL_S were considered FL_S (Suppl. Table 2) (online only).

Shortfin mako catch records were assigned to sex-specific maturity stages, representing neonate, YOY, immature, or mature individuals as follows: shortfin makos ≤68 cm FL_{OTB} were considered neonates on the basis of the average size at birth (63.2 cm FL_{OTB}*) and the size of the largest full-term embryo observed (estimated at 68 cm FL_{OTB}*; Mollet et al., 2000). Sharks >68 cm FL_{OTB} and <100 cm FL_{OTB} were classified as YOY (Natanson et al., 2006). For the older age classes, L_{50} estimates for males and females could be used to separate immature from mature sharks; however, misclassifications would result for both categories and distribution patterns potentially could be obscured because of individuals that fall into the transitional size range. To minimize the extent of overlap between the immature and mature sizes, sharks smaller than the smallest observed mature shark were considered immature. All sharks greater than the largest observed immature specimen by sex were considered to be mature. This method eliminated the portion of the length distribution during which maturity stage is the most uncertain and, therefore, the majority of the potential for differences in maturity stage to obscure distribution patterns.

To visualize potential variation in the spatial distribution of the life stages of shortfin makos, catch locations were binned by sex, maturity stage, and season and aggregated over a 1°-by-1° grid by using functions available in the R package tidyverse (vers. 1.2.1; Wickham, 2017). The seasons were winter (January–March), spring

Table 1

Number of shortfin makos (*Isurus oxyrinchus*), by sex, captured per month in the western North Atlantic Ocean between 1971 and 2018 for maturity analyses and between 1962 and 2018 for investigation of demographic structure. Values for maturity analyses include both dissected and visually assigned specimens. I=immature; T=transitional (length range, where individuals are approaching maturity, bracketed by the smallest mature and largest immature female (263.0 and 291.0 cm FL, respectively); and M=mature.

	Maturity analyses		Demographic structure							
			Male				Female			
Month of Capture	Male	Female	Total	I	T	M	Total	I	T	M
January	7	2	474	322	67	85	383	376	5	2
February	0	2	394	243	69	82	317	311	4	2
March	7	0	250	150	25	75	164	161	1	2
April	7	3	507	301	107	99	273	271	1	1
May	13	5	485	311	72	102	381	377	1	3
June	166	126	893	744	75	74	1258	1255	3	0
July	70	115	1650	1445	104	101	2254	2250	2	2
August	85	88	1404	1169	102	133	1758	1753	3	2
September	15	6	814	638	77	99	909	897	6	6
October	8	2	814	607	95	112	710	709	1	0
November	1	2	742	527	91	124	552	551	0	1
December	0	0	382	252	42	88	351	346	4	1

(April–June), summer (July–September), and fall (October–December) (Campana et al.[6]). The distribution of neonate and YOY catch records were examined for patterns related to pupping and nursery grounds.

Results

We examined 731 (351 female and 380 male) shortfin makos for maturity and completed full dissections of 197 females and 241 males. Females and males ranged in size from 70.6 to 338.5 cm FL_{OTB} and from 70.0 to 283.0 cm FL_{OTB}, respectively (Fig. 1). Several male shortfin makos in this sample are larger than previously measured males (260 cm FL_{OTB}; Natanson et al., 2006); however, these measurements are verified and can be considered to represent an accurate size increase. The majority of specimens were collected from recreational fishermen at shark fishing tournaments in the United States (88% sexes combined, 91% of females, and 86% of males; Suppl. Table 1 (online only)) and between June and August (94% of females and 85% of males; Table 1). No specimens of either sex were obtained in December; males and females were caught in all other months with the exception of February and March, respectively (Table 1).

Maturity indicators

Females The relationships of the measurements of oviduct width, oviducal gland width, uterus diameter, ovary length, ovary width, ovary weight, and follicle diameter to FL indicate a sharp increase in size of ~250–270 cm FL_{OTB}, as exemplified by the relationship between the oviducal gland width and FL (Fig. 2, Suppl. Fig. 2 (online only)). Only the relationship between FL and uterus length is essentially linear, indicating that growth of the uterus is relatively constant over ontogeny, rather than being indicative of size at maturity.

Immature females On the basis of organ measurements and the visual assessment used to assign status at dissection (full dissection: n=170; total: n=325), immature females ranged in length from 70.6 to 291.0 cm FL_{OTB}. Immature females have undeveloped ovaries with small follicles with little or no yolk; most follicles appear white to clear (Table 2). Maximum follicle size is generally ≤1 mm at this stage. Immature ovaries are embedded in epigonal tissue that progressively thins out in the larger immature females, ultimately becoming a thin, transparent sheath around the main ovary as the female matures. The immature uterus appears narrow and constricted with the oviducal gland appearing as a slight widening of the oviduct. Female shortfin makos >250 cm FL_{OTB} are starting to mature, and this transition to maturity is first observed in the development of the ovary. By the time a female is 250 cm FL_{OTB}, the ovary is clearly increasing

---

[6] Campana, S. E., J. Gibson, J. Brazner, L. Marks, and W. Joyce. 2008. Status of basking sharks in Atlantic Canada. Can. Sci. Advis. Secr. Res. Doc. 2008/004, 56 p. [Available from website.]

Table 2

Size ranges of measurements and descriptions of organs used to determine maturity stages of female shortfin makos (*Isurus oxyrinchus*) captured in the western North Atlantic Ocean between 1971 and 2018. Sharks in the size ranges associated with the immature and mature stages generally conform to those assignments (unless otherwise noted), whereas sharks in the transitional range can be either immature or mature. Follicles classified as uncertain could indicate a specimen is transitional or mature. Table format adapted from Walker (2005). *n*=number of specimens.

Organ	Index	Size range of measurements	Description	Maturity classification
Upper oviduct				
n=175	UO-1	≤7 mm	Thin tubular structure	Immature
	UO-2	>7 to ≥15 mm		Transitional
	UO-3	>15 mm	Thickened tubular structure	Mature
Oviducal gland				
n=168	OG-1	≤11 mm	Undifferentiated from oviduct	Immature
	OG-2	>11 to ≤35 mm	Increased width distinguishable from oviduct	Probably immature
	OG-3	>35 mm	Enlarged and bulbous	Probably mature
	OG-4	>49 mm	Enlarged and bulbous	Mature
Ovarian follicles				
n=111	OF-1	≤1 mm	Small and white	Immature
	OF-2	>1 mm	Larger with yolk	Uncertain
Ovary length				
n=166	OL-1	≤160 mm	Clear follicles barely distinguishable from epigonal	Immature
	OL-2	>160 to ≤210 mm	White or opaque follicles distinguishable; thinning epigonal	Transitional
	OL-3	>210 mm	Thin epigonal surrounding cream- to yellow-colored yolked follicles[†]	Mature
Ovary width				
n=171	OW-1	≤50 mm	Thin; follicles barely distinguishable from epigonal	Immature
	OW-2	>50 to ≤110 mm	Widening area of distinguishable follicles	Transitional
	OW-3	>110 mm	Wide area of follicles surrounded by thin epigonal	Mature
Uterus length				
n=112	UL-1	≤280 mm	Thin tubular structure indistinguishable from upper oviduct	Immature
	UL-2	>280 to ≤470 mm[‡]	Elongated tube, distinguishable from lower oviduct	Transitional
	UL-3	>470 mm	Large, often flaccid tubular structure	Mature
Uterus width				
n=181	UW-1	≤38 mm[§]	Thin tubular structure	Immature
	UW-2	>38 to ≤70 mm	Widening tube distinguishable from upper oviduct	Transitional
	UW-3	>70 mm	Large, distended tubular structure	Mature

[†] Mature and transitional ovaries can appear similar.

[‡] One specimen had a size larger than this range as a juvenile.

[§] One specimen had a size smaller than this range as an adult.

Table 3

Size ranges of measurements and descriptions of organs used to determine maturity stages of male shortfin makos (*Isurus oxyrinchus*) captured in the western North Atlantic Ocean between 1971 and 2018. Sharks in the size ranges associated with the immature and mature stages generally conform to those assignments, whereas sharks in the transitional range can be either immature or mature. Table format adapted from Walker (2005). *n*=number of specimens.

Organ	Index	Size range of measurements	Description	Maturity classification
Left clasper length				
n=237	LCL-1	≤185 mm	Soft, do not freely rotate, do not extend beyond pelvic fins, tip does not flex	Immature
	LCL-2	>85 to ≤221 mm	Soft to plastic, starting to rotate and extend beyond pelvic fins, tip does not flex	Transitional
	LCL-3	>221 mm	Rigid, freely rotate and flex at tip, extend beyond pelvic fins	Mature
Testis diameter				
n=209	TD-1	≤20 mm	Small testis encased in epigonal	Immature
	TD-2	>20 to ≤42 mm	Larger testis, epigonal decreasing in proportion	Transitional
	TD–3	>42 mm	Large testis with minimal epigonal	Mature
Testis length				
n=209	TL-1	≤70 mm	Thin testis encased in epigonal	Immature
	TL-2	>70 to ≤120 mm	Elongated testis, distinguishable from epigonal	Transitional
	TL-3	>120 mm	Long, distended testis from epigonal	Mature
Testis weight				
n=80	TW-1	≤45 g		Immature
	TW-2	≥45 to 90≤ g		Transitional
	TW-3	>90 g		Mature

in size, particularly in length (Fig. 3). An increase in size of all other organs can be seen in female shortfin makos >250 cm $\mathrm{FL}_{\mathrm{OTB}}$ (Suppl. Fig. 2) (online only).

The transitional length range, where individuals are approaching maturity, is bracketed by the smallest mature and largest immature female (263.0 and 291.0 cm $\mathrm{FL}_{\mathrm{OTB}}$, respectively). In this range, organ measurements in an individual may or may not be in the mature size range. The majority of immature sharks (92%) examined had a membrane separating the urogenital sinus from the cloaca. Of the 8% that did not, the majority (70%) were approaching the transitional length range. In general, the transitional ovary is larger and contains larger follicles than the smaller immature ovaries; however, in most cases, the follicles are not as large as in the mature stages. In smaller transitional individuals, reproductive organs are in various stages of development. However, by the time a female is 260 cm $\mathrm{FL}_{\mathrm{OTB}}$, organs are beginning to mature, as indicated by the marked increase in most morphometric measurements during the transitional length range (Fig. 2, Suppl. Fig. 3 (online only)). In and of itself, this increase in growth does not demonstrate maturity because most individuals are still immature until ~275 cm $\mathrm{FL}_{\mathrm{OTB}}$.

Mature females Adult females ranged from 263.0 to 338.5 cm $\mathrm{FL}_{\mathrm{OTB}}$ (*n*=26). Of those sampled, 3 were pregnant, 4 were postpartum, and 18 were staged as resting. The maturity stage of 1 specimen (either newly mature or resting) could not be determined with available information. The 3 pregnant females were 270.4, 285.0, and 301.0 cm $\mathrm{FL}_{\mathrm{OTB}}$ and were caught in January, February, and November, respectively, in the Gulf of Mexico. The largest trophonemata measured in this study (5 and 10 mm) were taken from 2 of the pregnant females. The postpartum females ranged in length from 289.0 to 325.0 cm $\mathrm{FL}_{\mathrm{OTB}}$. A recently postpartum female was caught in February in the Gulf of Mexico, and 3 specimens that had given birth within the season but had begun to recover were caught off Long Island in the summer (June: *n*=2; August: *n*=1).

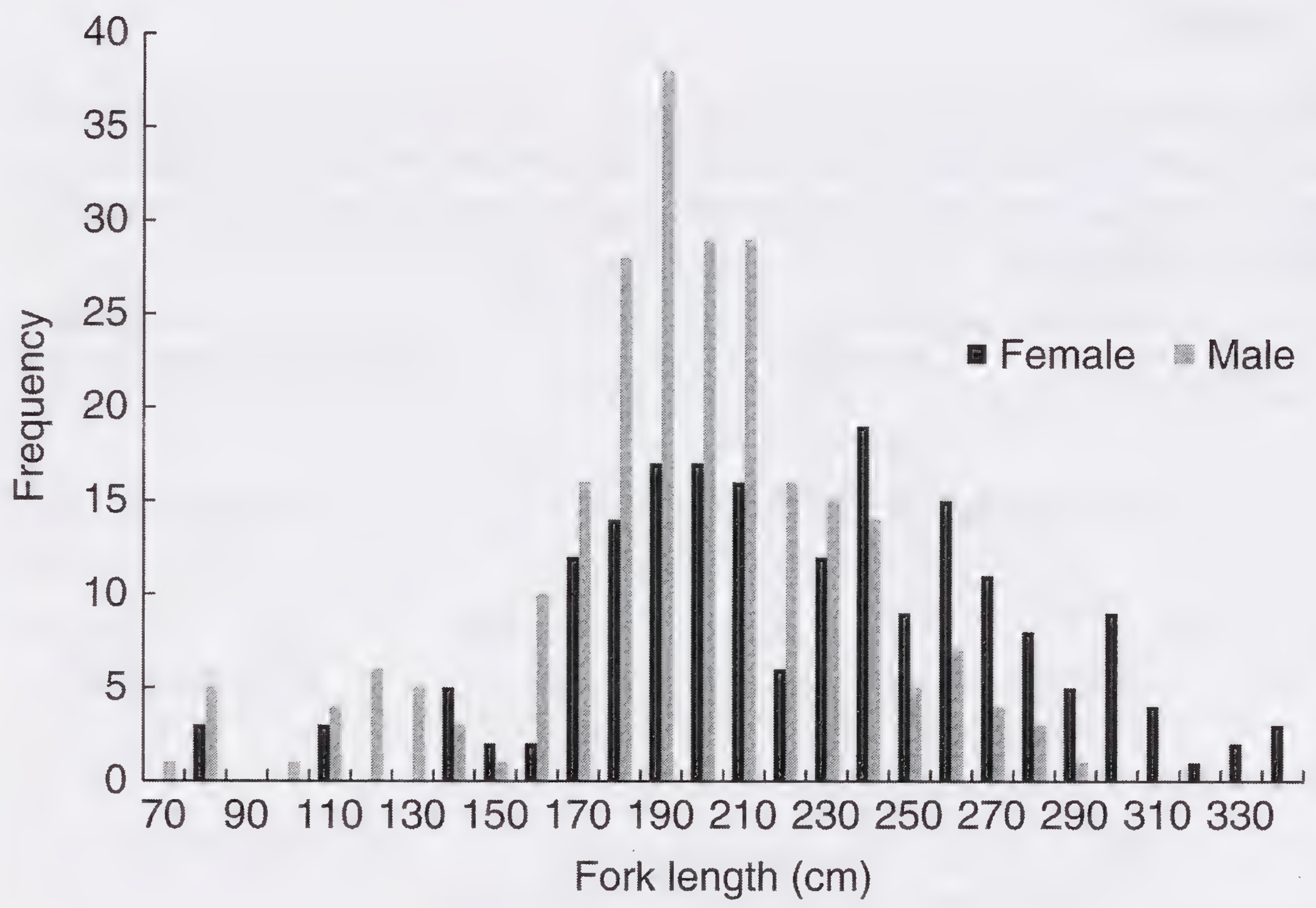

Figure 1

Size-frequency distributions for male (n=243) and female (n=197) shortfin makos (*Isurus oxyrinchus*) caught between the Gulf of Mexico and Newfoundland, Canada, during 1971–2018 and dissected for this study. n=number of specimens.

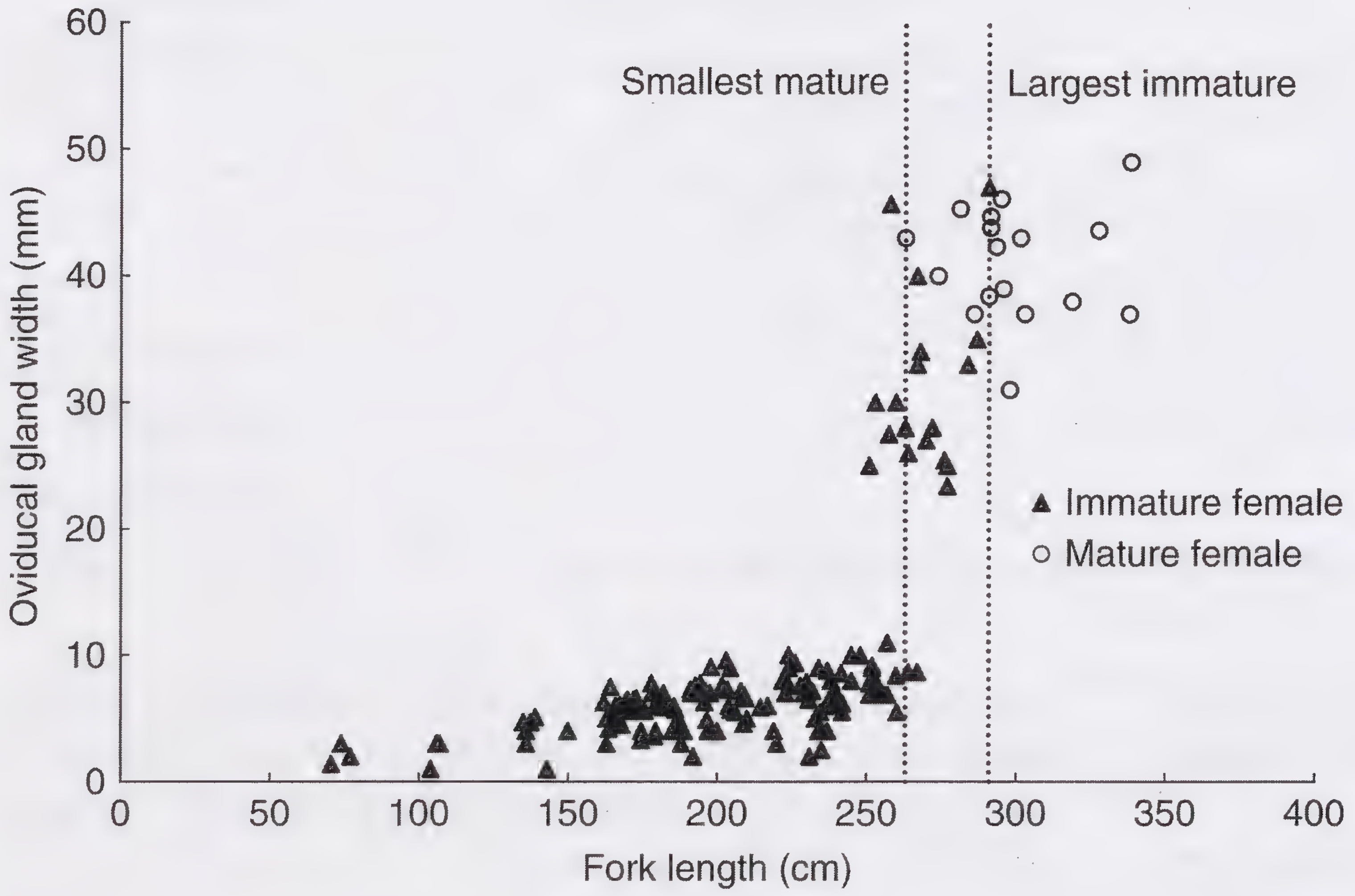

Figure 2

Relationship of oviducal gland width (in millimeters) to fork length (in centimeters) of female shortfin makos (*Isurus oxyrinchus*) caught between the Gulf of Mexico and Newfoundland, Canada, during 1971–2018. Black triangles and open circles indicate specimens in the immature and mature stages, respectively. The vertical dotted lines represent the lengths of the smallest mature and largest immature specimens.

The large range of follicle sizes observed in the resting stage (1.5–5.9 mm) is most likely indicative of the amount of time the individuals had been recovering from their most recent parturition. Although females with follicles of 3.6 mm are usually mature (Table 2), it is difficult to classify these stages on the basis of appearance of the ovary alone, because of the similarity of some resting ovaries to some immature ovaries. Stage must be determined in combination with other organ characteristics, particularly follicle and uterus size and condition (Natanson and Gervelis, 2013). Resting stage females have expanded but recovered uteri indicating that they have previously given birth; some have small trophonemata (0.0–1.5 mm), and the condition of their ovaries indicates they had not given birth in the current season.

Males On the basis of organ measurements and the visual assessment used to assign status at dissection (full dissection: n=241; total: n=379), immature males ranged in length from 70.0 to 187.1 cm FL_{OTB} (Suppl. Table 1) (online only). Measurements of clasper length (Fig. 4) verified visual accounts of the morphology during dissection, and a strong change in clasper growth rate at maturity was observed. Testis diameter, length, and weight as well as siphon sac size had approximately linear relationships with shark length, particularly after ~150 cm FL_{OTB} (Fig. 5, Suppl. Fig. 3 (online only)).

Clasper length, testis diameter, length, and weight, and siphon sac length show a rapid increase in growth at ~150 cm FL_{OTB} (Figs. 4 and 5, Suppl. Fig. 3 (online only)), which levels off at ~175 cm FL for clasper length (Fig. 4). Siphon sacs are undeveloped and short in immature males, usually not extending far past the pelvic fins. There is a marked increase in growth once an animal reaches ~150 cm FL_{OTB} (Suppl. Fig. 3) (online only), and the siphon sacs expand anteriorly along the abdomen but do not reach the level of the pectoral fins by the time they fully develop. The degree of rigidity of the claspers is the best overall indicator of maturity. Mature males have rigid claspers, with the ability of the clasper to rotate freely and of the rhipidion to splay, whereas immature males do not have these qualities (Table 3). There were very few exceptions (n=7) in which males did not have fully rigid claspers but had all other organs in the mature range, indicating that these males were approaching maturity. These specimens ranged in FL_{OTB} from 175.0 to 221.0 cm, with the larger 3 males (200.0–221.0 cm FL_{OTB}) having claspers that were partially rigid with sperm present and the smaller 4 specimens (175.0–187.4 cm FL_{OTB}) having claspers that were soft and flexible. The latter fish were at the transitional size for male maturity (172.8–187.1 cm FL_{OTB}). Immature males with rigid claspers (n=4) ranged

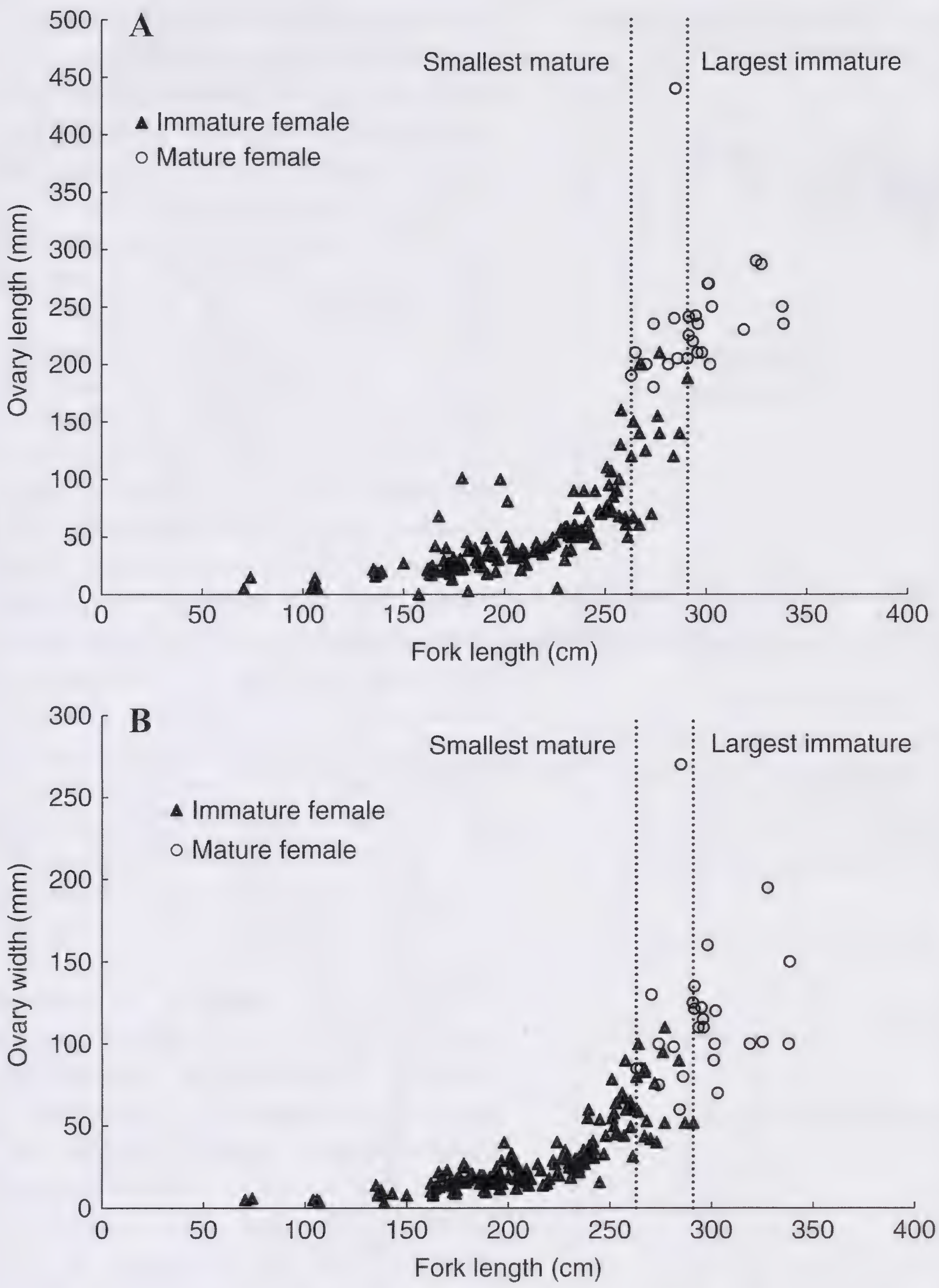

Figure 3

Relationship (**A**) of ovary length (in millimeters) to fork length (in centimeters) and (**B**) of ovary width (in millimeters) to fork length (in centimeters) of female shortfin makos (*Isurus oxyrinchus*) caught from the Gulf of Mexico to Newfoundland, Canada, during 1971–2018. Black triangles and open circles indicate specimens in the immature and mature stages, respectively. The vertical dotted lines represent the lengths of the smallest mature and largest immature specimens.

in size from 176.0 to 187.0 cm FL_{OTB}, lengths that are also in the transitional range for maturity. Although individual variation exists in body length and in the order that organ development takes place, clasper calcification appears to be the last phase of maturation.

Median length and weight at maturity

The estimated L_{50} for females was 279.8 cm FL_{OTB} (95% confidence interval [CI]: 273.8–286.6), and the estimated WT_{50} for females was 274.8 kg (95% CI: 255.4–274.0; Fig. 6). For males, the estimated L_{50} was 181.6 cm FL_{OTB} (95% CI: 179.9–188.4) and the WT_{50} was 63.8 kg (95% CI: 62.0–74.0; Fig. 6). Converting both L_{50} estimates into FL_S for comparison with the catch data resulted in 274.2 cm FL_S for females and 178.0 cm FL_S for males.

Demographic structure

On the basis of the estimated median size at maturity, 88% of the specimens were classified as immature; of these, immature females outnumbered immature males and mature males outnumbered mature females in all seasons (Table 1). Mature as well as immature animals of both sexes were caught in similar areas in all months, with the exception of mature females, which were not caught in June and October (Figs. 7 and 8, Suppl. Figs. 4 and 5 (online only)). These movements could be related to shifts in the fishing fleets, but some generalizations can be made by season and sex. Although there were few captures of mature females, catches occurred in the Gulf of Mexico in fall and winter, shifting slightly onto the continental shelf in spring and summer. Young-of-the-year and neonate sharks were found primarily on the western side of the North Atlantic Ocean from the Gulf of Mexico up to the Flemish Cap with a small concentration in the northern Gulf of Mexico (Figs. 7 and 8).

Discussion

The reproductive parameters estimated in this study provide improved sex-specific inputs for stock assessment of shortfin makos in the North Atlantic Ocean. Our sampling was done throughout a vast geographical range and resulted in a data set that was an order of magnitude larger than those of previous studies on male or female reproduction. Although our sampling was concentrated in the west, it is representative of the entire region, given the strong evidence for one population in the North Atlantic Ocean. Conventional tag and recapture data from 1148 shortfin makos indicate 1) mixing of individuals tagged in Europe and in the United States in an area west of the Azores of Portugal; 2) movement from the western to the eastern Atlantic Ocean; and 3) movement into and out of the Gulf of Mexico and the Caribbean Sea (Kohler and Turner, 2019). Our estimate of female L_{50} (279.8 cm FL_{OTB}, 274.2 cm FL_S*) is slightly larger than the previous estimate by Mollet et al. (2000)

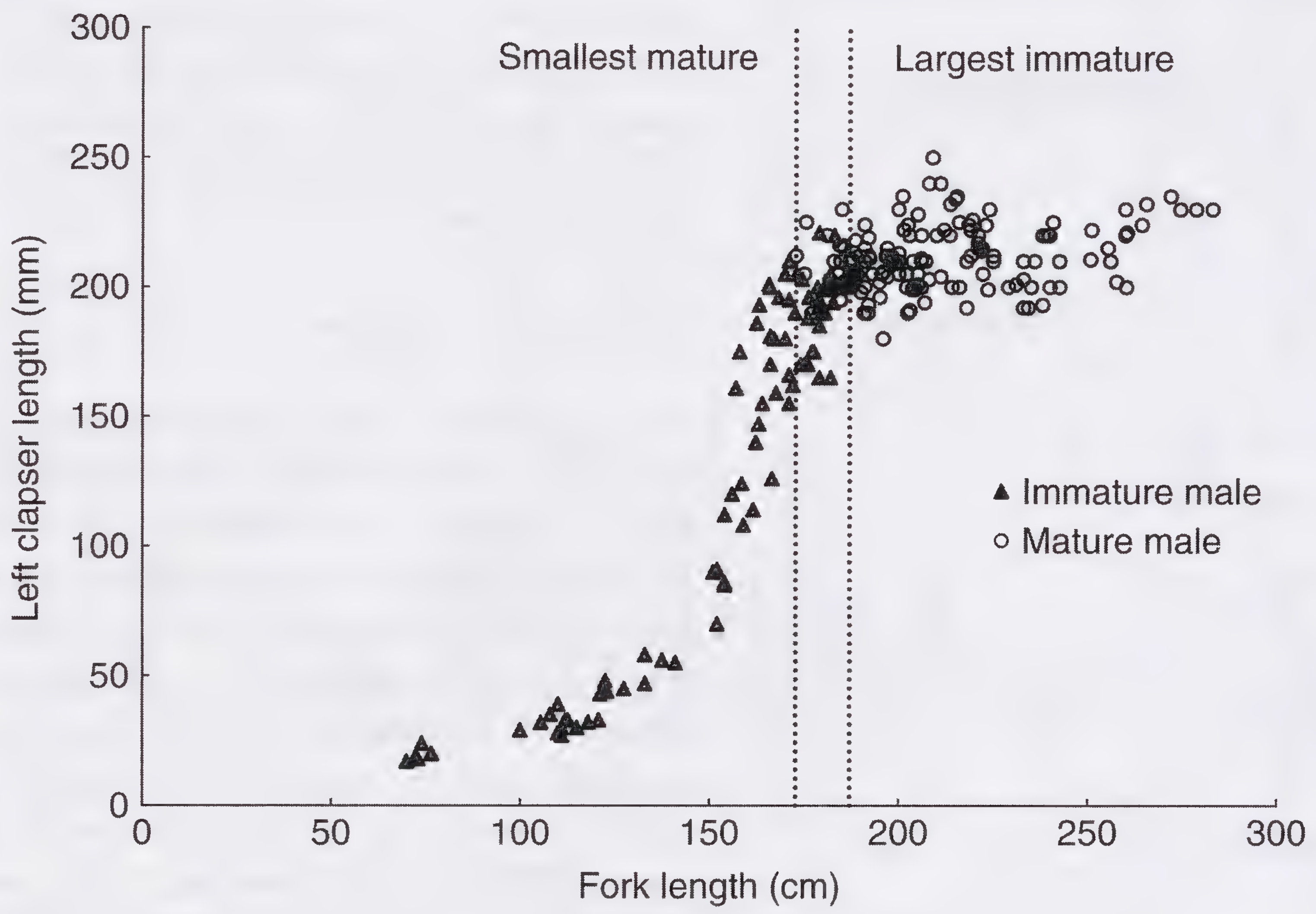

Figure 4

Relationship of left outer clasper length (in millimeters) to fork length (in centimeters) of male shortfin makos (*Isurus oxyrinchus*) caught between the Gulf of Mexico and Newfoundland, Canada, during 1971–2018. Black triangles and open circles indicate specimens in the immature and mature stages, respectively. The vertical dotted lines represent the lengths of the smallest mature and largest immature specimens.

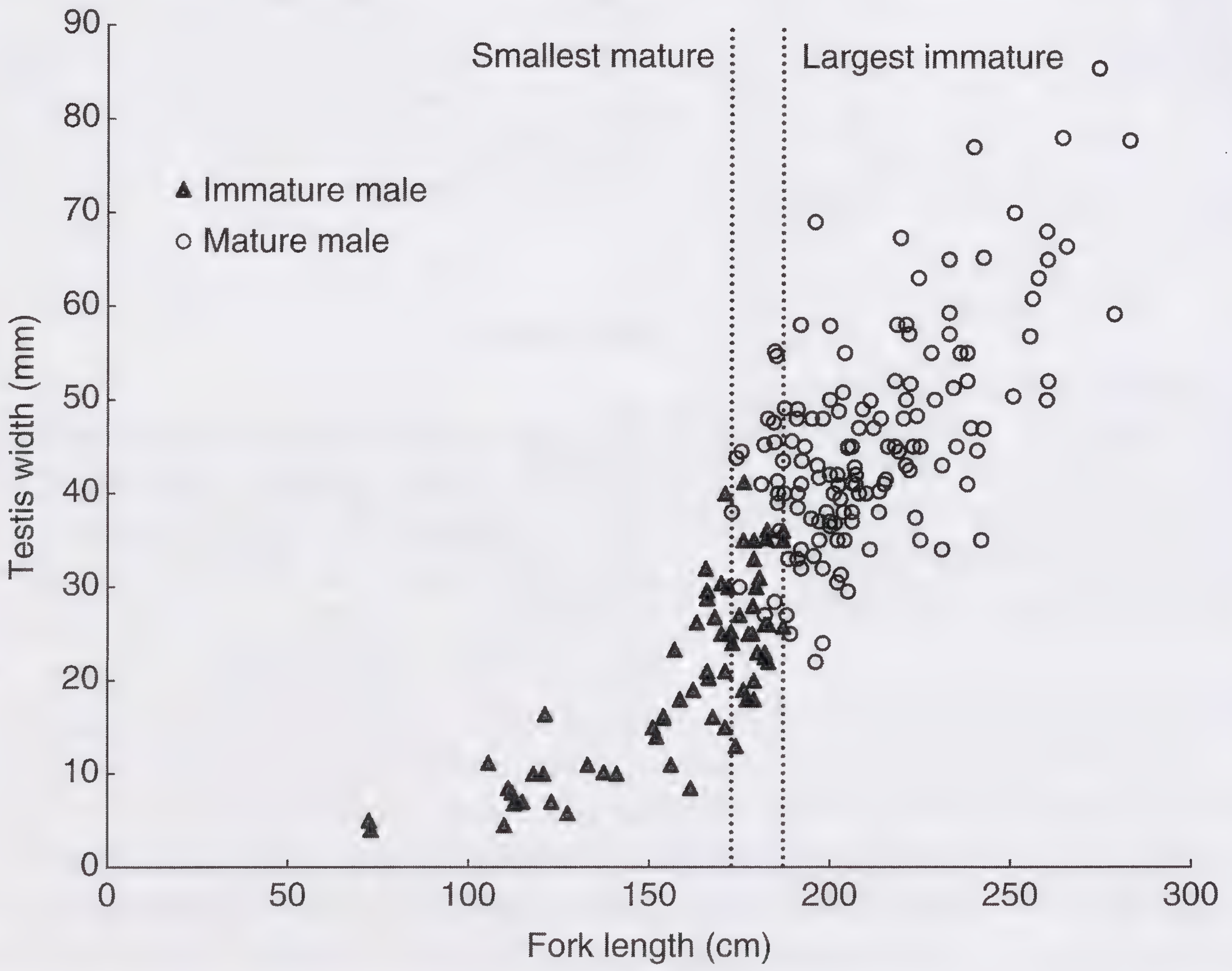

Figure 5

Relationship of right testis width (in millimeters) to fork length (in centimeters) of male shortfin makos (*Isurus oxyrinchus*) caught between the Gulf of Mexico and Newfoundland, Canada, during 1971–2018. Black triangles and open circles indicate specimens in the immature and mature stages, respectively. The vertical dotted lines represent the lengths of the smallest mature and largest immature specimens.

(275 cm FL_{OTB}*), although their value is within the 95% CI of this study. Our estimate for male L_{50} (181.6 cm FL_{OTB}, 178.0 cm FL_S*) is similar to the previous estimate from a study in waters of Portugal in the eastern North Atlantic Ocean (180 cm FL_{OTB}; Maia et al., 2007).

On the basis of existing age–length relationships, age at L_{50} were estimated for males at 7.5 years (Natanson et al., 2006; Rosa et al.[7]); the estimate for females was slightly over 19 years, when following Natanson et al. (2006), and 22 years, when following Rosa et al.[7] The dissection data provide a comprehensive view of the maturity of this species for the western North Atlantic Ocean, and the evidence for one stock supports the use of these data for characterizing maturity of the entire population in the North Atlantic Ocean. The fact that maturity estimates have not changed markedly over time increases our confidence in their accuracy, making our updated values the best available to describe maturity and to inform age- and sex-structured models used for stock assessment (ICCAT[4]).

The growth patterns of individual reproductive organs indicate increased energetic investment in reproduction in advance of maturity in both male and female shortfin makos, although not all organs are as useful for distinguishing between immature and mature individuals. With the exception of uterus length, which grew gradually relative to length, measurements of internal reproductive organs of females increased sharply as sharks matured. Similar to Mollet et al. (2000), we found that uterus width and oviducal gland growth were suitable for distinguishing between immature and mature females and reproductive stage. Although the maximum follicle diameter also increases with FL (Mollet et al., 2000), there is overlap in follicle size between all maturity stages because of the nature of the lamnid ovary and mode of embryonic nutrition, indicating that follicle diameter alone is not useful for determining stage of maturity.

---

[7] Rosa, D., F. Mas, A. Mathers, L. J. Natanson, A. Domingo, J. Carlson, and R. Coelho. 2017. Age and growth of shortfin mako in the north Atlantic, with revised parameters for consideration to use in the stock assessment. Int. Comm. Conserv. Atlantic Tunas, ICCAT SCRS/2017/111, 22p. [Working paper.]

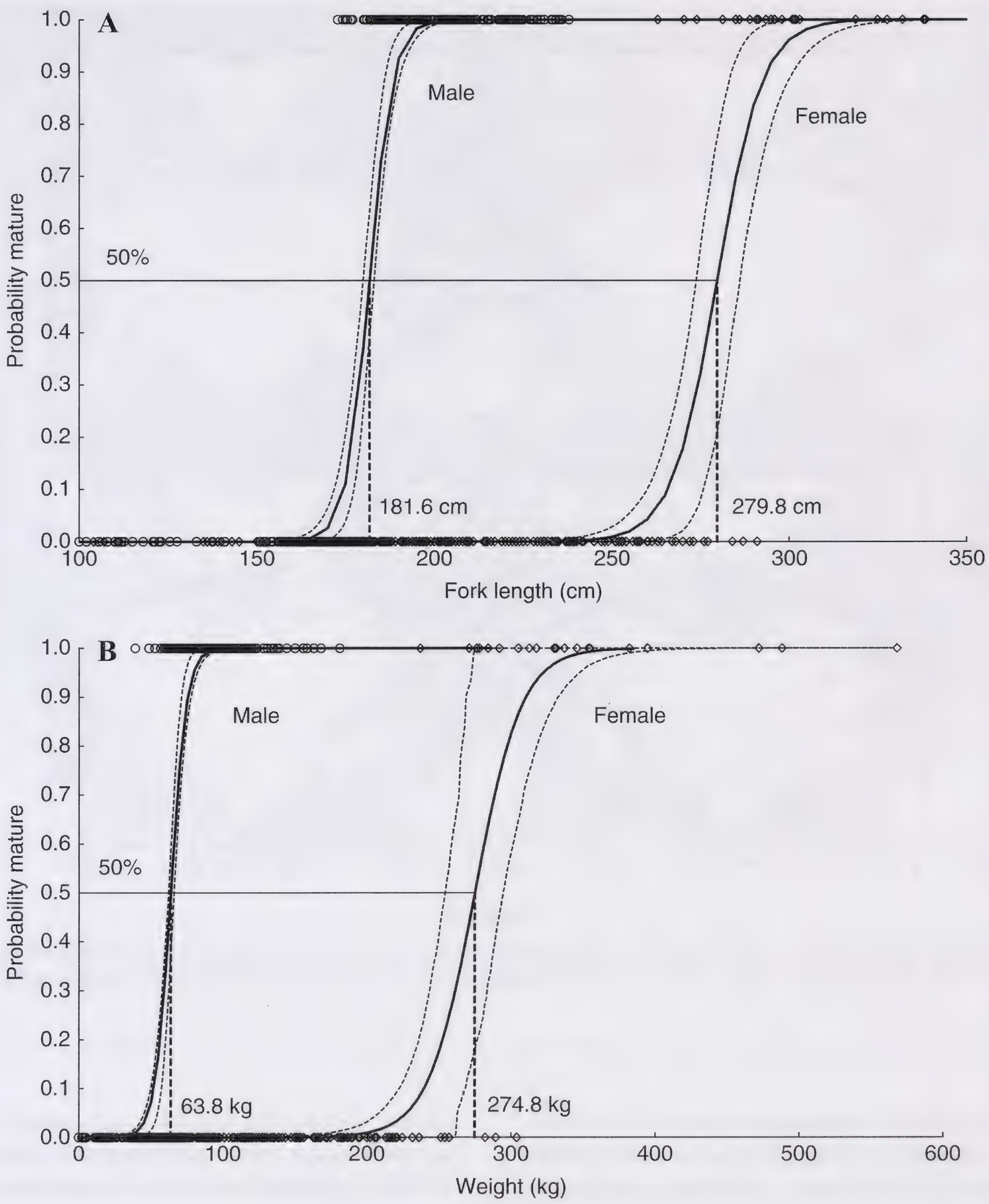

Figure 6

Maturity ogives for female (open diamond) and male (open circle) shortfin makos (*Isurus oxyrinchus*) caught in the western North Atlantic Ocean during 1971–2018, based on (**A**) fork length (in centimeters) and (**B**) weight (in kilograms). A horizontal line indicates the median size at 50% maturity. The dashed curved lines indicate 95% confidence intervals.

For males, clasper length and calcification are the most accurate means of determining maturity. It is not uncommon in elasmobranchs that the secondary sexual characteristics (including clasper rigidity, rotation, and the ability of the rhipidion to splay open) develop after the primary sexual organs and are the defining criteria for maturity (Clark and von Schmidt, 1965). At a minimum, future studies on the reproductive dynamics of shortfin makos should combine comprehensive visual assessments (e.g., presence or absence of embryos and condition of ovaries and uterus) with morphometric measurements (on the organs that show the most rapid growth to body size in females and on clasper length and rigidity in males) to accurately assign maturity stage.

The overlap observed in the demographic structure in the seasonal distributions of the 2 sexes as well as among the different life history stages of shortfin makos were unexpected, given that habitat partitioning and sex and size segregation is common in sharks (Haulsee et al., 2018). Immature males, adult males, immature females, and adult females were found together in every month, with the exception of June and October when mature

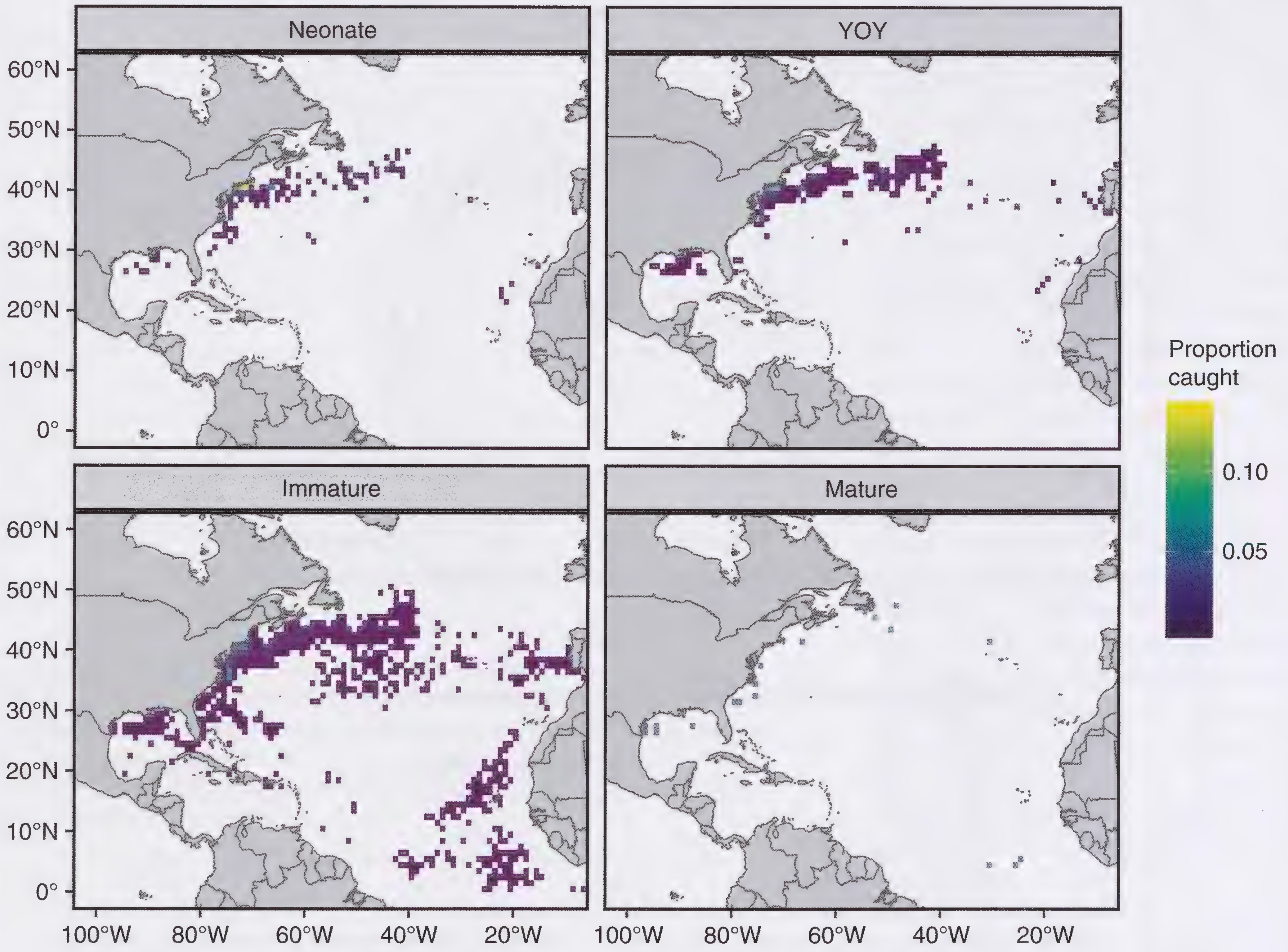

Figure 7

Maps showing the distribution of female shortfin makos (*Isurus oxyrinchus*) caught in the western North Atlantic Ocean during 1962–2018, by maturity status. Data are presented as proportion caught in 1° squares. YOY=young of the year.

females were not caught. Segregation in space and in particular by depth has been previously reported for shortfin makos in the South Pacific Ocean, with males being predominantly found in the west and females in the east and with larger fish spending time at greater depths than smaller fish (Mucientes et al., 2009). Similar to Muicientes et al. (2009), more mature males were captured than mature females in our study, possibly as a result of mature females being absent from the areas targeted by commercial fishing operations or remaining at depths that are out of the range of the fishing gear.

Although the distribution data used in this study were spatially and temporally dependent on fishing effort, the same is true for the majority of data used in other studies to describe the distributions of pelagic sharks (Mucientes et al., 2009; Heupel et al., 2018). Some gear configuration changes (Federal Register, 2004; Coelho and Muñoz-Lechuga, 2019) may have influenced the catchability of sharks over time (Reinhardt et al., 2018), but no management or systematic changes in the distribution of fishing effort would have affected the geographic range of the catch data used. The majority of the catch data used to infer distributions, however, originated from the western North Atlantic Ocean (87% came from west of longitude 45°W); therefore, there remains the possibility that spatial segregation occurs at a larger geographical scale. The fact that immature shortfin makos in our data were predominantly female but that Maia et al. (2007) found the majority of specimens taken off the coast of Portugal to be male is consistent with this hypothesis. Incorporating more distribution data from the Northeast Atlantic Ocean is needed to fully understand demographic structure and seasonal movement patterns of shortfin makos in the North Atlantic Ocean.

The identification of pupping and nursery areas for sharks is crucial to protect vulnerable life stages and support conservation goals (Heupel et al., 2007; Kinney and Simpfendorfer, 2009; Heupel et al., 2018). Unless movement following birth is substantial, the distribution of the youngest age classes should delineate potential birthing and nursery areas. Although the distribution data of mature females from this study and others (Branstetter, cited in Depperman, 1953; Branstetter, 1981; Gilmore, 1993; Mollet et al., 2000) indicates that the Gulf of Mexico is a possible

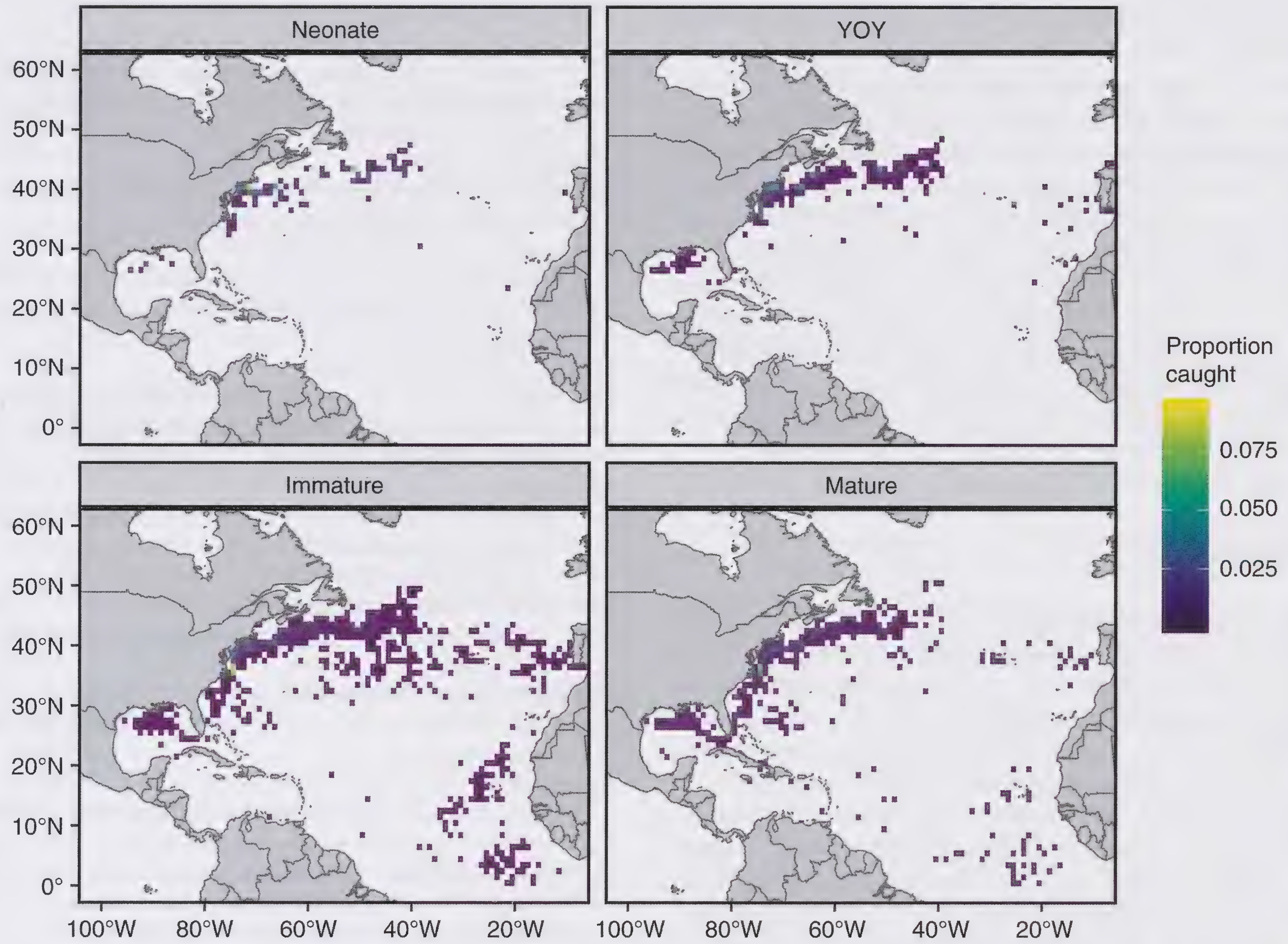

Figure 8

Maps showing the distribution of male shortfin makos (*Isurus oxyrinchus*) caught in the western North Atlantic Ocean during 1962–2018, by maturity status. Data are presented as proportion caught in 1° squares. YOY=young of the year.

gestation and parturition area from winter to spring, the distribution of neonates is much more widespread along the coast of North America and largely overlaps with the distribution of older immature sharks and adults. Neonate and YOY shortfin makos have also been found off Africa and Portugal (Maia et al., 2007), in waters that may prove to be important birthing or nursery areas with more intensive sampling in the Northeast Atlantic Ocean.

The suggestion of a nursery ground of some degree off Portugal is supported by Maia et al. (2007), who reported captures of birth-size individuals (<70 cm FL_{OTB}) in May and July. Maia et al. (2007) question the probability of pups swimming against the current to migrate from a southern pupping ground to Portugal. However, the new evidence of northern pupping on the western side of the Atlantic Ocean indicates that there could also be pupping on the northern area of the eastern Atlantic Ocean or that pups may be using northern surface currents to move from the western to the eastern Atlantic Ocean. Because the coastal areas off Portugal are considered unattractive to sharks (Maia et al., 2007), portions of the western North Atlantic Ocean, which are productive and the location of many shark nursery grounds (Castro, 1993), may be the main parturition and nursery areas for shortfin makos. Data from long-term tracking studies also indicate considerable use of the shelf between South Carolina and Nova Scotia, Canada, by primarily juvenile shortfin makos (Byrne et al., 2017), but additional fishery-independent data are needed to define these boundaries.

The updated reproductive and maturity estimates for both sexes and spatiotemporal patterns in the distribution of life history stages from this study can be used to improve the reliability of science-based advice, as well as to evaluate the likely effect of conservation measures such as size limits. Conservation measures to protect the shortfin mako have been implemented in commercial and recreational fisheries following the ICCAT[5] recommendations. For example, in an initial effort to limit mortality and reduce overfishing by recreational fishermen, the United States imposed size limits for 2019 of 210 cm FL_S and 180 cm FL_S for female and male shortfin makos, respectively. The female size limit is below the new L_{50} and the male limit is just below the new L_{50}, indicating that these management measures will reduce but not remove fishing pressure on mature individuals. Both the United States and Canada have banned the retention of live shortfin makos by commercial fleets, and Canada prohibited all retention of shortfin makos in recreational fisheries (COSEWIC, in press; Federal Register, 2019). Such measures are timely given that updated projections from the North Atlantic Ocean assessment model indicate continued population declines (ICCAT^4). However, there is still a need to better understand the seasonality and segregation of mature females, gestation, and parturition activities in the Gulf of Mexico and along the continental shelf, to develop mitigation options and aid in stock recovery. Ideally, future work on shortfin makos would rely on increased collection of fishery-independent data from sparsely sampled areas.

Acknowledgments

We thank the officials and participants of the many shark tournaments between southern New Jersey and Nova Scotia as well as commercial fishermen for allowing us to sample their landed shortfin mako. We also thank the NMFS Pelagic Observer Program for their data. Portuguese data were collected by the National Data Collection Program within the scope of the European Union Data Collection Framework and within project MAKO-WIDE funded by the Portuguese Foundation for Science and Technology (Ref: FAPESP/19740/2014). Lastly, we thank all individuals involved in Canada's At-Sea Observer Program.

Literature cited

Babcock, E. A., and H. Nakano.
2008. Data collection, research, and assessment efforts for pelagic sharks by the International Commission for the Conservation of Atlantic Tunas. *In* Sharks of the open ocean: biology, fisheries and conservation (M. D. Camhi, E. K. Pikitch, and E. A. Babcock, eds.), p. 472–477. Blackwell Publishing, Oxford, UK.

Barreto, R. R., W. K. T. de Farias, H. Andrade, F. M. Santana, and R. Lessa.
2016. Age, growth and spatial distribution of the life stages of the shortfin mako, *Isurus oxyrinchus* (Rafinesque, 1810) caught in the western and central Atlantic. PLoS ONE 11(4):e0153062.

Bigelow, H. B., and W. C. Schroeder.
1948. Sharks. *In* Fishes of the western North Atlantic. Part 1: lancelets, cyclostomes, sharks (J. Tee-Van, C. M. Breder, S. F. Hildebrand, A. E. Parr, and W. C. Schroeder, eds.), p. 59–546. Mem. Sears Found. Mar. Res., Yale Univ. Press, New Haven, CT.

Bradley, D., E. Conklin, Y. P. Papastamatiou, D. J. McCauley, K. Pollock, B. E. Kendall, S. D. Gaines, and J. E. Caselle.
2017. Growth and life history variability of the grey reef shark (*Carcharhinus amblyrhynchos*) across its range. PLoS ONE 12(2):e0172370.

Branstetter, S.
1981. Biological notes on the sharks of the north central Gulf of Mexico. Contrib. Mar. Sci. 24:13–34.

Byrne, M. E., E. Cortés, J. J. Vaudo, G. C. McN. Harvey, M. Sampson, B. M. Wetherbee, and M. Shivji.
2017. Satellite telemetry reveals higher fishing mortality rates than previously estimated, suggesting overfishing of an apex marine predator. Proc. R. Soc., B 284:20170658.

Canty, A., and B. Ripley.
2017. boot: bootstrap R (S-Plus) functions. R package, vers. 1.3-20. [Available from website.]

Casey, J. G., and H. W. Pratt Jr.
1985. Distribution of the white shark, *Carcharodon carcharias*, in the western North Atlantic. Mem. South. Calif. Acad. Sci. 9:2–14.

Casey, J. G., and N. E. Kohler.
1992. Tagging studies on the shortfin mako shark (*Isurus oxyrinchus*) in the western North Atlantic. Aust. J. Freshw. Res. 43:45–60.

Castro, J. I.
1993. The shark nursery of Bulls Bay, South Carolina, with a review of shark nurseries of the southeastern coast of the United States. Environ. Biol. Fish. 38:37–48.
2009. Observations on reproductive cycles of some viviparous North American sharks. Aqua Int. J. Ichthyol. 15: 205–222.

Clark, E., and K. von Schmidt.
1965. Sharks of the central Gulf Coast of Florida. Bull. Mar. Sci. 15:13–83.

Compagno, L. J. V.
2001. Sharks of the world. An annotated and illustrated catalogue of shark species known to date. Vol. 2: bullhead, mackerel, and carpet sharks (Heterodontiformes, Lamniformes and Orectolobiformes). FAO species catalogue for fishery purposes 1, 269 p. FAO, Rome.

Coelho, R., and R. Muñoz-Lechuga.
2019. Hooking mortality of swordfish in pelagic longlines: comments on the efficiency of minimum retention sizes. Rev. Fish Biol. Fish. 29:453–463.

Coelho, R., J. Mejuto, A. Domingo, K. Yokawa, K.-M. Liu, E. Cortés, E. V. Romanov, C. da Silva, F. Hazin, F. Arocha, et al.
2018. Distribution patterns and population structure of the blue shark (*Prionace glauca*) in the Atlantic and Indian Oceans. Fish Fish. 19:90–106.

COSEWIC (Committee on the Status of Endangered Wildlife in Canada).
In press. COSEWIC status report on shortfin mako *Isurus oxyrinchus* Atlantic population. COSEWIC, Ottawa, Canada.

Cortés, E.
1998. Demographic analysis as an aid in shark stock assessment and management. Fish. Res. 39:199–208.
2002. Incorporating uncertainty into demographic modeling: application to shark populations and their conservation. Conserv. Biol. 16:1048–1062.
2004. Life history patterns, demography, and population dynamics. *In* Biology of sharks and their relatives (J. C. Carrier, J. A. Musick, and M. R. Heithaus, eds.), p. 449–470. CRC Press, Boca Raton, FL.

Cortés, E., F. Arocha, L. Beerkircher, F. Carvalho, A. Domingo, M. Heupel, H. Holtzhausen, M. N. Santos, M. Ribera, and C. Simpfendorfer.
2010. Ecological risk assessment of pelagic sharks caught in Atlantic pelagic longline fisheries. Aquat. Living Resour. 23:25–34.

Depperman, B.
1953. Maternity model mako. Sports Afield, March.

Dulvy, N. K., J. K. Baum, S. Clarke, L. J. V. Compagno, E. Cortés, A. S. Domingo, S. Fordham, S. Fowler, M. P. Francis, C. Gibson, et al.

2008. You can swim but you can't hide: the global status and conservation of oceanic pelagic sharks and rays. Aquat. Conserv. 18:459–482.

Federal Register.

2004. Atlantic highly migratory species (HMS); pelagic longline fishery. Fed. Regist. 69:40734–40758. [Available from website.]

2019. Atlantic highly migratory species; shortfin mako shark management measures; final amendment 11. Fed. Regist. 84:5358–5377. [Available from website.]

Francis, M. P.

2006. Morphometric minefields—towards a measurement standard for chondrichthyan fishes. Environ. Biol. Fish. 77:407–421.

Francis, M. P., and C. Duffy.

2005. Length at maturity in three pelagic sharks (*Lamna nasus, Isurus oxyrinchus,* and *Prionace glauca*) from New Zealand. Fish. Bull. 103:489–500.

Francis, M. P., S. E. Campana, and C. M. Jones.

2007. Age under-estimation in New Zealand porbeagle sharks (*Lamna nasus*): is there an upper limit to ages that can be determined from shark vertebrae? Mar. Freshw. Res. 58:10–23.

Gilmore, R. G.

1993. Reproductive biology of lamnoid sharks. Environ. Biol. Fish. 38:95–114.

Haddon, M.

2011. Modelling and quantitative methods in fisheries, 2nd ed., 465 p. CRC Press, Boca Raton, FL.

Hamlett, W. C.

1999. Male reproductive system. *In* Sharks, skates and, rays: the biology of elasmobranch fishes (W. C. Hamlett, ed.), p. 444–470. Johns Hopkins Univ. Press, Baltimore, MD.

Hamlett, W. C., and T. J. Koob.

1999. Female reproductive system. *In* Sharks, skates, and rays: the biology of elasmobranch fishes (W. C. Hamlett, ed.), p. 398–443. Johns Hopkins Univ. Press, Baltimore, MD.

Harry, A. V., A. J. Tobin, and C. A. Simpfendorfer.

2013. Age, growth and reproductive biology of the spot-tail shark, *Carcharhinus sorrah*, and the Australian blacktip shark, *C. tilstoni*, from the Great Barrier Reef World Heritage Area, north-eastern Australia. Mar. Freshw. Res. 64:277–293.

Haulsee, D. E., M. W. Breece, L. M. Brown, B. M. Wetherbee, D. A. Fox, and M. J. Oliver.

2018. Spatial ecology of *Carcharias taurus* in the northwestern Mid-Atlantic coastal ocean. Mar. Ecol. Prog. Ser. 597:191–206.

Heupel, M. R., J. K. Carlson, and C. A. Simpfendorfer.

2007. Shark nursery areas: concepts, definition, characterization and assumptions. Mar. Ecol. Prog. Ser. 337: 287–297.

Heupel, M. R., S. Kanno, A. P. B. Martins, and C. A. Simpfendorfer.

2018. Advances in understanding the roles and benefits of nursery areas for elasmobranch populations. Mar. Freshw. Res. 70:897–907.

Jensen, C. F., L. J. Natanson, H. L. Pratt Jr., N. E. Kohler, and S. E. Campana.

2002. The reproductive biology of the porbeagle shark (*Lamna nasus*) in the western North Atlantic Ocean. Fish. Bull. 100:727–738.

Kinney, M. J., and C. A. Simpfendorfer.

2009. Reassessing the value of nursery areas to shark conservation and management. Conserv. Lett. 2:53–60.

Kohler, N. E., and P. A. Turner.

2019. Distribution and movements of Atlantic shark species: a 52-year retrospective atlas of mark and recapture data. Mar. Fish. Rev. 81(2):1–93.

Kohler, N. E., J. G. Casey, and P. A. Turner.

1995. Length-weight relationships for 13 species of sharks from the western North Atlantic. Fish. Bull. 93:412–418.

Maia, A., N. Queiroz, H. N. Cabral, A. M. Santos, and J. P. Correia.

2007. Reproductive biology and population dynamics of the shortfin mako, *Isurus oxyrinchus* Rafinesque, 1810, off the southwest Portuguese coast, eastern North Atlantic. J. Appl. Ichthyol. 23:246–251.

Mollet, H. F., G. Cliff, H. L. Pratt Jr., and J. D. Stevens.

2000. Reproductive biology of the female shortfin mako, *Isurus oxyrinchus* Rafinesque, 1810, with comments on the embryonic development of lamnoids. Fish. Bull. 98: 299–318.

Mucientes, G. R., N. Queiroz, L. L. Sousa, P. Tarroso, and D. W. Sims.

2009. Sexual segregation of pelagic sharks and the potential threat from fisheries. Biol. Lett. 5:156–159.

Natanson, L. J., and B. J. Gervelis.

2013. The reproductive biology of the common thresher shark in the western North Atlantic Ocean. Trans. Am. Fish. Soc. 142:1546–1562.

Natanson, L. J., N. E. Kohler, D. Ardizzone, G. M. Cailliet, S. P. Wintner, and H. F. Mollet.

2006. Validated age and growth estimates for the shortfin mako, *Isurus oxyrinchus*, in the North Atlantic Ocean. Environ. Biol. Fish. 77:367–383.

Patterson, K., R. Cook, C. Darby, S. Gavaris, L. Kell, P. Lewy, B. Mesnil, A. Punt, V. Restrepo, D. W. Skagen, et al.

2001. Estimating uncertainty in fish stock assessment and forecasting. Fish Fish. 2:125–157.

Pratt, H. L., Jr.

1996. Reproduction in the male white shark. *In* Great white sharks: the biology of *Carcharodon carcharias.* Proceedings of the symposium on the biology of the white shark; Bodega, CA, 4 March 1993 (A. P. Klimley and D. G. Ainley, eds.), p. 131–138. Acad. Press, San Diego, CA.

Pratt, H. L., Jr., and J. G. Casey.

1983. Age and growth of the shortfin mako, *Isurus oxyrinchus*, using four methods. Can. J. Fish. Aquat. Sci. 40: 1944–1957.

Quinn, T. J., II.

2003. Ruminations on the development and future of population dynamics models in fisheries. Nat. Resour. Model. 16:341–392.

R Core Team.

2018. R: a language and environment for statistical computing. R Foundation for Statistical Computing, Vienna, Austria. [Available from website.]

Reinhardt, J. F., J. Weaver, P. J. Latham, A. Dell'Apa, J. E. Serafy, J. A. Browder, M. Christman, D. G. Foster, and D. R. Blankinship.

2018. Catch rate and at-vessel mortality of circle hooks versus J-hooks in pelagic longline fisheries: a global meta-analysis. Fish Fish. 19:413–430.

Rigby, C. L., R. Barreto, J. Carlson, D. Fernando, S. Fordham, M. P. Francis, R. W. Jabado, K. M. Liu, A. Marshall, N. Pacoureau, et al.

2019. *Isurus oxyrinchus*. The IUCN Red List of Threatened Species 2019: e.T39341A2903170. [Available from website.]

Tanaka, S., G. M. Cailliet, and K. G. Yudin.

1990. Differences in growth of the blue shark, *Prionace glauca*: technique or population? *In* Elasmobranchs as living resources: advances in the biology, ecology, systematics, and status of the fisheries (H. L. Pratt Jr., S. H. Gruber, and T. Taniuchi, eds.), p. 177–187. NOAA Tech. Rep. NMFS 90.

Walker, T. I.
2005. Reproduction in fisheries science. *In* Reproductive biology and phylogeny of Chondrichthyes: sharks, rays and chimaeras (W. C. Hamlett, ed.), p. 81–127. Science Publishers Inc., Enfield, NH.

Wickham, H.
2017. tidyverse: easily install and load the ‘tidyverse’. R package, vers. 1.2.1. [Available from website.]

Zuur, A. F., E. N. Ieno, and C. S. Elphick.
2010. A protocol for data exploration to avoid common statistical problems. Methods Ecol. Evol. 1:3–14.

National Marine
Fisheries Service
NOAA

Fishery Bulletin
established in 1881

Spencer F. Baird
First U.S. Commissioner
of Fisheries and founder
of *Fishery Bulletin*

Genetic identification of blue rockfish (*Sebastes mystinus*) and deacon rockfish (*S. diaconus*) to enable life history analyses for stock assessment

Joseph J. Bizzarro (contact author)[1,2]
Elizabeth A. Gilbert-Horvath[2]
E. J. Dick[2]
Aaron M. Berger[3]
Katherine T. Schmidt[4]
Don Pearson[2]
Christine Petersen[5]
Lisa A. Kautzi[6]
Rebecca R. Miller[1,2]
John C. Field[2]
John Carlos Garza[2,7]

Email address for contact author: joe.bizzarro@noaa.gov

[1] Cooperative Institute for Marine Ecosystems and Climate
University of California, Santa Cruz
110 McAllister Way
Santa Cruz, California 95060

[2] Fisheries Ecology Division
Southwest Fisheries Science Center
National Marine Fisheries Service, NOAA
110 McAllister Way
Santa Cruz, California 95060

[3] Fishery Resource Analysis and Monitoring Division
Northwest Fisheries Science Center
National Marine Fisheries Service, NOAA
2032 SE OSU Drive
Newport, Oregon 97365

[4] West Coast Region
National Marine Fisheries Service, NOAA
650 Capitol Mall, Suite 5-100
Sacramento, California 95814

[5] Bonneville Power Administration
P.O. Box 3621
Portland, Oregon 97232

[6] Marine Resources Program
Oregon Department of Fish and Wildlife
2040 SE Marine Science Drive
Newport, Oregon 97365

[7] Department of Ocean Sciences
University of California, Santa Cruz
1156 High Street
Santa Cruz, California 95064

Abstract—To better inform stock assessment and management decisions, we used multiple approaches for estimating and comparing species-specific characteristics of the spatiotemporal composition of catch and life history traits of blue rockfish (*Sebastes mystinus*) and deacon rockfish (*S. diaconus*). We confirmed the species-level distinction of blue rockfish and deacon rockfish by using the results of genetic identification of individual fish from fin tissue samples and otoliths. Those results reveal the systematic relationships of these species with other rockfish species and enabled an evaluation of differences in distribution and life history (growth) between the 2 species in different management areas. Our evaluation of population structure found no significant differentiation within deacon rockfish and slight differentiation in blue rockfish that may not be biologically significant. Along the U.S. Pacific coast, deacon rockfish accounted for the majority of individuals sampled north of Monterey Bay, California, whereas blue rockfish were the more frequently observed species in waters of Monterey Bay and southern California. Modest but significant differences in growth parameters between the 2 species were observed by species, sex, and state (California or Oregon). The multidisciplinary nature of this study and the techniques and protocols we established provide a model for future research on and assessment of species complexes.

Modern genetic analyses are uncovering many phenotypically similar but genetically distinct species in otherwise well-characterized groups of organisms. In marine environments, the discovery of cryptic or visually similar species typically is not a function of an infrequent encounter rate, because they often occur in regions that have been heavily exploited and monitored for decades (e.g., Gharrett et al., 2005; Quattro et al., 2013). Several such recent discoveries have been made within rockfishes (*Sebastes* spp.), an extremely diverse group of more than 100 ecologically and economically important species that are primarily distributed in the northeastern Pacific Ocean (Eschmeyer et al., 2017). This high species diversity is a consequence of a rapid rate of speciation (Johns and Avise, 1998), which is ongoing, with nascent reproductive isolation and incipient species found throughout the genus (Venerus et al., 2013). For example, in the California Current, both the rougheye rockfish (*Sebastes aleutianus*) and the vermilion rockfish (*S. miniatus*) were previously considered single species, but each is now known to represent 2 morphologically similar but genetically distinct species: rougheye rockfish (*S. aleutianus*) and blackspotted rockfish (*S. melanostictus*) (Gharrett et al., 2005, 2006; Orr and Hawkins, 2008), and vermilion rockfish (*S. miniatus*)

Manuscript submitted 27 February 2019.
Manuscript accepted 10 February 2020.
Fish. Bull. 118:37–50 (2020).
Online publication date: 28 February 2020.
doi: 10.7755/FB.118.1.4

The views and opinions expressed or implied in this article are those of the author (or authors) and do not necessarily reflect the position of the National Marine Fisheries Service, NOAA.

and sunset rockfish (*S. crocotulus*) (Hyde et al., 2008). In a more extreme example from the northwestern Pacific Ocean, the nominal dark-banded rockfish (*S. inermis*) was discovered to be 3 distinct species that recently separated because of differential resource utilization (i.e., niche differentiation; Kai et al., 2002).

The discovery of unrecognized diversity within species that were previously considered to be monotypic expands our understanding of biodiversity and provides avenues for further study, but it also presents significant management challenges. Species or stocks are commonly used as management units; however, the presence of morphologically indistinguishable but genetically distinct taxa creates heterospecificity that can hamper the design of appropriate management and conservation measures (Tellier et al., 2011). This is particularly true if there are substantive differences between the species in life history (e.g., growth, maturity, or fecundity) or in distribution and habitat associations, differences that could lead to differential exploitation histories and management effectiveness (Cope and Punt, 2011; Cope et al., 2011). Consequently, several authors have emphasized the importance of conducting genetic and life history analyses to disentangle species complexes and to identify divergent lineages and potential subpopulations within rockfish species, to ensure that they are managed appropriately (Buonaccorsi et al., 2005; Tuckey et al., 2007; Hess et al., 2014).

The results of recent genetic analysis indicate that the nominal blue rockfish (*S. mystinus*) (Jordan and Gilbert, 1881) is actually 2 recently diverged but morphologically similar species: the blue rockfish (*S. mystinus*) and the deacon rockfish (*S. diaconus*) (Burford et al.[1]; Burford and Bernardi, 2008; Burford et al., 2011a; Frable et al., 2015). Although these species have been difficult to visually distinguish, species-specific differences in coloration, size of the symphyseal knob, ventrum shape, and length of anal-fin spines align with genetic differentiation (Burford and Bernardi, 2008; Frable et al., 2015).

In addition to genetic and morphological differentiation, differences in geographic distribution, and possibly in depth, have been observed for blue rockfish and deacon rockfish. Deacon rockfish range from the Channel Islands off southern California to Vancouver Island, Canada (Burford, 2009; Frable et al., 2015), and have been commonly reported at depths of 8–72 m (but have been observed in deeper water at Cobb Seamount, 46°46′N, 130°49′W; Love[2]) (Fig. 1). Blue rockfish range from northern Baja California, Mexico (Klingbeil and Knaggs, 1976), to central Oregon (Frable et al., 2015) and occur from surface waters to seafloor depths of at least 156 m (Love, 2011; Love[2]). Frable et al. (2015) have reported anecdotal evidence that adult deacon rockfish are more frequently found offshore in deeper water than adult blue rockfish; however, scant data are available to characterize relative abundance of these 2 species in the broad region of their co-occurrence.

Historical catch and demographic (age and length) data cannot be used to identify blue rockfish and deacon rockfish to the species level, leaving little alternative but to develop a stock assessment of the 2 species together as a complex (Dick et al.[3]). Although this species complex constitutes a minor component of commercial landings throughout its range, it has historically been the most frequently landed rockfish stock in the California recreational fishery and is also an important recreational fishery target off Oregon (Miller and Geibel, 1973; Dick et al.[3]). Therefore, quantifying differences in growth between the 2 species and evaluating potential spatiotemporal shifts in their relative abundance are critical to alleviating concerns that a single management strategy may not be appropriate for both species.

In this study, we combined genetic identification with otolith-based age and growth analyses to further elucidate differences between blue rockfish and deacon rockfish, describing and comparing patterns of variation in abundance and life history. We used highly informative microsatellite genetic markers to determine the specific identity of numerous biological samples collected over ~40 years. These identifications enabled estimation of 1) patterns of inter- and intraspecific genetic variation, 2) the contribution of each species to historical and recent fishery landings along the U.S. Pacific coast that were used to evaluate the evidence for spatiotemporal differences in relative abundance, and 3) age and growth parameters for blue rockfish and deacon rockfish that were used to determine if growth differed between species and (broad-scale) regions.

Materials and methods

Genetics

Material for genetic analyses was obtained from otoliths and fin tissue samples. Otoliths were available from archived samples that were collected from hook-and-line surveys and recreational fisheries sampling off California between 1976 and 1984 and were identified as blue rockfish at the time of collection (Table 1). Otoliths were removed from juvenile and adult fish (number of samples [n]=1655), then rinsed and air-dried, often leaving a small amount of tissue on the otolith surface from which DNA could be extracted. Fin tissue samples were collected from juveniles and adults off California and Oregon during several surveys and sampling programs between 2009 and

---

[1] Burford, M., M. Carr, and G. Bernardi. 2006. Speciation and genetic structure in a marine fish with an extended pelagic larval phase: an analysis of both the juvenile and adult populations of blue rockfish (*Sebastes mystinus*). Univ. Calif. Mar. Counc., Coast. Environ. Qual. Initiative Pap. 039, 9 p. [Available from website.]

[2] Love, M. 2018. Personal commun. Mar. Sci. Inst., Univ. Calif., Santa Barbara, Santa Barbara, CA 93106-6150.

[3] Dick, E. J., A. Berger, J. Bizzarro, K. Bosley, J. Cope, J. Field, L. Gilbert-Horvath, N. Grunloh, M. Ivens-Duran, R. Miller et al. 2017. The combined status of blue and deacon rockfishes in U.S. waters off California and Oregon in 2017, 309 p. Agenda item E.8, attach. 9. Pacific Fish. Manage. Counc., Portland, OR. [Available from website.]

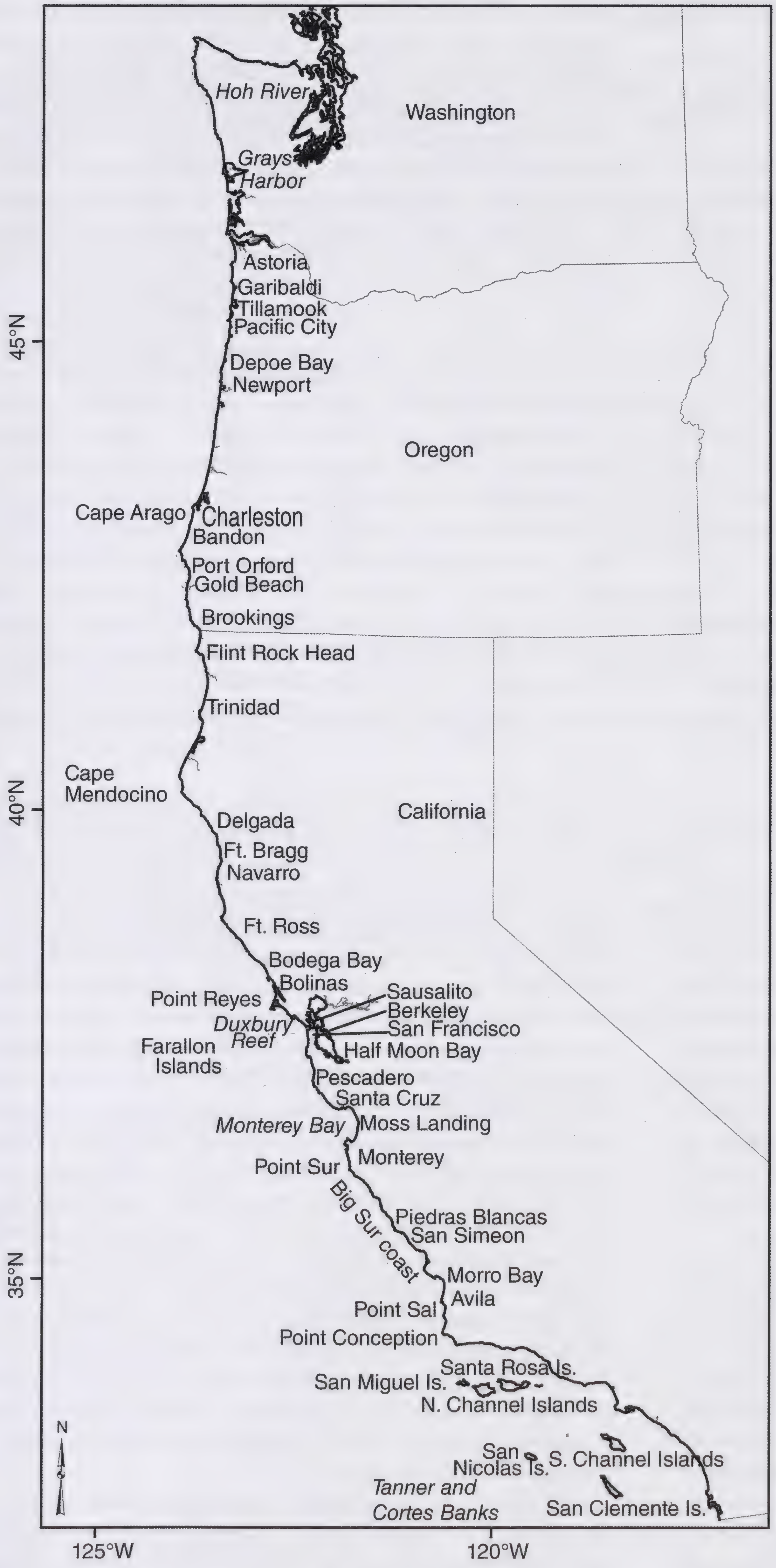

Figure 1

Map depicting the locations of ports of landing along the U.S. Pacific coast where samples of blue rockfish (*Sebastes mystinus*) and deacon rockfish (*S. diaconus*) were collected off California, Oregon, and Washington during 2004–2017 and 1976–1984. Other place-names referenced in the text also are shown.

2017, and most individuals were visually identified as either blue rockfish or deacon rockfish (Table 1). Young-of-the-year (YOY; age-0) rockfish were collected off California and Oregon from 2004 to 2016 during mid-water trawl surveys conducted for pelagic rockfish juveniles (Sakuma et al., 2006, 2016). Small pieces of fin tissue were taken from juveniles and adults (*n*=1140) and from YOY rockfish (*n*=192), and they were either air-dried or stored in 95% ethanol. Morphological differences that can be used to distinguish pelagic YOY blue rockfish from deacon rockfish have not been described; therefore, these samples were identified as blue rockfish or deacon rockfish by using genetic analysis (Table 1).

Purified genomic DNA was extracted by using DNeasy 96 Blood and Tissue Kits[4] (Qiagen Inc., Germantown, MD). The following 9 microsatellite markers were used for genotyping: Seb25, Spi12, Sra6-52, Sth45 (Roques et al., 1999; Sekino et al., 2000; Gómez-Uchida et al., 2003; Buonaccorsi et al., 2004), Seb9, Sme13, Spi10, Sra15-8, and Sth37, the last of which were previously employed by Pearse et al. (2007) for identification of rockfish species. Polymerase chain reaction (PCR) reagent components were as described in Venerus et al. (2013), and the thermal cycling conditions that were used are provided in Supplementary Table 1 (online only). The PCR products were electrophoresed on an Applied Biosystems 3730 DNA Analyzer (Thermo Fisher Scientific Inc., Waltham, MA), by using a fragment analysis run module. Allele calling was performed by using Applied Biosystems GeneMapper Software, vers. 4.0 (Thermo Fisher Scientific Inc.).

The genetic species identification process used in this study involved a combination of assignment tests and ancestry analysis. In the assignment tests, genotypes were compared to a reference data set containing visually identified and genetically verified blue rockfish (*n*=24) and deacon rockfish (*n*=26), as well as 42 other *Sebastes* species, including all of those commonly found in the California Current (Supplementary Table 2)

---

[4] Mention of trade names or commercial companies is for identification purposes only and does not imply endorsement by the National Marine Fisheries Service, NOAA.

Table 1

Region, time period, and life stage (age 0 and age 1 or older [age 1+]) sampled and sample size (n) of blue rockfish (*Sebastes mystinus*) and deacon rockfish (*S. diaconus*) associated with source information for each study component: genetic, species composition (SppComp), and age and growth (A&G) analyses. Samples used for the genetic component were genetically identified, whereas samples from the other components were a combination of genetic (1976–1984) and field (2004–2017) identifications. Surveys of pelagic young-of-the-year (YOY, age 0) rockfish were conducted by the National Marine Fisheries Service (NMFS) Southwest Fisheries Science Center (SWFSC) and the Pacific Whiting Conservation Cooperative. Hook-and-line surveys of juveniles and adults were conducted by the California Department of Fish and Wildlife, NMFS Northwest Fisheries Science Center, and the Oregon Department of Fish and Wildlife (ODFW). Unpublished data of S. Beyer were collected by the SWFSC Fisheries Ecology Division.

				Sample size (n)		
Region	Source	Time period	Life stage	Genetic	SppComp	A&G
California	Pelagic YOY	2004–2005, 2013, 2014, 2016	0	192	392	0
	Hook and-line surveys	1976–1977, 2010–2015	1+	165	184	182
	Sport fisheries sampling	1978, 1980–1984	1+	1419	311	280
	Various surveys	2004–2006, 2010–2015	1+	344	463	0
	Schmidt, 2014	2009–2012	1+	780	416	621
	Beyer, unpubl. data	2011–2012	1+	0	0	17
Oregon and Washington	Pelagic YOY	2004–2005	0	0	55	0
	Commercial fisheries sampling	2008–2016	1+	0	2753	1578
	Sport fisheries sampling	2008–2016	1+	0	7662	3747
	ODFW	2016–2017	1+	87	0	109

(online only). To assess the robustness of these results, 3 assignment analyses were conducted by using 2 software programs, GeneClass2 (Piry et al., 2004) and gsi_sim (Anderson et al., 2008). In GeneClass2, the semi-Bayesian method (Rannala and Mountain, 1997) and the frequency-based method (Paetkau et al., 2004) were employed. For the Paetkau method, the frequency of missing alleles was set to 0.01. Gsi_sim uses a Bayesian simulation method to estimate species (or population) of origin. We employed 25,000 sweeps of the Markov chain Monte Carlo method, following 5000 sweeps of burn-in, to calculate for each individual the posterior probability of membership in each species (P of Z-scores). For both methods, assignment of individuals to reference species (described previously) employed a probability threshold of 0.95.

The assignment results were then compared to arrive at a consensus species identification for each individual: assignment probabilities of 90% and above were considered high confidence, whereas probabilities below 90% were considered low confidence. Because low-confidence assignments are potentially inaccurate, only the high-confidence species assignments were considered as reliable identifications. Individuals that had a low-confidence assignment in one or more of the 3 methods were classified as having low confidence overall. Accordingly, only those individuals with concordant, high-confidence species assignments in all 3 methods were assigned a species identification. This conservative approach was taken to minimize or avoid spurious species assignments and to exclude any potential hybrids.

Multi-locus genotype data were analyzed by using STRUCTURE, vers. 2.3.4 (Pritchard et al., 2000), to determine the degree of genetic distinctiveness of the 2 species. This analysis differs from the assignment analysis because it uses Markov chain Monte Carlo simulation to estimate ancestry of individuals in a fractional manner, given a hypothesis about K, the number of genetic groups in the sample as a whole. In this analysis, all samples were considered to be of unknown species affiliation and were not compared to the reference data set as in the assignment analysis, and a location or population prior was not provided. Therefore, the STRUCTURE analysis provided a quasi-independent estimation of genetic species classifications. Analysis parameters included 50,000 burn-in sweeps to ensure an unbiased starting point for the Markov chain, 150,000 iterations without replacement, and 5 replicate runs each for hypothetical K of 2–4. Although a K value of 2 was assumed a priori to be most likely for these data, higher K values were included to detect genotypes from any other species that might be present in the data set. Then, by using STRUCTURE's fractional ancestry output for a K value of 2, individuals having >0.90 membership proportion in 1 of the 2 inferred clusters, corresponding to blue rockfish or deacon rockfish, were categorized as members of that cluster.

The final genetic species identification was made on the basis of a comparison of the high-confidence individual assignments and the STRUCTURE ancestry membership results. Species-level identification of individuals with high confidence in only one method (assignment or ancestry) was considered a *probable* species identification. Individuals with non-concordant results or low-confidence results in both methods were not identified to species and were omitted from further analyses.

Spatial genetic structure was evaluated at 2 levels: by sampling region within species (blue rockfish, n=1072; deacon rockfish, n=822) and by sampling region between species. Regions were established on the basis of fishing block number assigned by the state of California, fishing port, or latitude and longitude of the collection site (Table 2). Temporal samples were pooled within each region. All available samples, regardless of life stage (adult or juvenile), were included in order to maximize spatial coverage. Because sampling took place over multiple years at most locations, the inclusion of mixed life stages was not expected to bias the regional results. Omitted from this analysis were individuals whose collection site could not be identified or assigned to a fishing block (blue rockfish, n=16; deacon rockfish, n=9) and individuals from 4 regions with too few samples (n<9). Estimates of the pairwise interpopulation fixation index, F_{ST}, were calculated between regions and between the 2 species by region, by using Genetix, vers. 4.05 (Belkhir et al., 2004). Statistical significance was assessed with 4999 permutations, and the resulting P-values were adjusted for multiple comparisons by using a strict Bonferroni correction applied to an α of 0.05. Genetic summary statistics (expected and observed heterozygosity and mean number of alleles per locus) were calculated for each region by using the Microsatellite Toolkit, MSTools, vers. 3.1 (Park, 2002), an add-in for Microsoft Excel (Microsoft Corp., Redmond, WA).

Species composition

Total counts of blue rockfish and deacon rockfish were obtained from a variety of fishery-dependent and fishery-independent sources off California, Oregon, and Washington, including visual identification of specimens from the recent time period (2004–2017) and genetic analysis of historical samples (1976–1984). These data then were used to estimate and compare species composition along the U.S. Pacific coast. Samples of juvenile and adult individuals (age 1 or older [age 1+]) were obtained from historical and recent hook-and-line, spearing, and scuba collections conducted in California (n=1374) and Oregon (n=10,415) (Table 1). A comparatively small number of pelagic YOY rockfish were collected by trawling in California (n=392) and Oregon (n=55) during 2004–2016 (Table 1).

The resolution of sample locations was variable and depended on collection method. For the purposes of this evaluation, we assigned the location of samples to the port of landing, a reasonable assumption for specimens sampled primarily from recreational fisheries. The following ports along the coast of Oregon were combined for mapping and

Table 2

Summary statistics for sampling regions used in analysis of population genetic structure of blue rockfish (*Sebastes mystinus*) and deacon rockfish (*S. diaconus*). Material for genetic analyses was obtained from otoliths of blue rockfish and deacon rockfish collected off California (1976–1984) and from fin tissue samples of rockfish caught off California and Oregon (2009–2017). The latitudes for the northern and southern boundaries of the defined regions are given in decimal degrees. Also provided are the number of samples (n) for regions with >8 sampled individuals, expected and observed heterozygosity (H_E and H_O, respectively), and mean number of alleles per locus (MNA).

Region (north to south)	Species	Northern boundary (latitude)	Southern boundary (latitude)	n	H_E	H_O	MNA
Oregon coast	Blue	44.534	42.067	16	0.5064	0.5042	4.33
Oregon coast	Deacon	44.548	42.775	64	0.5176	0.5102	5.44
Northern California	Deacon	41.757	41.000	20	0.4976	0.4693	4.22
Mendocino coast	Deacon	40.500	39.133	49	0.5097	0.4303	5.00
Bodega Bay	Blue	38.467	38.167	14	0.5435	0.5659	4.22
Bodega Bay	Deacon	38.422	38.037	66	0.5120	0.5084	5.78
Farallon Islands	Blue	37.883	37.714	33	0.5018	0.4345	5.33
Farallon Islands	Deacon	37.883	37.734	99	0.5152	0.4642	6.11
Half Moon Bay	Blue	37.433	37.162	145	0.5260	0.5118	8.11
Half Moon Bay	Deacon	37.388	37.163	328	0.5190	0.4879	7.44
Monterey Bay	Blue	36.983	36.544	367	0.4979	0.4589	8.56
Monterey Bay	Deacon	36.983	36.544	136	0.5204	0.5170	6.44
Big Sur coast	Blue	36.474	36.031	38	0.4877	0.4679	5.22
Big Sur coast	Deacon	36.564	36.300	21	0.5477	0.5248	5.22
Morro Bay	Blue	35.703	35.000	172	0.4889	0.4616	7.56
Morro Bay	Deacon	35.703	35.000	30	0.5035	0.5254	5.00
Santa Barbara Channel	Blue	34.442	34.349	18	0.4293	0.4405	4.44
Northern Channel Islands	Blue	34.141	33.883	178	0.4755	0.4475	7.11
Northern Channel Islands	Deacon	34.141	34.017	9	0.5696	0.6497	3.67
Southern California shore	Blue	34.007	32.806	21	0.5183	0.5351	5.11
Southern Channel Islands	Blue	33.495	32.450	70	0.4833	0.4481	6.22

analysis: Tillamook (ports Astoria, Tillamook, Pacific City, and Garibaldi), Newport (ports Depoe Bay and Newport), Bandon (ports Bandon and Charleston), and Brookings (ports Brookings, Gold Beach, and Port Orford) (Fig. 1). The following ports and locations off the coast of California were combined for mapping and analysis: Point Reyes (ports Point Reyes and Fort Ross), Bolinas (ports Bolinas and Duxbury Reef), San Francisco Bay (ports Berkeley, San Francisco, and Sausalito), Santa Cruz (ports Santa Cruz, Davenport, and Moss Landing), Cortes Bank (ports Cortes and Tanner Banks), and the Southern California Bight (Fig. 1).

Species compositions of age-0 and age-1+ blue rockfish and deacon rockfish at ports in California and Oregon were summarized and displayed visually by using geographic information system software (ArcMap, vers. 10.4.1, Esri, Redlands, CA). In central California, for which data exist from historical and recent collections (Table 1), the relative percentage of blue rockfish and deacon rockfish was calculated for each time period.

Spatiotemporal patterns in species composition were investigated and compared with results from generalized linear models (GLMs) and generalized linear mixed models (GLMMs) by using a subset of data from port sampling in California. Species composition data (observed counts of each species) from central California were divided into the following groups, or port complexes, by proximity: Morro Bay Complex (from San Simeon to Avila), Monterey Bay Complex (from Monterey to Santa Cruz), and San Francisco Bay Complex (from Half Moon Bay to Bolinas). Data from southern California were not analyzed because deacon rockfish rarely were observed, whereas data from northern California were excluded because the sample size (n=71) was considered inadequate to reliably characterize species composition. Count data by species were fit by using a binomial GLM with a logit-link function and a logit-normal GLMM with observation-level random effects to determine if species compositions were influenced by spatial location or temporal occurrence. In these models, the number of positive occurrences of blue rockfish was considered the response variable, and location (Morro Bay Complex, Monterey Bay Complex, or San Francisco Bay Complex) and time period (historical, 1976–1984, or recent, 2004–2014) were included as categorical covariates. Model diagnostics were conducted to evaluate fit, and the Akaike information criterion (AIC) was used to select the best model for the data (Akaike, 1974). All analyses and diagnostics were conducted with statistical software R, vers. 3.3.2 (R Core Team, 2016).

Age and growth

Numerous studies evaluated age and growth of the blue rockfish and deacon rockfish complex prior to the description of deacon rockfish as a separate species, by using various methods (e.g., surface ages versus break and burn; for a review, see Laidig et al., 2003) and structures (e.g., scales or otoliths). Our species-specific data on age and growth were differentiated by using high-confidence genetic identifications for samples from California and visual field identifications for samples from Oregon, where they are considered reliable (Hannah et al.[5]).

Age estimates were derived from otoliths that were collected from recreational fisheries and research surveys in waters of California (Table 1). Otoliths collected between 1976 and 1984 were from fish identified to species with genetic analysis, whereas most contemporary samples (2005–2015) were from fish that were visually identified and then had their identity confirmed through genetic analyses. All otoliths of each species were aged by using the break-and-burn method (Beamish, 1979; Kimura et al., 1979), including otoliths from relatively small individuals that may have also been aged with surface reads.

Otoliths from blue rockfish and deacon rockfish off Oregon were primarily collected from fish taken by the recreational ocean-boat and commercial fleets, mainly by using hook-and-line methods (Table 1), but some otoliths were from fish collected during surveys that were conducted between December 2016 and February 2017 to target small fish (<24 cm fork length [FL]) that were poorly sampled by fishing fleets. These otoliths also were aged by using the break-and-burn method, except for a few otoliths collected from small, young individuals.

Aging error was evaluated by comparing estimates from otoliths that had been independently read twice by the same reader (within-reader variation) and by 2 different readers (between-reader variation). To evaluate within-reader aging error for samples from California, 587 otoliths were aged twice by the same person (blind reads), and the results were compared with age bias plots (after Campana et al., 1995). Within-reader aging error for samples from Oregon was assessed in the same manner by randomly selecting and comparing age estimates from 20% of all aged otoliths (n=1123). Between-reader aging error was evaluated for California and Oregon readers by comparing final reads for each region with a subset of 257 otoliths.

Age and length data for all species, both sexes, and different regions were fit by using the von Bertalanffy (1957) growth function:

$$L_t = L_\infty \left(1 - e^{-k(t - t_0)}\right)$$

where L_t = FL (in millimeters) of fish at a given age t (in years);
L_∞ = theoretical average maximum length (in millimeters);
k = growth coefficient (per year); and
t_0 = theoretical age at size zero.

The L_∞, k, and t_0 were estimated by using the nls (nonlinear least squares) function in R. The AIC was used to evaluate the relative fit of different regression models.

---

[5] Hannah, R. W., D. W. Wagman, and L. A. Kautzi. 2015. Cryptic speciation in the blue rockfish (*Sebastes mystinus*): age, growth and female maturity of the blue-sided rockfish, a newly identified species, from Oregon waters. Oregon Dep. Fish Wildl., Fish Div., Inf. Rep. 2015–01, 24 p. [Available from website.]

Four separate comparisons were made to assess potential sources of variability in age and growth parameters. The initial baseline analysis pooled the 2 species and states (Oregon and California) and compared only sexes. Subsequent analyses added categorical covariates for species and then state to the original model. Finally, to assess spatial differences in age and growth of female blue rockfish within the region of California, we evaluated data that were collected from specimens sampled north of Point Conception by Schmidt (2014) and sampled south of Point Conception in a hook-and-line survey (for a description of survey methods, see Harms et al., 2008).

Results

Genetics

Fin tissue samples yielded a much greater proportion of sufficient data for species identification than did otoliths, but species discrimination was reliable regardless of source material (Table 3). Most tissue samples produced sufficient genetic data for identification, and 91.2% of them were either verified (83.6%) or probable (7.6%) blue rockfish or deacon rockfish. In contrast, less than half of the otolith samples yielded sufficient data for identification, with 33.8% verified and 8.7% probable identifications (Table 3). Failure to yield a consensus species identification could have been caused by a variety of factors, such as poorly preserved DNA, missing data, or individuals of other *Sebastes* species visually misidentified as blue rockfish or deacon rockfish.

Table 3

Comparison of species identification results obtained from genetic analysis of recent fin tissue (2009–2016) and historical otolith (1976–1984) samples of blue rockfish (*Sebastes mystinus*) and deacon rockfish (*S. diaconus*) off the Pacific coast of the United States. See the "Materials and methods" section for criteria used to assign *verified* and *probable* identifications to other *Sebastes* species. The values in the last row (None) are for samples for which no species assignment was made, because of ambiguous or discrepant results or missing data. *n*=number of samples.

	Fin tissue		Otolith	
Species identification	*n*	%	*n*	%
Blue rockfish (verified)	630	46.5	309	18.9
Deacon rockfish (verified)	503	37.1	243	14.9
Blue rockfish (probable)	68	5.0	90	5.5
Deacon rockfish (probable)	35	2.6	52	3.2
Other *Sebastes* species	8	0.6	17	1.0
None	112	8.3	920	56.4
Total	1356	100	1631	100

Concordance between visual and genetic identifications was high, indicating that blue rockfish and deacon rockfish can be reliably distinguished in the field. Visual and genetic identifications matched in 96.3% of samples for which both were available (*n*=1042). Discrepant visual identifications were skewed toward deacon rockfish being identified as blue rockfish (*n*=33), whereas only 2 blue rockfish were visually identified as deacon rockfish. Two individuals that were visually identified as potential hybrids were genetically identified with high confidence as deacon rockfish.

Distributions of pairwise F_{ST} estimates within and between species displayed a distinctly bimodal pattern with nonoverlapping distributions (Supplementary Figure) (online only). Mean pairwise F_{ST} was at least 2 orders of magnitude larger among interspecific comparisons (0.1545 [standard deviation (SD) 0.0216]) than among the intraspecific comparisons, for which mean pairwise F_{ST} was almost zero (blue rockfish: 0.0057 [SD 0.0123]; deacon rockfish: 0.0007 [SD 0.0042]). All 110 of the interspecific F_{ST} comparisons differed significantly from zero following Bonferroni correction, whereas only 5 of 55 intraspecific comparisons for blue rockfish differed significantly and none of the 45 pairwise comparisons for deacon rockfish were significant. For blue rockfish, 4 of the significantly different within-species comparisons involved the location of Half Moon Bay and regions more to the south, and the comparison for the regions of Oregon and the northern Channel Islands also differed significantly.

Measures of genetic diversity were similar both between blue rockfish and deacon rockfish within the same region and between geographic regions within each species (Table 2). In 2-tailed *t*-tests for independent means, observed heterozygosity (H_O) and mean number of alleles per locus (MNA) did not differ significantly between the 2 species (H_O, $t=-1.307$, $P=0.207$; MNA: $t=0.982$, $P=0.338$). In addition, there was no significant correlation between latitude and H_O within blue rockfish (coefficient of correlation [r]=0.325, $P=0.329$) or deacon rockfish ($r=-0.584$, $P=0.077$), consistent with intraspecific genetic homogeneity over a broad geographic scale.

Species composition

The relative proportion of deacon rockfish increased with latitude and dominated samples from north of Monterey Bay, whereas blue rockfish were caught more frequently farther south (Fig. 2). From Pescadero, California, to Hoh River, Washington, 81.1% of YOY (*n*=322) and 85.7% of age-1+ individuals (*n*=10,889) were deacon rockfish, whereas from south of Pescadero, 71.2% of YOY (*n*=125) and 87.0% of juveniles and adults (*n*=900) were blue rockfish. Deacon rockfish were especially dominant off Oregon and Washington (age 0: 98.2%, *n*=55; age 1+: 86.1%, *n*=10,415) but were rarely encountered south of Point Conception (age 0: 0.0%, *n*=24; age 1+: 2.7%, *n*=293).

Comparisons of age-1+ catch composition indicated significant spatial differences in the relative proportions of blue rockfish and deacon rockfish (Fig. 3). Models that

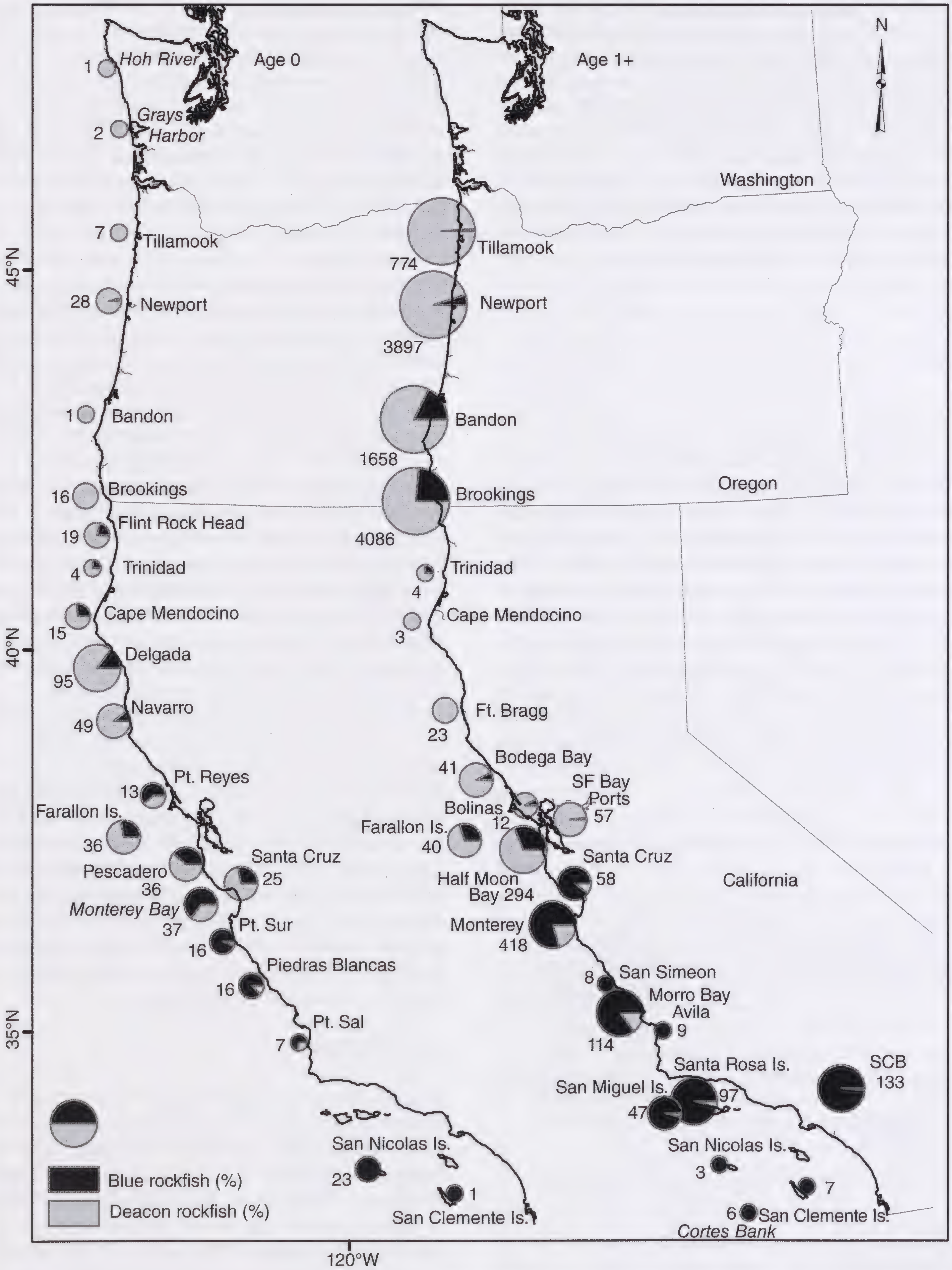

Figure 2

Relative proportion of blue rockfish (*Sebastes mystinus*) and deacon rockfish (*S. diaconus*), including young of the year (age 0) from pelagic surveys and juveniles and adults (age 1 or older [age 1+]) from hook-and-line collections, sampled at designated ports throughout the U.S. Pacific coast (for time periods of sampling, see Table 1). Numbers indicate sample size. SCB=Southern California Bight; SF=San Francisco.

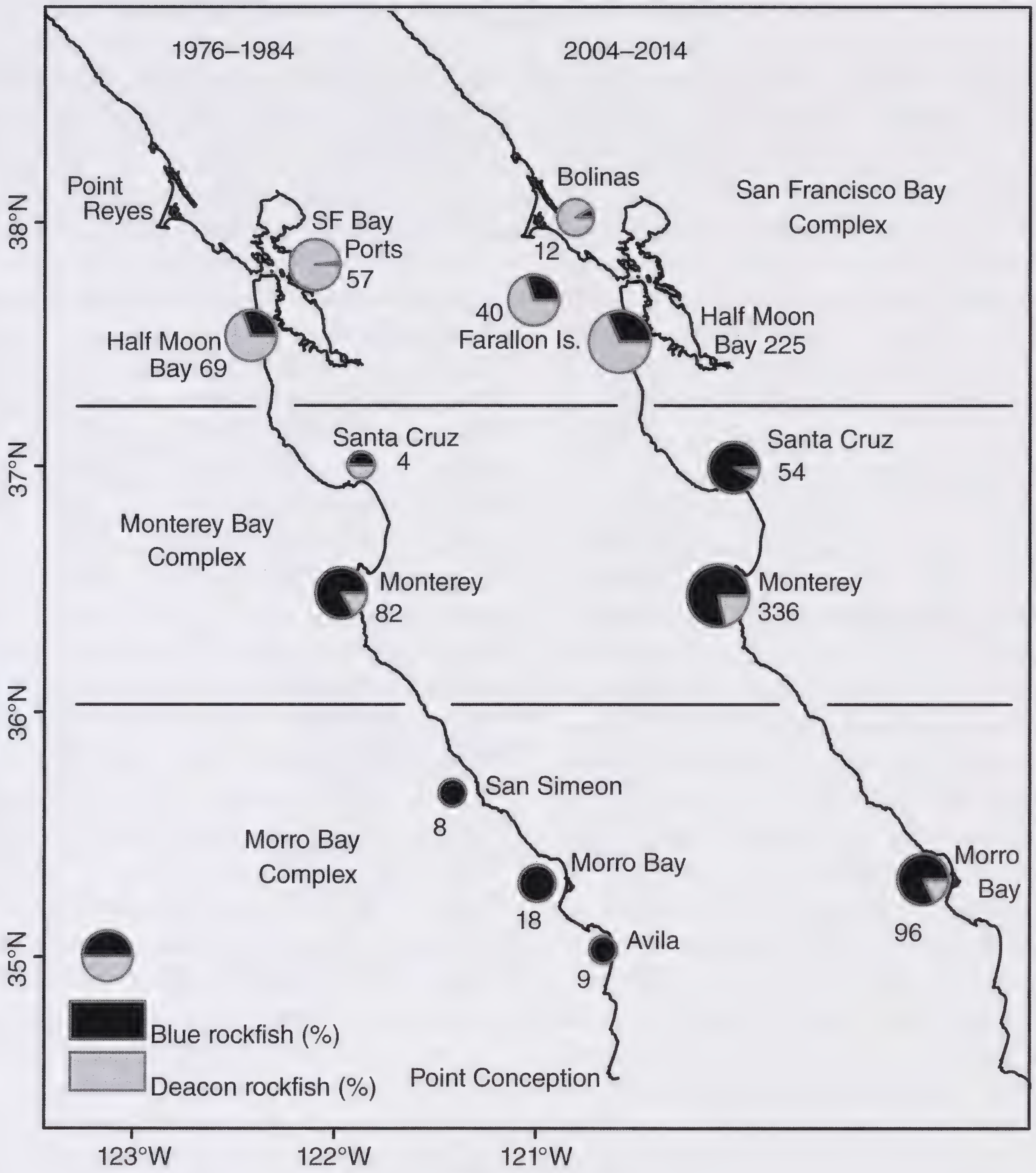

Figure 3

Relative proportion of juvenile and adult blue rockfish (*Sebastes mystinus*) and deacon rockfish (*S. diaconus*) from hook-and-line collections sampled historically (1976–1984) and recently (2004–2014) at designated ports in central California. Numbers indicate sample size.

incorporated observation-level random effects and included only location (AIC: 98.5) or location and time period (difference in AIC values [ΔAIC]: 1.9) as covariates had similar fits that were not improved when an interaction term was added (ΔAIC: 22.2). A significantly greater proportion of blue rockfish was caught in the Monterey Bay Complex (80.7%, n=476) than in the San Francisco Bay Complex (26.3%, n=403) (Z=–5.41, P<0.001); however, no significant difference in proportion of blue rockfish was found between catch compositions from the Monterey Bay and Morro Bay Complexes (87.0%, n=131, Z=1.57, P=0.110). The overall proportion of blue rockfish was not significantly different between historical (1976–1984) and recent (2004–2014) time periods (Z=0.135, P=0.892).

Age and growth

The most parsimonious age and growth model for all data from both species included all 3 distinguishing variables: species, sex, and state (Table 4). Species-sex and sex (only) models had relatively poor fits, but results from them are provided for comparative purposes (Table 4). For both species in both states, females grew slower and reached larger maximum sizes than males (Table 4, Fig. 4). Female blue rockfish and female deacon rockfish from Oregon also had similar estimated growth rates and maximum FLs (Table 4). Off California, both sexes of deacon rockfish grew to larger sizes at slower rates than did both sexes of blue rockfish (Table 4, Fig. 4).

Table 4

The von Bertalanffy growth function (VBGF) parameters and sample sizes (n) for age and growth models that incorporate different combinations of species, sex, and state for blue rockfish (*Sebastes mystinus*), deacon rockfish (*S. diaconus*), and both species. Samples were collected off California and Oregon during 1976–1984 and 2009–2017. The VBGF parameters are the theoretical average maximum length (L_∞), annual growth coefficient (k), and theoretical age at size zero (t_0). Sex and region information were combined for blue rockfish sampled off California. Models were compared by using Akaike information criterion (AIC). Values for L_∞ are give in fork length in centimeters. Also provided is the difference in AIC values between each model and the best fit (0) model (ΔAIC).

Model	ΔAIC	Species	Sex	State	n	$L\infty$	k	t_0
California-Oregon (Sex)	1567.9	Both	Female	California, Oregon	4989	37.5	0.21	–1.44
		Both	Male	California, Oregon	1545	30.3	0.38	–0.39
California-Oregon (Species-Sex)	1239.6	Blue	Female	California, Oregon	1463	37.1	0.19	–1.84
		Blue	Male	California, Oregon	217	30.5	0.30	–0.76
		Deacon	Female	California, Oregon	3526	37.8	0.22	–1.27
		Deacon	Male	California, Oregon	1328	30.3	0.39	–0.38
California-Oregon (Species-Sex-State)	0.0	Blue	Female	Oregon	931	38.0	0.20	2.13
		Blue	Male	Oregon	131	30.6	0.34	–1.02
		Blue	Female	California	532	35.5	0.15	–3.04
		Blue	Male	California	86	31.0	0.19	–2.30
		Deacon	Female	Oregon	3198	37.8	0.21	–1.51
		Deacon	Male	Oregon	1174	30.1	0.40	–0.69
		Deacon	Female	California	328	41.3	0.13	–2.81
		Deacon	Male	California	154	33.8	0.16	–2.91
California (Sex)	0.0	Blue	Female	California	404	34.5	0.17	–2.64
California (Sex-Region)	60.1	Blue	Female	Northern California	292	34.2	0.17	–2.44
		Blue	Female	Southern California	112	37.3	0.13	–5.08

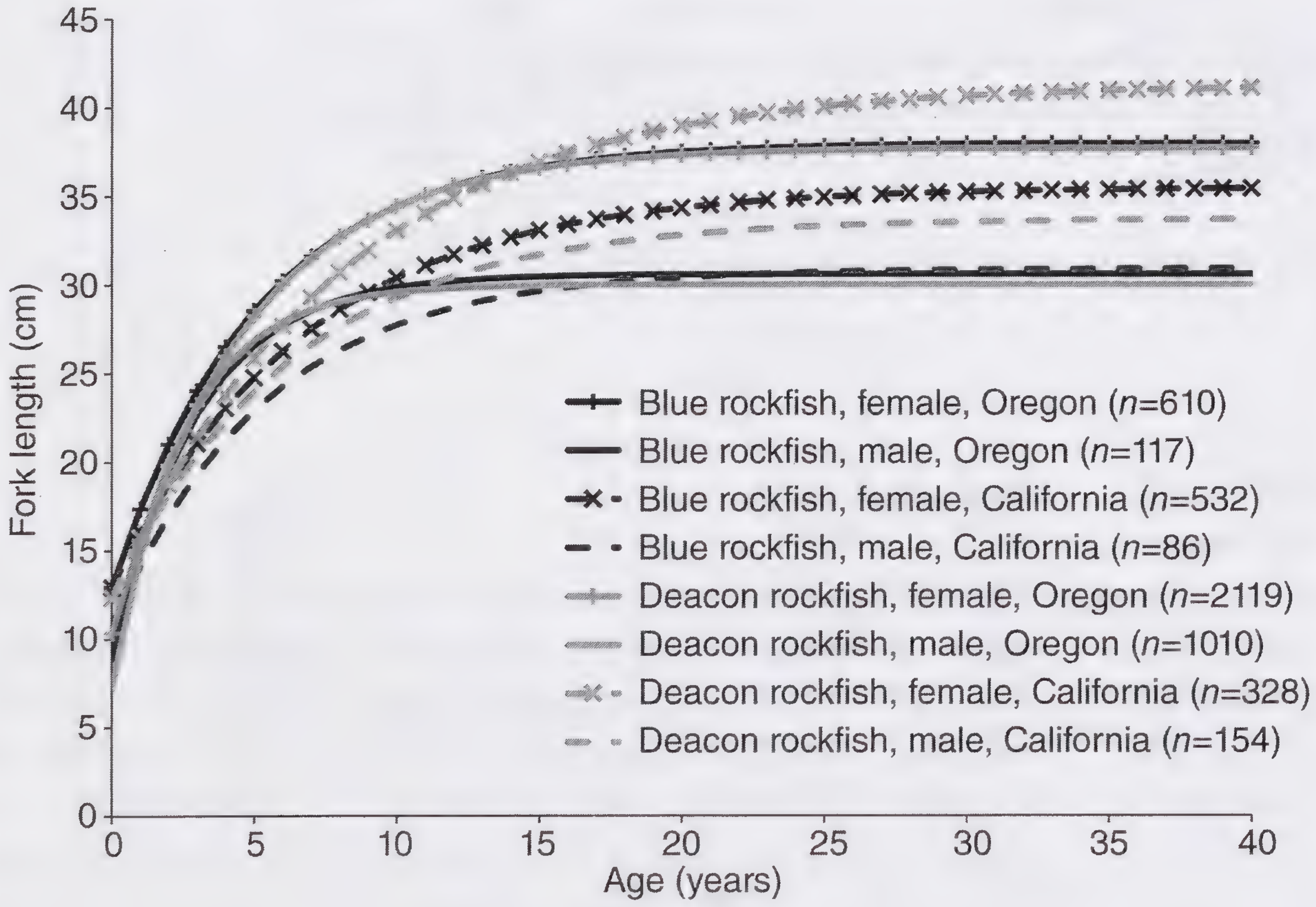

Figure 4

Fitted von Bertalanffy growth curves for female and male blue rockfish (*Sebastes mystinus*) and deacon rockfish (*S. diaconus*) collected from waters of either California or Oregon. For time periods of sampling, see Table 1. n=number of samples.

Female blue rockfish in southern California grew slower and reached slightly larger maximum sizes than female blue rockfish in northern California (Table 4); however, the more parsimonious model combined fish from both regions (Table 4). The combined model was heavily influenced by the larger sample size in the northern California data set, and the growth parameter estimates of the statewide and northern California models were nearly the same (Table 4).

Discussion

The use of genetic techniques to provide species identification of archived samples and to validate recent field identifications of blue rockfish and deacon rockfish enabled the separate estimation and comparison of biological traits for these 2 sister species. The application of this information to a recent stock assessment for the blue rockfish and deacon rockfish complex provided contextual information for the interpretation of reference points and uncertainty in the stock assessment model results and for the development of management recommendations and research needs (Dick et al.[3]). Furthermore, the high concordance between visual and genetic identification provides more evidence that blue rockfish and deacon rockfish can be reliably distinguished in the field by using morphological characteristics and coloration (Burford and Bernardi, 2008; Frable et al., 2015). The methods used in our study could be applied to other groups to estimate biological traits for taxa that are part of species complexes, particularly in situations in which recent sample data are sparse but archived collections of otoliths or other material exist to inform growth and demographic studies.

The results of our population genetic analyses confirm blue rockfish and deacon rockfish as a pair of significantly diverged species with limited intraspecific geographic structure (e.g., little to no population structure within the species range). Geographically, blue rockfish and deacon rockfish are highly differentiated from each other in regions throughout California and Oregon. Within species, however, deacon rockfish appear to be panmictic from southern California to central Oregon, indicating high gene flow over ~1300 km. For blue rockfish, although high gene flow also was the dominant pattern, some potential genetic structure was found, with significant differentiation between Oregon and the Channel Islands (the most geographically distant sampling sites in this study). In addition, Half Moon Bay was differentiated from most regions between the Farallon Islands off San Francisco and southern California (a distance of ~430 km). However, no evidence indicates a straightforward pattern of isolation by distance. Our results are generally consistent with a model of gene flow over hundreds of kilometers. The extent to which factors such as genotyping error and pooling of individuals over collection years affect our results is unclear. Further research might examine fine-scale population genetic patterns (e.g., temporal, latitudinal, depth, and distance from shore) within this species to validate and identify the drivers of this apparent differentiation. In addition, whether blue rockfish and deacon rockfish interbreed when they are sympatric is not known, and future studies may attempt to identify potential hybrids between the 2 species.

The high concordance between visual and genetic species identification in this study demonstrates the efficacy of distinguishing blue rockfish and deacon rockfish by either method alone. However, there is room for improvement in both methods. Additional distinguishing characteristics for deacon rockfish might improve the accuracy of visual identification in the field; in contrast, blue rockfish were only rarely misidentified. The genetic species identification process was designed to be rigorous, but the 9-marker species identification panel was developed by using high-quality DNA extracted from modern samples. Degradation and cross-contamination of DNA among the historical samples rendered many such samples unusable, leading to the use of greatly increased sample sizes to compensate for widespread instances of missing data. Data derived from low-quality samples are prone to allelic dropout and elevated genotyping error; hence, a conservative approach was taken during the species identification process to account for these limitations and for the lack of corroborative visual identifications for historical samples.

Blue rockfish and deacon rockfish are sympatric between Morro Bay and central Oregon, but there appears to be an abrupt shift in relative abundance between Monterey Bay and San Francisco Bay. Previous work has indicated that adults of both species had a high degree of spatial overlap and similar relative abundance in the approximately 450-km stretch of coast from Cape Arago, Oregon, to Cape Mendocino, California (Burford, 2009), and that the distribution of newly recruited juveniles shifted slightly to the south of the adult distribution (Burford et al., 2011b). However, several differences between this and prior studies may confound direct comparisons, including collection years (1976–1984 and 2004–2017 in our study versus 1999–2002 in previous studies), methods (scuba, spearing, and hook and line in our study and hook and line in prior studies), and sampling locations (Burford et al.[1]; Burford et al., 2011b). Burford et al. (2011b) suggested that temporal differences in species composition between life stages provide evidence of a southern shift in distribution of deacon rockfish during cold-water years. More data are needed to determine and compare the distribution, abundance, and habitat associations of these species, especially where they co-occur in similar relative abundance and particularly in the broad and poorly sampled region from north of San Francisco to the border of California and Oregon.

There are several sources of potential bias that should be considered when evaluating our species composition results. Data were collected opportunistically from a variety of ports and integrated across seasons and years, adding a degree of spatiotemporal variability that was unaccounted for in the calculation of descriptive statistics. Although the results of regression modeling indicate significant spatial and spatiotemporal differences, relatively few samples were collected for statistical comparisons, especially during the historical time period. Our relatively simple model also did not account for all sources of variability (e.g., fishing depth, hook type, size, selectivity, or bait type), increasing the possibility of Type 1 error.

The results of this study provide species-specific age and growth information for blue rockfish and deacon rockfish by sex and state, filling a life history data gap that has important management implications. Several previous age and growth studies were conducted on blue rockfish and deacon rockfish prior to the description of the complex as 2 separate species, with 4 of these conducted in California (Miller and Geibel, 1973; MacGregor, 1983; Karpov et al., 1995; Laidig et al., 2003) and 2 studies conducted in Oregon (McClure, 1982; Hannah et al.[5]). Because age and growth parameters varied between blue rockfish and deacon rockfish in our study and between sexes of the species complex in prior studies (McClure, 1982; Laidig et al., 2003), direct comparisons of age and growth estimates are limited to those studies that fit separate growth models for females and males.

We found that, in waters of California, deacon rockfish grow to larger sizes at slower rates than blue rockfish. However, our species-specific results are generally consistent with those of Laidig et al. (2003) for the blue rockfish and deacon rockfish complex; they found that males (k=0.195) grew faster than females (k=0.149) but that females reached larger maximum sizes. The oldest assigned and maximum predicted ages (at L_∞) were greater in Laidig et al. (2003) than in our study, most likely because Laidig et al. (2003) included several very large fish (>40 cm FL) in their analysis, whereas such fish were largely absent from our samples.

Growth rates of the blue rockfish and deacon rockfish complex have been reported to be faster for individuals collected off Oregon (McClure, 1982; male: k=0.23; female: k=0.31) than for those collected off California (Laidig et al., 2003), consistent with our results. Concordance with the results of Hannah et al.[5] is unsurprising because their age estimates compose a portion (~10%) of our data for deacon rockfish. However, McClure (1982) reported much larger sizes at age, possibly as a result of the use of surface reads instead of the break-and-burn technique (Laidig et al., 2003; this study), as surface reads may underestimate age in rockfish species (Chilton and Beamish, 1982; Munk, 2001).

Some caveats and considerations are provided to facilitate a thorough evaluation of the results of our age and growth analyses. We had low sample sizes for some of the modeled populations, including male blue rockfish in California and Oregon and deacon rockfish in California, and samples of both species were particularly sparse between San Francisco and the Oregon border. There also were few small juveniles in Oregon and large adults in California, potentially contributing to greater uncertainty in our region-specific estimates of growth parameters (t_0 and L_∞, respectively). Finally, although there was substantial agreement among ages between readers from California and Oregon (49% agreement to the same year), some bias was apparent, with 38% of age assignments reflecting an older age estimated by the California reader relative to the estimate by the Oregon reader (Dick et al.[3]). Because the age estimates were not validated by other methods, the accuracy of each set of reads cannot be evaluated.

Despite these caveats, our results provide a better understanding of the population genetics and life histories of a closely related pair of common, nearshore rockfish species and establish a foundation for future research and management of each species. It has been argued that managing species as a complex, because of data limitations or other factors, is reasonable only if the constituent species have similar life histories and if there is some realistic expectation that they will share similar population responses to fishing (Shertzer and Williams, 2008; Jiao et al., 2009; Cope et al., 2011). When there is evidence to indicate substantially different life histories, and therefore productivity levels, treating the complex as a single stock could raise significant conservation concerns because estimated fishing rates could be unsustainable for the less productive of the constituent species.

The most recent stock assessment treated blue rockfish and deacon rockfish as a complex because of a paucity of reliable species-specific life history, distribution, and abundance data and because of the inability to distinguish the 2 species in historical catch and landings data. The ability to demonstrate that growth was similar for the 2 species (within assessment areas) and to demonstrate that species composition did not vary significantly over time near the region where the greatest shift in abundance has been reported to occur (Dick et al.[3]) were key factors in the adoption of the species complex assessment. Despite these findings, the recent assessment was considered to be more uncertain than a typical single-species stock assessment, as has been the case for other stock assessments of multispecies complexes (e.g., Hicks et al., 2014). As a result, uncertainty buffers between allowed biological catches and overfishing limits that were greater than those for single-species assessments based on data of comparable quality (NMFS[6]) were recommended and adopted by fishery managers.

The information presented from this study can be used to direct future biological and fisheries research so that the life histories (including reproductive biology, which was not addressed in this study), ecological interactions, and needs for management of blue rockfish and deacon rockfish can be better understood. This information is particularly important for groundfish fisheries in the California Current because there remain several instances in which historical data pool 2 (or more) species that are now known to be distinct, such as the vermillion rockfish and sunset rockfish complex (Hyde et al., 2008) and the rougheye rockfish and blackspotted rockfish complex (Gharrett et al., 2005, 2006). Although the stock of blue rockfish and deacon rockfish off California was estimated to be slightly below target biomass and the stock off Oregon was well above the reference target (Dick et al.[3]), the assumption that the status and population trends of the 2 constituent species in each region are similar remains uncertain. The ability to differentiate morphologically similar species and stocks for assessments is largely contingent on the reliability of the approach used to distinguish them in the fishery; however, data collection programs for both commercial and recreational fisheries in some regions have not yet resolved catch and compositional data to the species level. Future research should therefore focus on collection of sex- and species-specific data to facilitate the development of separate stock assessments for each species.

Acknowledgments

We thank the following colleagues for their assistance: S. Beyer, T. Buell, E. Campbell, C. Columbus, L. Correa, A. Dauble, N. Kashef, T. Laidig, M. McFarland, S. Ralston, P. Rankin, K. Sakuma, S. Sogard, D. Stafford, N. Yochum, and M. Yoklavich. Funding was provided by the National Marine Fisheries Service's Improve a Stock Assessment Program. The authors J. Bizzarro and E. Gilbert-Horvath contributed equally to this manuscript.

---

[6] NMFS (National Marine Fisheries Service). 2018. Pacific coast groundfish fishery 2019–2020 harvest specifications and management measures: analytical document organized as a preliminary draft environmental assessment, 118 p. Agenda item E.4, Suppl. rev. attach. 2. Natl. Mar. Fish. Serv., Seattle, WA. [Available from website.]

Literature cited

Akaike, H.
1974. A new look at the statistical model identification. IEEE Trans. Autom. Control 16:716–723.

Anderson, E. C., R. S. Waples, and S. T. Kalinowski.
2008. An improved method for predicting the accuracy of genetic stock identification. Can. J. Fish. Aquat. Sci. 65:1475–1486.

Beamish, R. J.
1979. New information on the longevity of Pacific Ocean perch (*Sebastes alutus*). J. Fish. Res. Board Can. 36:1395–1400.

Belkhir, K. P., P. Borsa, L. Chikhi, N. Raufaste, and F. Bonhomme.
2004. GENETIX 4.05, logiciel sous Windows pour la génétique des populations. Laboratoire génome, populations, interactions. CNRS UMR 5000, Univ. Montpellier II, Montpellier, France. [Available from website.]

Buonaccorsi, V. P., M. Westerman, J. Stannard, C. Kimbrell, E. Lynn, and R. D. Vetter.
2004. Molecular genetic structure suggests limited larval dispersal in grass rockfish, *Sebastes rastrelliger*. Mar. Biol. 145:779–788.

Buonaccorsi, V. P., C. A. Kimbrell, E. A. Lynn, and R. D. Vetter.
2005. Limited realized dispersal and introgressive hybridization influence genetic structure and conservation strategies for brown rockfish, *Sebastes auriculatus*. Conserv. Genet. 6:697–713.

Burford, M. O.
2009. Demographic history, geographical distribution and reproductive isolation of distinct lineages of blue rockfish (*Sebastes mystinus*), a marine fish with a high dispersal potential. J. Evol. Biol. 22:1471–1486.

Burford, M. O., and G. Bernardi.
2008. Incipient speciation within a subgenus of rockfish (*Sebastosomus*) provides evidence of recent radiations within an ancient species flock. Mar. Biol. 154:701–717.

Burford, M. O., G. Bernardi, and M. H. Carr.
2011a. Analysis of individual year-classes of a marine fish reveals little evidence of first-generation hybrids between cryptic species in sympatric regions. Mar. Biol. 158:1815–1827.

Burford, M. O., M. H. Carr, and G. Bernardi.
2011b. Age-structured genetic analysis reveals temporal and geographic variation within and between two cryptic rockfish species. Mar. Ecol. Prog. Ser. 442:201–215.

Campana, S. E., M. C. Annand, and J. I. McMillan.
1995. Graphical and statistical methods for determining the consistency of age determinations. Trans. Am. Fish. Soc. 124:131–138.

Chilton, D. E., and R. J. Beamish.
1982. Age determination methods for fishes studied by groundfish program at the Pacific Biological Station. Can. Spec. Publ. Fish. Aquat. Sci. 60, 102 p.

Cope, J. M., and A. E. Punt.
2011. Reconciling stock assessment and management scales under conditions of spatially varying catch histories. Fish. Res. 107:22–38.

Cope, J. M., J. DeVore, E. J. Dick, K. Ames, J. Budrick, D. L. Erickson, J. Grebel, G. Hanshew, R. Jones, L. Mattes, et al.
2011. An approach to defining stock complexes for U.S. West Coast groundfishes using vulnerabilities and ecological distributions. North Am. J. Fish. Manage. 31:589–604.

Eschmeyer W. N., R. Fricke, and R. van der Laan (eds.).
2017. Catalog of fishes: genera, species, references. [Available from website, accessed October 2017.]

Frable, B. W., D. W. Wagman, T. N. Frierson, A. Aquilar, and B. L. Sidlauskas.
2015. A new species of *Sebastes* (Scorpaeniformes: Sebastidae) from the northeastern Pacific, with a redescription of the blue rockfish, *S. mystinus* (Jordan and Gilbert, 1881). Fish. Bull. 113:355–377.

Gharrett, A. J., A. P. Matala, E. L. Peterson, A. K. Gray, Z. Li, and J. Heifetz.
2005. Two genetically distinct forms of rougheye rockfish are different species. Trans. Am. Fish. Soc. 134:242–260.

Gharrett, A. J., C. W. Mecklenburg, L. W. Seeb, Z. Li, A. P. Matala, A. K. Gray, and J. Heifetz.
2006. Do genetically distinct rougheye rockfish sibling species differ phenotypically? Trans. Am. Fish. Soc. 135:792–800.

Gómez-Uchida, D., E. A. Hoffman, W. R. Ardren, and M. A. Banks.
2003. Microsatellite markers for the heavily exploited canary (*Sebastes pinniger*) and other rockfish species. Mol. Ecol. Notes 3:387–389.

Harms, J. H., J. A. Benante, and R. M. Barnhart.
2008. The 2004–2007 hook and line survey of shelf rockfish in the Southern California Bight: estimates of distribution, abundance, and length composition. NOAA Tech. Memo. NMFS-NWFSC-95, 110 p.

Hess, J. E., P. Chittaro, A. Elz, E. A. Gilbert-Horvath, V. Simon, and J. C. Garza.
2014. Cryptic population structure in the severely depleted cowcod, *Sebastes levis*. Can. J. Fish. Aquat. Sci. 71:81–92.

Hicks, A., C. Wetzel, and J. Harms.
2014. The status of rougheye rockfish (*Sebastes aleutianus*) and blackspotted rockfish (*S. melanostictus*) as a complex along the U.S. West Coast in 2013, 136 p. Pac. Fish. Manage. Counc., Portland, OR. [Available from website.]

Hyde, J. R., C. A. Kimbrell, J. E. Budrick, E. A. Lynn, and R. D. Vetter.
2008. Cryptic speciation in the vermilion rockfish (*Sebastes miniatus*) and the role of bathymetry in the speciation process. Mol. Ecol. 17:1122–1136.

Jiao, Y., C. Hayes, and E. Cortés.
2009. Hierarchical Bayesian approach for population dynamics modelling of fish complexes without species-specific data. ICES J. Mar. Sci. 66:367–377.

Johns, G. C., and J. C. Avise.
1998. Tests for ancient species flocks based on molecular phylogenetic appraisals of *Sebastes* rockfishes and other marine fishes. Evolution 52:1135–1146.

Jordan, D. S., and C. H. Gilbert.
1881. Description of *Sebastichthys mystinus*. Proc. U.S. Natl. Mus. 4:70–72.

Kai, Y., K. Nakayama, and T. Nakabo.
2002. Genetic differences among three colour morphotypes of the black rockfish, *Sebastes inermis*, inferred from mtDNA and AFLP analyses. Mol. Ecol. 11:2591–2598.

Karpov, K. A., D. P. Albin, and W. H. Van Buskirk.
1995. The marine recreational fishery in northern and central California: a historical comparison (1958-86), status of stocks (1980-86), and effects of changes in the California Current. Calif. Dep. Fish Game, Fish Bull. 176, 192 p.

Kimura, D. K., R. R. Mandapat, and S. L. Oxford.
1979. Method, validity, and variability in the age determination of yellowtail rockfish (*Sebastes flavidus*), using otoliths. J. Fish. Res. Board Can. 36:377–383.

Klingbeil, R. A., and E. H. Knaggs.
1976. Southern range extensions of the blue rockfish, *Sebastes mystinus*; the flag rockfish, *S. rubrivinctus*; and the shortbelly rockfish, *S. jordani*. Calif. Fish Game 62(2):160.

Laidig, T. E., D. E. Pearson, and L. L. Sinclair.
2003. Age and growth of blue rockfish (*Sebastes mystinus*) from central and northern California. Fish. Bull. 101:800–808.

Love, M. S.
2011. Certainly more than you want to know about the fishes of the Pacific Coast: a postmodern experience, 650 p. Really Big Press, Santa Barbara, CA.

MacGregor, J. S.
1983. Growth of the blue rockfish (*Sebastes mystinus*). CalCOFI Rep. 24:216–225.

McClure, R. E.
1982. Neritic reef fishes off central Oregon: aspects of life histories and recreational fishery. M.S. thesis, 94 p. Oregon State Univ., Corvallis, OR.

Miller, D. J., and J. J. Geibel.
1973. Summary of blue rockfish and lingcod life histories; a reef ecology study; and giant kelp, *Macrocystis pyrifera*, experiments in Monterey Bay, California. Calif. Dep. Fish Game, Fish Bull. 158, 131 p. [Available from website.]

Munk, K. M.
2001. Maximum ages of groundfishes in waters off Alaska and British Columbia and considerations on age determination. Alaska Fish. Res. Bull. 8:12–21.

Orr, J. W., and S. Hawkins.
2008. Species of the rougheye rockfish complex: resurrection of *Sebastes melanostictus* (Matsubara, 1934) and a redescription of *Sebastes aleutianus* (Jordan and Evermann, 1898) (Teleostei: Scorpaeniformes). Fish. Bull. 106:111–134.

Paetkau, D., R. Slade, M. Burden, and A. Estoup.
2004. Genetic assignment methods for the direct, real-time estimation of migration rate: a simulation-based exploration of accuracy and power. Mol. Ecol. 13:55–65.

Park, S. D. E.
2002. Trypanotolerance in West African cattle and the population genetic effects of selection. Ph.D. thesis, 241 p. Trinity College, Dublin, Ireland. [Available from website.]

Pearse, D. E., L. Wooninck, C. A. Dean, and J. C. Garza.
2007. Identification of northeastern Pacific rockfish using multilocus nuclear DNA genotypes. Trans. Am. Fish. Soc. 136:272–280.

Piry, S., A. Alapetite, J.-M. Cornuet, D. Paetkau, L. Baudouin, and A. Estoup.
2004. GENECLASS2: a software for genetic assignment and first-generation migrant detection. J. Hered. 95:536–539.

Pritchard, J. K., M. Stephens, and P. Donnelly.
2000. Inference of population structure using multilocus genotype data. Genetics 155:945–959.

Quattro, J. M., W. B. Driggers III, J. M. Grady, G. F. Ulrich, and M. A. Roberts.
2013. *Sphyrna gilberti* sp. nov., a new hammerhead shark (Carcharhiniformes, Sphyrnidae) from the western Atlantic Ocean. Zootaxa 3702:159–178.

R Core Team.
2016. R: a language and environment for statistical computing. R Foundation for Statistical Computing, Vienna, Austria. [Available from website, accessed October 2016.]

Rannala, B., and J. L. Mountain.
1997. Detecting immigration by using multilocus genotypes. Proc. Natl. Acad. Sci. U.S.A. 94:9197–9201.

Roques, S., D. Pallotta, J.-M. Sévigny, and L. Bernatchez.
1999. Isolation and characterization of polymorphic microsatellite markers in the North Atlantic redfish (Teleostei: Scorpaenidae, genus *Sebastes*). Mol. Ecol. 8:685–687.

Sakuma, K. M., S. Ralston, and V. G. Wespestad.
2006. Interannual and spatial variation in the distribution of young-of-the-year rockfish (*Sebastes* spp.): expanding and coordinating a survey sampling frame. CalCOFI Rep. 47:127–139.

Sakuma, K. M., J. C. Field, N. J. Mantua, S. Ralston, B. B. Marinovic, and C. N. Carrion.
2016. Anomalous epipelagic micronekton assemblage patterns in the neritic waters of the California Current in spring 2015 during a period of extreme ocean conditions. CalCOFI Rep. 57:163–183.

Schmidt, K. T.
2014. Life history changes in female blue rockfish, *Sebastes mystinus*, before and after overfishing in central California. M.S. thesis, 94 p. Calif. State Univ., Monterey Bay, CA.

Sekino, M., N. Takagi, M. Hara, and H. Takahashi.
2000. Microsatellites in rockfish *Sebastes thompsoni* (Scorpaenidae). Mol. Ecol. 9:634–636.

Shertzer, K. W., and E. W. Williams.
2008. Fish assemblages and indicator species: reef fishes off the southeastern United States. Fish. Bull. 106:257–269.

Tellier, F., J. M. A. Vega, B. R. Broitman, J. A. D. Vásquez, M. Valero, and S. Faugeron.
2011. The importance of having two species instead of one in kelp management: the *Lessonia nigrescens* complex. Cah. Biol. Mar. 52:455–465.

Tuckey, T., N. Yochum, J. Hoenig, J. Lucy, and J. Cimino.
2007. Evaluating localized vs. large-scale management: the example of tautog in Virginia. Fisheries 32:21–28.

Venerus, L. A., J. E. Ciancio, C. Riva-Rossi, E. A. Gilbert-Horvath, A. E. Gosztonyi, and J. C. Garza.
2013. Genetic structure and different color morphotypes suggest the occurrence and bathymetric segregation of two incipient species of *Sebastes* off Argentina. Naturwissenschaften 100:645–658.

von Bertalanffy, L.
1957. Quantitative laws in metabolism and growth. Q. Rev. Biol. 32:217–231.

National Marine
Fisheries Service
NOAA

Fishery Bulletin
established in 1881

Spencer F. Baird
First U.S. Commissioner
of Fisheries and founder
of *Fishery Bulletin*

Spatial variability in the fecundity of Atlantic sharpnose sharks (*Rhizoprionodon terraenovae*) in the northern Gulf of Mexico

William B. Driggers III (contact author)[1]
Matthew D. Campbell[1]
Kristin M. Hannan[2]
Eric R. Hoffmayer[1]
Christian M. Jones[1]
James A. Sulikowski[3]

Email address for contact author: william.driggers@noaa.gov

[1] Mississippi Laboratories
Southeast Fisheries Science Center
National Marine Fisheries Service, NOAA
3209 Frederic Street
Pascagoula, Mississippi 39567

[2] Riverside Technology Inc.
Mississippi Laboratories
Southeast Fisheries Science Center
National Marine Fisheries Service, NOAA
3209 Frederic Street
Pascagoula, Mississippi 39567

[3] School of Mathematical and Natural Sciences
Arizona State University
4701 West Thunderbird Road
Glendale, Arizona 85306

Abstract—Spatial variability in life history characteristics, including age at maturity, growth rates, and reproductive periodicity, has been documented for a number of shark species. Among causative factors hypothesized to induce dissimilarities, clinal variation is most often linked to temperature. However, if spatial differences in prey abundance were the causative factor, it could be masked by clinal variation. If prey abundance is the actual driver, intraspecific differences should be evident over a broad longitudinal range (i.e., constant water temperature) characterized by a demarcation of low and high productivity. In this study, Atlantic sharpnose sharks (*Rhizoprionodon terraenovae*) were collected for 1 year throughout the northern Gulf of Mexico (GOM) by using standardized bottom longline gear. Reproductive data were collected from 253 gravid females, and mean (4.2 versus 3.4 embryos) and median (4 versus 3 embryos) brood sizes were higher west of longitude 88°W than to the east. Based on fisheries survey data, spatial trends in abundance of Atlantic croaker (*Micropogonias undulatus*), a common prey item, coincided with that of Atlantic sharpnose sharks, and both were more abundant west of 88°W. Although differences in brood sizes appear minor, potential lifetime reproductive output for females was calculated to be over 2 times greater in the western versus the eastern GOM.

An essential component for appropriately assessing and effectively managing populations of elasmobranchs (sharks, skates, and rays) is accurate species-specific information pertaining to reproductive biology (Walker, 2005). However, intraspecific differences in important reproductive characteristics, such as size at maturity, size at birth, and reproductive periodicity, have been shown to occur within some shark species (e.g., Lombardi-Carlson et al., 2003; Sulikowski et al., 2007; Driggers and Hoffmayer, 2009), complicating the management process. For example, Yamaguchi et al. (2000) examined the reproductive biology of starspotted smooth-hounds (*Mustelus manazo*) at 5 locations in the eastern Pacific Ocean and found that individuals at the northernmost sampling location had a higher age and size at maturity and longer reproductive cycle than conspecifics at lower latitudes. Because of the importance of reproductive data as inputs into demographic and population models (Cortés, 2002), it is imperative to describe the life history of a species at various locations throughout its range and to not assume that these variables are spatially constant.

Intraspecific variability in reproductive traits for sharks has largely been documented along latitudinal clines (e.g., Taniuchi et al., 1993; Horie and Tanaka, 2002; Lombardi-Carlson et al., 2003). For example, Parsons (1993) examined several reproductive characteristics for bonnetheads (*Sphyrna tiburo*) off the west coast of Florida in the western North Atlantic Ocean and reported, among other differences, that females at a higher latitude had a longer gestation period, had a larger size at maturity, and gave birth to larger offspring than females at a lower latitude.

Manuscript submitted 26 August 2019.
Manuscript accepted 20 February 2020.
Fish. Bull. 118:51–62 (2020).
Online publication date: 4 March 2020.
doi: 10.7755/FB.118.1.5

The views and opinions expressed or implied in this article are those of the author (or authors) and do not necessarily reflect the position of the National Marine Fisheries Service, NOAA.

Similarly, Colonello et al. (2007) found that female angular angel sharks (*Squatina guggenheim*) off the coast of South America mature at larger sizes at higher latitudes than conspecifics at lower latitudes.

Among studies that have documented spatial disparities in reproductive traits, several hypotheses focusing on regional differences in prey availability, temperature, mortality, and energetics related to migrations have been formulated (e.g., Parsons, 1993; Yamaguchi et al., 2000; Sulikowski et al., 2007; Walker, 2007). Most studies that have examined geographic variability in reproductive traits for sharks have in total (e.g., Yamaguchi et al., 2000; Colonello et al., 2007) or in part (e.g., Lombardi-Carlson et al., 2003; Walker, 2007) attributed observed disparities to differences in water temperatures associated with changes in latitude. Cope (2006) suggested that, in addition to latitudinal variability as a cause for different reproductive traits, regional differences in fishing pressure could result in varying intraspecific life histories. This hypothesis was later supported by Walker (2007), who suggested that length-selective fishing mortality resulted in differences in sizes at maturity and maternity for gummy sharks (*Mustelus antarcticus*) at 2 locations off southern Australia. Walker (2007) also stated that another possible explanation was differences in environmental conditions between sampling locations. Parsons (1993) considered variability in prey abundance along the west coast of Florida as a cause of the reproductive differences found in bonnetheads; however, he concluded differences were related to seasonal variation in water temperature and photoperiod.

If spatial differences in prey availability could result in variability in important life history characteristics, one would expect to see differences within a shark species inhabiting a broad longitudinal range (i.e., constant water temperature) characterized by a strong demarcation of relatively low and high productivity. Therefore, the objective of this study was to compare the fecundity of Atlantic sharpnose sharks (*Rhizoprionodon terraenovae*) between the eastern and western areas of the northern Gulf of Mexico (GOM), with the former region characterized by low productivity and the latter by high productivity (e.g., Riley, 1937).

Materials and methods

Atlantic sharpnose sharks were collected throughout the northern GOM from April through October 2011 by using standardized bottom longline gear. The gear consisted of 1.8 km of 4.0-mm diameter monofilament mainline with 100 gangions constructed with a size 148 snap, 3.7 m of 3.0-mm diameter monofilament leader, and a 15/0 circle hook (model no. 39960D, O. Mustad & Son A.S.[1], Gjovik, Norway) and was set at depths of 7–459 m (mean: 99.8 m [standard deviation (SD) 100.0]). Four bottom longline vessels sampled throughout U.S. waters of the northern GOM for 20 days in each month. Biologists on each vessel were requested to retain and freeze a maximum of 10 female sharks greater than 650 mm fork length (FL) during each 20-d period. This size was selected because it approximately coincided with estimates of size at 50% maturity for female Atlantic sharpnose sharks (e.g., Driggers et al.[2]). All collected sharks were subsequently transported to the National Marine Fisheries Service, Southeast Fisheries Science Center, Mississippi Laboratories for reproductive data collection.

Hoffmayer et al. (2013) proved that there is significant seasonal variability in the timing of ovulation, mating, and parturition among Atlantic sharpnose sharks in the northern GOM. Because reproductive asynchrony could obfuscate potential differences in the reproductive biology of this species when comparing the eastern and western GOM, we chose to focus solely on fecundity. To assess fecundity, each specimen was thawed and an incision was made from the cloaca to the pectoral girdle. An incision was then made in each uterus, and contents were removed. The number of embryos in the uteri was then counted, and the sex of all individuals within each brood was recorded. Unfertilized eggs and embryos in very early stages of development were not included in counts because of the uncertainty of correctly identifying a blastodisc in frozen and subsequently thawed specimens. Therefore, as development of embryos within a single brood is synchronous and thus negates potential bias associated with omitting all uterine eggs in the blastodisc stage of development, only macroscopically visible embryos were included in counts.

To determine the longitude that would be used to separate the northern GOM into eastern and western areas, a map of catch per unit of effort (CPUE, defined as number of Atlantic sharpnose sharks caught per 100 hook hours) for all longline sets was generated with the mapping software Surfer (vers. 11.5.1069; Golden Software, Golden, CO), by using a point kriging function and semivariogram model with a linear component, anisotropy angle of 0, and anisotropy ratio and variogram slope of 1. Using the same methods, we mapped the distribution of Atlantic croaker (*Micropogonias undulatus*), a primary prey species of Atlantic sharpnose sharks in the northern GOM (Bethea et al., 2006; Higgs et al., 2012), to examine similarities in the spatial abundance of predator and prey. Data on catch of Atlantic croaker (defined as kilograms per trawl hour) were retrieved from the Southeast Area Monitoring and Assessment Program (SEAMAP) Trawl Survey database (available from website, accessed May 2017). Trawl survey data, which were collected yearly during June–July and October–November, were limited to the years 2009–2014 and collected by using the methods described by Rester[3].

---

[1] Mention of trade names or commercial companies is for identification purposes only and does not imply endorsement by the National Marine Fisheries Service, NOAA.

[2] Driggers, W. B., III, E. R. Hoffmayer, J. K. Carlson, and J. Loefer. 2013. Reproductive parameters for Atlantic sharpnose sharks (*Rhizoprionodon terraenovae*) from the western North Atlantic Ocean. Southeast Data, Assessment, and Review SEDAR34-WP-30, 5 p. [Available from website.]

Prior to conducting analyses, data related to the lengths of all females captured, to the lengths of all gravid females, and to brood size were investigated to identify outliers on a regional basis. Outliers were defined as those points that were 3 times above or below the upper and lower quartiles. We employed t-tests to compare region-specific lengths of female sharks for all captured individuals, length of gravid females, and brood sizes. If data did not adhere to the assumptions of normality and homoscedasticity, as indicated by skewness, kurtosis, and F-tests, data were log-transformed. If the assumptions of parametric statistics were still not met after transformation, Mann–Whitney W (length) and Kolmogorov–Smirnov (distributions) tests were used to compare data between regions. Regression analyses were used to examine the relationship between maternal body length and brood size for each region and for both areas combined. Length and brood-size data were log-transformed, and analysis of covariance (ANCOVA) was used to determine if there was a difference in regression lines between the eastern and western GOM. To describe the relationship for combined areas, 21 regression models were fitted, and the one selected to best represent the relationship was chosen on the basis of the highest coefficient of determination (r^2). Further, to examine if there was a latitudinal effect on brood size, a linear regression was conducted on latitude of capture of gravid females and the associated brood sizes. All statistical tests were considered significant at an α of 0.05.

To examine the potential lifetime reproductive output (PLRO) of 2 hypothetical female Atlantic sharpnose sharks with disparate mean brood sizes, the total number of offspring attributable to these females over their lifetimes was calculated. On the basis of the results of Driggers et al.[2] and Hoffmayer et al. (2013), it was assumed that in the northern GOM, female Atlantic sharpnose sharks mature at an age of 1.3 years, have a maximum longevity of 17.2 years, reproduce annually, and gestate for approximately 1 year and that the sex ratio of embryos is 1:1. Although mating occurs over a protracted period, the earliest stages of gestation are generally observed in July (Hoffmayer et al., 2013). Therefore, we assumed that the age at first maternity for Atlantic sharpnose sharks in the northern GOM was 3 years. We made a simplifying assumption that the mortality rate of the female, her offspring, and subsequent generations was zero throughout each hypothetical female's lifetime. Additionally, we did not account for the relationship between length and brood size because growth models specific to the eastern and western regions of the northern GOM were not available to back-transform size at age.

To test if prey availability affects the fecundity of female Atlantic sharpnose sharks in the eastern and western GOM, we examined condition factor between the 2 regions. Because body weight of females can vary widely depending on reproductive condition (e.g., state of maturity, degree of embryo development, and brood size) and female Atlantic sharpnose sharks are not completely reproductively synchronous in the northern GOM, we examined the condition factor of males as a proxy. Males were better suited for this analysis because their body weight is less affected by reproductive state. Although testis weight does vary throughout the year, the resolution of scales used in the field was 0.25 kg; therefore, seasonal change in testis weight was considered undetectable. Furthermore, because weights were obtained at sea, vessel motion could have increased measurement error. As a result, regression analyses were applied to length and weight data from all males, with the exception of specimens that were damaged because of depredation, and the model best describing the relationship was fit to the data. The best fit model was considered that with the highest r^2. Those data points that had Studentized residuals greater than 2 in absolute value were considered outliers and were removed from the data set.

Region-specific length–weight regressions were then analyzed by using ANCOVA after parameters were log-transformed. Additionally, non-transformed length and weight data were used to calculate Fulton's condition factor (K), as outlined in Froese (2006). Prior to calculating K, all length and weight data, which were originally recorded in millimeters and kilograms, were converted into centimeters and grams, respectively. Despite trying multiple transformations (e.g., cube root, log, and square), these data did not conform to the assumptions of parametric statistics. As a result, Mann–Whitney W (length) and Kolmogorov–Smirnov (distributions) tests were used to compare K values between regions.

Data from males collected on the West Florida Shelf were also used to examine latitudinal effects on body length and weight. Data were limited to males for the reasons outlined previously and were truncated to include only mature sharks captured east of 85°W. Males were considered mature if they had calcified claspers that freely rotated 180° and had a functional rhipidion. The spatial limit was applied so that males outside of the latitudinal cline were excluded (i.e., shelf axis runs north–south and excludes an expansive east–west component). Regression analyses were performed with latitude and body size (i.e., length and weight) as the independent and dependent variables, respectively.

Results

A total of 1173 longline sets were conducted (Fig. 1), resulting in the capture of 4082 Atlantic sharpnose sharks. Females (number of specimens [n]=1943) and males (n=1910) ranged in size from 278 to 992 mm FL (mean: 726.6 mm FL [SD 104.3]) and from 296 to 915 mm FL (mean: 726.9 mm FL [SD 86.7]), respectively (sex and lengths were not recorded for 229 individuals because of

---

[3] Rester, J. K. (ed.). 2011. SEAMAP environmental and biological atlas of the Gulf of Mexico, 2009. Gulf States Mar. Fish. Comm., no. 198, 74 p. [Available from website.]

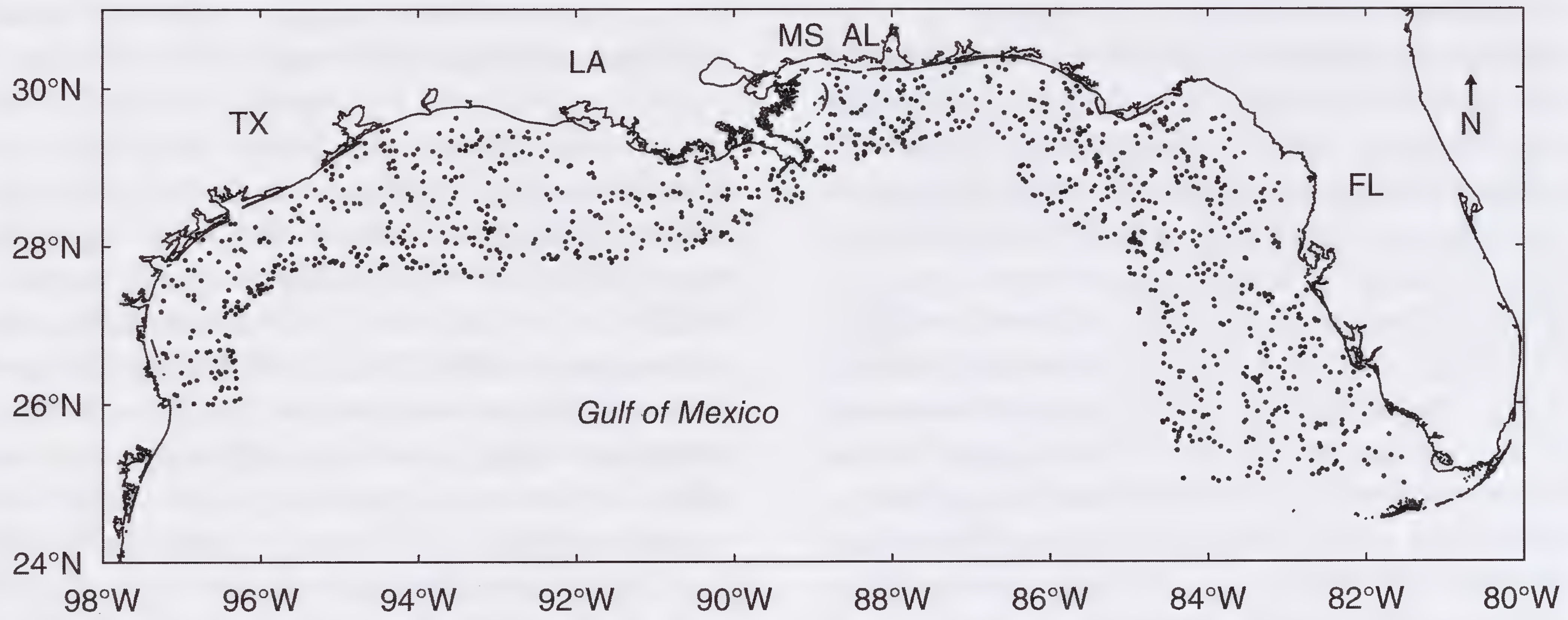

Figure 1

Map showing the distribution of 1173 bottom longline sets conducted to capture Atlantic sharpnose sharks (*Rhizoprionodon terraenovae*) in the northern Gulf of Mexico during April–October 2011. Black circles indicate individual longline set locations. Gear was set in waters off Texas (TX), Louisiana (LA), Mississippi (MS), Alabama (AL), and Florida (FL).

damage inflicted by other sharks). In the western GOM, females ranged in size from 278 to 992 mm FL (n=1590; mean: 735.1 mm FL [SD 102.7]), and in the eastern GOM, they ranged from 390 to 884 mm FL (n=353; mean: 687.8 mm FL [SD 102.6]). Males ranged in size from 296 to 915 mm FL in the western GOM (n=1697; mean: 731.8 mm FL [SD 86.0]) and from 384 to 860 mm FL in the eastern GOM (n=213; mean: 684.1 mm FL [SD 84.5]). Visual inspection of the interpolated distribution map based on CPUE of Atlantic sharpnose sharks throughout the northern GOM revealed a distinct discontinuity in the abundance of the species at approximately 88°W (Fig. 2). Therefore, for the purposes of subsequent analyses, the western GOM was defined as that region west of 88°W, and the eastern GOM was defined as the area east of 88°W.

Outliers omitted from the data sets were limited to one 278-mm-FL female collected in the western GOM and 3 broods of 8 embryos observed in the eastern GOM. Mean sizes of females captured in the eastern and western GOM were 687.9 mm FL (SD 102.6) and 735.1 mm FL (SD 102.1), respectively, and there was a significant difference in the median sizes of females captured in the 2 regions: 695 mm FL in the east and 760 mm FL in the west (W=356,870, P<0.01) (Fig. 3). Similarly, among gravid female specimens examined (n=253), there was a significant difference in the mean FL among individuals in the eastern (752.2 mm FL [SD 64.5]) and western (779.5 mm FL [SD 54.2]) GOM (t=−2.89, P<0.01) (Fig. 4). There was no significant relationship between latitude and body length (F=1.26, P=0.27) or weight (F=2.27, P=0.14) for mature males on the West Florida Shelf.

During this study, brood-size data were collected from 253 gravid females (eastern GOM: n=42; western GOM: n=211), ranging in size from 647 to 935 mm FL (mean: 775.0 mm FL [SD 56.8]) (Fig. 5). There was no significant difference between the slopes (F=2.12, P=0.15) or intercepts (F=0.27, P=0.61) for the relationship between maternal FL and brood size when comparing specimens collected in the eastern and western GOM. There was a significant positive relationship between maternal FL and brood size (F=305.88, P<0.01, r^2=0.55) for data collected from the combined areas (Fig. 6); this relationship was described by the following equation:

$$brood\ size = \sqrt{-58.1084 + 0.000129332 \times FL^2}.$$

However, there was no significant relationship between latitude and brood size (F=2.48, P=0.12, r^2=0.58) (Fig. 7). There was a significant difference in the mean brood size between the 2 regions (t=−3.03, P<0.01) with mean brood sizes of 3.4 embryos (SD 1.4) and 4.2 embryos (SD 1.7) in the eastern and western GOM, respectively. When including those values considered outliers (i.e., 3 broods of 8 embryos from the eastern GOM), data were not normally distributed and could not be made so through transformation. However, median brood size was significantly lower (W=5398.5, P=0.02) among gravid females in the eastern GOM (median: 3 embryos; mean: 3.7 embryos [SD 1.8]) than in the western GOM (median: 4 embryos; mean: 4.2 embryos [SD 1.7]) (Fig. 5).

Under the previously stated assumptions, the total number of offspring the hypothetical females would give birth to in the eastern and western GOM during each mother's lifetime (first generation of each mother's 15 broods [B1–15, G1]) would be 51 and 63, respectively. During the 17-year lifespans of the 2 hypothetical females, the 5 generations associated with each female's first brood (i.e., B1, G1–5) would produce 64.1 young in the eastern

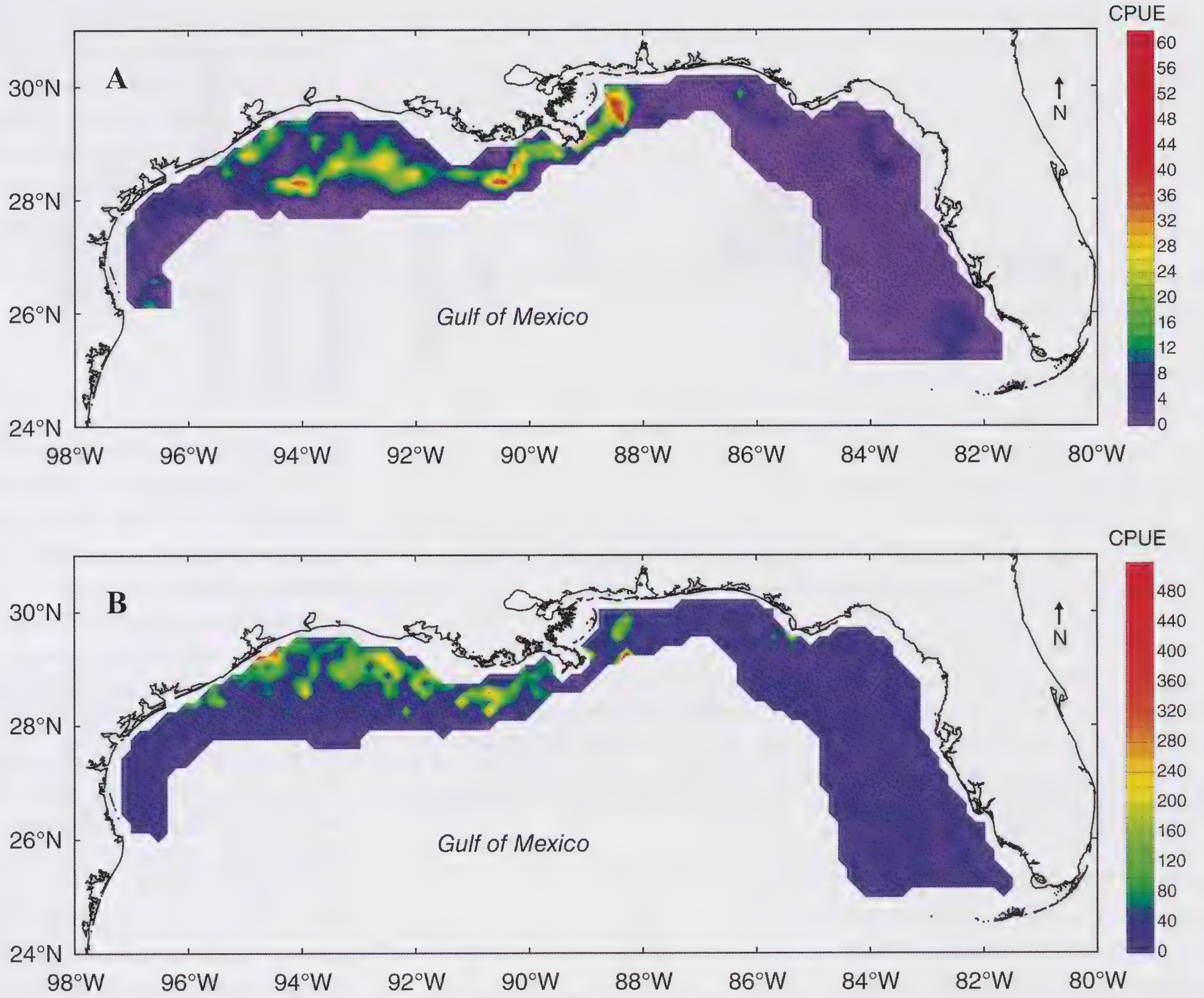

Figure 2

(**A**) Map showing spatial abundance of Atlantic sharpnose sharks (*Rhizoprionodon terraenovae*) collected with bottom longline gear in the northern Gulf of Mexico during April–October 2011. The catch per unit of effort (CPUE), the number of sharks caught per 100 hook hours, is used as the measure of abundance and is indicated with the color scale. (**B**) Map showing spatial abundance of Atlantic croaker (*Micropogonias undulatus*), a common prey item of Atlantic sharpnose sharks, in the northern Gulf of Mexico based on data from Southeast Area Monitoring and Assessment Program trawl surveys conducted during 2009–2014. The CPUE, the weight in kilograms of croaker caught per hour, is indicated with the color scale.

GOM and 152.1 young in the western GOM. Further, over each mother's lifetime, all broods (B1–15) and generations (G1–5) would result in a PLRO of 394.2 and 814.0 pups in the eastern and western GOM, respectively (Table 1).

A total of 1910 males were collected throughout the study area. For 1884 of those specimens, length and weight data were available. Data collected from 97 individuals were determined to be outliers (i.e., Studentized residuals >2) and were removed from subsequent analyses. Of the retained data, male body sizes were 296–915 mm FL and 0.2–5.6 kg in the western GOM (n=1587) and 384–860 mm FL and 0.5–4.2 kg in the eastern GOM (n=200). Neither length nor weight data met the assumptions of parametric statistics; however, the median length (755 versus 691 mm FL; W=219,880, P<0.01) and weight (3.3 versus 2.4 kg; W=235,136, P<0.01) of males were greater in the western GOM than in the eastern GOM. There was no significant difference in the slope of regression lines between log FL and log weight for male Atlantic sharpnose sharks in the 2 regions (F=0.62, P=0.43); however, the intercepts were significantly different (F=123.78, P<0.01), indicating that, at a given FL, the mean weight of a male Atlantic sharpnose shark is greater in the western GOM than in the eastern GOM.

Condition factors for male Atlantic sharpnose sharks in the western GOM ranged from 0.56 to 1.03 (mean: 0.78 [SD 0.08]) and from 0.62 to 0.88 in the eastern GOM (mean: 0.73 [SD 0.06]). The median K values were significantly different between the 2 regions (W=228636, P<0.01), with the median K being higher in the western GOM (0.72) than in the eastern GOM (0.78). Similarly, the distribution of K values in the 2 regions were significantly different (Kolmogorov–Smirnov statistic: 4.84, $P<0.01$) (Fig. 8). Visual inspection of the interpolated distribution map based on CPUE of Atlantic croaker throughout the region revealed a distinct discontinuity in the abundance of the species at approximately 88°W; the same spatial discontinuity was observed for CPUE of Atlantic sharpnose sharks (Fig. 2).

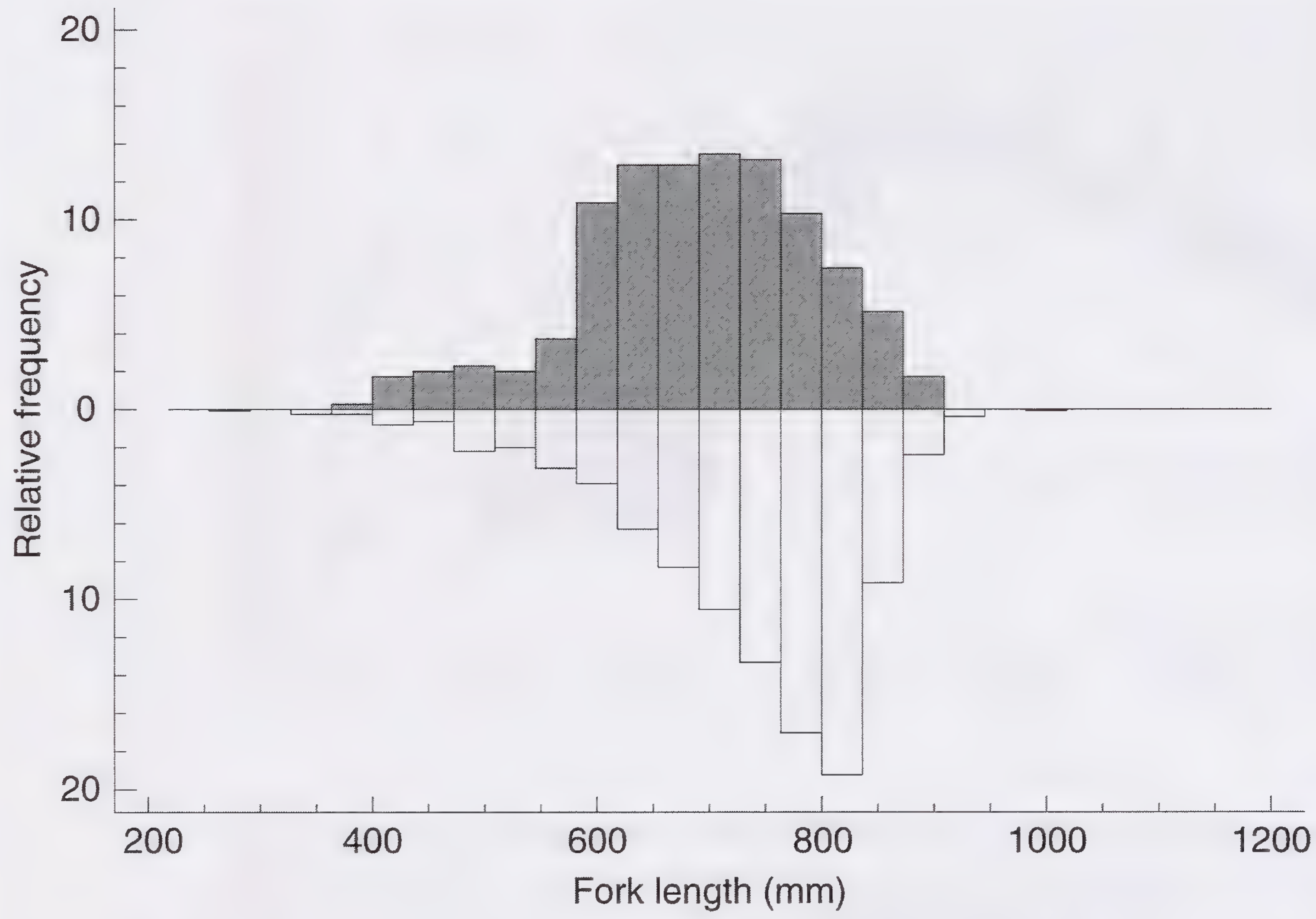

Figure 3

Length–frequency histogram of female Atlantic sharpnose sharks (*Rhizoprionodon terraenovae*) captured in the northern Gulf of Mexico during this study between April and October 2011. Gray and white bars represent individuals captured in the eastern (number of specimens [*n*]=353) and western (*n*=1590) Gulf of Mexico, respectively. The eastern and western regions of the Gulf of Mexico are separated by the longitude 88°W.

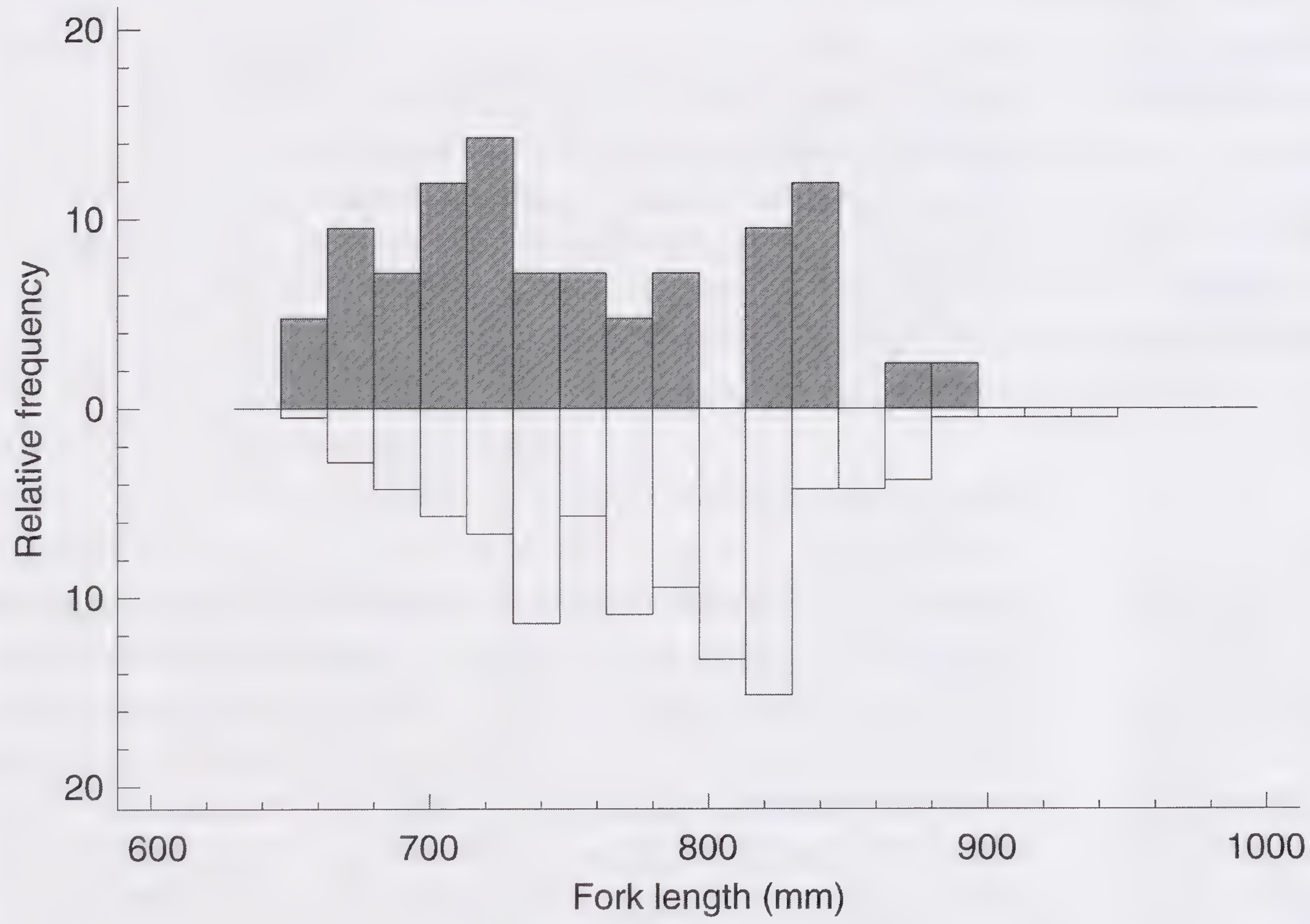

Figure 4

Length–frequency histogram of gravid female Atlantic sharpnose sharks (*Rhizoprionodon terraenovae*) captured between April and October 2011 in the northern Gulf of Mexico and examined during this study. Gray and white bars represent individuals captured in the eastern (number of specimens [*n*]=42) and western (*n*=211) Gulf of Mexico, respectively. The eastern and western regions of the Gulf of Mexico are separated by the longitude 88°W.

Discussion

The phenomenon of spatial variation in the reproductive biology of elasmobranchs has been demonstrated by a number of studies, with many authors hypothesizing that this variability is primarily related to temperature and is therefore often associated with latitudinal gradients (e.g., Menni and Lessa, 1998; Yamaguchi et al., 2000; Tovar-Ávila et al., 2007). To our knowledge, the first evidence for temperature-based spatial variability among elasmobranch conspecifics is attributable to Olsen (1954), who demonstrated that, among other differences, female topes (*Galeorhinus galeus*) ovulated 3 months earlier off Australia and gave birth 1 month earlier off Tasmania, in warmer areas compared with cooler areas. Similarly, Springer (1960) stated that female sandbar sharks (*Carcharhinus plumbeus*) in the western North Atlantic Ocean likely have smaller pups and give birth at a later date in cooler versus warmer waters. Conversely, Lombardi-Carlson et al. (2003) found that bonnetheads within the GOM have larger sizes at birth in cooler waters. However, Lombardi-Carlson et al. (2003) also reported that bonnetheads inhabiting higher latitudes gave birth at a later date, similar to what Springer (1960) suggested for sandbar sharks.

Unlike in other studies, the differences in brood sizes observed in our study could not be explained by temperature. To examine if temperature was responsible for differences in brood size, we took 2 approaches: 1) direct comparison of the relationship between brood size and latitude and 2) comparison of mature male body size along the West Florida Shelf as a proxy to determine if there was an increase in body size along

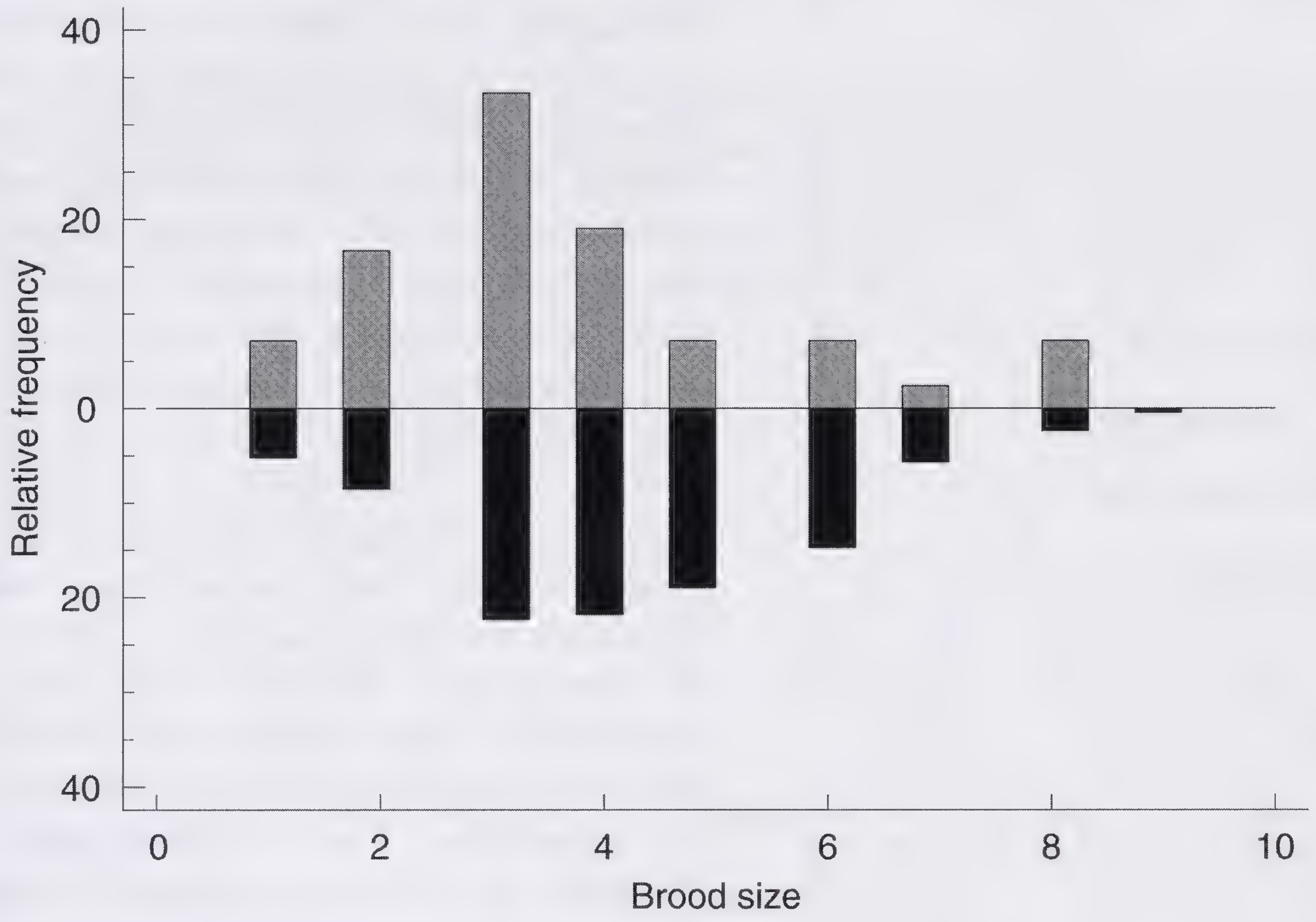

Figure 5

Frequency distributions of brood size for gravid female Atlantic sharpnose sharks (*Rhizoprionodon terraenovae*) captured in the northern Gulf of Mexico during this study in April–October 2011. Gray and black bars represent broods examined from the eastern (number of specimens [*n*]=42) and western (*n*=211) Gulf of Mexico, respectively. The eastern and western regions of the Gulf of Mexico are separated by the longitude 88°W.

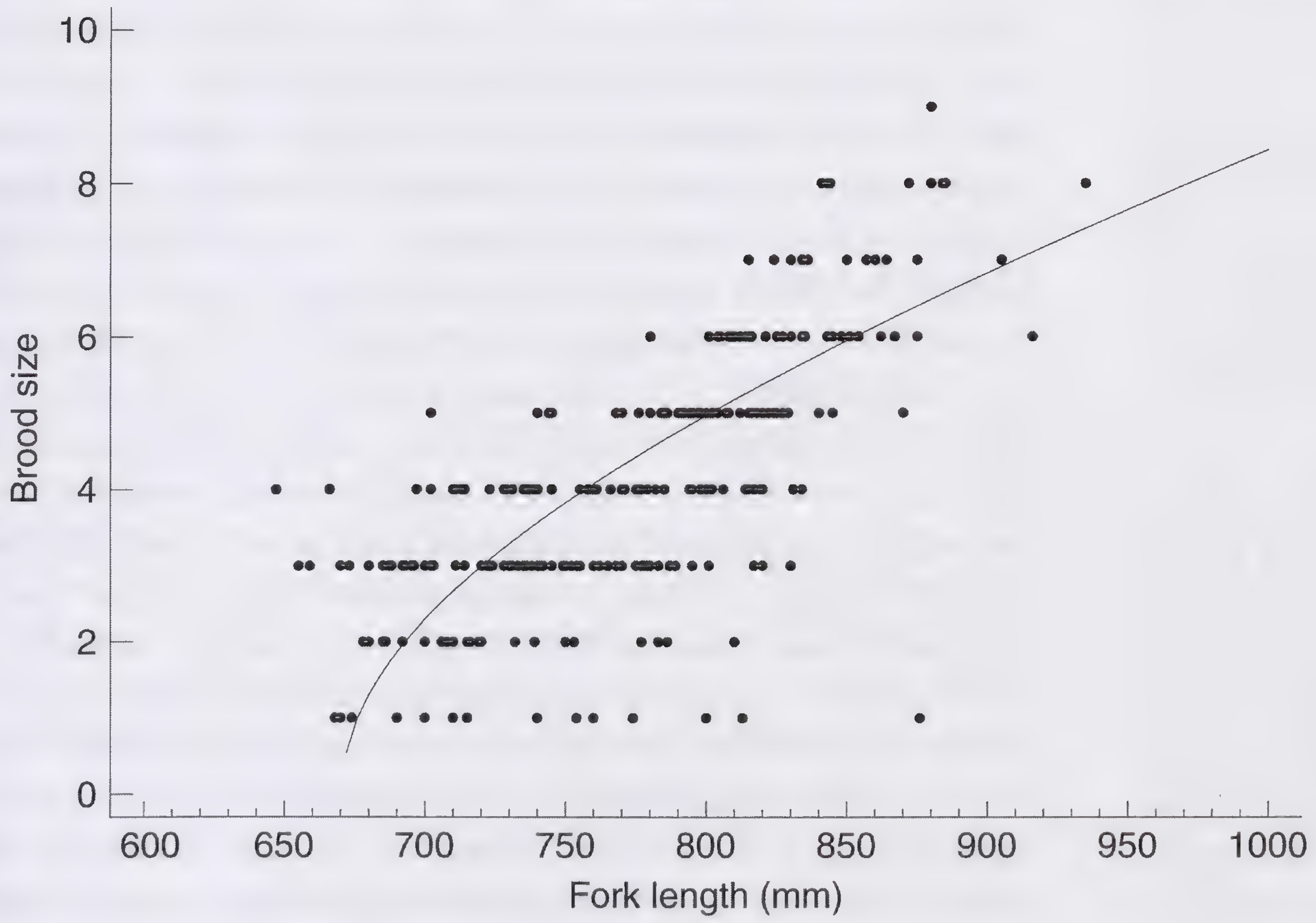

Figure 6

Relationship between maternal fork length and brood size for Atlantic sharpnose sharks (*Rhizoprionodon terraenovae*) collected in the northern Gulf of Mexico during this study between April and October 2011.

the latitudinal cline. Recall that males were analyzed to avoid the confounding issues of female body weight changing throughout the reproductive cycle (e.g., embryos in varying states of development). In addition, we chose to use mature males as a proxy for females to remove spatial variability in the number of young of the year and juveniles that could potentially obfuscate trends we were examining. By using only mature individuals, we limited this analysis to individuals that were approaching the growth asymptote. Although it would have been ideal to examine females, we were able to assign maturity status to males on the basis of non-lethal, external examinations, eliminating the need to sacrifice females and rely on subjective maturity assignments that could have resulted in inclusion of nulliparous individuals or those that were entering their first reproductive cycle as mature individuals.

In the case of the relationship between brood size and latitude of capture, there was no significant relationship between the 2 variables. Similarly, there was no significant difference in the length and weight of mature males along the West Florida Shelf over latitudes ranging from approximately 25°N to 30°N. Furthermore, although a significant relationship existed between size and fecundity for Atlantic sharpnose sharks in the combined areas, the results of the ANCOVA indicate no significant difference in the brood size of similarly sized females in the eastern and western GOM. However, the mean and median sizes of females were larger in the western GOM.

The homogeneity in body length of Atlantic sharpnose sharks across the West Florida Shelf is not consistent with what has been observed for bonnetheads, which are reported to be larger with increasing latitude off the west coast of Florida (Parsons, 1993; Lombardi-Carslon et al., 2003). The disparity between our results and those of Parsons (1993) and Lombardi-Carslon et al. (2003) is likely related to the migratory habits between the 2 species. For example, on the basis of acoustic monitoring, Heupel et al. (2006) reported that bonnetheads in Charlotte Harbor, Florida, are resident within estuaries proximal to the monitoring site and rarely make long-distance seasonal migrations. This finding is supported by tag-recapture data and genetic analyses indicating that bonnetheads have a fine-scale population structure in the eastern GOM and that, when migrating from a specific estuary, they move into

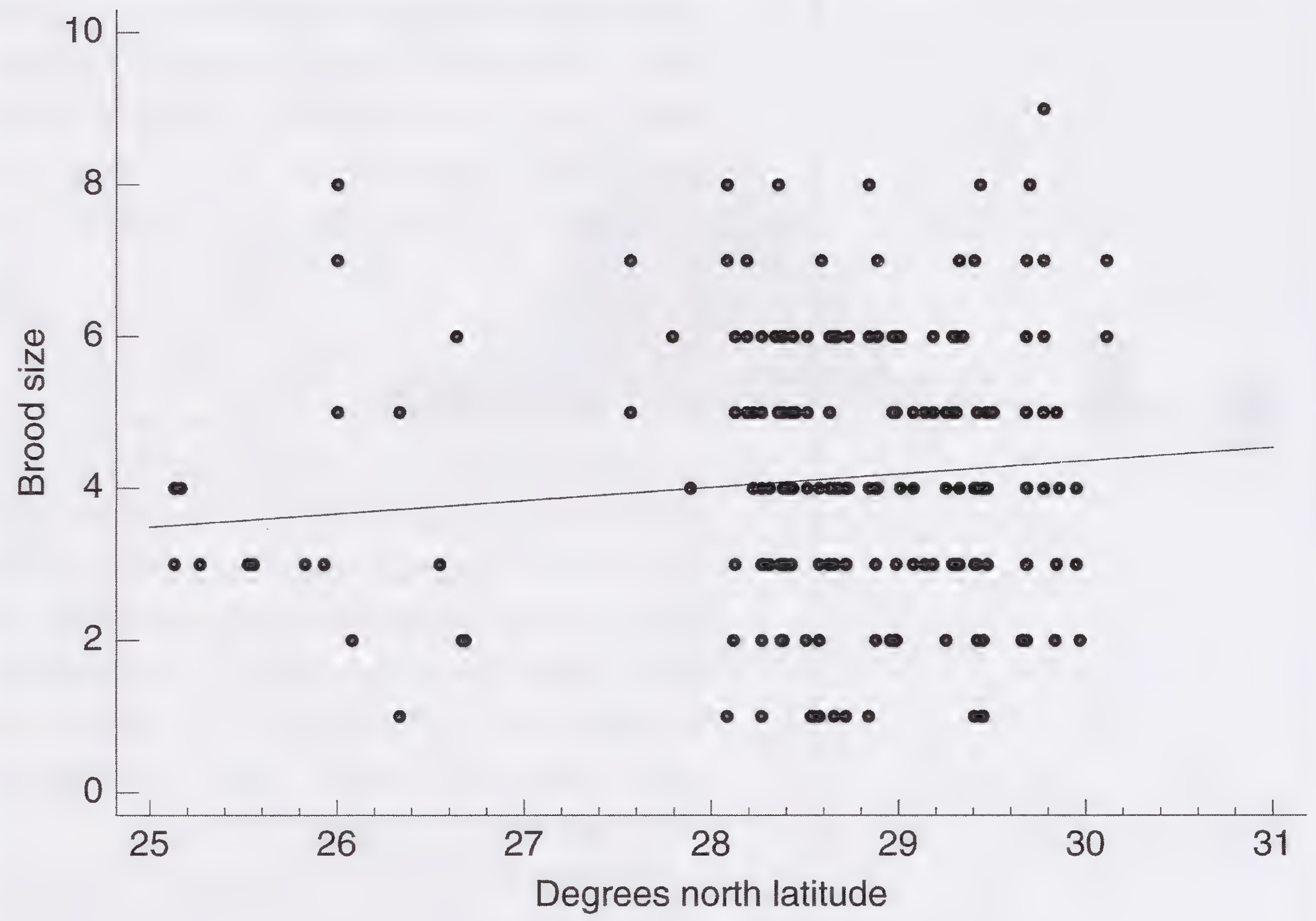

Figure 7

Relationship between latitude of capture and brood size for female Atlantic sharpnose sharks (*Rhizoprionodon terraenovae*) collected in the northern Gulf of Mexico during this study between April and October 2011.

neighboring systems (Tyminski et al.[4]; Portnoy et al., 2015; Fields et al., 2016). Unlike for bonnetheads, no fine-scale population structure has been observed for Atlantic sharpnose sharks in the northern GOM (Heist et al., 1996; Davis et al., 2019) and tag-recapture data show relatively larger scale movements in the region compared with those of bonnetheads (Tyminski et al.[4]; Deacy[5]). If brood size is affected by temperature, the phenomenon would be expected to be most evident in a species, such as bonnetheads, that has been shown to make limited movements outside of spatially discrete areas along a latitudinal cline.

Despite no evidence of latitudinal variability in the fecundity of Atlantic sharpnose sharks being found in our study and for bonnetheads by Lombardi-Carlson et al. (2003), such a trend has been identified for other species. For example, Chen et al. (1981) found higher brood sizes of Japanese spurdogs (*Squalus japonicus*) with increasing latitude between 2 sampling locations in the Indo-Pacific along a latitudinal cline of approximately 350 km. Other species for which similar trends of larger broods associated with increasing latitude have been observed include the shortspine dogfish (*S. mitsukurii*) and gummy shark (Lenanton et al., 1990; Taniuchi et al., 1993), along latitudinal clines of approximately 125–930 km. Conversely, Yamaguchi et al. (2000) found that the brood size of starspotted smooth-hounds decreased with latitude in similarly sized females over a latitudinal cline of approximately 1800 km. However, Yamaguchi et al. (2000) also noted a significant positive relationship between maternal length and brood size, a relationship that has been established for numerous shark species (e.g., Ford, 1921), and reported that females at higher latitudes attained longer lengths than conspecifics at lower latitudes. We found neither a difference in size-specific fecundity of Atlantic sharpnose sharks along the West Florida Shelf nor a difference in body size along a latitudinal cline of approximately 600 km. However, we did find significant differences in these characteristics between the eastern and western GOM, indicating a factor other than latitude or temperature is responsible for the observed differences.

Although our sampling occurred over a period of only 1 year, it is possible that the higher fecundity of Atlantic sharpnose sharks in the western GOM versus the eastern GOM is a density-dependent response to a past reduction in population size within that region. Rose et al. (2001) reviewed density dependence among fish species, defined compensatory changes as those that increase or decrease population growth when density is low and high, respectively, and stated that depensatory changes slow population growth rates at low densities. Studies of density-dependent change in shark populations have largely focused on temporal differences in growth rates, size and age at maturity, and fecundity for affected populations (e.g., da Silva and Ross[6]; Sminkey and Musick, 1995; Sosebee, 2005). For example, Taylor and Gallucci (2009) determined that, for spiny dogfish (*Squalus acanthias*) in the northeast Pacific Ocean, age at maturity decreased while fecundity increased over a 60-year period. Carlson and Baremore (2003) compared data on the life history of Atlantic sharpnose sharks published between 1979 and 1984 with direct estimates obtained from necropsies and vertebral analysis from 1998 to 2001 and found that, although size and age at maturity decreased and growth rates increased between the 2 periods, no change was evident in size at parturition or fecundity.

If the differences we observed in fecundity between the eastern and western GOM were related to a change in population density, fecundity should have been highest in the area of lowest adult abundance or of highest adult mortality. However, results of our study indicate that

---

[4] Tyminski, J. P., R. E. Hueter, and J. Morris. 2013. Tag-recapture results of bonnethead (*Sphyrna tiburo*) and Atlantic sharpnose (*Rhizoprionodon terraenovae*) sharks in the Gulf of Mexico and Florida coastal waters. Southeast Data, Assessment, and Review SEDAR34-WP-31, 13 p. [Available from website.]

[5] Deacy, B. 2018. Personal commun. Southeast Fish. Sci. Cent., Natl. Mar. Fish. Serv., 3500 Delwood Beach Rd., Panama City, FL 32408-7403.

[6] da Silva, H. M., and M. R. Ross. 1993. Reproductive strategies of spiny dogfish, *Squalus acanthias*, in the NW Atlantic. ICES CM 1993/G:51, 18 p. [Available from website.]

Table 1

Potential lifetime reproductive output (PLRO) of 2 hypothetical female Atlantic sharpnose sharks (*Rhizoprionodon terraenovae*) in the eastern and western regions of the northern Gulf of Mexico. The numbers of pups in the columns on either side of the age column represent the brood size (B1–15) attributable to each female (first generation, G1) and her female offspring (subsequent 4 generations, G2–G5) throughout the 17-year lifespan of the original 2 hypothetical females. The eastern and western regions of the Gulf of Mexico are separated by the longitude 88°W.

Western region					Age (years)	Eastern region				
					0					
					1					
					2					
				$4.2_{B1,G1}$	3	$3.4_{B1,G1}$				
				$4.2_{B2,G1}$	4	$3.4_{B2,G1}$				
				$4.2_{B3,G1}$	5	$3.4_{B3,G1}$				
			$8.8_{B1,G2}$	$4.2_{B4,G1}$	6	$3.4_{B4,G1}$	$5.8_{B1,G2}$			
			$8.8_{B2,G2}$	$4.2_{B5,G1}$	7	$3.4_{B5,G1}$	$5.8_{B2,G2}$			
			$8.8_{B3,G2}$	$4.2_{B6,G1}$	8	$3.4_{B6,G1}$	$5.8_{B3,G2}$			
		$18.5_{B1,G3}$	$8.8_{B4,G2}$	$4.2_{B7,G1}$	9	$3.4_{B7,G1}$	$5.8_{B4,G2}$	$9.8_{B1,G3}$		
		$18.5_{B2,G3}$	$8.8_{B5,G2}$	$4.2_{B8,G1}$	10	$3.4_{B8,G1}$	$5.8_{B5,G2}$	$9.8_{B2,G3}$		
		$18.5_{B3,G3}$	$8.8_{B6,G2}$	$4.2_{B9,G1}$	11	$3.4_{B9,G1}$	$5.8_{B6,G2}$	$9.8_{B3,G3}$		
	$38.9_{B1,G4}$	$18.5_{B4,G3}$	$8.8_{B7,G2}$	$4.2_{B10,G1}$	12	$3.4_{B10,G1}$	$5.8_{B7,G2}$	$9.8_{B4,G3}$	$16.7_{B1,G4}$	
	$38.9_{B2,G4}$	$18.5_{B5,G3}$	$8.8_{B8,G2}$	$4.2_{B11,G1}$	13	$3.4_{B11,G1}$	$5.8_{B8,G2}$	$9.8_{B5,G3}$	$16.7_{B2,G4}$	
	$38.9_{B3,G4}$	$18.5_{B6,G3}$	$8.8_{B9,G2}$	$4.2_{B12,G1}$	14	$3.4_{B12,G1}$	$5.8_{B9,G2}$	$9.8_{B6,G3}$	$16.7_{B3,G4}$	
$81.7_{B1,G5}$	$38.9_{B4,G4}$	$18.5_{B7,G3}$	$8.8_{B10,G2}$	$4.2_{B13,G1}$	15	$3.4_{B13,G1}$	$5.8_{B10,G2}$	$9.8_{B7,G3}$	$16.7_{B4,G4}$	$28.4_{B1,G5}$
$81.7_{B2,G5}$	$38.9_{B5,G4}$	$18.5_{B8,G3}$	$8.8_{B11,G2}$	$4.2_{B14,G1}$	16	$3.4_{B14,G1}$	$5.8_{B11,G2}$	$9.8_{B8,G3}$	$16.7_{B5,G4}$	$28.4_{B2,G5}$
$81.7_{B3,G5}$	$38.9_{B6,G4}$	$18.5_{B9,G3}$	$8.8_{B12,G2}$	$4.2_{B15,G1}$	17	$3.4_{B15,G1}$	$5.8_{B12,G2}$	$9.8_{B9,G3}$	$16.7_{B6,G4}$	$28.4_{B3,G5}$
Total PLRO=814.0 pups						Total PLRO=394.2 pups				

Atlantic sharpnose sharks are most abundant in the western GOM, where fecundity is the highest.

Spatial differences in the abundance of Atlantic sharpnose sharks were evident with greater abundance west than east of 88°W. The clear demarcation in abundance is similar to that reported for nurse sharks (*Ginglymostoma cirratum*) by Hannan et al. (2012), who found that nurse sharks were most abundant east of 88°W and largely absent to the west of that longitude. The authors hypothesized that the distribution of nurse sharks was driven primarily by the presence of hard-bottom substrate. Similarly, Portnoy et al. (2014), using genetic analyses of nuclear encoded microsatellites and mitochondrial DNA, described the population structure of blacknose sharks (*Carcharhinus acronotus*) in the western North Atlantic Ocean and reported a barrier to gene flow in the northern GOM corresponding with the Mississippi River Delta, in close proximity to 88°W. Portnoy et al. (2014) went on to speculate that the outflow of freshwater from the Mississippi River created a barrier to movement across the GOM for the stenohaline blacknose shark. Results of genetic analyses of Atlantic sharpnose sharks indicates that there is one genetic stock of the Atlantic sharpnose shark throughout the northern GOM (Heist et al., 1996; Todd et al., 2004; Davis et al., 2019). However, of the 118 tagged Atlantic sharpnose sharks for which recapture data were available from previous studies, only 3 individuals moved between the eastern and western GOM (Kohler et al., 1998; Bethea and Grace[7]; Hendon et al.[8]). Therefore, demarking the eastern and western GOM at 88°W is well supported and coincided with a discontinuity in the distribution of the predominant prey of Atlantic sharpnose sharks.

The diet of Atlantic sharpnose sharks is primarily composed of teleosts, which have made up approximately 66% of the identifiable remains in examinations of stomach contents (Cortés, 1999). Bethea et al. (2006) examined ontogenetic differences in the diet of Atlantic sharpnose sharks in the eastern GOM and reported that the Atlantic croaker was the most commonly identified prey within adult stomachs (6.5% index of relative importance [IRI]; all other identified species had an IRI ≤2.4%) despite their absence among the 7 most abundant prey species that were present in the study area. Higgs et al. (2012) examined the diet of

---

[7] Bethea, D. M., and M. A. Grace. 2013. Tag and recapture data for Atlantic sharpnose, *Rhizoprionodon terraenovae*, and bonnethead shark, *Sphyrna tiburo*, in the Gulf of Mexico and US South Atlantic: 1998–2011. Southeast Data, Assessment, and Review SEDAR34-WP-04, 19 p. [Available from website.]

[8] Hendon, J. M., E. R. Hoffmayer, and G. R. Parsons. 2013. Tag and recapture data for Atlantic sharpnose, *Rhizoprionodon terraenovae*, and bonnethead, *Sphyrna tiburo*, sharks caught in the northern Gulf of Mexico from 1998–2011. Southeast Data, Assessment, and Review SEDAR34-WP-33, 8 p [Available from website.]

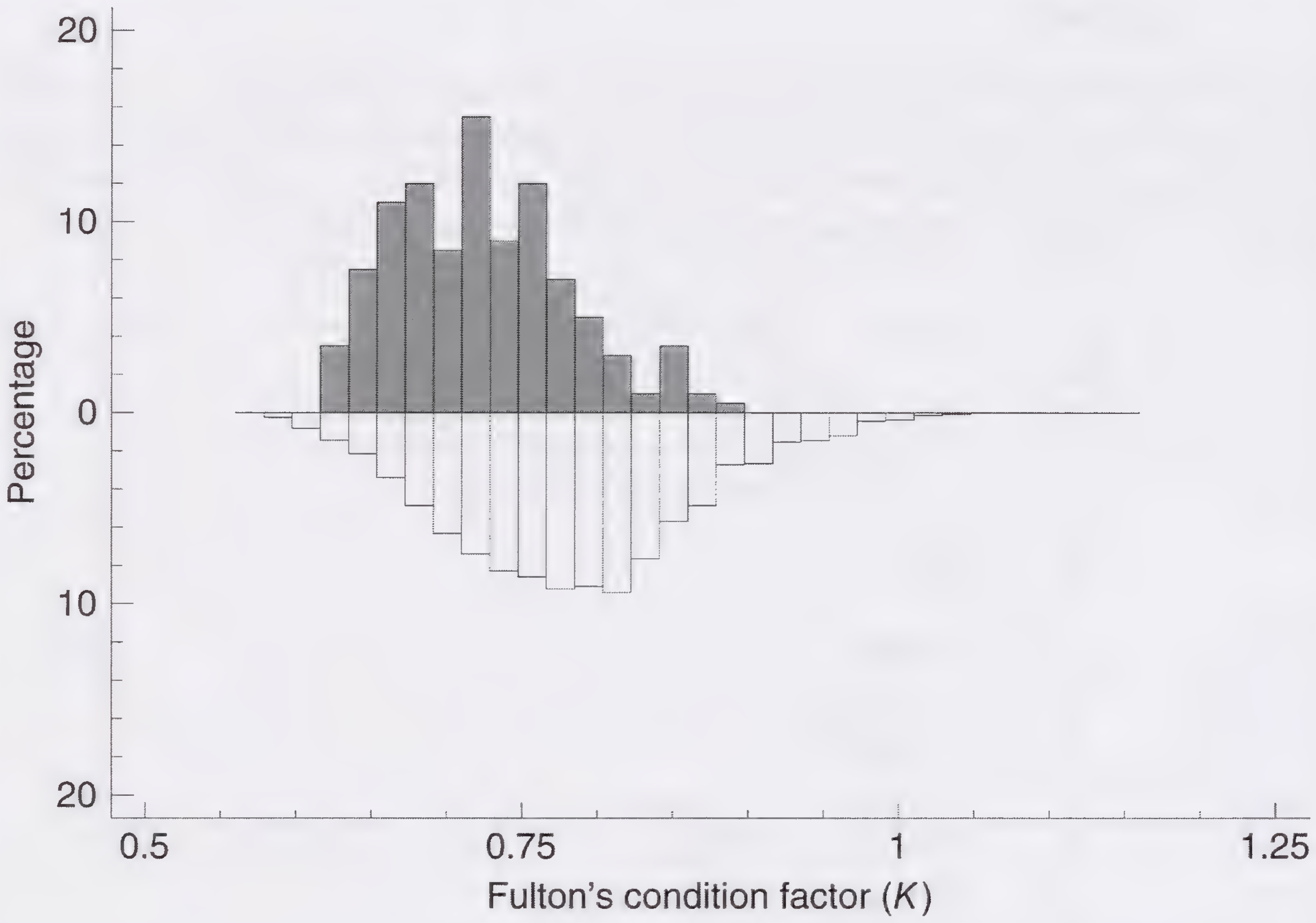

Figure 8

Fulton's condition factor (*K*) of male Atlantic sharpnose sharks (*Rhizoprionodon terraenovae*), plotted for specimens from the eastern Gulf of Mexico (n=200, gray bars) and for those from the western Gulf of Mexico (n=1583, white bars). Sharks were collected between April and October 2011. The eastern and western regions of the Gulf of Mexico are separated by the longitude 88°W.

Atlantic sharpnose sharks in the western GOM and, like Bethea et al. (2006), found the Atlantic croaker to be the dominant prey species (reported to have the highest IRI of all species, but no value was given). Results of these studies indicate that the Atlantic croaker is a preferred prey species of Atlantic sharpnose sharks and, as such, the similarity in the distributions of predator and prey reported herein are not unexpected.

In terms of CPUE during SEAMAP trawl surveys, among species that are potential prey for Atlantic sharpnose sharks, the Atlantic croaker ranks 16th in the eastern GOM (1.82 kg/h) and 1st in the western GOM (91.60 kg/h). Further, among the 15 most frequently caught potential prey species during SEAMAP trawl surveys in the 2 regions, the CPUE of prey was almost 3 times greater in the western GOM (174.62 kg/h) than in the eastern GOM (64.66 kg/h) (Pollack and Hanisko[9]). Given the strong spatial relationship between Atlantic sharpnose sharks and Atlantic croaker, prey availability appears to be a more plausible explanation of the observed differences in brood size between regions.

The higher abundance of prey in the western GOM had 2 noticeable effects on Atlantic sharpnose sharks in that region: the condition factor of male Atlantic sharpnose sharks (and females by proxy) was higher in the western GOM and both sexes attained larger sizes in that region. Although there was a significant relationship between maternal length and brood size, this relationship was not significantly different between regions; therefore, there was no statistical difference in the brood size of similarly sized females between areas. This finding indicates that the larger brood sizes observed in the western GOM were related to the larger maximum size of females, and we postulate that larger female and brood sizes are a direct effect of prey availability. Future research should examine potential differences in embryonic growth between regions to determine if excess energy is directed to developing larger embryos rather than larger broods within similarly sized females, perhaps through a common-garden experimental design. However, because of the protracted and asynchronous reproductive cycles of female Atlantic sharpnose sharks in the northern GOM (Hoffmayer et al., 2013), we were not able to compare size at birth between the eastern and western GOM.

The difference of 0.6 pups per brood in the mean brood size of females between the eastern and western GOM, superficially, appears minor. Discussion of reproductive value (e.g., Fisher, 1930) and net reproductive rate are hampered by the lack of region-specific growth models necessary to back-transform age at size as would be required to calculate age-specific fecundity, age-specific mortality rates, and intrinsic rates of increase. However, the PLRO calculated in this study for 2 hypothetical females indicates the significance of the disparity. In both scenarios, which include multiple generations, the hypothetical female in the western GOM would be responsible for the production of more than 2 times the number of sharks than the hypothetical female in the eastern GOM. Therefore, even small changes in reproductive value, which may be statistically insignificant, can have large effects on population size.

The higher reproductive potential of Atlantic sharpnose sharks in the western versus the eastern GOM has numerous implications, such as variable population recovery rates, spatial variability in forage base for predators of Atlantic sharpnose sharks, possible effects on distributions of larger sharks, and potential region-specific mesopredator release and trophic cascades if populations of predators of Atlantic sharpnose sharks decline in the GOM. Future research should model the effects of varying abundance levels of Atlantic sharpnose sharks on the ecology of the 2 areas. Further, the results of this study underline the need to examine the life history of wide-ranging species throughout their range rather than assuming that traits of individuals from a discrete location are applicable to individuals over broad expanses, particularly those for which individuals show limited movement (e.g., small coastal sharks). Seemingly small differences in important life history characteristics, such as fecundity, could have significant effects on rebound potential for species adversely impacted by recreational and commercial fisheries.

---

[9] Pollack, A., and D. Hanisko. 2017. Unpubl. data. Miss. Lab., Southeast Fish. Sci., Cent., Natl. Mar. Fish. Serv., 3209 Frederic St., Pascagoula, MS 39567-4112.

Acknowledgments

We thank the captains and crews of the NOAA Ship *Oregon II*, F/V *Black Jack IV*, F/V *Daytona*, F/V *Gulfsearch*, and F/V *Beau Rivage* for their assistance in the collection of specimens.

Literature cited

Bethea, D. M., J. K. Carlson, J. A. Buckel, and M. Satterwhite.
2006. Ontogenetic and site-related trends in the diet of the Atlantic sharpnose shark *Rhizoprionodon terraenovae* from the northeast Gulf of Mexico. Bull. Mar. Sci. 78:287–307.

Carlson, J. K., and I. E. Baremore.
2003. Changes in biological parameters of Atlantic sharpnose shark *Rhizoprionodon terraenovae* in the Gulf of Mexico: evidence for density-dependent growth and maturity? Mar. Freshw. Res. 54:227–234.

Chen, C., T. Taniuchi, and Y. Nose.
1981. Some aspects of reproduction in the pointed-snout dogfish *Squalus japonicus* taken off Nagasaki and Choshi. Bull. Jpn. Soc. Sci. Fish. 47:1157–1164.

Colonello, J. H., L. O. Lucifora, and A. M. Massa.
2007. Reproduction of the angular angel shark (*Squatina guggenheim*): geographic differences, reproductive cycle, and sexual dimorphism. ICES J. Mar. Sci. 64:131–140.

Cope, J. M.
2006. Exploring intraspecific life history patterns in sharks. Fish. Bull. 104:311–320.

Cortés, E.
1999. Standardized diet compositions and trophic levels of sharks. ICES J. Mar. Sci. 56:707–717.
2002. Incorporating uncertainty into demographic modeling: application to shark populations and their conservation. Conserv. Biol. 16:1048–1062.

Davis, M. M., P. de J. Suárez-Moo, and T. S. Daly-Engel.
2019. Genetic structure and congeneric range overlap among sharpnose sharks (genus *Rhizoprionodon*) in the northwest Atlantic Ocean. Can. J. Fish. Aquat. Sci. 76:1203–1211.

Driggers, W. B., III, and E. R. Hoffmayer.
2009. Variability in the reproductive cycle of finetooth sharks, *Carcharhinus isodon*, in the northern Gulf of Mexico. Copeia 2009:390–393.

Fields, A. T., K. A. Feldheim, J. Gelsleichter, C. Pfoertner, and D. D. Chapman.
2016. Population structure and cryptic speciation in bonnethead sharks *Sphyrna tiburo* in the south-eastern U.S.A. and Caribbean. J. Fish Biol. 89:2219–2233.

Fisher, R. A.
1930. The genetical theory of natural selection, 272 p. Clarendon Press, Oxford, UK.

Ford, E.
1921. A contribution to our knowledge of the life-histories of the dogfishes landed at Plymouth. J. Mar. Biol. Assoc. U.K. 12:468–505.

Froese, R.
2006. Cube law, condition factor and weight-length relationships: history, meta-analysis and recommendations. J. Appl. Ichthyol. 22:241–253.

Hannan, K. M., W. B. Driggers III, D. S. Hanisko, L. M. Jones, and A. B. Canning.
2012. Distribution of the nurse shark, *Ginglymostoma cirratum*, in the northern Gulf of Mexico. Bull. Mar. Sci. 88:73–80.

Heist, E. J., J. A. Musick, and J. E. Graves.
1996. Mitochondrial DNA diversity and divergence among sharpnose sharks, *Rhizoprionodon terraenovae*, from the Gulf of Mexico and the Mid-Atlantic Bight. Fish. Bull. 94:664–668.

Heupel, M. R., C. A. Simpfendorfer, A. B. Collins, and J. P. Tyminski.
2006. Residency and movement patterns of bonnethead sharks, *Sphyrna tiburo*, in a large Florida estuary. Environ. Biol. Fish. 76:47–67.

Higgs, J. M., E. R. Hoffmayer, J. M. Hendon, and C. M. Butler.
2012. Diet of Atlantic sharpnose shark, *Rhizoprionodon terraenovae*, from the north-central Gulf of Mexico: initial findings. Proc. Gulf Caribb. Fish. Inst. 65:156–158.

Hoffmayer, E. R., W. B. Driggers III, L. M. Jones, J. M. Hendon, and J. A. Sulikowski.
2013. Variability in the reproductive biology of the Atlantic sharpnose shark in the Gulf of Mexico. Mar. Coast. Fish. 5:139–151.

Horie, T., and S. Tanaka.
2002. Geographical variation of maturity size of the cloudy catshark, *Scyliorhinus torazame*, in Japan. J. Fac. Mar. Sci. Technol. Tokai Univ. 53:111–124.

Kohler, N. E., J. G. Casey, and P. A. Turner.
1998. NMFS Cooperative Tagging Program, 1962–93: an atlas of shark tag and recapture data. Mar. Fish. Rev. 60(2):1–87.

Lenanton, R. C. J., D. I. Heald, M. Platell, M. Cliff, and J. Shaw.
1990. Aspects of the reproductive biology of the gummy shark, *Mustelus antarcticus* Günther, from waters off the south coast of western Australia. Aust. J. Mar. Freshw. Res. 41:807–822.

Lombardi-Carlson, L. A., E. Cortés, G. R. Parsons, and C. A. Manire.
2003. Latitudinal variation in life-history traits of bonnethead sharks, *Sphyrna tiburo*, (Carcharhiniformes: Sphyrnidae) from the eastern Gulf of Mexico. Mar. Freshw. Res. 54:875–883.

Menni, R. C., and R. P. Lessa.
1998. The chondrichthyan community off Maranhão (northeastern Brazil). II. Biology of species. Acta Zool. Lillo. 44:69–89.

Olsen, A. M.
1954. The biology, migration, and growth rate of the school shark, *Galeorhinus australis* (Macleay) (Carcharhinidae) in south-eastern Australian waters. Aust. J. Mar. Freshw. Res. 5:353–410.

Parsons, G. R.
1993. Geographic variation in reproduction between two populations of the bonnethead shark, *Sphyrna tiburo*. Environ. Biol. Fish. 38:25–35.

Portnoy, D. S., C. M. Hollenbeck, C. N. Belcher, W. B. Driggers III, B. S. Frazier, J. Gelsleichter, R. D. Grubbs, and J. R. Gold.
2014. Contemporary population structure and post-glacial genetic demography in a migratory marine species, the blacknose shark, *Carcharhinus acronotus*. Mol. Ecol. 23:5480–5495.

Portnoy, D. S., J. B. Puritz, C. M. Hollenbeck, J. Gelsleichter, D. Chapman, and J. R. Gold.
2015. Selection and sex-biased dispersal in a coastal shark: the influence of philopatry on adaptive variation. Mol. Ecol. 24:5877–5885.

Riley, G. A.
1937. The significance of the Mississippi River drainage for biological conditions in the northern Gulf of Mexico. J. Mar. Res. 1:60–74.

Rose, K. A., J. H. Cowan Jr., K. O. Winemiller, R. A. Myers, and R. Hilborn.
2001. Compensatory density dependence in fish populations: importance, controversy, understanding and prognosis. Fish Fish. 2:293–327.

Sminkey, T. R., and J. A. Musick.
1995. Age and growth of the sandbar shark, *Carcharhinus plumbeus*, before and after population depletion. Copeia 1995:871–883.

Sosebee, K. A.
2005. Are density-dependent effects on elasmobranch maturity possible? J. Northw. Atl. Fish. Sci. 35:115–124.

Springer, S.
1960. Natural history of the sandbar shark *Eulamia milberti*. Fish. Bull. 178:1–38.

Sulikowski, J. A., W. B. Driggers III, T. S. Ford, R. K. Boonstra, and J. K. Carlson.
2007. Reproductive cycle of the blacknose shark *Carcharhinus acronotus* in the Gulf of Mexico. J. Fish Biol. 70:428–440.

Taniuchi, T., H. Tachikawa, M. Shimizu, and Y. Nose.
1993. Geographical variations in reproductive parameters of shortspine spurdog in the North Pacific. Nippon Suisan Gakkaishi 59:45–51.

Taylor, I. G., and V. F. Gallucci.
2009. Unconfounding the effects of climate and density dependence using 60 years of data on spiny dogfish (*Squalus acanthias*). Can. J. Fish. Aquat. Sci. 66:351–366.

Todd, T. N., L. S. Waldbeser, and R. Ward.
2004. Use of single-stranded conformational polymorphisms (SSCP) to detect species relationship and population structure in the Atlantic sharpnose shark (*Rhizoprionodon terraenovae*) and the Caribbean sharpnose shark (*R. porosus*). Proc. Gulf Caribb. Fish. Inst. 55:294–305.

Tovar-Ávila, J., T. I. Walker, and R. W. Day.
2007. Reproduction of *Heterodontus portusjacksoni* in Victoria, Australia: evidence of two populations and reproductive parameters for the eastern population. Mar. Freshw. Res. 58:956–965.

Walker, T. I.
2005. Reproduction in fisheries science. *In* Reproductive biology and phylogeny of Chondrichthyes: sharks, batoids and chimaeras (W. C. Hamlett, ed.), p. 81–127. Science Publishers Inc., Enfield, NH.
2007. Spatial and temporal variation in the reproductive biology of gummy shark *Mustelus antarcticus* (Chondrichthyes: Triakidae) harvested off southern Australia. Mar. Freshw. Res. 58:67–97.

Yamaguchi, A., T. Taniuchi, and M. Shimizu.
2000. Geographic variations in reproductive parameters of the starspotted dogfish, *Mustelus manazo*, from five localities in Japan and in Taiwan. Environ. Biol. Fish. 57:221–233.

National Marine
Fisheries Service
NOAA

Fishery Bulletin
established in 1881

Spencer F. Baird
First U.S. Commissioner
of Fisheries and founder
of *Fishery Bulletin*

Postrelease survival of green sturgeon (*Acipenser medirostris*) encountered as bycatch in the trawl fishery that targets California halibut (*Paralichthys californicus*), estimated by using pop-up satellite archival tags

Phaedra Doukakis (contact author)[1]
Ethan A. Mora (deceased)[2,3]
Susan Wang[4]
Paul Reilly[5]
Russ Bellmer (retired)[5]
Kristine Lesyna[6]
Travis Tanaka[5]
Natnael Hamda[2,3]
Mary L. Moser[7]
Daniel L. Erickson[1]
Jason Vestre[8]
Jon McVeigh[8]
Kevin Stockmann[8]
Kristen Duncan[8]
Steven T. Lindley[2]

Email address for contact author: phaedra.doukakis@noaa.gov

[1] Ocean Associates Inc.
National Marine Fisheries Service, NOAA
4007 North Abingdon Street
Arlington, Virginia 22207

[2] Southwest Fisheries Science Center
National Marine Fisheries Service, NOAA
110 McAllister Way
Santa Cruz, California 95060

[3] Cooperative Institute for Marine Ecosystems and Climate
University of California Santa Cruz
1156 High Street
Santa Cruz, California 95060

[4] West Coast Region
National Marine Fisheries Service, NOAA
501 West Ocean Boulevard, Suite 4200
Long Beach, California 90802

[5] Fisheries Branch
California Department of Fish and Wildlife
830 S Street
Sacramento, California 95814

[6] Belmont Field Office and Laboratory
Marine Region
California Department of Fish and Wildlife
350 Harbor Boulevard
Belmont, California 94002

[7] Northwest Fisheries Science Center
National Marine Fisheries Service, NOAA
2725 Montlake Boulevard East
Seattle, Washington 98112

[8] West Coast Groundfish Observer Program
Northwest Fisheries Science Center
National Marine Fisheries Service, NOAA
2725 Montlake Boulevard East
Seattle, Washington 98112

Abstract—Understanding postrelease effects of incidental capture on fish species of conservation concern is critically needed. We collaborated with commercial fishermen to estimate postrelease survival of green sturgeon (*Acipenser medirostris*) captured and released from bottom trawls used to target California halibut (*Paralichthys californicus*). We developed a method for interpreting acceleration, depth, and temperature data transmitted from pop-up satellite archival tags to classify the fate of individuals following capture and release in fishing operations. We first deployed SeaTag-MOD satellite tags on known living and dead sturgeon to develop a support vector machine that uses accelerometer readings to classify tagged fish as alive or dead. In 2015 and 2016, fishermen and West Coast Groundfish Observer Program observers tagged 76 green sturgeon (69–135 cm fork length) encountered as bycatch, yielding 51 useable data sets. Eleven sturgeon were classified as having died after release, 9 of which died within our designated 21-d (504 h) study period. Some green sturgeon entered the San Francisco Bay Delta after being tagged, indicating movement between ocean and estuary environments. Research is needed to understand how to minimize effects of handling time and trawl bycatch mortality.

Quantifying the impacts of incidental capture and release on marine species is a difficult but critical fisheries management requirement (Davis, 2002; Suuronen, 2005; Davies et al., 2009; Brooke et al., 2012). Fish encountered as bycatch may experience effects such as delayed mortality or reductions in fitness (Davis, 2002; Suuronen, 2005; Suuronen and Erickson, 2010; Wilson et al., 2014). Delayed mortality can be an important factor in the recovery of fish listed under the U.S. Endangered Species Act (Collins et al., 2000; ASSRT, 2007).

Postrelease survival in fish species has traditionally been examined by holding fish in net pens after capture (e.g., Davis, 2002; Parker et al., 2003; Weltersbach and Strehlow, 2013),

Manuscript submitted 29 April 2019.
Manuscript accepted 18 February 2020.
Fish. Bull. 118:63–73 (2020).
Online publication date: 13 March 2020.
doi: 10.7755/FB.118.1.6

The views and opinions expressed or implied in this article are those of the author (or authors) and do not necessarily reflect the position of the National Marine Fisheries Service, NOAA.

using experimental gear (e.g., Erickson and Pikitch[1]), or studying fish activity through telemetry (Hoolihan et al., 2011; Beardsall et al., 2013; Campana et al., 2016). Common factors contributing to mortality in these and other studies include time out of water on deck, water and air temperature, tow velocity and duration, and fish size and handling practices (Olla et al., 1997; Davis et al., 2001; Davis and Parker, 2004; Suuronen and Erickson, 2010; Gale et al., 2013; Mandelman et al., 2013). Predation after release can also be a factor (Raby et al., 2014). Cook et al. (2019) reviewed potential sources of stress that lead to postrelease mortality and predation in fish species. They observed that simulating actual fishery practices is critical for correctly assessing bycatch effects.

Involving the fishing community in fisheries research has many benefits (Johnson and van Densen, 2007; Yochum et al., 2011). Cooperative research can facilitate enhanced knowledge of the fisheries resource while engendering trust and communication among policymakers, scientists, and fishermen. Moreover, involving the fishing community can increase data collection capacity and validity. Fishermen may also become more invested in the results and willing to address conservation challenges.

Sturgeon and paddlefish species (Acipenseriformes) are among the most threatened of all fish families, according to the IUCN Red List of Threatened Species (IUCN, 2018). Historic overfishing, illegal fishing and trade, and habitat modification and destruction have contributed to their decline (Pikitch et al., 2005). Although directed catch has been eliminated for most sturgeon species, mortality due to incidental capture still threatens the recovery of depleted populations (Stein et al., 2004; Beardsall et al., 2013; Dunton et al., 2015; Breece et al., 2016).

Green sturgeon (*Acipenser medirostris*) inhabit coastal bays, estuaries, rivers, and nearshore environments along the western seaboard of North America and are taken as bycatch in a number of fisheries (NMFS, 2015; NMFS[2]). Bycatch of green sturgeon is a factor in recovering the Southern distinct population segment (DPS), which is listed as threatened under the Endangered Species Act (Federal Register, 2006; NMFS[2]). The Southern DPS recovery plan recognizes reducing fisheries bycatch and estimating postrelease effects as priority tasks (NMFS[2]). The Northern DPS of green sturgeon, a National Marine Fisheries Service (NMFS) species of concern (Federal Register, 2006), coexists with the Southern DPS in estuarine and marine habitats (NMFS[2]), and fish from the 2 DPS are morphologically indistinguishable (NMFS[2]). Directed fishing has been virtually eliminated for green sturgeon in West Coast rivers and nearshore environments because coast-wide regulations prohibit retention (NMFS[2]).

The bottom-trawl fishery that targets California halibut (*Paralichthys californicus*) and operates out of San Francisco and Half Moon Bay, California, encounters green sturgeon at a rate higher than that of other fisheries for which we have data (Richerson et al.[3]). The NMFS West Coast Groundfish Observer Program (WCGOP) has recorded bycatch of green sturgeon in the fishery since 2002. Between 2007 and 2017, estimated annual encounters of green sturgeon in the fishery ranged from 29 individuals in 2011 to 665 individuals in 2015. Analysis of genetic samples taken from specimens of the green sturgeon caught in the fishery over that time period (n=104) indicates that over 95% of the animals encountered are from the threatened Southern DPS (Anderson et al., 2017). The majority of green sturgeon encountered in the fishery are immature individuals that are less than 140 cm fork length [FL] and greater than 59 cm FL (Richerson et al.[3]). Southern DPS green sturgeon reproduce in the Sacramento River system and rear in the San Francisco Bay Delta (NMFS[2]). The fishery operates in waters of the Pacific Ocean more than 5.6 km (3 nautical miles) offshore from this delta (Fig. 1). Immediate mortality of green sturgeon in the fishery (i.e., finding dead green sturgeon in the bottom-trawl net) is only very rarely observed in WCGOP onboard sampling.

We collaborated with fishermen that target California halibut and with WCGOP observers to measure postrelease survival of green sturgeon encountered in the California halibut bottom-trawl fishery. We developed a method for interpreting data transmitted from pop-up satellite archival tags (PSATs) to classify the fate of green sturgeon after release and were able to estimate postrelease survival in normal California halibut bottom-trawl operations. We tested the hypothesis that there is no postrelease mortality of green sturgeon captured as bycatch in this fishery.

Material and methods

We had 3 objectives: 1) characterize the patterns of tag sensor data (accelerometer data) of known living and dead green sturgeon, 2) train an algorithm to classify accelerometer data into *alive* and *dead* classes, and 3) use the

---

[1] Erickson, D., and E. Pikitch. 1999. Survival of trawl-caught and discarded sablefish, 21 p. Northwest Fish. Sci. Cent., Natl. Mar. Fish. Serv., NOAA, Newport, OR. [Available from Northwest Fish. Sci. Cent., 2725 Montlake Blvd. E., Seattle, WA 98112.]

[2] NMFS (National Marine Fisheries Service). 2018. Recovery plan for the Southern distinct population segment of North American green sturgeon (*Acipenser medirostris*), 88 p. Calif. Cent. Valley Off., West Coast Reg., Natl. Mar. Fish. Serv., NOAA, Sacramento, CA. [Available from website.]

[3] Richerson, K., J. E. Jannot, Y.-W. Lee, J. McVeigh, K. Somers, V. Tuttle, and S. Wang. 2019. Observed and estimated bycatch of green sturgeon in 2002–2017 U.S. West Coast groundfish fisheries. Northwest Fish. Sci. Cent. Observer Program, Natl. Mar. Fish. Serv., NOAA, Seattle, WA. [Available from website.]

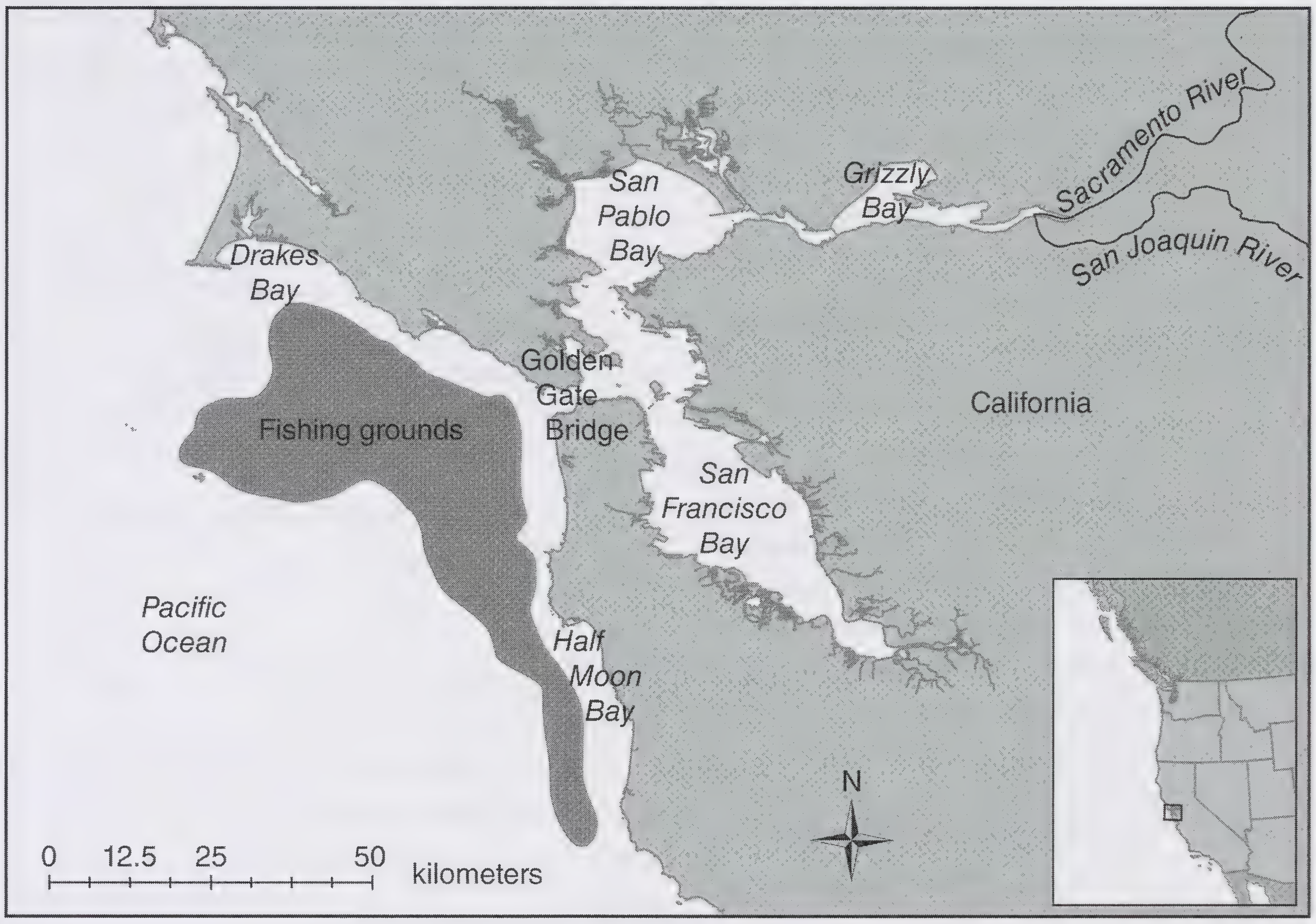

Figure 1

Map of the San Francisco Bay Delta and the approximate fishing grounds of the bottom-trawl fishery that targets California halibut (*Paralichthys californicus*) as defined by analysis of data from the West Coast Groundfish Observer Program, which has been recording data on bycatch of green sturgeon (*Acipenser medirostris*) in this fishery since 2002.

algorithm along with other information to classify the fate of green sturgeon captured and released during normal fishing operations of the bottom-trawl fishery that targets California halibut (Fig. 2).

During 2015 and 2016, green sturgeon were captured and tagged in the bottom-trawl fishery that operates out of San Francisco, California, and Half Moon Bay, California, and targets California halibut (Fig. 1). We used PSATs (SeaTag-MOD[4] tags, Desert Star Systems, Marina, CA) to log acceleration on 3 axes, along with tag depth and water temperature. In all cases, the tags were attached to the base of the dorsal fin of the sturgeon by using clear 2-mm monofilament fishing line crimped into a loop of approximately 150 mm (Erickson and Hightower, 2007). This loose attachment allowed the tags to float vertically above the dorsal fin when the fish was stationary, trail freely alongside or above the fish when the fish was swimming, and undulate with the tailbeat. The tags were programmed to log readings from the sensors every 4 min. The length of tag deployment (number of days attached to the fish) varied for each objective.

Characterizing sensor readings for green sturgeon with known fates

To characterize the data patterns of living and dead green sturgeon, we attached PSATs to known living and dead sturgeon in 2 separate trials (Suppl. Table 1) (online only). In the first trial, we attached PSATs to 3 living, captive green sturgeon (approximately 90, 100, and 110 cm FL) held for 7.5 h in a 1.5-m deep circular tank with a 4-m diameter. The fish swam naturally during the trial, and the position of tags ranged from vertical when the fish were stationary to nearly vertical (partially horizontal) when the fish were mobile. In the second trial, we attached a PSAT to a dead white sturgeon (*A. transmontanus*) (104 cm FL) in the Pacific Ocean off northern California for 96 h.

We used accelerometer readings, from PSAT deployments for which the fates of fish were known, to train the support vector machine (SVM) and to classify individuals on the basis of data patterns into 1 of 2 states: alive or dead. The SVM is a machine-learning algorithm designed for binary classification (Burges, 1998; Bishop, 2006; Raschka, 2015; Sugiyama, 2016; Watt et al., 2016). After training and testing the SVM, we developed a classification workflow by using Scikit-learn (vers. 0.18.1; Pedregosa et al., 2011) for implementing the algorithm.

---

[4] Mention of trade names or commercial companies is for identification purposes only and does not imply endorsement by the National Marine Fisheries Service, NOAA.

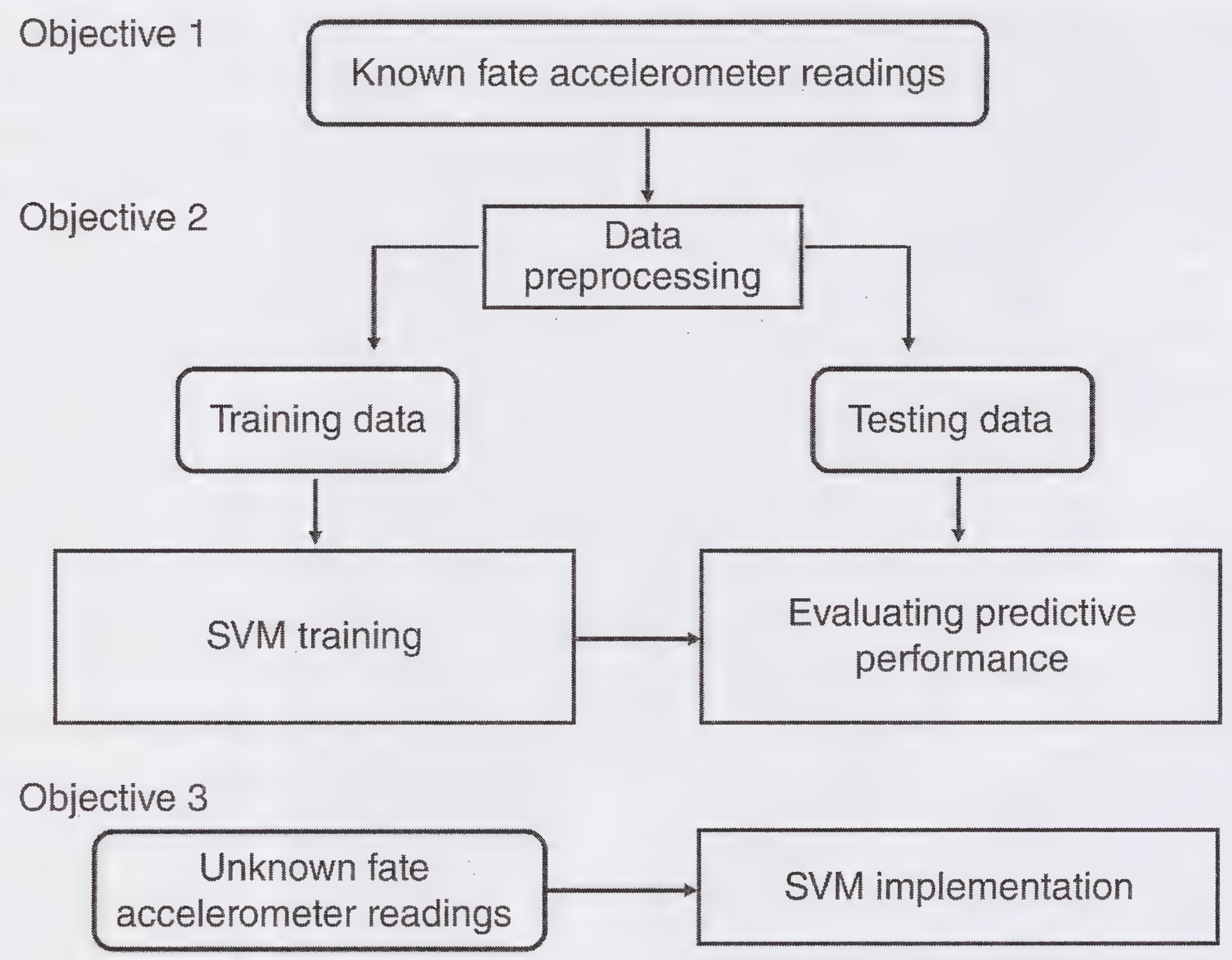

Figure 2

Schematic description of the model development and implementation process used to estimate postrelease survival of green sturgeon (*Acipenser medirostris*) in the bottom-trawl fishery that targets California halibut (*Paralichthys californicus*) in nearshore waters of the Pacific Ocean just west of the San Francisco Bay Delta. The first objective was to characterize the patterns of tag sensor data (accelerometer readings) of green sturgeon with known fates. The second objective was to train an algorithm, a support vector machine (SVM), to classify accelerometer data into *alive* and *dead* classes. The third objective was to use the algorithm along with other information to classify the fate of green sturgeon captured and released from May 2015 through September 2016 during normal fishing operations of the California halibut bottom-trawl fishery.

The SVM constructs 2 hyperplanes (decision boundaries) that separate binary classes while preserving the greatest margin between them. The margin is defined as the distance between the hyperplanes and the data points closest to a hyperplane (support vectors) (Raschka, 2015). If we assume that the 2 classes are linearly separable, the objective is to find hyperplanes with the smallest generalization error between observations from accelerometer data and predictions from the model (the SVM).

The positive (living) and negative (dead) individuals and hyperplanes that are parallel to the decision boundary can be mathematically expressed as follows:

$$W_0 + W^{\mathrm{T}}X_{\mathrm{pos}} = 1 \text{ and} \tag{1}$$

$$W_0 + W^{\mathrm{T}}X_{\mathrm{neg}} = -1, \tag{2}$$

where W_0 = a bias factor;
W = a vector that weights values for each set of accelerometer readings;
T = the transpose of the vectors W;
X_{pos} = accelerometer readings for the positive (living) individuals; and
X_{neg} = accelerometer readings for the negative (dead) individuals.

The goal is to train the SVM for optimal classification of fish as positive or negative while iteratively estimating W. Therefore, the separation problem is to determine the hyperplane such that

$$W_0 + W^{\mathrm{T}}X_{\mathrm{pos}} \geq 1 \text{ and} \tag{3}$$

$$W_0 + W^{\mathrm{T}}X_{\mathrm{neg}} \leq -1. \tag{4}$$

If we subtract Equation 1 from Equation 2, we get the following equation:

$$W^{\mathrm{T}}(X_{\mathrm{pos}} - X_{\mathrm{neg}}) = 2. \tag{5}$$

The length of the vector (w) can be defined as follows:

$$\| w \| = \sqrt{\sum_{\mathrm{j}=1}^{\mathrm{m}} w_{\mathrm{j}}^2} \,. \tag{6}$$

Normalizing Equation 5 by using the length of the vector w, we arrive at Equation 7:

$$\frac{W^{\mathrm{T}}(X_{\mathrm{pos}} - X_{\mathrm{neg}})}{\| w \|} = \frac{2}{\| w \|} \,. \tag{7}$$

The SVM finds the hyperplane that has the largest margin, by maximizing Equation 7 and constraining the samples of data so that they are classified correctly as follows:

$$W_0 + W^{\mathrm{T}} x^{(\mathrm{i})} \geq 1 \quad \text{if } y^{(\mathrm{i})} = 1 \text{ and} \tag{8}$$

$$W_0 + W^{\mathrm{T}} x^{(\mathrm{i})} < -1 \quad \text{if } y^{(\mathrm{i})} = -1, \tag{9}$$

where $y^{(\mathrm{i})}$ = the data classes (i.e., the dependent variables); and
$x^{(\mathrm{i})}$ = accelerometer readings.

The constraint equation requires that negative data points fall on one side of the negative hyperplane and that positive data points fall behind the positive hyperplane. Here, the hyperplanes correspond to alive and dead classifications as follows:

$$y^{(\mathrm{i})}(W_0 + W^{\mathrm{T}} x^{(\mathrm{i})}) \geq 1. \tag{10}$$

This mathematical approach assumes the data separated by the hyperplane are linearly separable. However, this assumption fails for our data set. To address this issue, we used a modified kernel method in which kernel functions $K(X^{(\mathrm{i})}, X^{(\mathrm{j})})$ transform the training data (Burges, 1998; Bishop, 2006; Raschka, 2015; Watt et al., 2016). This method creates nonlinear combinations of the original features to project them onto a higher dimensional space where they become linearly separable (Bishop, 2006; Raschka, 2015). We applied the radial basis function kernel, also known as the *Gaussian kernel* (Equation 11):

$$K\left(x^{(\mathrm{i})}, x^{(\mathrm{j})}\right) = \mathrm{e}^{\left(\frac{\|x^{(\mathrm{i})} - x^{(\mathrm{j})}\|}{2\sigma^2}\right)}. \tag{11}$$

Here, $\gamma = \frac{1}{2\sigma^2}$ is a free parameter (hyperparameter) that is to be optimized.

Training and testing the algorithm

The accelerometer readings obtained in the work for our first objective were randomly divided into training and testing data samples at a ratio of 4:1 (training:testing). Prior to the training and testing process, the samples of tag sensor data (X_i) were transformed to $X_{std,i}$ by using their respective means (μ_i) and standard deviations (σ_i^2) with the following equation:

$$X_{std,i} = \frac{(X_i - \mu_i)}{\sigma_i}. \tag{12}$$

The goal of normalization is to change the accelerometer readings to a common scale without distorting differences in the ranges of values. The standardization step avoids biasing the machine-learning algorithm toward numerically large values. After normalization, the model was trained by using the SVMs in Scikit-learn. We used the stochastic gradient-descent optimization technique to estimate the model parameters. To avoid over-fitting, we applied a 10-fold cross-validation technique (Sugiyama, 2016) in which the training data set was divided into 10 groups and the model was trained iteratively by using 9 groups and validated with the remaining group. After training, the model was implemented to test classification accuracy.

During the training and testing of the model, we encountered data imbalance between the alive and dead classes. Among the 1676 data points we obtained, only 284 data points (less than 17%) were labeled as *alive* because the tag deployment on living green sturgeon was 7.5 h. In contrast, the dead white sturgeon was monitored for 96 h. Because this data imbalance can lead to a biased classification performance (Murphy, 2012), we resampled the alive class and randomly replicated it to increase the number of data points for this class in the sample. To avoid over-fitting, we evaluated the performance of the SVM classifier by using precision as an additional classification metric. By combining the 2 classification performance metrics (i.e., accuracy and precision), we were able to balance the bias–variance tradeoff of the SVM classifier.

Once trained, we used the classification algorithm to assist with the interpretation of accelerometer data from deployments on green sturgeon captured as bycatch in the commercial California halibut bottom-trawl fishery.

Classifying fates of captured green sturgeon

To apply our model and measure postrelease survival, green sturgeon were captured as bycatch on 6 bottom-trawl vessels during normal fishing operations that targeted California halibut and tagged with PSATs between 13 May 2015 and 7 September 2016 (Fig. 1). Sturgeon tagged with PSATs were measured (in FL) and released as soon as possible. To encourage return of the tags for enhanced data recovery and redeployment, PSATs had a reward label.

From fish handled by an observer, we collected a tissue sample (1-cm^2 clip from the pectoral fin) for genetic analysis to determine whether the fish belonged to the Southern or Northern DPS. No live wells were available on the cooperating vessels; green sturgeon were removed from the haul and processed as soon as possible. We rated the condition of the fish as good (no apparent damage or stress), fair (flushed appearance, minor abrasions), or poor (serious abrasions, bleeding, or obvious injury) (NWFSC[5]) and recorded the additional time on deck needed for WCGOP processing and tagging (i.e., obtaining weight, length, fin clip, and photograph, and tagging with passive integrated transponder tags, in some cases, and PSATs). We recorded the date, time, and GPS location at which each fish was released as well as the associated trip and haul number. For each haul, we recorded the starting and ending dates, times, locations, and depths.

Initially, multiple fish in a single haul were tagged, and tagged fish were as small as 69 cm FL. Concern over introducing confounding factors (e.g., extended time on deck when tagging multiple fish and potential tag effects on smaller fish) led to changes in our protocol to tag only fish ≥80 cm FL in each haul. We tagged the first captured fish of sufficient size. Prior to these changes, the maximum number of fish tagged in a single haul was 3, and this number was taken only once; 2 fish were tagged in each of 5 other hauls. All other hauls had either 1 fish in the haul or had only 1 fish tagged out of multiple individuals caught. Five tagged fish were <80 cm FL.

Tags were programmed to remain attached to the fish for at least 21 d, after which they would release, float to the surface, and begin broadcasting data to satellites. We selected 21 d as the time frame that mortality of green sturgeon could be attributed to the effects of trawl capture, on the basis of a literature survey of similar approaches. Because of logistics involved with programming and transport to fishermen and observers, tags were sometimes deployed for more than 21 d.

We used multiple lines of evidence to determine the fate of tagged individuals: location, depth, temperature, and acceleration data. The GPS location at release of the tagged fish, as recorded by the tag, was compared with the time and estimated location of the first PSAT broadcast. Variable depth recordings that were not characterized by regular, repeating tidal signatures indicated swimming. In contrast, depth recordings from PSATs on dead fish had a tidal signature (as in the record from the PSAT deployment on the known dead white sturgeon). Data from temperature sensors often indicate the difference between the cooler ocean waters near the release location and the warmer waters of the San Francisco Bay Delta. Accelerometer data for each individual were classified by our trained algorithm. For each tag deployment, we plotted the classified accelerometer data by time and a smoothing trend line (moving average of 200 readings) to visualize any trends in activity during a deployment.

---

[5] NWFSC (Northwest Fisheries Science Center). 2019. 2019 training manual: West Coast Groundfish Observer Program, 529 p. Northwest Fish. Sci. Cent., Natl. Mar. Fish. Serv., NOAA, Seattle, WA. [Available from website.]

For each PSAT deployment, we summarized these lines of evidence, wrote a narrative of what likely happened to each fish after release, and ultimately classified each deployment as a survival or a mortality. We then implemented the Kaplan–Meier survival estimator—in the package survival, vers. 2.38 (Therneau and Grambsch, 2000; Therneau, 2015), in statistical software R, vers. 3.3.2 (R Core Team, 2016)—to determine the proportion of individuals that had survived 21 d (504 h) following capture and release from the fishery (Kaplan and Meier, 1958).

Although not the central goal of our study, we used stepwise logistic regression analysis (RStudio, vers. 1.0.44, RStudio Inc., Boston, MA) to evaluate the association of potential explanatory variables (e.g., tow duration, tow depth, fish length, and processing time; Suppl. Table 2 (online only)) with postrelease survival. We included continuous variables that were consistently recorded and had a wide range of values. Null values were excluded from the logistic regression model. We assumed that a *P*-value ≤0.05 indicates that a result is statistically significant.

Results

Characterizing sensor readings for green sturgeon with known fates

Temperature and depth data and accelerometer readings from PSAT deployments on known dead and living sturgeon were downloaded, plotted, and visually examined. The PSAT deployed on the known dead white sturgeon recorded consistently cool water temperatures (approximately 12°C), and the depth record indicated tidal fluctuations consistent with a stationary carcass on the seafloor. Accelerometer data indicate that the tag was almost entirely upright with minimal lateral sway. The PSATs deployed on 3 green sturgeon known to be alive all recorded shallow depths (<1 m) and stable water temperatures (18°C) experienced in the tank. Accelerometer readings were variable, indicating the occurrence of periods of apparent swimming (lateral swaying) and stationary periods during which the tag was upright (see examples in Supplementary Figures 1–3) (online only).

Training and testing the algorithm

The model correctly classified 97.7% and 96.3% of the dead individuals in the training and testing data sets, respectively (Table 1). More living than dead individuals were misclassified for both the training (~7%) and testing (6%) data sets (Table 1). Overall, the model accurately classified 96.9% of the data points, with better classification accuracy for the fates of tagged fish determined to be dead (98.7%) than for those determined to be alive (88.0%).

Classifying fates of captured green sturgeon

Fishermen attached PSATs to 19 green sturgeon, and observers tagged 57 fish. Of these 76 PSAT deployments, 51 yielded sufficient data to contribute to our analysis. Of these 51 data sets, 37 were from recovered tags and 14 were from broadcasted data summaries. Examples of the accelerometer, depth, and temperature data from PSAT deployments can be found in Supplementary Figures 1–3 (online only). The length of tagged fish ranged from 69 to 135 cm FL (median: 98 cm FL) (Fig. 3). For 3 of the 5 fish <80 cm FL, data from PSAT deployments could not be used for classification (because of insufficient data recovery); the other 2 fish were determined to have survived for 21 d. A median of 7.5 min was estimated for the time required to process and tag an individual (Suppl. Table 2) (online only). This value does not represent total time out of the water, given the additional time necessary to extract a green sturgeon from a haul and ensure safe conditions for processing.

After release, green sturgeon often entered San Francisco Bay or remained in nearshore waters of the Pacific Ocean and close to their release locations. Citizens found and returned tags that had popped off and drifted to shore. These tags were generally recovered from ocean beaches between Drakes Bay and Half Moon Bay (Fig. 1). Within the San Francisco Bay Delta, PSATs were recovered from directly below the Golden Gate Bridge to inland waters at the confluence of the Sacramento and San Joaquin Rivers. Some deployments yielded both broadcast summaries and archival data; in these cases, we used the more complete archival data (see the "Discussion" section). For the 51 deployments with sufficient data, 24 tags were recovered or had first broadcasts within the San Francisco Bay Delta, and 21 tags were recovered or had first broadcasts in the ocean (near their recovery locations). For the other 6 deployments, the recovery or first broadcast location of the tag could not be determined.

The length of time that a tag remained attached to a fish ranged from 3 to 47 d (83–1128 h). In most cases, tags were attached to the fish for more than 21 d. Three tags detached prematurely because of poor tag attachment and were omitted from the study at the time of detachment (categorized as *censored*; Suppl. Table 2 (online only)). Of the 51 green sturgeon for which data were recovered, we estimated that 11 died, 9 within 4.5 d (107 h) of release, and 2 died after the 21-d (504-h) study period at 569 h and 679 h after release (Table 2). We, therefore, reject the hypothesis that there is no postrelease mortality of green sturgeon captured as bycatch in this fishery. The estimated survival rate was 82% (95% confidence interval: 72–94%) during the 21-d study period.

The results of analysis with the full regression model indicate that mortality (within 504 h postrelease) was not significantly related to tow duration (*P*=0.6438), tow

Table 1

Accuracy of the support vector machine (SVM) model in classifying an individual green sturgeon (*Acipenser medirostris*) as dead or alive. We collected accelerometer data from pop-up satellite archival tags (PSATs) deployed on known living and dead sturgeon. Data were derived from 2 experiments conducted in 2015. In the first, we attached PSATs to 3 living, captive green sturgeon (approximately 90, 100, and 110 cm FL) held for 7.5 h in a 1.5-m-deep circular tank with a 4-m diameter. In the second, we attached a PSAT to a dead white sturgeon (*A. transmontanus*) (104 cm FL) in the Pacific Ocean off northern California for 96 h. We obtained 284 accelerometer readings from the live green sturgeon and 1392 accelerometer readings from the dead white sturgeon. The accelerometer readings were randomly divided into training and testing data samples at a ratio of 4:1 (training:testing) and used to develop a SVM model to classify each accelerometer reading as representing a living or dead sturgeon. The data in this table compare the actual and predicted (by using the SVM model) number and percentage of accelerometer readings classified as representing a living or dead sturgeon.

Overall accuracy of classification by SVM

		Predicted classification (no. of accelerometer readings)	
	Classification	Dead	Alive
Actual classification (no. of accelerometer readings)	Dead	1374	18
	Alive	34	250

Accuracy of classification by SVM: training data

		Predicted classification (percentage of accelerometer readings)	
	Classification	Dead	Alive
Actual classification (percentage of accelerometer readings)	Dead	97.7%	7%
	Alive	2.3%	93%

Accuracy of classification by SVM: testing data

		Predicted classification (percentage of accelerometer readings)	
	Classification	Dead	Alive
Actual classification (percentage of accelerometer readings)	Dead	96.3%	6%
	Alive	3.7%	94%

depth (P=0.5623), fish length (P=0.5424), processing time (P=0.7214), air temperature (P=0.8808), or water temperature (P=0.9266). These variables were dropped by the model in further analysis with the stepwise regression model. Catch weight was not included in this analysis because of the frequency of associated null values. The time that elapsed between the end of the tow (i.e., the start of the haul back of the trawl net) and the release of the tagged green sturgeon (Suppl. Table 2) (online only) remained in the final model and significantly affected postrelease survival (P=0.0315). It should be noted that the same relationship was found when the model considered mortality occurring more than 504 h after release.

Discussion

We successfully developed a method for interpreting archival tagging data to classify the fate of tagged green sturgeon. Our approach is unique in that it relies primarily on an algorithm trained by data from deployments of PSATs on individuals with known fates rather than on assessments of mortality based on continuous or threshold depth or on descent of depth readings (Poisson et al., 2014; Hutchinson et al., 2015). Given that sturgeon are mostly bottom dwelling and can sometimes occupy a range of depths that could be perceived as constant (i.e., within the range of error of the depth sensor), we developed the approach detailed herein. Our approach is similar to that developed by Whitney et al. (2016) in its use of accelerometer data in combination with depth and temperature data.

Our success in arriving at a survival estimate can be attributed to a few factors. Foremost was the cooperation with fishermen and observers, which provided a low-cost mechanism for tagging green sturgeon without additional research or vessel effort and a study design that tested our hypothesis in regular fishing conditions. The high rate of tag retrieval was also important. Data obtained from recovered tags were sufficient for determining mortality or survival 90% of the time; broadcast data were

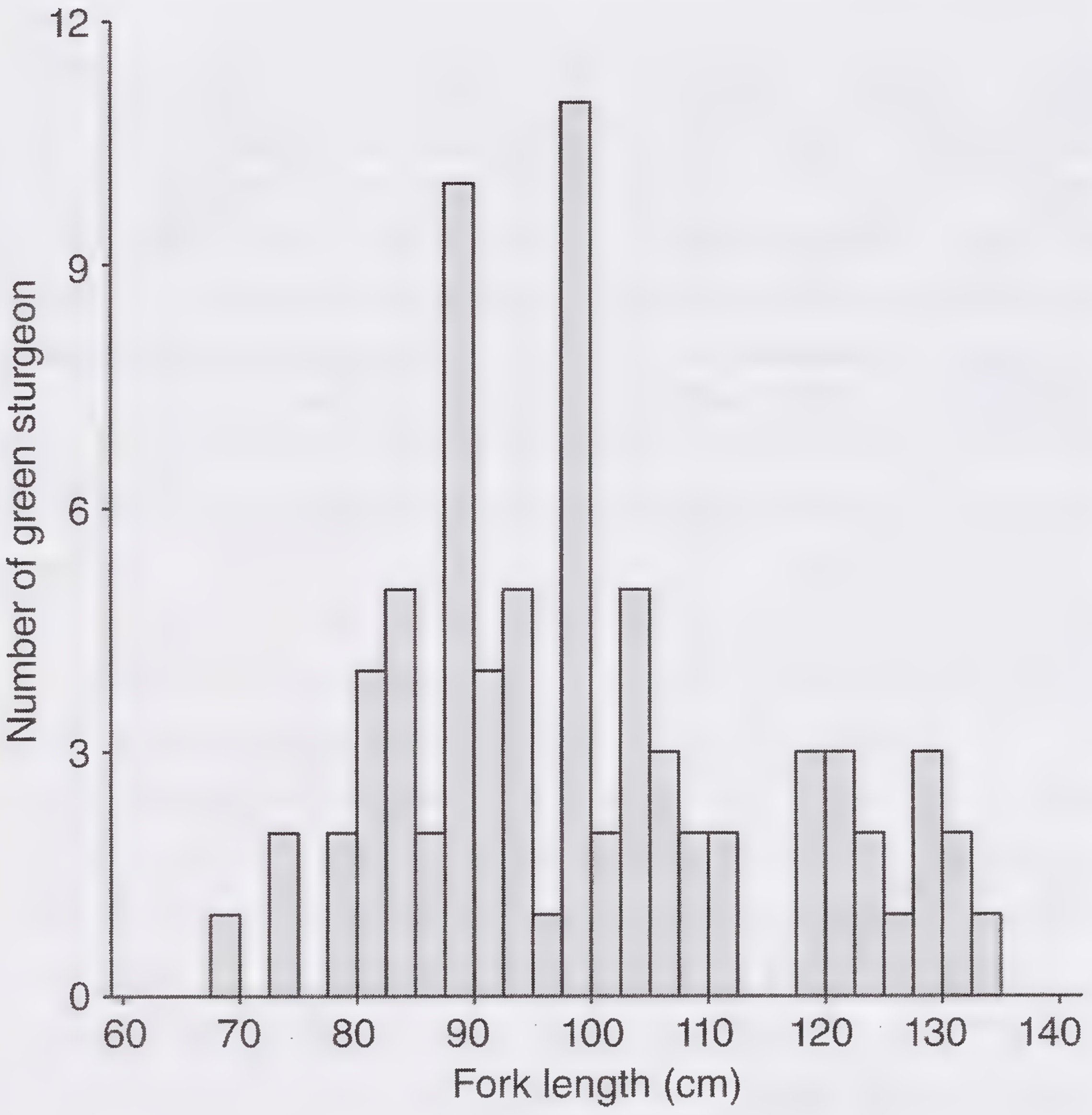

Figure 3

Length–frequency histogram for green sturgeon (*Acipenser medirostris*) tagged after capture as bycatch between May 2015 and September 2016 on 6 bottom-trawl vessels that targeted California halibut (*Paralichthys californicus*) off San Francisco and Half Moon Bay.

Table 2

Kaplan–Meier estimates of survival of green sturgeon (*Acipenser medirostris*) as each dead individual exits the study. Between May 2015 and September 2016, individuals were captured as bycatch and tagged on 6 bottom-trawl vessels that targeted California halibut (*Paralichthys californicus*) in nearshore waters of the Pacific Ocean just west of the San Francisco Bay Delta. The number at risk is the number of green sturgeon with tags still attached for at least the corresponding hours after release. For example, 16 individuals had tags that remained attached for more than 678 h after release. We attributed any mortality occurring before 504 h to the effects of trawl capture. SE=standard error of the mean; CI=confidence interval.

Hours after release	Number at risk	Survival rate	SE	95% CI
0.53	51	0.98	0.02	0.94–1.00
4.33	50	0.96	0.03	0.91–1.00
4.80	49	0.94	0.03	0.88–1.00
6.58	48	0.92	0.04	0.85–1.00
8.62	47	0.90	0.04	0.82–0.99
14.63	46	0.88	0.05	0.80–0.98
17.85	45	0.86	0.05	0.77–0.96
104.09	43	0.84	0.05	0.75–0.95
107.34	42	0.82	0.05	0.72–0.94
569.05	27	0.79	0.06	0.68–0.92
678.67	16	0.74	0.07	0.61–0.90

sufficient for determining mortality or survival 70% of the time. The location of our study was such that many of our tags were found on beaches near recreational and urban areas. Broadcast data were inferior to archived data from the returned tags because weather often hindered satellite transmissions, leading to gaps in the broadcast data summaries. In future studies, the use of broadcast data in other areas or from different tags may result in more complete broadcast data. We also benefitted from baseline information from a previous study of green sturgeon that used pop-up satellite tagging (Erickson and Hightower, 2007). Hence, signatures within our data, including tidal patterns and evidence of animals moving into warmer or cooler waters, helped determine the fates of sturgeon.

The temperature and depth data as well as the location of first broadcast or recovery of tags indicate that some green sturgeon entered the environment of the San Francisco Bay Delta after being tagged and released in the Pacific Ocean. Given previous research (Anderson et al., 2017), the majority of these fish were likely Southern DPS individuals that had reared in the delta environment. The results of earlier work indicate that Southern DPS green sturgeon rear in freshwater and estuarine environments for up to 4 years before transitioning to saltwater environments and migrating up the coast, returning to freshwater only to spawn (Beamesderfer et al., 2007). Our research adds evidence to published studies (e.g., Lindley et al., 2011; Miller, 2017) that Southern DPS green sturgeon move in and out of San Francisco Bay before maturing and migrating to northern estuaries.

Finding an appropriate method to acquire accelerometer data for sturgeon was a challenge. Although we tagged captive green sturgeon, other options could provide data to refine our results. Captive white sturgeon in commercial aquariums with tanks of much greater volume could be used, but fish in such tanks are often not in the size range of fish tagged in our field study. Moser et al. (2018) provided accelerometer data from live, free-swimming green sturgeon shortly after capture and release from gill nets in Willapa Bay, Washington. These green sturgeon ranged from 45 to 167 cm FL, with the majority of those fish larger than the green sturgeon in our study. The data of Moser et al. (2018) were also collected by tags that were not freely moving but held in place along the body axis. Despite these differences, it might be possible to incorporate elements of their accelerometer data to inform our classification model in the future. Using PSATs on green sturgeon from gill-net bycatch could provide an interesting comparison and insights into the relative threats of these 2 fisheries to green sturgeon.

Additional studies and modeling are needed to understand the effects of the estimated level of postrelease mortality on the threatened Southern DPS. Population estimates based on adult abundance have recently been developed for the Southern DPS (Mora et al., 2018), allowing evaluation of population-level impacts of bycatch mortality on status and recovery. The California halibut bottom-trawl fishery primarily interacts with immature individuals of the Southern DPS (Anderson et al., 2017; Richerson et al.[3]). With some additional efforts, data from this fishery could be used to refine the overall estimate of abundance for the Southern DPS and allow for a more robust analysis of effects from postrelease mortality. It should be noted that fishery bycatch mortality is only one factor that affects the Southern DPS; recovery will require improved access to spawning and rearing areas (NMFS[2]).

Our study was not designed to examine specific factors contributing to postrelease mortality and involved green sturgeon caught during normal fishing operations. Although we collected ancillary data on each haul for which green sturgeon were tagged, hauls and fishing effort were not sufficiently dispersed across the different variables, sample sizes were small, and data were recorded inconsistently for some variables. Therefore, our inability to identify certain factors as significant contributors to postrelease mortality should not be taken as conclusive evidence that these factors have no effect. In our study, the total time that a tagged sturgeon spent in the net during haul back and on deck for processing and tagging was the only variable that may have significantly affected mortality. Given this result and literature evidence (e.g., Parker et al., 2003; Davis and Parker, 2004; Beardsall et al., 2013; Cook et al., 2019), WCGOP protocols have been changed to minimize time out of water for green sturgeon encountered in the fishery. Creating onboard environments conducive to improved survival (e.g., shade, use of a hose or other water source to keep individuals continuously wet and cool, and possible construction of live wells) will also be explored.

A rational next step is to design a properly stratified study to evaluate the contribution of different factors to the capture and survival of green sturgeon in the bottom-trawl fishery that targets California halibut. A future study could also incorporate an examination of stress responses (Lankford et al., 2005; Webb and Doroshov, 2011; Beardsall et al., 2013; McLean et al., 2019). Reports by fishermen and observers further indicate that California sea lions (*Zalophus californianus*) and Steller sea lions (*Eumetopias jubatus*) are sometimes present in the area where green sturgeon are released. Postrelease predation could be a factor (Cook et al., 2019). Ingestion of sturgeon fitted with pop-up satellite tags could be inferred from tag data that indicates movement patterns (e.g., Kerstetter et al., 2004) or stomach temperature (e.g., Béguer-Pon et al., 2012) of a predator.

Trawl-net modifications that reduce encounters or lethal interactions with green sturgeon should also be explored, given that bycatch avoidance is the best mechanism to reduce postrelease mortality. Research should be undertaken in collaboration with fishermen and with the objective of maintaining a viable fishery while reducing interactions with green sturgeon. Although examples of trawl-net modifications meant to exclude sturgeon are lacking, visual studies (e.g., Piasente et al., 2004; Jones et al., 2008) could inform designs that minimize interactions and maintain viability of the target fishery.

Acknowledgments

This project was supported by the NMFS Southwest Fisheries Science Center and National Cooperative Fisheries Fund and by the NMFS West Coast Region and Office of Protected Resources. Fishermen targeting California halibut and WCGOP observers were essential to the success of this work. We are grateful to R. Morse (West Coast Region affiliate) for his assistance with geographical information system analyses and map generation. We dedicate this work to our colleague E. Mora, who passed away on 22 May 2019. He was the powerhouse behind the study, a giant in the world of green sturgeon research, and a one-of-a-kind colleague.

Literature cited

Anderson, E. C., T. C. Ng, E. D. Crandall, and J. C. Garza.
2017. Genetic and individual assignment of tetraploid green sturgeon with SNP assay data. Conserv. Genet. 18: 1119–1130.

ASSRT (Atlantic Sturgeon Status Review Team).
2007. Status review of Atlantic sturgeon (*Acipenser oxyrinchus oxyrinchus*), 174 p. Report to Northeast Reg. Off., Natl. Mar. Fish. Serv., NOAA, Gloucester, MA. [Available from website.]

Beamesderfer, R. C. P., M. L. Simpson, and G. J. Kopp.
2007. Use of life history information in a population model for Sacramento green sturgeon. Environ. Biol. Fish. 79: 315–337.

Beardsall, J. W., M. F. McLean, S. J. Cooke, B. C. Wilson, M. J. Dadswell, A. M. Redden, and M. J. W. Stokesbury.
2013. Consequences of incidental otter trawl capture on survival and physiological condition of threatened Atlantic sturgeon. Trans. Am. Fish. Soc. 142:1202–1214.

Béguer-Pon, M., J. Benchetrit, M. Castonguay, K. Aarestrup, S. E. Campana, M. J. W. Stokesbury, and J. J. Dodson.
2012. Shark predation on migrating adult American eels (*Anguilla rostrata*) in the Gulf of St. Lawrence. PLoS ONE 7(10):e46830.

Bishop, C. M.
2006. Pattern recognition and machine learning, 738 p. Springer-Verlag, New York.

Breece, M. W., D. A. Fox, K. J. Dunton, M. G. Frisk, A. Jordaan, and M. J. Oliver.
2016. Dynamic seascapes predict the marine occurrence of an endangered species: Atlantic sturgeon *Acipenser oxyrinchus oxyrinchus*. Methods Ecol. Evol. 7:725–733.

Brooke, S. G., L. L. Desfosse, and W. A. Karp.
2012. Estimating overall fish bycatch in U.S. commercial fisheries. Mar. Fish. Rev. 74(3):1–5.

Burges, C. J. C.
1998. A tutorial on support vector machines for pattern recognition. Data Min. Knowl. Disc. 2:121–167.

Campana, S. E., W. Joyce, M. Fowler, and M. Showell.
2016. Discards, hooking, and post-release mortality of porbeagle (*Lamna nasus*), shortfin mako (*Isurus oxyrinchus*), and blue shark (*Prionace glauca*) in the Canadian pelagic longline fishery. ICES J. Mar. Sci. 73:520–528.

Collins, M. R., S. G. Rogers, T. I. J. Smith, and M. L. Moser.
2000. Primary factors affecting sturgeon populations in the southeastern United States: fishing mortality and degradation of essential habitats. Bull. Mar. Sci. 66:917–928.

Cook, K. V., A. J. Reid, D. A. Patterson, K. A. Robinson, J. M. Chapman, S. G. Hinch, and S. J. Cooke.
2019. A synthesis to understand responses to capture stressors among fish discarded from commercial fisheries and options for mitigating their severity. Fish Fish. 20:25–43.

Davies, R. W. D., S. J. Cripps, A. Nickson, and G. Porter.
2009. Defining and estimating global marine fisheries bycatch. Mar. Policy 33:661–672.

Davis, M. W.
2002. Key principles for understanding fish bycatch discard mortality. Can. J. Fish. Aquat. Sci. 59:1834–1843.

Davis, M. W., and S. J. Parker.
2004. Fish size and exposure to air: potential effects on behavioral impairment and mortality rates in discarded sablefish. North Am. J. Fish. Manage. 24:518–524.

Davis, M. W., B. L. Olla, and C. B. Schreck.
2001. Stress induced by hooking, net towing, elevated sea water temperature and air in sablefish: lack of concordance between mortality and physiological measures of stress. J. Fish Biol. 58:1–15.

Dunton, K. J., A. Jordaan, D. O. Conover, K. A. McKown, L. A. Bonacci, and M. G. Frisk.
2015. Marine distribution and habitat use of Atlantic sturgeon in New York lead to fisheries interactions and bycatch. Mar. Coast. Fish. 7:18–32.

Erickson, D. L., and J. E. Hightower.
2007. Oceanic distribution and behavior of green sturgeon. Am. Fish. Soc. Symp. 56:197–211.

Federal Register.
2006. Endangered and threatened wildlife and plants: threatened status for southern distinct population segment of North American green sturgeon. Fed. Reg. 71:17757–17766. [Available from website.]

Gale, M. K., S. G. Hinch, and M. R. Donaldson.
2013. The role of temperature in the capture and release of fish. Fish Fish. 14:1–33.

Hoolihan, J. P., J. Luo, F. J. Abascal, S. E. Campana, G. De Metrio, H. Dewar, M. L. Domeier, L. A. Howey, M. E. Lutcavage, M. K. Musyl, et al.
2011. Evaluating post-release behaviour modification in large pelagic fish deployed with pop-up satellite archival tags. ICES J. Mar. Sci. 68:880–889.

Hutchinson, M. R., D. G. Itano, J. A. Muir, and K. N. Holland.
2015. Post-release survival of juvenile silky sharks captured in a tropical tuna purse seine fishery. Mar. Ecol. Prog. Ser. 521:143–154.

IUCN (International Union for Conservation of Nature).
2018. The IUCN Red List of Threatened Species. Vers. 2018-1. [Available from website, accessed July 2018.]

Johnson, T. R., and W. L. T. van Densen.
2007. Benefits and organization of cooperative research for fisheries management. ICES J. Mar. Sci. 64:834–840.

Jones, E. G., K. Summerbell, and F. O'Neill.
2008. The influence of towing speed and fish density on the behavior of haddock in a trawl cod-end. Fish. Res. 94:166–174.

Kaplan, E. L., and P. Meier.
1958. Nonparametric estimation from incomplete observations. J. Am. Stat. Assoc. 53:457–481.

Kerstetter, D. W., J. J. Polovina, and J. E. Graves.
2004. Evidence of shark predation and scavenging on fishes equipped with pop-up satellite archival tags. Fish. Bull. 102:750–756.

Lankford, S. E., T. E. Adams, R. A. Miller, and J. J. Cech Jr.
2005. The cost of chronic stress: impacts of a nonhabituating stress response on metabolic variables and swimming performance in sturgeon. Physiol. Biochem. Zool. 78: 599–609.

Lindley, S. T., D. L. Erickson, M. L. Moser, G. Williams, O. P. Langness, B. W. McCovey Jr., M. Belchik, D. Vogel, W. Pinnix, J. T. Kelly, et al.
2011. Electronic tagging of green sturgeon reveals population structure and movement among estuaries. Trans. Am. Fish. Soc. 140:108–122.

Mandelman, J. W., A. M. Cicia, G. W. Ingram Jr., W. B. Driggers III, K. M. Coutre, and J. A. Sulikowski.
2013. Short-term post-release mortality of skates (family Rajidae) discarded in a western North Atlantic commercial otter trawl fishery. Fish. Res. 139:76–84.

McLean, M. F., M. K. Litvak, S. J. Cooke, K. C. Hanson, D. A. Patterson, S. G. Hinch, and G. T. Crossin.
2019. Immediate physiological and behavioural response from catch-and-release of wild white sturgeon (*Acipenser transmontanus* Richardson, 1836). Fish. Res. 214:65–75.

Miller, E. A.
2017. Niche partitioning by green sturgeon (*Acipenser medirostris*) and white sturgeon (*A. transmontanus*) in the San Francisco Estuary and Sacramento River. Ph.D. diss., 174 p. Univ. Calif. Davis, Davis, CA.

Mora, E. A., R. D. Battleson, S. T. Lindley, M. J. Thomas, R. Bellmer, L. J. Zarri, and A. P. Klimley.
2018. Estimating the annual spawning run size and population size of the Southern Distinct Population Segment of green sturgeon. Trans. Am. Fish. Soc. 147: 195–203.

Moser, M. L., S. C. Corbett, B. J. Burke, and O. P. Langness.
2018. Potential for use of accelerometers to monitor green sturgeon *Acipenser medirostris* (Ayres, 1854) behavior after handling. J. Appl. Ichthyol. 34:405–411. website

Murphy, K. P.
2012. Machine learning: a probabilistic perspective, 1104 p. MIT Press, Cambridge, MA.

NMFS (National Marine Fisheries Service).
2015. Southern distinct population segment of the North American green sturgeon. 5-year review: summary and evaluation, 38 p. West Coast Reg., Natl. Mar. Fish. Serv., NOAA, Long Beach, CA. [Available from website.]

Olla, B. L., M. W. Davis, and C. B. Schreck.
1997. Effects of simulated trawling on sablefish and walleye pollock: the role of light intensity, net velocity and towing duration. J. Fish Biol. 50:1181–1194.

Parker, S. J., P. S. Rankin, R. W. Hannah, and S. B. Schreck.
2003. Discard mortality of trawl-caught lingcod in relation to tow duration and time on deck. North Am. J. Fish. Manage. 23:530–542.

Pedregosa, F., G. Varoquaux, A. Gramfort, V. Michel, B. Thirion, O. Grisel, M. Blondel, P. Prettenhofer, R. Weiss, V. Dubourg, et al.
2011. Scikit-learn: machine learning in Python. J. Mach. Learn. Res. 12:2825–2830.

Piasente, M., I. A. Knuckey, S. Eayrs, and P. E. McShane.
2004. In situ examination of the behaviour of fish in response to demersal trawl nets in an Australian trawl fishery. Mar. Freshw. Res. 55:825–835.

Pikitch, E. K., P. Doukakis, L. Lauck, P. Chakrabarty, and D. L. Erickson.
2005. Status, trends and management of sturgeon and paddlefish fisheries. Fish Fish. 6:233–265.

Poisson, F., J. D. Filmalter, A.-L. Vernet, and L. Dagorn.
2014. Mortality rate of silky sharks (*Carcharhinus falciformis*) caught in the tropical tuna purse seine fishery in the Indian Ocean. Can. J. Fish. Aquat. Sci. 71:795–798.

Raby, G. D., J. R. Packer, A. J. Danylchuk, and S. J. Cooke.
2014. The understudied and underappreciated role of predation in the mortality of fish released from fishing gears. Fish Fish. 15:489–505.

Raschka, S.
2015. Python machine learning, 454 p. Packt Publishing, Birmingham, UK.

R Core Team.
2016. R: a language and environment for statistical computing. R Foundation for Statistical Computing, Vienna, Austria. [Available from website, accessed November 2016]

Stein, A. B., K. D. Friedland, and M. Sutherland.
2004. Atlantic sturgeon marine distribution and habitat use along the Northeastern coast of the United States. Trans. Am. Fish. Soc. 133:527–537.

Sugiyama, M.
2016. Introduction to statistical machine learning, 534 p. Morgan Kaufman, Waltham, MA.

Suuronen, P.
2005. Mortality of fish escaping trawl gears. FAO Fish. Tech. Pap. 478, 72 p. FAO, Rome.

Suuronen, P., and D. L. Erickson.
2010. Mortality of animals that escape fishing gears or are discarded after capture: approaches to reduce mortality. *In* Behavior of marine fishes: capture process and conservation challenges (P. He, ed.), p. 265–294. Blackwell Publishing Ltd., Ames, IA.

Therneau, T. M.
2015. A package for survival analysis in S. Vers. 2.38. [Available from website, accessed May 2017.]

Therneau, T. M., and P. M. Grambsch.
2000. Modeling survival data: extending the Cox model, 350 p. Springer, New York.

Watt, J., R. Borhani, and A. K. Katsaggelos.
2016. Machine learning refined: foundations, algorithms, and applications, 298 p. Cambridge Univ. Press, Cambridge, UK.

Webb, M. A. H., and S. I. Doroshov.
2011. Importance of environmental endocrinology in fisheries management and aquaculture of sturgeons. Gen. Comp. Endocrinol. 170:313–321.

Weltersbach, M. S., and H. V. Strehlow.
2013. Dead or alive—estimating post-release mortality of Atlantic cod in the recreational fishery. ICES J. Mar. Sci. 70:864–872.

Whitney, N. M., C. F. White, A. C. Gleiss, G. D. Schwieterman, P. Anderson, R. E. Hueter, and G. B. Skomal.
2016. A novel method for determining post-release mortality, behavior, and recovery period using acceleration data loggers. Fish. Res. 183:210–221.

Wilson, S. M., G. D. Raby, N. J. Burnett, S. G. Hinch, and S. J. Cooke.
2014. Looking beyond the mortality of bycatch: sublethal effects of incidental capture on marine animals. Biol. Conserv. 171:61–72.

Yochum, N., R. M. Starr, and D. E. Wendt.
2011. Utilizing fishermen knowledge and expertise: keys to success for collaborative fisheries research. Fisheries 36:593–605.

National Marine
Fisheries Service
NOAA

Fishery Bulletin
established in 1881

Spencer F. Baird
First U.S. Commissioner
of Fisheries and founder
of *Fishery Bulletin*

Growth of juvenile Atlantic sturgeon (*Acipenser oxyrinchus oxyrinchus*) in response to dual-season spawning and latitudinal thermal regimes

Erin L. Markin (contact author)[1]
David H. Secor[2]

Email address for contact author: erin.markin@noaa.gov

[1] Horn Point Laboratory
Center for Environmental Science
University of Maryland
2020 Horns Point Road
Cambridge, Maryland 21613
Present address for contact author: Office of Protected Species
National Marine Fisheries Service, NOAA
1315 East-West Highway
Silver Spring, Maryland 20910

[2] Chesapeake Biological Laboratory
Center for Environmental Science
University of Maryland
P.O. Box 38
Solomons, Maryland 20688

Abstract—Populations of Atlantic sturgeon (*Acipenser oxyrinchus oxyrinchus*) occur over a broad latitudinal range, such that size-dependent winter mortality of juveniles could select for latitudinal countergradient variation in growth rate of juveniles. To investigate latitudinal countergradient variation in growth between populations, growth of strains of the Saint John River (New Brunswick, Canada) and the Altamaha River (Georgia) was compared in a common-garden experiment by exposing juveniles (Altamaha River strain: mean length of 178 mm [standard deviation (SD) 8.1]; Saint John River strain: mean length of 180 mm [SD 9.2]) to simulated temperature regimes representing the latitudinal range of this subspecies (in the Saint John, Choptank, and Edisto Rivers). No strain effect was detected. To evaluate thermal phenology, a growth-degree-day (GDD) model was developed from responses of fish in a laboratory. Growth degree days were predicted for juveniles that spawned in the fall and for systems south of Chesapeake Bay, where supraoptimal summertime temperatures occur. Predicted lengths of age-1 Atlantic sturgeon generally fell within the range of values reported in literature. Results of analyses with the GDD model support evidence that spawning occurs in the fall only in systems south of the New York Bight, and the model could be applied in evaluation of scenarios of warming and dual-season spawning throughout the range of this subspecies.

Manuscript submitted 17 April 2019.
Manuscript accepted 28 February 2020.
Fish. Bull. 118:74–86 (2020).
Online publication date: 23 March 2020.
doi: 10.7755/FB.118.1.7

The views and opinions expressed or implied in this article are those of the author (or authors) and do not necessarily reflect the position of the National Marine Fisheries Service, NOAA.

Conservation success of threatened and endangered sturgeon species is most sensitive to factors that influence first-year survival; therefore, juvenile sturgeon should receive the highest conservation priority (Gross et al., 2002; Secor et al., 2002). Age-0 and older juveniles (<100 cm total length [TL]) of the Atlantic sturgeon subspecies *Acipenser oxyrinchus oxyrinchus*, distinct population segments of which are protected as threatened or endangered under the U.S. Endangered Species Act (Federal Register, 2012a, 2012b), are encountered in over a dozen tributaries used for spawning (Hilton et al., 2016). Their growth and survival conditions may vary widely across the broad latitudinal range (of about 15° or 2200 km) in which these nursery systems occur (from the Satilla River in Florida [31° N] to the Saint Lawrence River in Canada [44°30′ N]). Assessment and conservation of juvenile production is confounded further by the recent discovery that, in some portions of their range, Atlantic sturgeon spawn in both spring and fall (Balazik et al., 2012; Hager et al., 2014; Balazik and Musick, 2015; Smith et al., 2015). Such dual-season spawning would result in 2 size modes associated with age-0 and age-1 juveniles in any given season. Therefore, to assess recruitment, lengths of sampled juveniles need to be discriminated between subannual spawning cohorts.

In some species that occur over broad latitudinal ranges, juvenile growth rates are faster at higher latitudes (Conover, 1992). Regions in higher latitudes support shorter growing seasons, earlier onsets of winter, and greater severity of winter (Yamahira and Conover, 2002) as well as scarcity of prey in winter (Shuter et al., 2012). In North America, the latitudinal gradient of shorter summers and longer winters in the north, compared with winters in the south, can result in systematic changes in population traits, such as spawning time, somatic growth, size and age at reproduction, and lifespan (Shuter et al., 2012), but juvenile growth may be particularly responsive to countergradient selection.

Atlantic silverside (*Menidia menidia*) occur over a latitudinal range similar to that of Atlantic sturgeon, and juveniles grow faster at higher latitudes, a difference in growth that has reproductive implications for this short-lived species (Conover and Present, 1990). For populations sampled from a representative range of latitudes, length of growing season varied by a factor of 2.5, but sizes of Atlantic silverside at the end of the season were similar across latitudes (Conover and Present, 1990). Northern strains of mummichog (*Fundulus heteroclitus*) had a higher capacity for growth when reared in a common-garden experiment with fish from southern latitudes (Schultz et al., 1996). Similarly, larval (Conover et al., 1997) and juvenile (Secor et al., 2000) striped bass (*Morone saxatilis*) obtained from higher latitudes grew faster than those from lower latitudes in common-garden experiments. Northern populations of lake sturgeon (*Acipenser fulvescens*) were smaller at a given age than southern populations, but they grew at a higher rate when growth was adjusted for expected thermal conditions (Power and McKinley, 1997). Therefore, countergradient variation in growth is expected for species that occur across wide temperate latitudinal ranges.

In temperate systems, cessation of growth and lethal temperatures during winter months are thought to drive latitudinal countergradient trends in juvenile growth (Conover, 1992; Schultz et al., 1996; Power and McKinley, 1997). Winter mortality may occur because of thermal stress, starvation, predation, disease, winter hypoxia, and physical disturbance (e.g., ice flows). However, it is thermal stress (e.g., inability to maintain homeostasis) and starvation (e.g., insufficient energy stores) that likely account for a significant proportion of winter mortality (Hurst, 2007). At higher latitudes, smaller body size and lower energy stores may increase winter mortality (Yamahira and Conover, 2002; Garvey and Marschall, 2003; Crossman et al., 2009; Pörtner and Peck, 2010; Shuter et al., 2012). Striped bass in the Hudson River in New York shifted from increasing length early in the growing season to increasing energy reserves toward the end of the growing season, presumably to reduce risk of winter mortality (Hurst and Conover, 2003). Atlantic silverside in northern latitudes accumulated energy stores faster than their southern counterparts, providing evidence that risk of winter starvation resulted in selection to accumulate energy during the first growing season (Schultz and Conover, 1997). There has been little research on winter mortality of sturgeon species. Crossman et al. (2009) observed that only 40% of stocked juvenile lake sturgeon survived their first winter, indicating that winter mortality could be an important agent of natural selection. Still, they observed no relationship between size and winter survival.

Seasonal changes in temperature that juveniles encounter during their first year of life, referenced here as *thermal phenology*, play an integral role in determining their growth and survival (Neuheimer and Taggart, 2007; Puckett et al., 2008; Humphrey et al., 2014). To evaluate thermal phenology, a valuable tool is the growth-degree-day (GDD) model, which integrates temperatures that a fish experiences together with thermal tolerance thresholds. The GDD method allows individual growth calendars to be tracked for differing hatch dates and regions, supporting simulation of thermal phenologies for growth of Atlantic sturgeon across latitudes. Although fish weight can be used as the principal growth variable explained by GDD, length of fish is preferred because it either does not change or changes positively on a seasonal basis (i.e., fish will not shrink in length) (Neuheimer and Taggart, 2007; Humphrey et al., 2014). In addition, length is the most commonly monitored measure of size, allowing us to compare model predictions with published length-at-age data.

To test if northern and southern populations of Atlantic sturgeon express countergradient variation in growth, we reared juveniles in common-garden experiments in 3 thermal regimes representative of the latitudinal range of this subspecies. In addition to this laboratory experiment, we applied a GDD model over the latitudinal range of Atlantic sturgeon to determine: 1) the number of GDD accumulated during the first year of life and 2) the predicted size of Atlantic sturgeon at the end of the first year of life (age: 1.0 year). Specific hypotheses included 1) juvenile growth rate will be positively associated with the latitude of their source strain, 2) strain growth rates will differ among thermal regimes, 3) accumulated GDD (juvenile growth performance) and size at age of 1.0 year will be less for northern strains than southern strains, and 4) the accumulated GDD and size at winter onset will be higher for Atlantic sturgeon that spawned in spring than for those that spawned in fall.

Materials and methods

Laboratory experiment

A comparison of juvenile growth between the strains of Atlantic sturgeon from the Saint John River in New Brunswick, Canada, and the Altamaha River in Georgia was conducted under controlled laboratory conditions. Atlantic sturgeon from the population in the Saint John River were provided by C. Ceapa (Acadian Sturgeon and Caviar Inc.[1], Saint John, Canada) in July 2013 (hatch date: 21 July 2013; water temperature: ~15°C) from a spawning by 1 female and 3–4 males. Atlantic sturgeon from the population in the Altamaha River were acquired from the U.S. Fish and Wildlife Bears Bluff National Fish Hatchery in Wadmalaw Island, South Carolina, in August 2013 (hatch date: 9 August 2013; water temperature: ~22°C) from a spawning by 1 female and 1 male. Upon arrival, larvae (~10 mm TL) were reared in freshwater

---

[1] Mention of trade names or commercial companies is for identification purposes only and does not imply endorsement by the National Marine Fisheries Service, NOAA.

(~17.8°C) and fed nauplii of brine shrimp (*Artemia* spp.) before being weaned to a commercial diet at ~35 mm TL and acclimated to water from the Choptank River (a tributary of Chesapeake Bay, Maryland) (salinity: ~10) until the start of the experiment.

Fish from the populations in the Altamaha and Saint John Rivers were exposed to 3 thermal regimes. Ambient seasonal temperatures at the Choptank River (intermediate latitude: data from in situ measurements; senior author, unpubl. data) were used for one thermal regime, and other regimes simulated the mean monthly temperatures recorded in the winter and spring of 2013 at the Edisto River, South Carolina (low latitude: data available from the National Estuarine Research Reserve System [NERRS] at website), and at the Saint John River (high latitude; Ceapa[2]). The treatment in which fish from the Saint John River strain were exposed to the thermal regime of the Edisto River received 6 replicates. The treatment in which fish from the Altamaha River strain were exposed to the thermal regime of the Saint John River received 6 replicates. The treatment in which both strains were exposed to the thermal regime of the Choptank River received 3 replicates.

Smaller tanks (148 L) were used for the Edisto and Saint John River thermal regimes, but owing to tank availability, larger tanks (1600 L) were used for the Choptank River thermal regime treatments. Seven fish were stocked into each tank and acclimated to the target temperature at a rate of 1°C/d. The experiment was conducted during December 2013–June 2014 for the thermal regime treatments that simulated temperatures in the Choptank River and Edisto River. Owing to a mechanical failure, the Saint John River thermal regime treatment was terminated in March 2014. The Saint John River and Edisto River thermal regimes were controlled by using heat exchangers in a partially recirculating aquaculture system with filtered (2 µm) water from the Choptank River. Salinity ranged from 8 to 12. Fish were fed an amount equal to 5% of their body weight per day (sturgeon booster diet, Zeigler Bros Inc., Gardners, PA) during the course of the experiment. The amount of food consumed or discarded was not quantified.

Weights in grams and TLs in millimeters were measured for all experimental fish and recorded at intervals of approximately 4 weeks. Because of the small initial size of the fish from the Altamaha River strain (mean: 178 mm TL [standard deviation (SD) 8.1] and 22 g [SD 3.0]) and the Saint John River strain (mean: 180 mm TL [SD 9.2] and 24 g [SD 3.1]), individual fish were not marked; therefore, lengths and weights for each tank were summed for statistical comparisons. Among treatments, there was no statistical difference in the initial lengths (analysis of variance [ANOVA]: between strains, sample size [n]=30, P=0.48; between thermal regimes, n=30, P=0.76) or in weights (ANOVA: between strains, n=30, P=0.06; between thermal regimes, n=30, P=0.84).

Growth-degree-day model and analysis

The GDDs were calculated for each temperature profile as follows:

$$GDD = \Sigma\,(T_{\mathrm{i}} - T_{\mathrm{th\text{-}min}}) \times \Delta d \text{ or} \quad (1)$$

$$GDD = \Sigma\,(T_{\mathrm{th\text{-}max}} - T_{\mathrm{i}}) \times \Delta d, \quad (2)$$

where T_{i} = the mean daily water temperature;
$T_{\mathrm{th\text{-}min}}$ = the minimum threshold (4°C);
$T_{\mathrm{th\text{-}max}}$ = the maximum threshold (28°C); and
Δd = the number of days between sampling.

Note that we assumed that fish cannot lose length; therefore, GDD was assigned a value of 0 if temperatures were outside the tolerance limits of the Atlantic sturgeon. The minimum and maximum thermal growth thresholds were selected at 4°C and 28°C on the basis of laboratory experiments and observations of thermal limits in Atlantic sturgeon (Dovel and Berggren, 1983; Mohler[3]; Niklitschek and Secor, 2005, 2009).

Repeated measures ANOVA, conducted in statistical software R, vers. 3.3.2 (R Core Team, 2016), was used to compare the effects of thermal regime and strain on the tank means for repeated measurements of length, weight, and specific growth rate. Four models were compared to determine the best covariance structure among repeated measures: 1) a baseline model assuming independence (model 1), 2) a model with dependence between tanks but no correlation between days (model 2), 3) a model with dependence between tanks and first-order autoregressive correlation (an autoregressive lag-1 covariance structure) between days (model 3), and 4) a model with dependence between tanks and autoregressive–moving average (1,1) correlation (autoregressive–moving average model) between days (model 4). The best model was determined by using the lowest Akaike information criterion (AIC), after which the final model structure was determined by using restricted maximum likelihood. Post-hoc comparisons were made by using Tukey's honestly significant difference to determine which comparisons were significant.

Growth degree days along a latitudinal gradient

Water temperature data for estuarine systems during the period 2008–2013 were obtained from 7 NERRS sites, representing the latitudinal distribution of Atlantic sturgeon: (1) Wells, Maine, (2) Great Bay, New Hampshire, (3) Hudson River, New York, (4) Chesapeake Bay, Maryland, (5) North Carolina, (6) the area from North Inlet to Winyah Bay, South Carolina (hereafter, referred to as *South Carolina*), and (7) Ashepoo–Combahee–Edisto Basin in South Carolina. For consistency and under the assumption that tidal freshwater areas represent a substantial fraction of habitats where growth of age-0 fish occurs,

---

[2] Ceapa, C. 2013. Personal commun. Acadian Sturgeon and Caviar Inc., 214 King St. E., Saint John, New Brunswick E2L 1H3, Canada.

[3] Mohler, J. W. 2004. Culture manual for the Atlantic sturgeon, *Acipenser oxyrinchus oxyrinchus*, 70 p. [Available from Region 5, U.S. Fish Wildl. Serv., 300 Westgate Center Dr., Hadley, MA.]

Table 1

Mean total length and weight of Atlantic sturgeon (*Acipenser oxyrinchus oxyrinchus*) during each sampling period for each thermal regime from December 2013 to March 2014. Thermal regimes included ambient seasonal temperatures at the Choptank River in Maryland (intermediate latitude) and mean monthly temperatures recorded in the winter and spring of 2013 at the Edisto River in South Carolina (low latitude) and at the Saint John River in Canada (high latitude). Standard deviations are given in parentheses.

	Total length (mm)			Weight (g)		
Sampling period	Saint John River	Choptank River	Edisto River	Saint John River	Choptank River	Edisto River
0	179 (11)	181 (6)	178 (7)	23 (4)	24 (3)	23 (2)
1	181 (10)	196 (5)	208 (11)	24 (4)	30 (5)	37 (4)
2	181 (10)	196 (5)	246 (17)	23 (3)	33 (4)	61 (10)
3	182 (11)	199 (5)	298 (13)	24 (4)	36 (4)	107 (10)

temperature records for a single station within each NERRS site corresponding with tidal freshwater or the lowest salinity station were used to estimate GDDs from daily average means for each station and then summed by month. For stations where winter water temperatures were not recorded, we assumed zero growth occurred during this season because water temperatures recorded before or after the missing period were at or below the thermal tolerance threshold for Atlantic sturgeon.

Using ANOVA, we compared GDD between NERRS sites and years. Additionally, cumulative GDD was calculated for the first year of life (age: 1.0 year) for each NERRS site, for Atlantic sturgeon that spawned in spring and for those that spawned in fall. Assumed spawning dates for sturgeon that spawned in spring were 1 July (Maine), 1 June (New Hampshire), 1 May (New York and Maryland), and 1 April (North Carolina and South Carolina), and assumed spawning dates for sturgeon that spawned in fall were 1 September (Maryland) and 1 October (North Carolina and South Carolina) (Dovel[4]; Smith et al., 1984; Gilbert[5]; Collins et al., 2000; Balazik et al., 2012). Tukey's honestly significant difference was used for post-hoc comparisons between sites and years.

Length at age 1 was predicted from combined experimental data by using a von Bertalanffy growth function with nonlinear regression:

$$L_{\mathrm{GDD}} = L_{\infty}\left(1 - e^{-K(GDD - GDD_0)}\right), \tag{3}$$

where L_{∞} = asymptotic length;
K = growth coefficient;
GDD = GDD at age 1; and
GDD_0 = GDD at hatch.

The model was fitted by using an iterative fitting procedure (Solver, Frontline Systems Inc., Incline Village, NV) within Microsoft Excel 2003 (Microsoft Corp., Redmond, WA). Adjustments to GDDs used in this model were needed for the growth period prior to the experiment, which was estimated as 1708 GDD=122 d×18°C. Predicted length at the onset of winter (1 January), from the assumed date of fall spawning was also calculated by using the von Bertalanffy growth function. Predicted length at the onset of summer (1 July) from the assumed date of spring spawning was also calculated by using the von Bertalanffy growth model for systems south of the Hudson River, New York.

Results

Laboratory experiment

The effect of thermal regime and strain on specific growth rate has been evaluated (Markin, 2017); therefore, the results reported here focus on effects on length and weight. Owing to the early termination of the experiment that used the Saint John River thermal regime, we did initial comparisons of thermal regimes for the abbreviated period December 2013–March 2014 (Table 1). Based on AIC criteria, ANOVA tests of average sturgeon length and weight responses used a within-tank autoregressive–moving average model between days (Table 2). There was no effect of strain on average fish length (P=0.82) or weight (P=0.88). Nor was there a significant interaction between thermal regime and strain on length (P=0.80) or weight (P=0.78). Therefore, these factors were dropped in the development of the final model. Both sturgeon length and weight were significantly influenced by thermal regime treatment (Table 3). As a result, regardless of strain, juveniles exposed to the Edisto River thermal regime were significantly larger (mean: 232.0 mm TL and 57.0 g) than those that experienced the Saint John River thermal regime (mean: 180.6 mm TL and 23.6 g; P<0.001) and the Choptank River thermal regime (mean: 192.8 mm TL and 30.7 g; P<0.03). Although higher growth

---

[4] Dovel, W. L. 1979. The biology and management of shortnose and Atlantic sturgeon of the Hudson River, 54 p. NY Dep. Environ. Conserv. final rep. Proj. no. AFS9-R. [Available from NY Dep. Environ. Conserv., 625 Broadway, Albany, NY 12233-0001.]

[5] Gilbert, C. R. 1989. Species profiles: life histories and environmental requirements of coastal fishes and invertebrates (Mid-Atlantic Bight)—Atlantic and shortnose sturgeons. U.S. Fish Wildl. Serv. Biol. Rep. 82 (11.122), 28 p. [Available from website.]

Table 2

Comparison of models used for repeated measures analysis of variance of total length and weight of Atlantic sturgeon (*Acipenser oxyrinchus oxyrinchus*) between thermal regimes. Three thermal regimes were used to represent the latitudinal range of this subspecies, with ambient seasonal temperatures at the Choptank River in Maryland and simulated temperatures of the Edisto River in South Carolina and the Saint John River in Canada. Total lengths were measured between December 2013 and March 2014. The models were designed with no covariance (model 1), with dependence between tanks only (model 2), with an autoregressive lag-1 covariance structure (model 3), and with autoregressive–moving average correlation (model 4). Values for Akaike information criterion (AIC) and the change in AIC (ΔAIC) are provided.

Model structure	Model	AIC	ΔAIC	Random
Length~thermal regime	1	1136.90	59.10	~1 | Tank
	2	1128.20	50.40	~1 | Tank
	3	1109.40	31.60	~1 | Tank
	4	1077.80	0.00	~1 | Tank
Weight~thermal regime	1	1051.80	34.90	~1 | Tank
	2	1022.30	5.40	~1 | Tank
	3	1035.40	18.50	~1 | Tank
	4	1016.90	0.00	~1 | Tank

Table 3

Summary of results from analysis of variance and Tukey's honestly significant difference pairwise comparisons between total length of Atlantic sturgeon (*Acipenser oxyrinchus oxyrinchus*) and the thermal regime to which fish were exposed in experiments conducted between December 2013 and March 2014. Thermal regimes included ambient seasonal temperatures at the Choptank River in Maryland and temperatures recorded at the Edisto River in South Carolina and the Saint John River in Canada. lsmean=least-square mean; SE=standard error of the mean.

Model structure	Treatment	lsmean	SE	df	Contrasts	*P*-value
Length~thermal regime	Saint John	180.3	10.2	27	Choptank–Saint John	0.86
	Choptank	189.6	10.2	27	Choptank–Edisto	0.02
	Edisto	239.0	14.4	27	Edisto–Saint John	<0.00
Weight~thermal regime	Saint John	23.7	6.0	27	Choptank–Saint John	0.82
	Choptank	30.1	8.6	27	Choptank–Edisto	0.01
	Edisto	63.9	6.0	27	Edisto–Saint John	<0.00

was observed for fish exposed to the Choptank River thermal regime, no significant difference was detected in the lengths of fish between the Saint John River (mean: 180.6 mm TL and 23.6 g) and the Choptank River (mean: 192.8 mm TL and 30.7 g) thermal regimes ($P>0.8$).

Because strain did not influence growth performance or interact with thermal regime, growth data were combined across all treatments to develop a predictive length-versus-GDD model for juveniles. A von Bertalanffy growth model best fit the nonlinear relationship (Fig. 1). The resulting equation was used to estimate growth of age-1 sturgeon along a latitudinal gradient, as discussed in subsequent sections:

$$length = 803.93\left(1 - e^{(-0.000167(\mathrm{GDD}-110.3))}\right), \qquad (4)$$

Growth degree days along a latitudinal gradient

For Atlantic sturgeon that spawned in spring, the accumulation of GDDs increased along a latitudinal gradient from Maine to Chesapeake Bay (n=35, P<0.01) (Fig. 2). Age-1 sturgeon in the 3 most northern systems (Maine, New Hampshire, and New York) accumulated significantly less GDD over the first year of life than more southerly sites. Age-1 sturgeon in the Chesapeake Bay region accumulated the most GDDs (mean: 4295 [SD 149]) compared with those in all other systems, particularly those in systems north of Chesapeake Bay. Between Chesapeake Bay and systems to its south, GDDs of fish were fairly similar. Latitudinal trends in GDDs were the result of days in each system experiencing suboptimal and supraoptimal temperatures (Table 4). Chesapeake Bay had the fewest number of days during which no growth occurred. Northern systems had

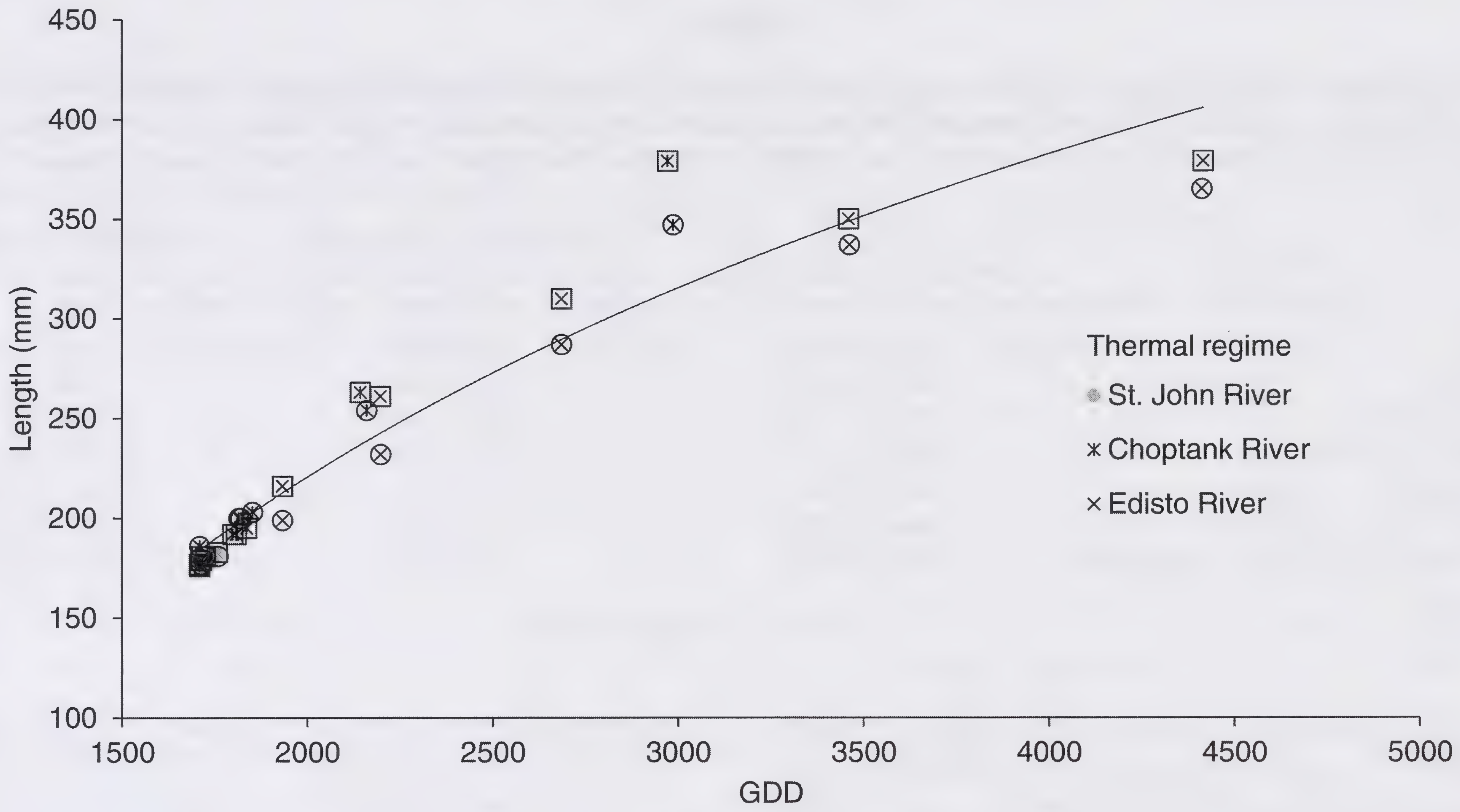

Figure 1

Relationship of total lengths and growth degree days (GDDs) of Atlantic sturgeon (*Acipenser oxyrinchus oxyrinchus*) for 3 thermal regimes that represent temperatures experienced by fish in the Edisto River in South Carolina, the Choptank River in Maryland, and the Saint John River in Canada and for 2 strains of Atlantic sturgeon from the Saint John River and the Altamaha River in Georgia, modeled by using a von Bertalanffy growth function. Total lengths were measured between December 2013 and March 2014. Open circles represent the strain from the Saint John River. Open squares represent the strain from the Altamaha River. Other symbols represent the thermal regimes, as indicated in the figure key.

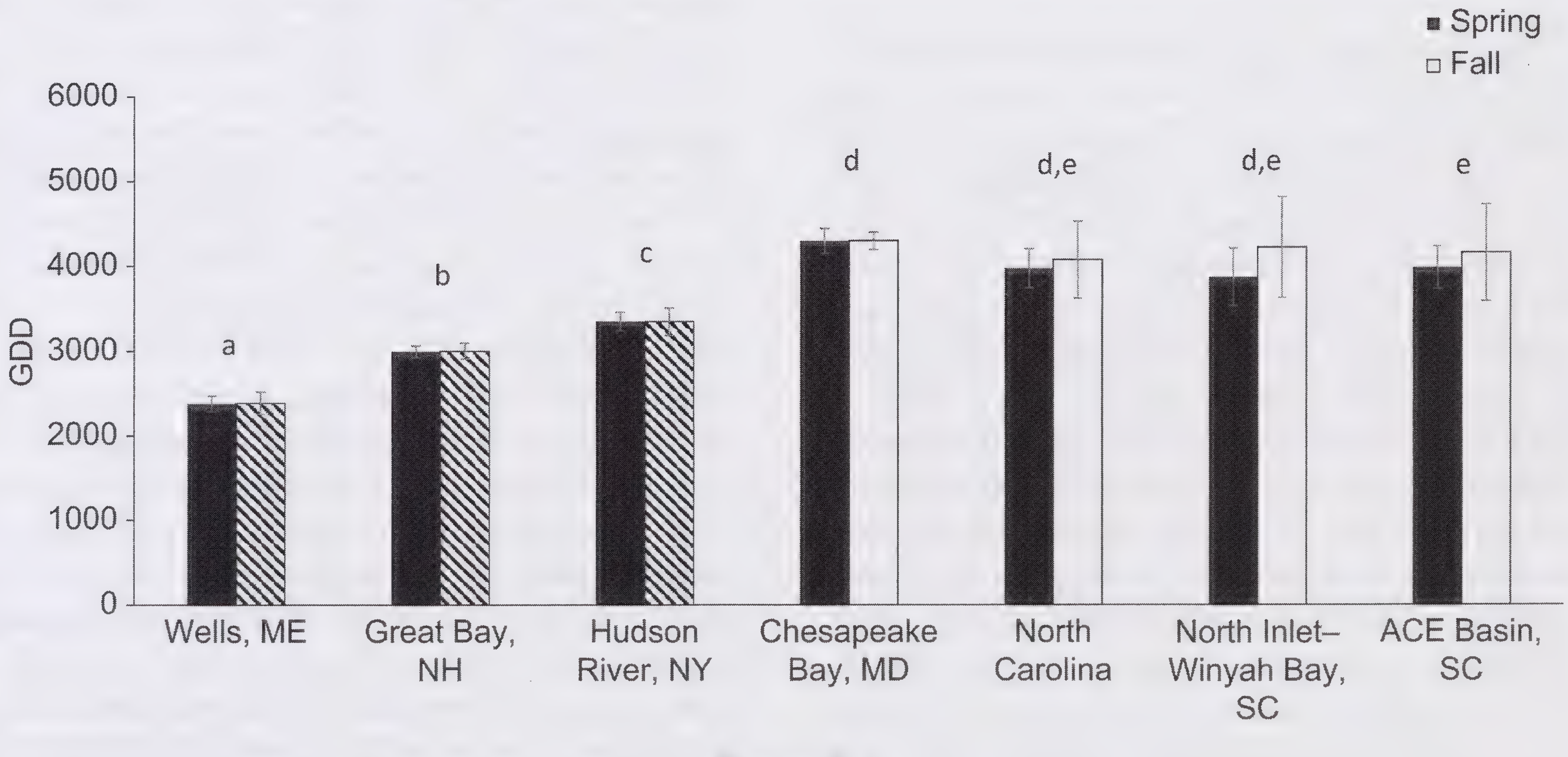

Figure 2

Accumulated growth degree days (GDD) of Atlantic sturgeon (*Acipenser oxyrinchus oxyrinchus*) in relation to their spawning cohort (fall and spring) and the thermal regimes to which they were exposed across a latitudinal range. Water temperature data used for thermal regimes were collected from National Estuarine Research Reserve System sites from Maine to South Carolina during 2008–2013. Different letters denote significant difference ($P<0.05$) according to results from analysis of variance and comparisons with Tukey's honestly significant difference. The bars with diagonal lines indicate a hypothetical scenario in which spawning occurs in fall in those locations. The southernmost site is the Ashepoo–Combahee–Edisto Basin (ACE Basin) in South Carolina. Error bars indicate standard deviations.

Table 4

Average annual growth degree days (GDDs) and the number of days of suboptimal and supraoptimal temperatures collected from the National Estuarine Research Reserve System (NERRS) sites across the latitudinal range of the Atlantic sturgeon (*Acipenser oxyrinchus oxyrinchus*) in the United States for the years 2008–2013. Standard deviations are given in parentheses.

NERRS site	Average annual GDD (d)	Average no. of days with suboptimal temperatures	Average no. of days with supraoptimal temperatures
Well, ME	197.3 (9.8)	123.8 (10.9)	0.0 (0.0)
Great Bay, NH	249.2 (9.7)	123.7 (9.6)	0.0 (0.0)
Hudson River, NY	277.7 (14.8)	119.2 (13.8)	0.7 (1.1)
Chesapeake Bay, MD	358.4 (14.5)	4.2 (6.0)	0.0 (0.0)
North Carolina	340.3 (28.2)	3.5 (4.8)	58.7 (20.0)
North Inlet–Winyah Bay, SC	348.5 (49.9)	2.0 (4.0)	62.0 (21.8)
Ashepoo–Combahee–Edisto Basin, SC	333.4 (50.2)	1.2 (2.6)	78.0 (22.5)

119–124 d with suboptimal temperatures, and southern systems had 59–79 d of supraoptimal temperatures. Sturgeon in systems where spawning is believed to occur in both spring and fall accumulated more GDDs during their first year of life than those in systems where spawning occurs only in spring (Fig. 2). In these systems, similar size at the age of 1.0 year was observed between fall and spring spawning cohorts for each system, but this result was largely an outcome of the simulation exercise in which each cohort experienced 365 d of GDDs for the same thermal regime. Slight deviations between cohorts are likely due to the difference in start times for the 2 cohorts.

Lengths along a latitudinal gradient

We estimated the TL of age-1 fish along a latitudinal gradient by using the accumulated GDD for each system during 2008–2012 (Table 5, Fig. 3). Age-1 Atlantic sturgeon that spawned in spring attained the smallest size in Maine (mean: 253.2 mm TL [SD 8.6]; range: 241.8–267.6 mm TL), whereas Chesapeake Bay produced the largest-sized Atlantic sturgeon (404.2 mm TL [SD 10.0]; range: 386.9–416.0 mm TL). Age-1 Atlantic sturgeon in New Hampshire had an estimated mean length of 307.0 mm TL (SD 5.7), in a range of 300.8–315.4 mm TL, and the mean length of age-1 sturgeon in New York was estimated to be 335.7 mm TL (SD 8.7), with a range of 321.5–346.0 mm TL. South of Chesapeake Bay, sizes of age-1 sturgeon were similar. Monthly lengths were estimated along a latitudinal gradient for Atlantic sturgeon that spawned in spring (Fig. 4, A–G) and fall (Fig. 5, A–D). For Atlantic sturgeon spawned in spring, the mean length after the first month of growth was estimated to be 45.6 mm TL (SD 6.0), in a range of 29.1–53.8 mm TL. For Atlantic sturgeon that spawned in fall, lengths after the first month of growth were estimated to have a mean of 53.4 mm TL (SD 4.0) and a range of 42.0–59.4 mm TL. Size at the onset of winter varied considerably for the fall cohort when exposed to a thermal regime that simulated temperatures in northern systems where the fall cohort is not observed, ranging from 22 to 102 mm TL from Maine to New York. In comparison, the size of fish in systems where the fall cohort is observed varied less: 119–174 mm TL for Chesapeake Bay and the systems south of it (Fig. 6). Juveniles that spawned in spring were considerably larger, with latitudinal trends mirroring trends in size at age of 1.0 year. Size at the onset of summer ranged from 108 to 157 mm TL for Chesapeake Bay and the systems south of it.

Discussion

In the laboratory experiment, we failed to detect an effect of strain on juvenile growth in a common-garden environment; therefore, the results of this study of Atlantic sturgeon do not support the existence of latitudinal countergradient growth variation. Although countergradient growth variation has been highlighted in other ectotherms that have wide latitudinal ranges (Conover et al., 2009), there are species for which countergradient growth variation has not been observed. Countergradient growth has not been reported for the California grunion (*Leuresthes tenuis*), possibly because of its oceanic life history (Brown et al., 2012). Populations of Atlantic cod (*Gadus morhua*) have responded similarly to a warm thermal regime, indicating that observed higher growth rates of southern populations were not a result of higher genetic capacities for growth (Purchase and Brown, 2001). For Atlantic salmon (*Salmo salar*) from 5 rivers in Norway that were reared in common thermal conditions in a previous study, no association between their river of origin and maximal or threshold growth rates was observed (Jonsson et al., 2001). In our study, Atlantic sturgeon had higher growth in warmer temperatures, a relationship that is expected for ectotherms, but the population of the Saint John River did not compensate for a shorter growing season with a greater capacity for growth. If strain does not influence growth, it should be possible to generalize thermal growth performance across latitudes and spawning periods and to predict sizes of juveniles across the range of this subspecies.

Seasonal observations of adult and early life stages in tributaries where Atlantic sturgeon spawn provide direct or circumstantial evidence for dual-season spawning for

Table 5

Reported and predicted total lengths of Atlantic sturgeon (*Acipenser oxyrinchus oxyrinchus*) at ages of 0–1 year along a latitudinal gradient from Canada to Georgia. Observed sizes are total lengths measured between December 2013 and March 2014; for some observed sizes, a mean is given instead of a range. Predicted sizes are estimates from nonlinear regression in this study. Modeled sampling months are hypothetical for this study.

Location	Observed size (mm)	Age (years)	Predicted size (mm)	Age (years)	Reported sampling period	Modeled sampling month	Source
Saint John River, Canada	217	1			May–October		Stewart et al. (2015)
Maine			241.8-267.6	1.0		June	This study
New Hampshire			300.8-315.4	1.0		May	This study
Connecticut River	225–640	1			May–October 2014		Savoy et al. (2017)
New York			321.5–346.0	1.0		April	This study
Hudson River, NY	323	0^+			October–May 1975, 1976, 1978		Dovel[a]
Hudson River, NY	502	1			October–May 1975–1978		Dovel[a]; Dovel and Berggren (1983)
Hudson River, NY	425–525	1			March–July		Peterson et al. (2000)
Hudson River, NY	450–550	1			August		Peterson et al. (2000)
Hudson River, NY	525–600	1			September		Peterson et al. (2000)
Hudson River, NY	575–625	1			October–December		Peterson et al. (2000)
Chesapeake Bay			386.9–416.0	1.0		April	This study
James River, VA	406–431[+]	Unknown			November		Balazik[b]
North Carolina			367.1–406.8	1.0		March	This study
South Carolina coastal rivers	550	1			Unknown		McCord et al. (2007); Schueller and Peterson (2010)
South Carolina			340.9–409.2	1.0		March	This study
Savannah River, SC/GA	410	0–1			Various		Peterson et al. (2008)
Ogeechee River, GA	310	0–1			May–December		Peterson et al. (2008)
Ogeechee River, GA	242–361	1			June–August 2007		Farrae et al. (2009)
Altamaha River, GA	379	0–1			June–August 2005		Peterson et al. (2008)
Altamaha River, GA	350–550	1			various		Schueller and Peterson (2010)
Satilla River, GA	340–540	1			September–July		Fritts et al. (2016)

[+] Total lengths were reported as 16–17 in.

[a] Dovel, W. L. 1979. The biology and management of shortnose and Atlantic sturgeon of the Hudson River, 54 p. Final report. Proj. no. AFS9-R. [Available from NY Dep. Environ. Conserv., 625 Broadway, Albany, NY 12233-0001.]

[b] Balazik, M. 2016. Personal commun. Virginia Commonwealth Univ., P.O. Box 842030, Richmond, VA 23284-2030.

populations in Maryland, Virginia, North Carolina, and South Carolina (Smith et al., 1984; Balazik et al., 2012; Hager et al., 2014; Balazik and Musick, 2015; Smith et al., 2015) and evidence that, in the Altamaha River, spawning of Atlantic sturgeon may occur only in the fall (Ingram and Peterson, 2016). Results from the GDD model indicate that thermal conditions experienced by northern populations (from Maine to New York), particularly in advance of their first winter, may be inadequate to support spawning in fall (Fig. 6). Smaller sizes at the onset of winter would

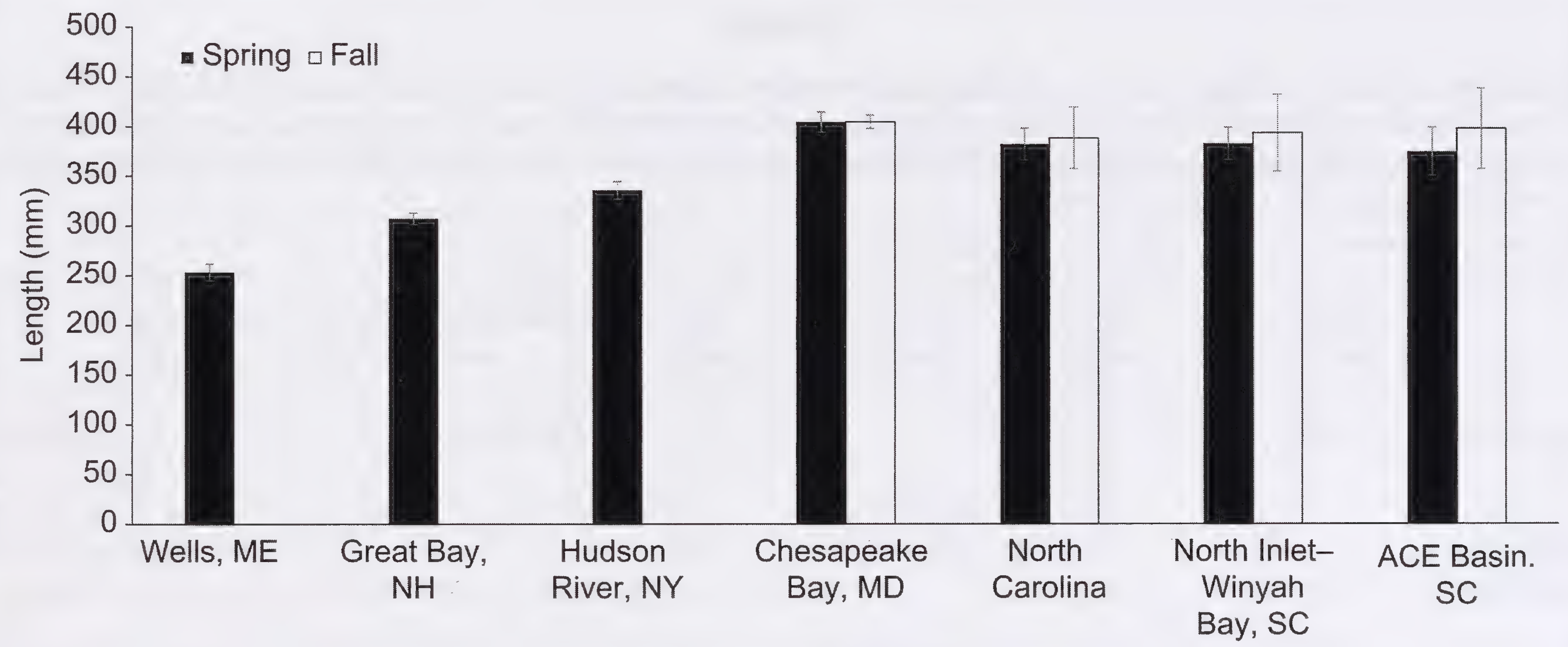

Figure 3

Total lengths of age-1 Atlantic sturgeon (*Acipenser oxyrinchus oxyrinchus*), by spawning cohort (fall and spring), along a latitudinal gradient of thermal regimes to which they were exposed. Water temperature data used for thermal regimes were collected from National Estuarine Research Reserve System sites from Maine to South Carolina during 2008–2013. The southernmost site is the Ashepoo–Combahee–Edisto Basin (ACE Basin) in South Carolina. Error bars indicate standard deviations.

be expected to result in increased mortality (Hurst, 2007), and future research should focus on factors that may drive winter mortality in sturgeon (e.g., starvation, predation, and thermal stress). Juveniles from northern populations that spawned in spring, albeit at smaller sizes than their counterparts from the southern population, must be sufficiently large at winter onset to weather the longer and more intense winters encountered at higher latitudes.

Interestingly, a strong difference in days with temperatures below the minimum threshold (<4°C) between the Hudson River (119.2 d [SD 13.8]) and Chesapeake Bay (4.2 d [SD 6.0]) is associated with the apparent shift from spawning in spring in the north to spawning in both spring and fall in the south. A supraoptimal thermal threshold may also curtail the incidence of dual-season spawning. In areas where spawning may occur exclusively in fall, as has been proposed for the Altamaha River (Ingram and Peterson, 2016), supraoptimal temperatures (>28°C) may curtail successful spawning events in spring or at least reduce growth and possibly survival of juveniles. Atlantic sturgeon experienced a sharp increase in the number of supraoptimal days between Chesapeake Bay (0.0 d) and North Carolina (mean: 58.7 d [SD 20]). With regional warming in coastal waters of Maryland and the southeastern United States (Kennedy et al.[6]; Najjar et al., 2010), increased supraoptimal days experienced could negatively affect Atlantic sturgeon that spawn in spring. If this results in a reduction of recruitment of individuals that spawn in spring, population persistence and recovery would increasingly depend on successful fall cohorts.

There is some evidence that, in systems where Atlantic sturgeon spawn in spring and fall, cohorts are genetically distinct (Balazik and Musick, 2015; Hilton et al., 2016; Farrae et al., 2017) and may use separate spawning grounds (Balazik and Musick, 2015). Further investigations are needed to determine if dual-season spawning is related to genetic differentiation and if larval and juvenile sturgeon are able to imprint on specific seasonal signals in tributaries where they spawn. If genetic differences exist, additional studies are needed to determine if there are growth differences between strains that spawn in spring and those that spawn in fall.

The laboratory design assumed that 1) the 2 sampled populations were representative of latitudinal differences in growth responses, 2) batch growth rates were representative of growth performance, 3) growth is linear between the upper and lower thresholds, and 4) hatchery-sourced cohorts were representative of naturally spawned juveniles. Although the 2 strains of Atlantic sturgeon used in this study—strains of fish from the Altamaha River and the Saint John River—represented the northern and southern parts of the latitudinal range, the addition of other strains would have strengthened inferences by providing a continuum of expected growth rates. The small size of the Atlantic sturgeon at the start of the experiment was not conducive to marking individual fish; hence, length and weight data were pooled by tank. Because individual growth rates can vary substantially within populations, investigation into the variability of growth among different population is warranted. Finally, using progeny from 1 spawning event in a hatchery may not well represent the genetic variability in wild populations. However, hatchery-reared Atlantic

---

[6] Kennedy, V. S., R. R. Twilley, J. A. Kleypas, J. H. Cowan Jr., and S. R. Hare. 2002. Coastal and marine ecosystems and global climate change: potential effects on U.S. resources, 52 p. Pew Center on Global Climate Change, Arlington, VA. [Available from website.]

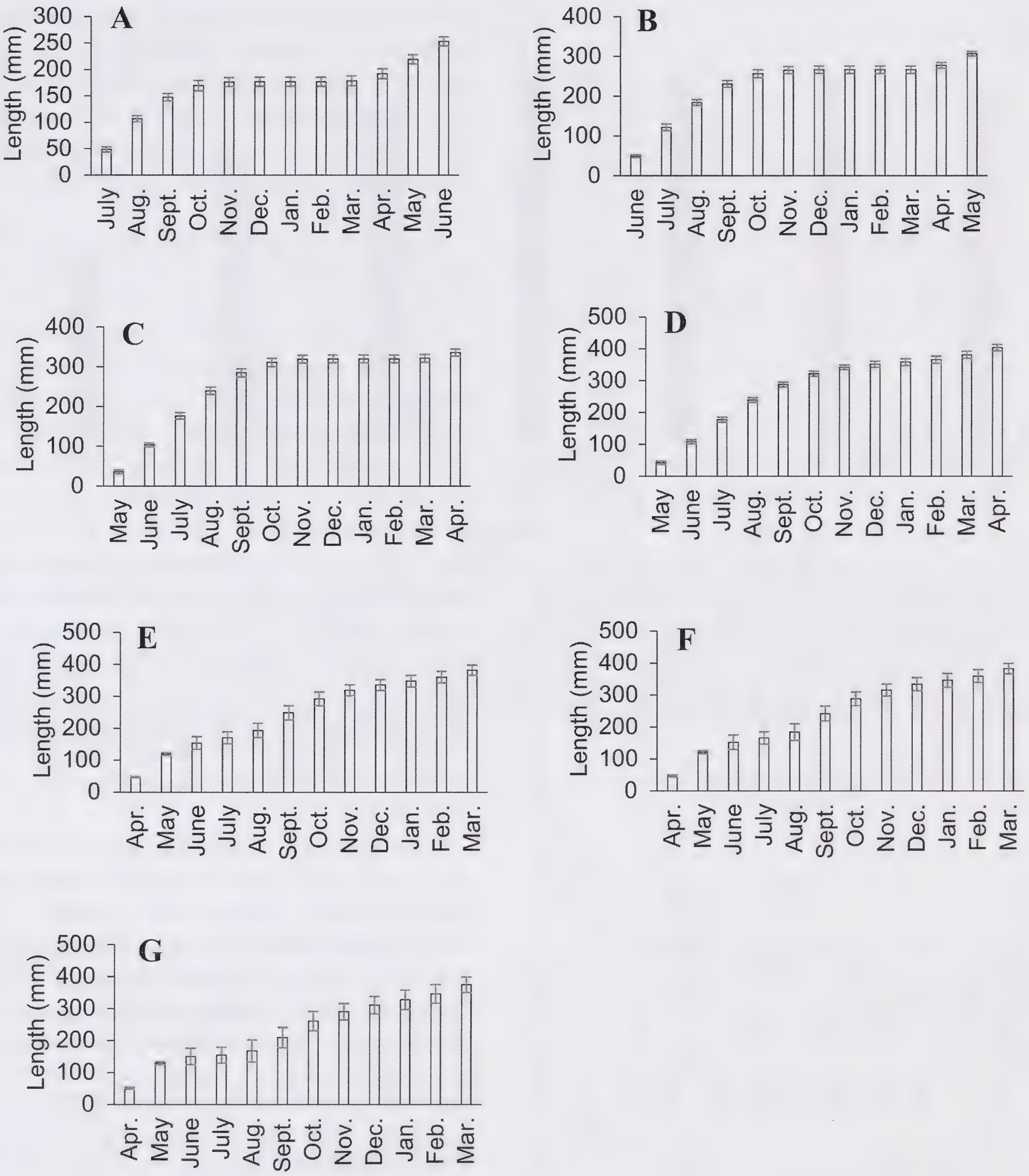

Figure 4

Monthly mean total lengths of Atlantic sturgeon (*Acipenser oxyrinchus oxyrinchus*) spawned in spring, across a latitudinal range during 2008–2012: (**A**) Wells, Maine; (**B**) Great Bay, New Hampshire; (**C**) Hudson River, New York; (**D**) Chesapeake Bay, Maryland; (**E**) North Carolina; (**F**) the area from North Inlet to Winyah Bay, South Carolina; and (**G**) Ashepoo–Combahee–Edisto Basin, South Carolina. Error bars indicate standard deviations.

sturgeon provide a reliable source for experimental research with known genetic parentage, and use of hatchery-reared sturgeon does not affect wild populations.

Important assumptions of the GDD model included 1) specification of lower and upper threshold temperatures of 4°C and 28°C and 2) specification of time of spawning associated with spring and fall periods (GDD along a latitudinal gradient; see the "Materials and methods" section), which likely vary with latitude. Investigations of thermal tolerances of Atlantic sturgeon have been primarily focused on the population in the Hudson River (Mohler[3]; Niklitschek and Secor, 2009). It is conceivable that these thresholds could vary among populations, and such differences would influence inferences made related to predictions of juvenile sizes. Still, the results of our laboratory experiments indicate that both strains experienced no growth for the thermal regime treatment that simulated the temperatures of the Saint John River at <4°C. In the Edisto River thermal regime experiment, fish were exposed briefly to 28°C, and this period coincided with a marked

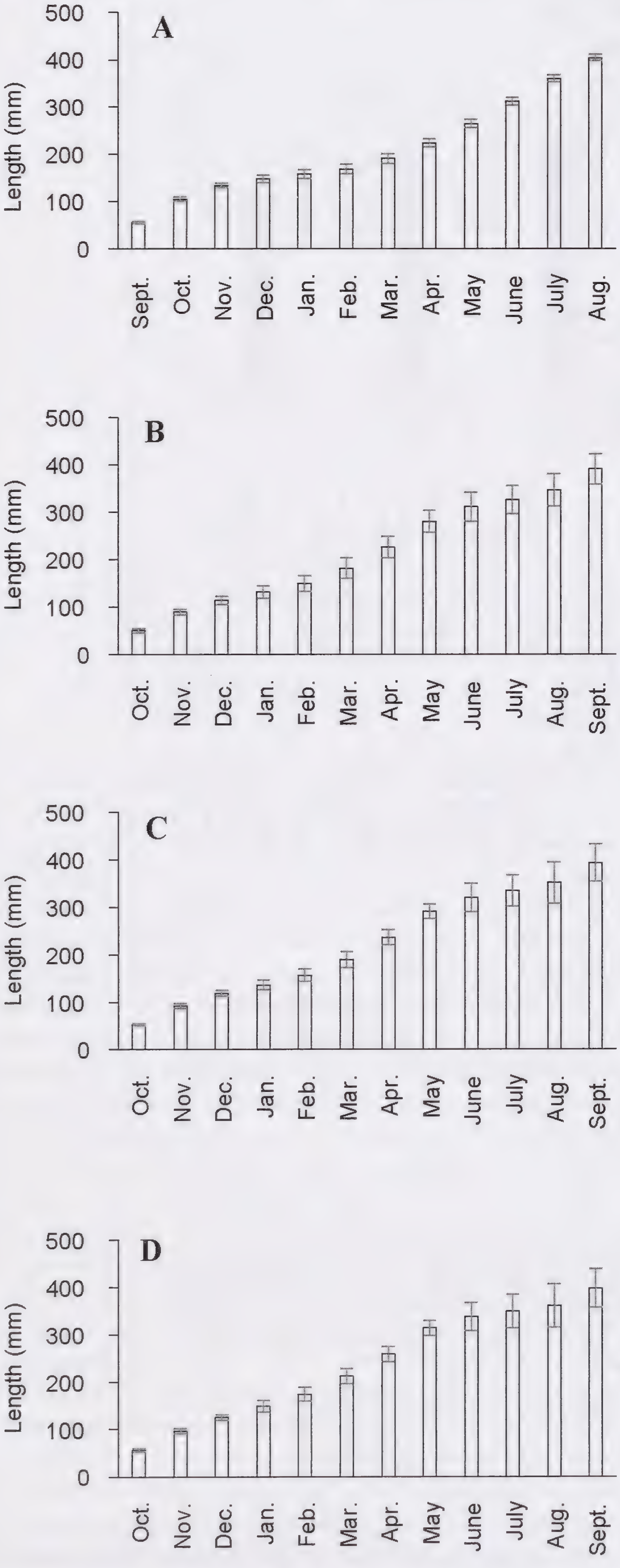

Figure 5

Monthly mean total lengths of Atlantic sturgeon (*Acipenser oxyrinchus oxyrinchus*) that spawned in fall, across a latitudinal range during 2008–2012: (**A**) Chesapeake Bay, Maryland; (**B**) North Carolina; (**C**) the area from North Inlet to Winyah Bay, South Carolina; and (**D**) Ashepoo–Combahee–Edisto Basin, South Carolina. Error bars indicate standard deviations.

decline in growth. Early termination of the Saint John River treatment constrained analysis on growth under this temperature regime, although results support the notion that the Saint John River strain performed similarly to the Altamaha River strain. Still, having measurements of growth over an entire year's thermal regime, starting at hatch, would improve the model used in determining size at the age of 1.0 year.

Reported ranges of juvenile sizes are highly variable across systems without a strong latitudinal trend. In part, this high variation relates to not knowing the exact age of juveniles, which is typically assigned according to size alone. Because collections occur in different seasons (spring, summer, and fall), sometimes without knowledge of spawning (spring or fall) cohort, ages may vary between 0.5 and 1.9 years. Indeed, discerning length thresholds for age-0 juveniles is a priority in surveys of Atlantic sturgeon (ASMFC, 2017), and for this priority, GDD growth predictions have application. The predicted lengths of age-1 sturgeon generally fell within the range reported in literature for age-1 Atlantic sturgeon, supporting the approach used in our study (Table 5). As expected, the predicted sizes at the age of 1.0 year indicate a strong latitudinal pattern across systems, whereas observed lengths do not. Further, the GDD model—if credible—can be used to predict juvenile age and hatch date period.

In conclusion, populations of Atlantic sturgeon in the Saint John River and the Altamaha River did not differ in their capacity for growth in thermal regimes that represented the latitudinal range of this subspecies. The results of comparisons of GDDs, as a measure of growth performance, among systems corroborate the observation of dual-season spawning in systems from Chesapeake Bay to South Carolina and provide a rationale for why this behavior may not occur in the more northern and extreme southern systems of the range. Accumulated GDDs can be used to predict lengths at date to improve assessments of juvenile occurrence and production. Further, juvenile growth performance associated with dual-season spawning can be forecast under different climate change scenarios by using the GDD model.

Acknowledgments

This work was funded by the NOAA Species Recovery Grants to States Program (grant no. NA13NMF4720042 to B. Richardson and D. Secor) and the Maryland Department of Natural Resources Fisheries Service. Our thanks to U.S. Fish and Wildlife Service Bears Bluff National Fish Hatchery and to Acadian Sturgeon and Caviar Inc. for supplying the fish. This study was conducted under National Marine Fisheries Service permit no. 17367 and the University of Maryland College Park Animal Use and Care permit F-HPL-14-09. This paper is contribution no. 5652 of the University of Maryland Center for Environmental Science.

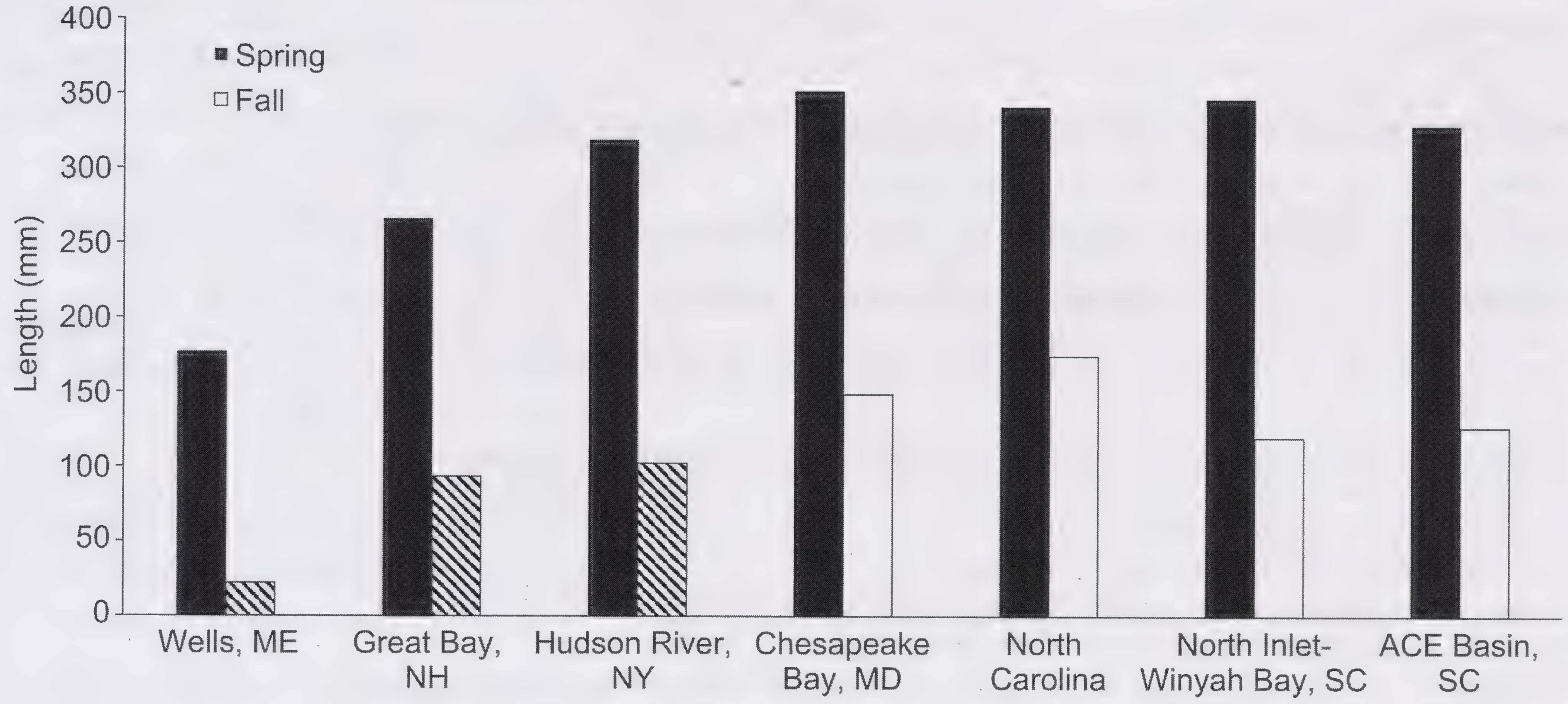

Figure 6

Total lengths of Atlantic sturgeon (*Acipenser oxyrinchus oxyrinchus*) that spawned in spring and fall at the onset of winter (1 January), by the thermal regimes to which they were exposed across a latitudinal range. Water temperature data used for thermal regimes were collected from National Estuarine Research Reserve System sites from Maine to South Carolina during 2008–2012. Open bars represent the cohort that spawns in fall, and black bars represent the cohort that spawns in spring. The bars with diagonal lines indicate a hypothetical scenario of spawning occurring in fall in those locations. The southernmost site is the Ashepoo–Combahee–Edisto Basin (ACE Basin) in South Carolina.

Literature cited

ASMFC (Atlantic States Marine Fisheries Commission).
2017. 2017 Atlantic sturgeon benchmark stock assessment and peer review report, 368 p. Atlantic States Mar. Fish. Comm., Arlington, VA. [Available from website.]

Balazik, M. T., and J. A. Musick.
2015. Dual annual spawning races in Atlantic sturgeon. PLoS ONE 10(5):e0128234.

Balazik, M. T., G. C. Garman, J. P. Van Eenennaam, J. Mohler, and L. C. Woods III.
2012. Empirical evidence of fall spawning by Atlantic sturgeon in the James River, Virginia. Trans. Am. Fish. Soc. 141:1465–1471.

Brown, E. E., H. Baumann, and D. O. Conover.
2012. Absence of countergradient and cogradient variation in an oceanic silverside, the California grunion *Leuresthes tenuis*. Mar. Ecol. Prog. Ser. 461:175–186.

Collins, M. R., T. I. J. Smith, W. C. Post, and O. Pashuk.
2000. Habitat utilization and biological characteristics of adult Atlantic sturgeon in two South Carolina rivers. Trans. Am. Fish. Soc. 129:982–988.

Conover, D. O.
1992. Seasonality and the scheduling of life history at different latitudes. J. Fish Biol. 41(sB):161–178.

Conover, D. O., and T. M. C. Present.
1990. Countergradient variation in growth rate: compensation for length of the growing season among Atlantic silversides from different latitudes. Oecologia 83:316–324.

Conover, D. O., J. J. Brown, and A. Ehtisham.
1997. Countergradient variation in growth of young striped bass (*Morone saxatilis*) from difference latitudes 1. Can. J. Fish. Aquat. Sci. 54:2401–2409.

Conover, D. O., T. A. Duffy, and L. A. Hice.
2009. The covariance between genetic and environmental influences across ecological gradients: reassessing the evolutionary significance of countergradient and cogradient variation. Ann. N.Y. Acad. Sci. 1168:100–129.

Crossman, J. A., P. S. Forsythe, E. A. Baker, and K. T. Scribner.
2009. Overwinter survival of stocked age-0 lake sturgeon. J. Appl. Ichthyol. 25:516–521.

Dovel, W. L., and T. J. Berggren.
1983. Atlantic sturgeon of the Hudson estuary, New York. New York Fish Game J. 30(2):140–172.

Farrae, D., P. M. Schueller, and D. L. Peterson.
2009. Abundance of juvenile Atlantic sturgeon in the Ogeechee River, Georgia. Proc. Annu. Conf. SEAFWA 63:172–176.

Farrae, D. J., W. C. Post, and T. L. Darden.
2017. Genetic characterization of Atlantic sturgeon, *Acipenser oxyrinchus oxyrinchus*, in the Edisto River, South Carolina and identification of genetically discrete fall and spring spawning. Conserv. Genet. 18:813–823.

Federal Register.
2012a. Endangered and threatened wildlife and plants; threatened and endangered status for distinct population segments of Atlantic sturgeon in the Northeast Region. Fed. Regist. 77:5880–5912. [Available from website.]
2012b. Endangered and threatened wildlife and plants; final listing. Determinations for two distinct population segments of Atlantic sturgeon (Acipenser oxyrinchus oxyrinchus) in the Southeast. Fed. Regist. 77:5914–5982. [Available from website.]

Fritts, M. W., C. Grunwald, I. Wirgin, T. L. King, and D. L. Peterson.
2016. Status and genetic character of Atlantic sturgeon in the Satilla River, Georgia. Trans. Am. Fish. Soc. 145:69–82.

Garvey, J. E., and E. A. Marschall.
2003. Understanding latitudinal trends in fish body size through models of optimal seasonal energy allocation. Can. J. Fish. Aquat. Sci. 60:938–948.

Gross, M. R., J. Repka, C. T. Robertson, D. H. Secor, and W. Van Winkle.
2002. Sturgeon conservation: insights from elasticity analysis. Am. Fish. Soc. Symp. 28:13–30.

Hager, C., J. Kahn, C. Watterson, J. Russo, and K. Hartman.
2014. Evidence of Atlantic sturgeon spawning in the York River system. Trans. Am. Fish. Soc. 143:1217–1219.

Hilton, E. J., B. Kynard, M. T. Balazik, A. Z. Horodysky, and C. B. Dillman.
2016. Review of the biology, fisheries, and conservation status of the Atlantic sturgeon, (*Acipenser oxyrinchus oxyrinchus* Mitchill, 1815). J. Appl. Ichthyol. 32(S1):30–66.

Humphrey, J., M. J. Wilberg, E. D. Houde, and M. C. Fabrizio.
2014. Effects of temperature on age-0 Atlantic menhaden growth in Chesapeake Bay. Trans. Am. Fish. Soc. 143:1255–1265.

Hurst, T. P.
2007. Causes and consequences of winter mortality in fishes. J. Fish Biol. 71:315–345.

Hurst, T. P., and D. O. Conover.
2003. Seasonal and interannual variation in the allometry of energy allocation in juvenile striped bass. Ecology 84:3360–3369.

Ingram, E. C., and D. L. Peterson.
2016. Annual spawning migrations of adult Atlantic sturgeon in the Altamaha River, Georgia. Mar. Coast. Fish. 8: 595–606.

Jonsson, B., T. Forseth, A. J. Jensen, and R. F. Næsje.
2001. Thermal performance in juvenile Atlantic salmon, *Salmo salar* L. Funct. Ecol. 15:701–711.

Markin, E.
2017. Atlantic sturgeon growth responses to dual seasonal spawning, latitudinal thermal regimes, and Chesapeake Bay environmental stressors. Ph.D. diss., 223 p. Univ. Maryland, College Park, MD. [Available from website.]

McCord, J. W., M. R. Collins, W. C. Post, and T. I. J. Smith.
2007. Attempts to develop an index of abundance for age-1 Atlantic sturgeon in South Carolina, USA. Am. Fish. Soc. Symp. 56:397–403.

Najjar, R. G., C. R. Pyke, M. B. Adams, D. Breitburg, C. Hershner, M. Kemp, R. Howarth, M. R. Mulholland, M. Paolisso, D. Secor, et al.
2010. Potential climate-change impacts on the Chesapeake Bay. Est. Coast. Shelf Sci. 86:1–20.

Neuheimer, A. B., and C. T. Taggart.
2007. The growing degree-day and fish size-at-age: the overlooked metric. Can. J. Fish. Aquat. Sci. 64:375–385.

Niklitschek, E. J., and D. H. Secor.
2005. Modeling spatial and temporal variation of suitable nursery habitats for Atlantic sturgeon in the Chesapeake Bay. Est. Coast. Shelf Sci. 64:135–148.
2009. Dissolved oxygen, temperature and salinity effects on the ecophysiology and survival of juvenile Atlantic sturgeon in estuarine waters: I. laboratory results. J. Mar. Biol. Ecol. 381(Suppl.):150–160.

Peterson, D. L., M. B. Bain, and N. Haley.
2000. Evidence of declining recruitment of Atlantic sturgeon in the Hudson River. North Am. J. Fish. Manage. 20: 231–238.

Peterson, D. L., P. Schueller, R. DeVries, J. Fleming, C. Grunwald, and I. Wirgin.
2008. Annual run size and genetic characteristics of Atlantic sturgeon in the Altamaha River, Georgia. Trans. Am. Fish. Soc. 137:393–401.

Pörtner, H. O., and M. A. Peck.
2010. Climate change effects on fishes and fisheries: towards a cause-and-effect understanding. J. Fish Biol. 77: 1745–1779.

Power, M., and R. S. McKinley.
1997. Latitudinal variation in lake sturgeon size as related to the thermal opportunity for growth. Trans. Am. Fish. Soc. 126:549–558.

Puckett, B. J., D. H. Secor, and S-J. Ju.
2008. Validation and application of lipofuscin-based age determination for Chesapeake Bay blue crabs. Trans. Am. Fish. Soc. 137:1637–1649.

Purchase, C. F., and J. A. Brown.
2001. Stock-specific changes in growth rates, food conversion efficiencies, and energy allocation in response to temperature change in juvenile Atlantic cod. J. Fish Biol. 58: 36–52.

R Core Team.
2016. R: a language and environment for statistical computing. R Foundation for Statistical Computing, Vienna, Austria. [Available from website, accessed October 2016.]

Savoy, T., L. Maceda, N. K. Roy, D. Peterson, and I. Wirgin.
2017. Evidence of natural reproduction of Atlantic sturgeon in the Connecticut River from unlikely sources. PLoS ONE 12(4):e0175085.

Schueller, P., and D. L. Peterson.
2010. Abundance and recruitment of juvenile Atlantic sturgeon in the Altamaha River, Georgia. Trans. Am. Fish. Soc. 139:1526–1535.

Schultz, E. T., and D. O. Conover.
1997. Latitudinal differences in somatic energy storage: adaptive responses to seasonality in an estuarine fish (Atherinidae: *Menidia mendia*). Oecologia 109:516–529.

Schultz, E. T., K. E. Reynolds, and D. O. Conover.
1996. Countergradient variation in growth among newly hatched *Fundulus heteroclitus*: geographic differences revealed by common-environment experiments. Funct. Ecol. 10:366–374.

Secor, D. H., T. E. Gunderson, and K. Karlsson.
2000. Effect of temperature and salinity on growth performance in anadromous (Chesapeake Bay) and nonanadromous (Santee-Cooper) strains of striped bass *Morone saxatilis*. Copeia 2000:291–296.

Secor, D. H., P. J. Anders, W. Van Winkle, and D. A. Dixon.
2002. Can we study sturgeons to extinction? What we do and don't know about the conservation of North American sturgeons. Am. Fish. Soc. Symp. 28:3–10.

Shuter, B. J., A. G. Finstad, I. P. Helland, I. Zweimüller, and F. Hölker.
2012. The role of winter phenology in shaping the ecology of freshwater fish and their sensitivities to climate change. Aquat. Sci. 74:637–657.

Smith, J. A., H. J. Flowers, and J. E. Hightower.
2015. Fall spawning of Atlantic sturgeon in the Roanoke River, North Carolina. Trans. Am. Fish. Soc. 144:48–54.

Smith, T. I. J., D. E. Marchette, and G. D. Ulrich.
1984. The Atlantic sturgeon fishery in South Carolina. North Am. J. Fish. Manage. 4:164–176.

Stewart, N. D., M. J. Dadswell, P. Leblanc, R. G. Bradford, C. Ceapa, and M. J. W. Stokesbury.
2015. Age and growth of Atlantic sturgeon from the Saint John River, New Brunswick, Canada. North Am. J. Fish. Manage. 35:364–371.

Yamahira, K., and D. O. Conover.
2002. Intra- vs. interspecific latitudinal variation in growth: adaptation to temperature of seasonality? Ecology 83: 1252–1262.

National Marine
Fisheries Service
NOAA

Fishery Bulletin
established in 1881

Spencer F. Baird
First U.S. Commissioner
of Fisheries and founder
of *Fishery Bulletin*

Development and implementation of a fully randomized sampling design for a fishery monitoring program

Jennifer Cahalan (contact author)[1]
Craig Faunce[2]

Email address for contact author: jcahalan@psmfc.org

[1] Pacific States Marine Fisheries Commission
7600 Sand Point Way NE
Seattle, Washington 98115

[2] Fisheries Monitoring and Analysis Division
Alaska Fisheries Science Center
National Marine Fisheries Service, NOAA
7600 Sand Point Way NE
Seattle, Washington 98115

Abstract—Fishery observer programs in the United States are mandated to collect fishery-dependent data. These monitoring programs must have clear objectives and be statistically sound despite the constraints imposed by commercial fishing operations. In addition, successful programs continuously self evaluate and improve. Decisions regarding sampling design must integrate the concerns and needs of industry and fisheries managers while ensuring the scientific integrity of the data. Here, we use examples from a large observer program to illustrate how the elements of a statistical design can be effectively implemented. With the rich economic resources of the fishing fleet in Alaska and a long history of observer coverage, the North Pacific Observer Program currently has high overall coverage rates and employs a statistically rigorous sampling design. The North Pacific Fishery Management Council receives 2 annual reports on the objectives and performance of fishery monitoring in the region. As fisheries management has become more sophisticated, data needs have increased. Balancing the amount and types of data collected with observer workloads is a critical component of designing sampling methods.

Manuscript submitted 29 May 2019.
Manuscript accepted 5 March 2020.
Fish. Bull. 118:87–99 (2020).
Online publication date: 23 March 2020.
doi: 10.7755/FB.118.1.8

The views and opinions expressed or implied in this article are those of the author (or authors) and do not necessarily reflect the position of the National Marine Fisheries Service, NOAA.

Monitoring catch and bycatch is an important component of successful fisheries management (Sutinen, 1999; Hilborn et al., 2005). Fisheries, meanwhile, benefit from an increased focus on accountability, sustainability, and compliance with seafood traceability standards that foster a positive public perception (Lewis and Boyle, 2017). Because fishery monitoring has had positive effects, numerous studies have been devoted to how fisheries can and should be monitored (e.g., van Helvoort, 1986; Davies and Reynolds, 2003; Zollett et al., 2015).

Few studies however have examined how scientifically and statistically robust monitoring programs are enacted (e.g., Cotter and Pilling, 2007; ICES[1]). If fisheries monitoring programs were well funded and provided with stable, noncompetitive objectives, establishing a successful program should be simple. However, the political, social, and economic landscape affecting such programs can change rapidly, often resulting in changing monitoring objectives. Consequently, there are no monitoring programs for many fisheries and bycatch species (e.g., Lewison et al., 2004; Roberson et al., 2018), and already established programs can be ill-equipped to address new mandates (Borges, 2015).

We have drawn on our experience with a large fisheries monitoring program to show how similar programs can successfully address multiple objectives while still adhering to a scientifically defensible sampling design. In particular, we focused on how design elements address the logistical constraints imposed on data collection from commercial fishing operations.

Materials and methods

Keys to a successful sampling design

Studies have described the effective design and components of fishery monitoring programs that gather useful data (e.g., Cotter and Pilling, 2007; Vølstad et al., 2014; ICES[1]). These design elements include randomized data collections over spatial and temporal scales (a probability sample), the collection of sufficient data, and the use of stratification and prespecification of sampling intensity to control precision of estimates. In order to meet the data needs of fisheries managers and scientific researchers, a monitoring program design must also make efficient use of available funding, use the time and energy of observers wisely, and maintain observer safety standards.

---

[1] ICES (International Council for the Exploration of the Sea). 2014. Report of the third workshop on practical implementation of statistical sound catch sampling programmes (WKPICS3); Copenhagen, Denmark, 19–22 November 2013. ICES CM 2013/ACOM:54, 109 p. [Available from website.]

Monitoring objectives

Data collected by fishery monitoring programs have many uses. These data include collections in support of stock assessments (NRC, 1998), ecosystem-based fisheries management (Gilman et al., 2017), avoidance of bycatch *hot spots* by industry and research partners (Gilman et al., 2006; O'Keefe et al., 2014), and detailed catch accounting (Karp et al., 2019). Because the fisheries data collected by these monitoring programs are used in analyses that meet a wide variety of management and scientific needs, it is often difficult to specify a single objective for these programs. Programs designed to meet the data needs for only one objective could potentially look very different depending on the specifics of both the objective and the target populations. For example, because of differences in the prevalence and spatial distribution of different bycatch species within groundfish fisheries, a monitoring program designed to collect biological samples and data (e.g., otoliths and length measurements) from specimens of a single targeted species might be very different than one designed to monitor bycatch of a less common species. Instead, the objective of these programs should be to collect representative data from the relevant fisheries such that characteristics of catch (e.g., species prevalence and at-sea discard rate) are accurately reflected in the monitoring data.

Probability sampling

A sampling design links the sample data and the sampled population. Unlike other types of sampling, such as proportional-to-size or adaptive sampling designs, a probability sampling design that makes the fewest assumptions about the characteristics of the sampled population (e.g., the catch or length distribution for specific species) is a necessity for most monitoring programs (Cotter et al., 2002).

The basic elements of a probability sample are well known: the target population is identified, and any differences between the target population and the sampling frame (sampled population) are identified. The sampled population is then divided into unambiguously defined sampling units so that each element of the population is in one and only one sampling unit, a method for randomly selecting units is prespecified, and data from the sampling unit are collected (e.g., Cochran, 1977; Thompson, 2012). In fisheries monitoring, it is often not possible to completely list all the sampling units in a population or it is infeasible to randomly select individual units without first selecting a larger grouping (i.e., random sample of fishing events, or hauls, without first selecting fishing trips). Regardless, these design principles can be incorporated into monitoring programs. Sampling of fishing effort can be naturally organized into a hierarchical structure (i.e., trips, then hauls, then samples), and leveraging this structure enables implementation of a probability design and yields efficiencies in sampling. Multistage cluster designs are used to sample each level of the target population independently. This design not only preserves the probability sample by allowing selection probabilities to be specified for each sampling unit but also may decrease logistical difficulties and costs.

Stratification and allocation

Stratification of the target population is used to decrease the variability in estimates or to increase cost effectiveness and logistical efficiency of sampling. Specification of sampling strata, sample allocation among strata, and minimal sample size targets are design components that can be used to develop sampling recommendations, and the methods for these components are well established. However, balancing the sampling needs for different species across different fisheries requires using different approaches to development of sampling recommendations, and, in particular, recommendations of sampling intensity.

When a single objective is clearly defined (e.g., estimation of single-species catch), minimization of variance for a given cost can be used to determine sampling rates, appropriate stratification, and other elements of the sample design (Cochran, 1977). However, for sampling of multiple species, the rate of variance minimization and recommended sample sizes will be different for each species, depending on the variance structure of the species within the catch. For example, Babcock et al.[2] demonstrated that, for species that are less common in the catch, higher sample rates are required to achieve the same precision as that for discards of more common species (i.e., discards of rarer species typically have higher variance between sampling units). Therefore, monitoring programs with multiple objectives need to balance the competing sample size recommendations for different objectives (i.e., species) and accommodate the logistical constraints inherent in sampling commercial catches. One way to address these issues is through the use of a probability sample with a sample size large enough to reasonably assure that all aspects of the monitored fisheries are represented in the collected data, minimizing the number and types of gaps in the data set.

Evaluation of implementation

Evaluating whether a sampling design has been successfully implemented is critical to ensuring that a monitoring program is efficient and that collected data are suitable

---

[2] Babcock, E. A., E. K. Pikitch, and C. G. Hudson. 2003. How much observer coverage is enough to adequately estimate bycatch?, 29 p. Oceana, Washington, DC. [Available from website.]

Table 1

Summary of the hierarchical structure and randomization of the sampling design used and data collected by the North Pacific Observer Program in 2018. This program of the National Marine Fisheries Service collects data that are representative of fishing activities throughout the federally managed groundfish fisheries off Alaska.

Hierarchy level	Sampling unit definition	Randomization method	Data collected	Constraints	How addressed
Primary	Trip	Binomial selection	Vessel and gear types, port of departure and return, delivery information	Cost	Fee, eliminating individual cost burden (works like insurance)
Secondary	Hauls	Constrained random	Fishing effort (date, location, depth, duration of trawl tows, number of hooks or pots fished)	Fatigue	Random sample of hauls within trips
Tertiary	Portions of catch (gear or weight)	Situation dependent; systematic random preferred	Species composition (proportions), percentage discarded by species	Space and physical ability	Maximization of sample size within constraints, use of multiple samples
Quaternary	Individual catch items (fish)	Systematic random preferred, simple random acceptable, varies with research needs	Length measurements, samples from specimens (e.g., otoliths, stomachs)	Time and availability of species	Annual collaboration with stock assessors to focus sampling on high-priority species

for use in a range of analytic activities. That data originating from observer programs are randomly collected and representative of fishing activities are basic underlying assumptions of many analyses, such as bycatch estimation and stock assessments. Evaluations of these basic assumptions should include assessment of spatial and temporal coverage of fishing activities, adequacy of sampling frames and definitions of sampling units, and effectiveness of stratification definitions.

Implementing these basic design elements can be difficult to achieve in commercial fisheries because of logistical and funding constraints that limit deployments of observers and because of the chaotic environment on deck where observers sample catches. However, in spite of these challenges, designing and implementing a probability-based sampling program is possible. From what we have learned in implementing the successful North Pacific Observer Program of the National Marine Fisheries Service (NMFS), we describe how all these elements and considerations can come together to create a working science-based sampling program.

Results

Case study: North Pacific Observer Program

Fisheries in the 3.77 million km^2 that make up the U.S. exclusive economic zone off Alaska are managed by the NMFS in consultation with the North Pacific Fishery Management Council (NPFMC). The waters off Alaska account for half of all annual U.S. seafood landings. In 2018, 1084 vessels fished with trawl, longline, pot, and jig gear in the U.S. exclusive economic zone off Alaska, catching over 2.3 million metric tons (t) of groundfish worth more than $2.5 billion (Ganz et al., 2019; Fissel et al., 2019). In-season, near real-time accounting of retained and discarded catch for federal fishery quota monitoring is supported in Alaska with data collected by the North Pacific Observer Program (DiCosimo et al., 2010).

The North Pacific Observer Program is the largest in the country; in 2018 over 400 observers and electronic monitoring (camera) systems were deployed for over 40,000 sea days (AFSC[3]). The goal of the North Pacific Observer Program is to collect data that are representative of fishing activities throughout the federally managed groundfish fisheries off Alaska. The North Pacific Observer Program employs a stratified multistage design in which the primary sampling units are individual trips taken by vessels. Within the fishing trip, the secondary sampling units are individual fishing events (hauls, or sets), tertiary sampling units are portions of the catch, and quaternary sampling units are individual fish; these sampling units are collected on the vessel once the observer is deployed (Table 1). Sampling occurs throughout the federally managed groundfish fisheries off Alaska; in 2018 over 58,000 fishing events (hauls) occurred on sampled trips.

Through annual deployment plans (ADPs), the NMFS defines how monitoring tools will be deployed for the following year. At the NPFMC October and December meetings, the NMFS prepares a draft and final ADP for NPFMC review. In the draft ADP, multiple competing deployment options, including alternative stratum definitions and sample allocations, are compared. After receiving input from the NPFMC, stakeholders, and the public, the NMFS presents in the final ADP only the preferred design, predicted total and observed fishing effort, and associated selection rates for the coming year (see Ganz and Faunce, 2019).

---

[3] AFSC (Alaska Fisheries Science Center) and Alaska Regional Office. 2019. North Pacific Observer Program 2018 annual report. AFSC Processed Rep. 2019-04, 148 p. [Available from website.]

Sampling design

The North Pacific Observer Program divides the fleet of vessels into 2 broad categories: those that are observed for every trip (full coverage) and those that are not (partial coverage). The first category consists of factory vessels (catcher-processors and motherships, with limited exceptions), catcher vessels participating in management programs that have transferable allocations of prohibited species catch as part of their catch-share program, catcher vessels using trawl gear that have requested full coverage for all fishing within the Bering Sea and Aleutian Islands, and inshore processors receiving or processing walleye pollock (*Gadus chalcogrammus*) caught in the Bering Sea under cooperative agreements (American…1998). These vessels are required to carry one or more observers for all of their trips and to pay for that observer coverage through companies certified by the NMFS to provide observers. In the second category, vessels without factories (catcher vessels) participating in open-access fisheries or in individual fishing quota fisheries carry an observer only on a randomly selected subset of their trips. Observers in partial coverage are provided through a contract between the NMFS and a single provider and are supported through ex-vessel fee revenues from the prior year.

In 2018, electronic monitoring was added as an alternative to observers for fishery monitoring of vessels in the partial coverage category (NMFS[4]). Vessels in the electronic monitoring sampling strata do not carry observers on any fishing trips but are equipped with video camera systems that record all fishing activities. Video files are later reviewed, all catch items are counted and identified to species, and the disposition (retained or discarded) of each item is recorded. Vessels that use non-trawl gear volunteer to participate in electronic monitoring for the upcoming year, and if selected by the NMFS to participate, have electronic monitoring enabled on a random subset of their trips. Vessels also pay the ex-vessel fee to support deployment of electronic monitoring—just as they would if the coverage was by observers. Data from these electronically monitored trips are combined with data from the trips monitored by observers to estimate the catch of each species.

With slight variations between years, the North Pacific Observer Program has stratified the partial coverage fleet for deployment of observers and electronic monitoring systems on the basis of vessel size and gear properties following an initial regression analysis by the NMFS that indicated these were the main drivers of differences in landed catch (Gasper et al., 2019). Vessels under 12 m (40 ft) and those using jig gear operating in the North Pacific Ocean are currently not required to be observed (zero coverage stratum) because they catch few fish and cannot easily and safely accommodate an observer. Stratum definitions must be based on trip qualities known before a trip begins so that selection rates can be properly assigned.

Allocation strategy

There is a strong impetus to maximize efficiency and utility of fishery monitoring data, especially at the trip level, because of stakeholder concerns about costs. The NMFS has focused sample allocation on discarded groundfish and minimization of data gaps, while the NPFMC has expressed a desire for the NMFS to prioritize monitoring of bycatch of Pacific halibut (*Hippoglossus stenolepis*) and Chinook salmon (*Oncorhynchus tshawytscha*), which are prohibited from being retained and sold by certain gear groups. To address these multiple objectives, a 2-step sample allocation process for observer deployment was developed.

First, baseline coverage rates were established following the results of simulated sampling of past fishing events (Gasper et al., 2019). Second, if annual funding is available for sampling effort (sea days converted to fishing trips) above these baseline observer coverage rates, additional effort is allocated according to a blended weighting for optimized sample allocation following Cochran (1977). The blended allocation weighting is the average of the 3 separate optimal allocation weightings derived from discarded total catch of groundfish and catch of the prohibited species Pacific halibut and Chinook salmon. Each weighting takes into account average trip cost and variance for the stratum during the year (Sullivan and Faunce, 2018).

Results of simulated sampling and analyses of past fishing events indicate that, at deployment rates of 15% or greater, the number of gear and area combinations with fewer than 3 trips observed decreased substantially (Gasper et al., 2019). With the use of this 2-step process, the deployment rates employed since 2018 are the combination of the base sampling effort (15% of trips) and additional optimized sampling effort (sea days) allocated to each stratum (NMFS[5]). In contrast, deployment of electronic monitoring is based on voluntary vessel participation and is set at 30% following NPFMC guidance (NMFS[4]).

---

[4] NMFS (National Marine Fisheries Service). 2017. 2018 annual deployment plan for observers in the groundfish and halibut fisheries off Alaska, 20 p. Natl. Mar. Fish. Serv., NOAA, Juneau, AK. [Available from: website.]

[5] NMFS (National Marine Fisheries Service). 2019. 2020 annual deployment plan for observers and electronic monitoring in the groundfish and halibut fisheries off Alaska, 18 p. Natl. Mar. Fish. Serv., NOAA, Juneau, AK. [Available from website.]

Selection of sampling units

Trips Within each partial coverage stratum, the sampling frame consists of all fishing trips that are required by law to be logged into an online application (the Observer Declare and Deploy System, available from website) or through a 24-h call center. Each logged trip represents a sampling unit, and for each sampling unit an observer or electronic monitoring system is assigned on the basis of a random 4-digit number between 0 and 1 generated when the trip is logged. If the number is at or below the selection rate stipulated in the ADP, that trip is selected for monitoring; otherwise it is not. The system in Alaska is 1 of 2 such declaration and selection systems in the country (see Palmer et al., 2016, for a description of the other). In Alaska, although selection rates differ between strata as a result of the allocation process defined in the ADP, each logged trip within a stratum receives the same selection probability. The rate of trip selection within each stratum is held constant for the calendar year.

Hauls Once an observer is deployed, the monetary sampling costs do not change (because the cost of deploying an observer has already been incurred), and estimates of costs are measured by an observer's time and energy. Factors to consider when developing methods for sampling on a vessel include randomizing sample selection, maximizing both the number and size of sampling units selected, and integrating sampling activities into a streamlined observer workflow. Sample size recommendations reflect what is logistically possible, and sampling rates are limited by an observers' access to the catch, the time available to sample, and their physical capacity.

Randomization of haul selection is achieved through the use of 2 alternative tools. The first tool is a modified table of random numbers that assigns a random number of hauls to be sampled followed by a number of hauls to be skipped. The second tool is a table that provides an observer with a 6-h break starting at a random hour of the day. Both of these tools give the observer periods during which non-sampling duties can be completed, provide rest periods for the observer, and decrease the ability of the vessel crew to predict which hauls will be sampled (as would be possible if a systematic design was used). Because it is required that all large organisms, such as marine mammals and sharks, caught in bycatch be available to the observer for all sampled hauls, randomization at the haul or set level is critical to accurate estimation of bycatch for these species.

Catch An observer is responsible for assessing the fishing activities on a vessel and for determining how sampling is best conducted. They define the population to be sampled, establish a sampling frame, define the sampling units, and randomly select a set of sampling units for data collection at each level of the hierarchy. Sampling frames and units are defined differently depending on fishing gear, observer experience, fishing operations and catch handling practices on a particular vessel, environmental conditions, and the general situation on the particular vessel. Observers are trained to maximize the fraction of the catch sampled in order to increase detection probabilities of rare species (e.g., seabirds, deep sea corals, and sharks) and to minimize sampling variance associated with haul-specific estimates of species-specific bycatch.

The sampling methods used by observers vary between fishing trips and between hauls within the same fishing trip, as a result of the varied sampling environments. Options for defining sampling frames and units vary dramatically across fisheries, and opportunities for randomizing selection of those units can be constrained by the gear used and by deck or factory configurations of individual vessels. Hence, the ability to adjust sampling in response to changing fishing conditions and vessel operations is critical to successful implementation of a credible randomized sampling design.

Since 2010, observers have recorded the type of sampling unit and the selection process used to randomize collection of their catch composition samples. Samples can be selected by using *strictly randomized methods* (simple or systematic random sampling in which sampling units are unambiguously defined), *randomized methods* in which randomization is incorporated into sample selection but either sampling units are not well defined or the entire catch is not available to be sampled (with a large difference between sampling frame and target populations), or non-random methods (which include both *opportunistic* sampling unit selection and complete enumeration [i.e., a *census* of the catch]).

Despite the range and diversity of fishing operations in Alaska, fishing operations that present similar sampling challenges can be grouped into 3 broad categories: 1) fixed-gear vessels (longline and pots) of any type, 2) catcher-processors that use trawl nets, and 3) catcher vessels that use trawl nets. The catch on fixed-gear vessels is sampled at one location (the roller on longline vessels or the sorting table or tote on pot vessels) in an orderly fashion as the catch is either brought on board or discarded. The observer defines sampling units and the sampling frame in terms of units of retrieved gear, such as segments of longline gear or predetermined numbers of pots. Catch is tallied at a vessel's rail from a systematic random selection of units (collection by using a strictly randomized method). Although defining sampling frames and randomizing selection of sampling units are straightforward, observers on these vessels work on deck often in severe weather conditions (extreme cold), limiting the size of individual samples. On larger vessels, gear retrieval can take in excess of 10 h, and in order to ensure adequate time to process samples (e.g., time to sort catch items and to collect weight and length data) and in order to allow an adequate rest period, time management can become a component of an observer's sampling design.

On trawl vessels, catch comes aboard in a more disorderly fashion than the process used on fixed-gear vessels, and sampling units and frames are defined in terms of catch weight. On catcher-processor vessels that use trawl nets, hauls can be in excess of 100 t. These catcher-processor and mothership vessels have a factory, and an observer has access to tools not available on catcher vessels. These tools include a motion-compensated platform scale, a flow scale that provides a continuous and cumulative weight of catch as it passes over the scale on a conveyor belt, and a dedicated sample station with specified minimal space requirements (4.5 m^2; Equipment…2019) to provide an area to store and process collected samples. Because catch passes into the factory on a series of conveyor belts past the observer's sample station, randomization is generally achieved by using systematic random sampling methods (strictly randomized collection). Although an observer works in the vessel factory and not on deck, sampling is conducted in an industrial setting designed and operated to move catch through the processing plant to the freezer as quickly as possible, limiting the amount of time an observer has to select and process samples.

Catcher vessels that use trawl nets often pose the most challenging sampling design scenarios. Similar to catcher-processors that use trawl nets, haul weight on these vessels can be over 100 t; however, catches typically range between 10 t and 70 t. Observers work on deck in a dynamic environment, and catch is available to the observer in an unorganized manner. On some catcher vessels, catch comes aboard directly into the trawl alleyway, and the net is often reset before the completion of sampling. Only a few tools, such as spring scales or small platform scales, are available to an observer, and totes or bin space for storing individual samples is limited. An observer may have little time to collect samples before the catch is stowed. Observers who work on deck are exposed to weather and sample under dynamic conditions in which the catch shifts within the trawl alley. In spite of this chaotic sampling environment on deck, methods have been developed to randomize sample collections on catcher vessels, and alternative methods have been explored (Cahalan et al., 2016). For example, some catcher vessels may dump catch from the codend of the trawl net onto the deck where the crew sorts and discards unwanted catch or fish can flow directly into the hold.

Using time as a proxy for fish weight, observers can define sampling units and a systematic sampling design and then randomly select proxy sampling units until the entire catch has been moved below deck (strictly randomized collection). In the more common situation, however, an observer samples catch directly from the trawl alley. An observer might randomly choose several places adjacent to the alleyway to select samples (collection by using a randomized method), or a captain might determine where the observer can safely collect a single sample (opportunistic collection). Scenarios in which observers resort to opportunistic sampling pose the most challenges, in terms of decisions on how to best define sampling units and to randomize selections given the working environment on deck.

Individual fish Lastly, individual fish are randomly selected from the samples of catch by using either a systematic or simple random sampling design to select fish of a specified species. Biological data, such as fish lengths, as well as otoliths and tissue samples (stomachs, gonads, and fins taken for genetics analysis) are collected from the randomly selected individuals. Bycatch of all prohibited species, including the Pacific halibut, the Pacific herring (*Clupea pallasii*), all Pacific salmon species (*Oncorhynchus* spp.), steelhead (*O. mykiss*), all king crab species (*Lithodes* spp. and *Paralithodes* spp.), and Tanner crab species (*Chionoecetes* spp.), have biological data collected by the observer at sea. Through an annual process, the scientists at the NMFS Alaska Fisheries Science Center, working with the North Pacific Observer Program, determine the species for which, and quantities of, collections of biological data and specimens will be specified in the observer sampling manual for the following year. The collection methods for most species are integrated into the sampling hierarchy.

Landed catch is not sampled by observers in the North Pacific Ocean with the single exception of the fisheries that target walleye pollock and for which there has been long-standing concerns over salmon bycatch (Faunce, 2015). To address these concerns, a separate, parallel sampling design has been implemented in which trips on catcher vessels within these fisheries are monitored at the point of shoreside delivery. From these monitored shoreside landings, observers count and obtain biological data from salmon caught as bycatch.

Program evaluation

The North Pacific Observer Program evaluates the past performance of the implementation of the sampling design and provides the results in an annual report to the NPFMC in June. The results of the evaluations in annual reports inform decisions about recommendations for improving the deployment of observers and electronic monitoring systems in the next ADP cycle. This annual cycle of review, revision, and refinement leads to continual improvement of stakeholder engagement and deployments of observers and electronic monitoring systems. Here, we focus on review of the 2 stages of the sampling design with the most utility to other programs: deployment of observers (trip selections) and catch sampling (Table 2).

Observer and electronic monitoring deployments The ability to deploy observers at prespecified rates is evaluated in annual reports by comparing the rate of trip selection programmed into the online trip logging application to the initial selection rate for each sampling stratum (Table 3). The magnitude of non-response and actual on-the-ground coverage rates are assessed by comparing the proportion of trips observed in each stratum (actual coverage rate) with the prespecified rate (Table 3).

Temporal and spatial patterns of observed trips should be representative of the total fishing effort to provide inference about catch and bycatch. Avoidance of observer coverage during periods of high bycatch or during fishery openings typically is reflected in departures from expected patterns of observer coverage over time. Differences in temporal fishing patterns between observed and unobserved fishing trips are assessed by comparing the cumulative distributions of the number of observed trips and the expected number of observed trips given the deployment

Table 2

Structure of the sampling hierarchy used in 2018 by the North Pacific Observer Program, National Marine Fisheries Service, to monitor groundfish fisheries off Alaska and to evaluate on an annual basis the performance and design of sampling. The evaluation method informs efforts to improve the deployment of observers and electronic monitoring systems in the next annual deployment plan (ADP). Action items address questions of whether or not collected data are representative of fishing activities.

Question	Representativeness question and evaluation methods	Action item
Primary sampling units: trips		
How well was fishing effort predicted in the ADP last year?	Comparison of actual fishing effort vs. distribution of simulated outcomes from ADP	If actual effort not within simulated distribution, corrective or alternative methods for predicting future fishing effort are made, and the density value chosen to set overage risk is reassessed.
Is the realized observation rate reasonable given the selection rate?	Binomial test and evaluation of trip cancellation rates (selected, not selected)	Disproportionate cancellations may be evidence of a deployment effect. Policy allowing multiple trips to be logged is recommended to be reevaluated.
Is the temporal distribution of observed trips reasonable given fishing activity?	Cumulative distribution of selected trips vs. all trips	Together with cancellation rates, departure may be evidence of a deployment effect. Evaluated with opening and closing of fisheries.
Are data representative in space?	Probability densities resulting from hypergeometric distribution	Single test results not given much value in isolation. If the suite of results point to observer effect, look at prior years. If such a pattern found, recommend higher coverage rates for strata.
Is the information on observed trips comparable to that on unobserved trips?	Permutation test	
Secondary sampling units: hauls		
Is the sample rate consistent with expectations outlined in the observer sampling manual (AFSC[1])?	Inspection of proportion of hauls sampled per trip	Feedback to the observer both at sea and during data quality control process.
Tertiary sampling units: portions of total catch		
Are randomized sample selection methods used?	Inspection of proportions of hauls sampled using different randomization schemes	Feedback to observer and additional coaching related to specific sampling situations. Recommendations for additional training may be made.
Are multiple samples collected?	Inspection of numbers of samples per haul for different sampling scenarios	
Are sampling units well defined?	Inspection of sample unit definitions recorded by observers. Inspection of consistency of size of samples (catcher vessels)	
Quaternary sampling units: individual catch items (fish)		
Are randomized sample selection methods used?	Inspection of randomization schemes used to select fish; amount of data deleted because of inappropriate selection methods	Feedback to observer and additional coaching related to specific sampling situations. Recommendations for additional training may be made.
Are lengths of individual randomly selected fish consistent with mean size of fish in the catch sample (tertiary sample)?	Comparisons of mean fish weights by species	

[1] AFSC (Alaska Fisheries Science Center). 2018. 2018 observer sampling manual. North Pac. Groundfish Obs. Program, Fish. Monit. Analysis Div., AFSC, Seattle, WA. [Available from website.]

Table 3

Table of results from evaluation of trip selection in 2018 for 3 main gear-based strata for the category of vessels with partial coverage. These results illustrate the ability of the North Pacific Observer Program, National Marine Fisheries Service, to assess whether or not random selection was achieved in sampling of the groundfish fisheries off Alaska by using the programmed rate of trip selection, realized rate expected, and realized rate. Programmed and expected selection rates are derived from the trip logging application, and realized rates are derived from landing reports and the observer program data on observer deployments. The observer program does not report selection rates realized beyond the nearest tenth of a percentage. Entries in the "Within expected range?" column refer to whether or not the actual value was within the 95% binomial confidence limits of the numbers in the "Programmed value" column. Evaluation of whether or not the programmed rate was implemented correctly includes tests of whether or not the random number generator of the trip selection application was functioning correctly. Evaluation of the expected rate includes tests of whether or not the trip selection application rate is equal to the programmed rate after user influence (e.g., trip cancellations and trip duration changes). Evaluation of the realized rate includes tests of whether or not the number of trips actually monitored was equal to the programmed rate. For complete results, see Ganz et al., 2019.

Stratum	Rate	Programmed value	Actual value	Within expected range?
Hook and line				
	Programmed	17.26	16.32	Yes
	Expected	17.26	17.67	Yes
	Realized	17.26	15.5	No
Hook and line electronic monitoring				
	Programmed	30.00	30.15	Yes
	Expected	30.00	34.10	No
	Realized	30.00	22.7	No
Pot				
	Programmed	16.21	16.38	Yes
	Expected	16.21	16.45	Yes
	Realized	16.21	15.5	Yes
Trawl				
	Programmed	20.18	20.07	Yes
	Expected	20.18	20.88	Yes
	Realized	20.18	20.3	Yes

rate, the total number of fishing trips that occurred, and the 95% confidence interval based on Bernoulli selection of individual trips (AFSC[3]). Deviations of the number of observed trips from the expected number of observed trips that coincide with fishery openings or closings are evidence of deployment effects.

Differences in the spatial distribution of the sample (observed trips) and the total population (all fishing trips in sampled strata) are also evaluated. The probability that the sample contains the number of trips actually observed in a geographic area given the number of trips that occurred in the area (from landings data) and the total number of trips fished is computed for each area (within each sampling stratum) and used to assess the spatial representativeness of observed trips. A low probability of the sample containing the number of trips actually observed (or a number of trips greater than expected) is indicative of departures from representative deployments. However, because multiple areas are assessed simultaneously, we must avoid the risk of making erroneous conclusions as a result of multiple comparisons (Greenland et al., 2016). Therefore, a finding of a greater number of areas with probabilities lower than our nominal error rate predicts (i.e., if the probability of the sample containing the number of trips actually observed is less than 0.05) is interpreted to be evidence of an overall deployment effect. For example, in an assessment of 20 areas, we expect that one of those areas could have a low (<0.05) probability (or one area with a more extreme result). If more areas were found in the current and prior years, then it is recommended that coverage rates for that stratum be increased.

Characteristics of observed and unobserved trips are compared to evaluate whether observed fishing trips are similar to (and exchangeable with) unobserved fishing trips. Currently, 6 characteristics that are known for both the observed and unobserved trips are assessed: trip duration, number of geographic areas fished, total landed weight, number of species landed, proportion of the landing accounted for by the predominant species, and vessel length (Ganz et al., 2019). Permutation tests are used to test the

Table 4

Percentage of hauls sampled in 2018 by the North Pacific Observer Program, National Marine Fisheries Service, within each gear and vessel type that achieved the specified randomization. In strictly randomized methods of sampling, sampling units are unambiguously defined, all units are available to be selected, and sample selection is either simple random or systematic random. In randomized methods, randomization is introduced to the sampling process, but sampling units cannot be well defined, all units are not available to the observer, or the entire sampling unit is not collected. Opportunistic sample unit selection is a non-random method. A census, another type of non-random method, is a complete enumeration or weight for the entire haul.

		Percentage of hauls by gear type			
Vessel type	Method	Pelagic trawl	Non-pelagic trawl	Longline	Pot
Catcher	Strictly randomized	33.5%	38.7%	91.5%	91.9%
	Randomized	42.5%	21.0%	1.2%	1.1%
	Opportunistic	24.0%	40.0%	0.8%	2.8%
	Census	0.1%	0.2%	6.4%	4.3%
Catcher-processor	Strictly randomized	98.4%	96.9%	99.1%	99.1%
	Randomized	0.1%	0.5%	0.5%	
	Opportunistic	0.2%	2.5%	0.3%	
	Census	1.4%	0.1%	0.1%	0.9%

probability that the observed difference in trip metrics between observed and unobserved trips derives from the same population. A preponderance of low *P*-values among tests is interpreted as evidence of an observer effect. However, low sample sizes can result in spurious results, and large sample sizes can lead to low *P*-values for very small differences. For these reasons, the North Pacific Observer Program presents the effect size (magnitude of the difference in the metric for observed and all trips) as well as the *P*-values to increase interpretability of test results with low *P*-values (to avoid confusion between no difference and no significant difference, as per Greenland et al., 2016).

Catch sampling In spite of the logistical difficulties of sampling on commercial fishing vessels, most hauls are sampled by using strictly randomized or randomized methods (Table 4). As expected on longline and pot vessels, close to 100% of hauls are sampled by using strictly randomized methods (Table 4). The most difficult sampling situation for observers is on catcher vessels that use trawl nets because defining sampling units and randomizing which units to select is complicated by catch handling and vessel operations. In spite of the logistical difficulties, observers resorted to opportunistic sampling in fewer than half the sampled hauls on catcher vessels that use trawl nets, and 60% of hauls were sampled with some randomization incorporated into sample selection.

Discussion

The Magnuson–Stevens Fishery Conservation and Management Reauthorization Act of 2006 (Magnuson–Stevens…2018), the Marine Mammal Protection Act (Marine…2018), and the Endangered Species Act (Endangered…2018) of the United States mandate not only collection of data for fisheries management of target species but also monitoring of the effects of fisheries on protected species (Moore et al., 2009). The observer programs tasked with this monitoring mandate have multiple, disparate sampling objectives that often change over time. In Alaska, we have chosen not to design the monitoring program to a specific fishery or to meet specific target precision goals. Because species-specific catches (including discards) have different underlying distributions and population structures that vary both with the time of year and in geographic space, it can be difficult to design sampling programs to meet species-specific (e.g., achieve a target-level precision for species-specific bycatch estimates) or short-term goals without decreasing the utility of the collected data for estimation specific to other species or analytic objectives. Sampling schemes that are optimal for less common species will not necessarily be optimal for target species. A diverse group of researchers and stakeholders, including statisticians, stock assessment scientists, social scientists (economists and anthropologists), members of the fishing industry, and fisheries managers, use data collected by observers, and they all have very different data needs and objectives. In all cases, analytic data users, and fisheries assessment and management, are affected by sparse and missing data. This issue of a lack of or low quality of data is particularly problematic for low-effort fisheries in which observers may not be able to sample from specific strata (i.e., areas and time of year).

The challenge in designing sampling programs that collect representative data useful to researchers and fisheries managers is surmountable. Sampling designs that do not make assumptions about the underlying population being sampled are preferred to model-based designs that incorporate assumptions (Cotter and Pilling, 2007). A hierarchical probability-based design for the federally managed fisheries off Alaska is used because it is feasible and necessary (e.g., it is impossible to randomly deploy observers to individual hauls or by weight of catch). This type of design makes efficient use of observer funds and sampling effort, and it allows flexibility to the data user in the estimators they chose. Because data collected under a probability-based sampling scheme can be used in both model-based estimation and more traditional design-based estimation processes, an analyst can choose to use design-based estimators when estimating bycatch of relatively common groundfish species or to use a model-based estimator (e.g., zero-inflated parametric models) to estimate the bycatch of a rare species (Allen et al., 2002; Dietrich et al., 2009; Stock et al., 2019).

Stratification decisions in the sampling design for deployment of observers or electronic monitoring systems can be based on logistical considerations aimed at reducing cost (e.g., Sun and Fine, 2016). Defining sampling strata on the basis of fishery (i.e., fishery-specific deployment of observers) can be problematic because factors describing the sampling units and strata need to be defined prior to fishing (Cochran, 1977), and although the intended target species is known prior to fishing, the realized target is not. Melvin et al. (2019) and Moore et al. (2009) have advocated fishery-specific solutions to monitoring for bycatch of seabirds and marine mammals, respectively, but we intentionally avoid inclusion of species in the stratum definitions for sampling in the North Pacific Ocean with the notable exception of dockside monitoring in the trawl fishery that targets walleye pollock. Because fisheries are not clearly defined prior to fishing and the North Pacific Observer Program cannot deploy into specific fisheries, the terms *fishery* or *métier*, which are often conflated, are not used (Ulrich et al., 2012).

Stratification decisions in the sampling design for deployment of observers or electronic monitoring systems can be based on statistical considerations aimed at reducing variance in the estimator (e.g., Wigley and Tholke, 2018). Although this objective is achieved by maximizing the differences between strata and minimizing differences within strata (Thompson, 2012), if poorly constructed, stratified sampling designs can lead to estimates with variances greater (not lower) than would be achieved with an unstratified design and the same overall sample size. In addition, for situations in which multiple estimation objectives (e.g., multiple species) exist, sample size and allocation decisions based on the minimization of variance must rely on assignment of relative importance of objectives, de facto decisions of which species are important and which are not. For example, Miller et al. (2007) used variance minimization to allocate sampling effort among gear-based strata to identify the ideal stratification of "small" and "large" vessels in the North Pacific Observer Program in the North Pacific Ocean. They synthesized multiple sampling objectives (i.e., species-specific estimates of catch and discards) into a single objective by weighting the individual species according to the management priorities at the time. This weighting required prioritizing the importance of species and fisheries not only in the current year but also in future years when sampling will take place.

Although this method of Miller et al. (2007) decreased variance of the species- and fishery-specific estimates of catch and discards that were investigated, this sample allocation may not be optimal or even appropriate for other data users who have sampling goals that are not related to catch or discards (e.g., collection of tissue samples for genetic analysis). Unlike the approach used by Miller et al. (2007), the method used by the North Pacific Observer Program addresses multiple species (not only a few high-profile species) across fisheries and multiple estimation goals, including catch estimation for in-season quota management, catch-at-age estimation used in the stock assessment process, estimation of bycatch of rare species such as marine mammals, and identification of population substructure through genetic analysis of tissue samples.

The question of how much coverage is enough is reasonable to ask but difficult to answer for any monitoring program. Babcock et al.[2] used simulation to show how variance decreases with increasing sample size and how more samples are required for species with increasing rarity, and they advocated setting precision-based targets to guide analyses of sample sizes. This type of analysis was used by NMFS (2004) to set a precision target for U.S. fisheries. The observer program in New England established a 30% coefficient of variation for its species within numerous fishery complexes. The result was a sample size that the program could not afford, and the program was scaled back. However, the NMFS was challenged in a legal suit on the grounds that it failed to achieve its own performance standard. In an eventual compromise, species that constituted small portions of total catch or for whom the recommended sampled sizes would have been large were eliminated from sample size recommendations and other filtering rules, prior to scaling back to affordable levels (Wigley et al.[6]; Wigley and Tholke, 2018).

In the North Pacific Observer Program, a different approach was taken to setting target sample rates and to making sample allocation decisions. The North Pacific Observer Program does not set coverage rates on the basis of predetermined precision criteria. Instead, it evaluates alternative stratifications and allocations in its draft ADP review process and compares the relative performance of each against the stratification used in the previous year and an equal allocation of available sample effort. Performance scores are based on the severity of data gaps generated—the greater the gap, the lower the score

---

[6] Wigley, S. E., P. J. Rago, K. A. Sosebee, and D. L. Palka. 2007. The analytic component to the Standardized Bycatch Reporting Methodology Omnibus Amendment: sampling design end estimation of precision and accuracy, 2nd ed. Northeast Fish. Sci. Cent. Ref. Doc. 07-09, 156 p. [Available from website.]

(NMFS[7]). Selection of the current baseline rate of 15% was derived in large part from an analysis that evaluated how the probability of having no data in a catch estimation post-stratum (defined by the dominant species in the catch during periods of 2–4 weeks) changed over a range of deployment rates (Gasper et al., 2019).

By instituting a baseline rate, the North Pacific Observer Program effectively curtailed the ability for managers to annually tailor coverage to meet short-term goals because only funds available after the baseline rate threshold had been reached were available for tailored use. Instead, the establishment of the base rate by the NMFS in Alaska has helped ensure that representative data are collected by the North Pacific Observer Program. Doing so also has created incentive for the NMFS and the NPFMC to obtain funding for coverage above 15% and retained the ability for targeted deployment to meet specific and often changing management priorities.

This concept of the use of different deployment strategies for observer programs is not a new one. The most striking example is when observers are also used to aid in enforcement programs. In Alaska, observers provide an invaluable resource for law enforcement agents by providing statements of potential violations (Porter, 2010). Furlong and Martin (2001) describe a program in which observer deployment is optimized to be greater in proportion to a vessel's demonstrated or suspected violation rate in cases where the deployment cost of an observer is directly borne by the vessel on a trip-by-trip basis. In this system, the incentive to comply is tied to the cost of observation. Such a deployment scheme would tackle the largest potential sources of bias, but it would not result in representative data at the fishery level (Benôit and Allard, 2009). The partial coverage fleet in Alaska funds observer coverage like insurance, wherein all participants pay into the program but only those that are selected have observer coverage. This funding system removes the economic penalties normally associated with industry-funded monitoring programs, and in our opinion greatly reduces the incentive for vessels to change fishing behavior when observers are onboard. Although evidence of this observer effect has been found in the past (Faunce and Barbeaux, 2011), recent complaints about observer deployment are often limited to new participants in a program and are generally focused on the logistical aspects of observation, such as the need for bunk space, food, or life-raft capacity.

To address the logistical difficulties of physical observation, the NPFMC began implementing electronic monitoring on longline vessels in 2014 and has expanded its use every year since. The NPFMC elected to use electronic monitoring for bycatch estimation rather than the less cumbersome compliance monitoring (monitoring only for compliance with regulations such as no discards; e.g., the use of electronic monitoring in Europe to help with enforcement of a discard ban; Borges et al., 2016). Vessels participating in electronic monitoring constitute their own deployment and estimation stratum within the current sample design of the North Pacific Observer Program (Ganz et al., 2019). However, electronic monitoring does not include collection of biological tissues or weight information; therefore, biological samples and data must be obtained elsewhere or inferred. Specifically, on vessels in the electronic monitoring stratum, staff review the video imagery of fishing activities recorded by camera systems, documenting the number and disposition (retained or discarded) of each species. The number of at-sea discards for these strata is estimated by using data derived from electronic monitoring in combination with species-specific mean weights of fish from the observed strata.

Although we have focused here on the deployment of observers, this design is equally applicable to the design of electronic monitoring programs and incorporation of electronic monitoring into observer-based monitoring programs. The reliance on other sampling strata to represent the electronic monitoring stratum highlights the need to set observer coverage rates so that data gaps are minimized and the necessary data elements from the observed strata can be used to "complete" data collected in the electronic monitoring strata, effectively reducing the number of gaps in biological data (inclusive of fish length and weight).

Although deployment rates in Alaska are set to ensure coverage in time and space, the intensity of sampling at sea is largely determined by the sampling environment. Once an observer is deployed, sampling design considerations shift to include the abilities of the observer, and decisions are based on what can be physically and logically achieved given that sampling occurs on vessels actively engaged in commercial fishing. The ability to adjust sampling in response to changing fishing conditions and vessel operations is critical to successful implementation of a credible randomized sampling design. Defining sampling units and having access to those sampling units in order to randomize selections is difficult in many situations. In spite of this challenge, the majority of samples are collected by using credible randomization methods.

Fully randomized designs have the added advantage of allowing sampling to be evaluated at all levels. Instituting randomized trip selection through the restructure of the North Pacific Observer Program in 2013 resulted in the ability to evaluate how well observers and electronic monitoring systems were deployed. Patterns and trends in observer coverage in the previous year are used to assess the effectiveness of the North Pacific Observer Program and to make recommendations for changes to be instituted the following year (as part of the processes for annual review and development of an ADP). Similarly, explicitly capturing information about how observers sample while they are deployed on fishing vessels allows evaluation of the effectiveness of sampling in terms of both accuracy of collected data and statistical robustness of sampling methods. These data are used to provide feedback directly to the observer after deployment and to adjust training and sampling methods for future years.

---

[7] NMFS (National Marine Fisheries Service). 2019. Draft 2020 annual deployment plan for observers and electronic monitoring in the groundfish and halibut fisheries off Alaska, 16 p. Natl. Mar. Fish. Serv., NOAA, Juneau, AK. [Available from website.]

Randomization, which has long been known to lower costs of sampling (relative to conducting a census of a population), results in representative data that can be used for a variety of purposes and estimators. Our experiences with the North Pacific Observer Program in Alaska have indicated that randomization can be achieved at each level and that these theoretical benefits can be realized in practice. The trip selection process used in Alaska has proven to be a robust method for the randomization of deployments of observers and electronic monitoring systems and, even though active fishing vessels are not perfect sampling platforms, credible at-sea sampling methods can be designed and implemented. We are not aware of another fishery monitoring program that makes annual evaluations of its performance and determines whether sampling objectives were met and whether departures from randomization could be detected. This annual cycle of evaluation and improvement of sampling methods is unique to Alaska and contributes to the success of the North Pacific Observer Program and the positive state of sustainable fisheries management in Alaska. The success of the North Pacific Observer Program in implementing random sampling while using state-of-the-art technology and efficiently collecting data for a variety of uses indicates that this observer program can be used as a model for other fishery monitoring programs with similar objectives.

Acknowledgments

We thank the many observers who are deployed to commercial fishing vessels that target groundfish species in Alaska and the staff of the Fisheries Monitoring and Analysis Division of the Alaska Fisheries Science Center who support observers and make observer data available to our many data users. Our gratitude goes to our colleagues J. Gasper and B. Mason, whose discussions have helped to form this manuscript, and to S. Lowe, C. Tribuzio, and 2 anonymous reviewers whose contributions greatly improved this manuscript.

Literature cited

Allen, M., D. Kilpatrick, M. Armstrong, R. Briggs, G. Course, and N. Pérez.
2002. Multistage cluster sampling design and optimal sample sizes for estimation of fish discards from commercial trawlers. Fish. Res. 55:11–24.

American Fisheries Act. Pub. L. 105-277, div. C, title 2. 112 Stat. 2681 (21 October 1998). [Available from website.]

Benôit, H. P., and J. Allard.
2009. Can the data from at-sea observer surveys be used to make general inferences about catch composition and discards? Can. J. Fish. Aquat. Sci. 66:2025–2039.

Borges, L.
2015. The evolution of a discard policy in Europe. Fish Fish. 16:534–540.

Borges, L., L. Cocas, and K. N. Nielsen.
2016. Discard ban and balanced harvest: a contradiction? ICES J. Mar. Sci. 73:1632–1639.

Cahalan, J., C. Faunce, J. Bonney, and R. Swanson.
2016. A field test of fisheries observer sampling methods for estimation of at-sea discards. Fish. Res. 174:219–233.

Cochran, W. G.
1977. Sampling techniques, 3rd ed., 448 p. John Wiley and Sons Inc., New York.

Cotter, A. J. R., and G. M. Pilling.
2007. Landings, logbooks and observer surveys: improving the protocols for sampling commercial fisheries. Fish Fish. 8:123–152.

Cotter, A. J. R., G. Course, S. T. Buckland, and C. Garrod.
2002. A PPS sample survey of English fishing vessels to estimate discarding and retention of North Sea cod, haddock, and whiting. Fish. Res. 55:25–35.

Davies, S. L, and J. E. Reynolds (eds.).
2003. Guidelines for developing an at-sea fishery observer programme. FAO Fish. Tech. Pap., 414, 116 p. FAO, Rome.

DiCosimo, J., R. D. Methot, and O. A. Ormseth.
2010. Use of annual catch limits to avoid stock depletion in the Bering Sea and Aleutian Islands management area (Northeast Pacific). ICES J. Mar. Sci. 67:1861–1865.

Dietrich, K. S., J. K. Parrish, and E. F. Melvin.
2009. Understanding and addressing seabird bycatch in Alaska demersal longline fisheries. Biol. Conserv. 142: 2642–2656.

Endangered Species Act. 16 U.S.C. 1531–1544 (2018). [Available from website.]

Equipment and operational requirements. 50 C.F.R. 679.28 (2019). [Available from website.]

Faunce, C. H.
2015. Evolution of observer methods to obtain genetic material from Chinook salmon bycatch in the Alaska pollock fishery. NOAA Tech. Memo. NMFS-AFSC-288, 28 p.

Faunce, C. H., and S. J. Barbeaux.
2011. The frequency and quantity of Alaskan groundfish catcher-vessel landings made with and without an observer. ICES J. Mar. Sci. 68:1757–1763.

Fissel, B., M. Dalton, B. Garber-Yonts, A. Haynie, S. Kasperski, J. Lee, D. Lew, A. Lavoie, C. Seung, K. Sparks, et al.
2019. Stock assessment and fishery evaluation report for the groundfish fisheries of the Gulf of Alaska and Bering Sea/Aleutian Islands area: economic status of the groundfish fisheries off Alaska, 2017, 320 p. [Available from website.]

Furlong, W. J., and P. M. Martin.
2001. Observer deployment in the fishery and regulatory self-enforcement. *In* Microbehavior and macroresults: proceedings of the tenth biennial conference of the International Institute of Fisheries Economics and Trade; Corvallis, OR, 10–14 July 2000 (R. S. Johnston and A. L. Shriver, eds.), 8 p. Int. Inst. Fish. Econ. Trade, Corvallis, OR. [Available from website.]

Ganz, P., and C. H. Faunce.
2019. An evaluation of methods used to predict commercial fishing effort in Alaska. NOAA Tech. Memo. NMFS-AFSC-395, 19 p.

Ganz, P., S. Barbeaux, J. Cahalan, J. Gasper, S. Lowe, R. Webster, and C. Faunce.
2019. Deployment performance review of the 2018 North Pacific Observer Program. NOAA Tech. Memo. NMFS-AFSC-397, 73 p.

Gasper, J., C. Tide, G. Harrington, J. Mondragon, J. Cahalan, S. Bibb, and G. Merrill.
2019. Supplement to the environmental assessment for restructuring the program for observer procurement and deployment in the North Pacific. NOAA Tech. Memo. NMFS-F/AKR-19, 168 p.

Gilman, E. L., P. Dalzell, and S. Martin.
2006. Fleet communication to abate fisheries bycatch. Mar. Policy 30:360–366.

Gilman, E., M. Weijerman, and P. Suuronen.
2017. Ecological data from observer programmes underpin ecosystem-based fisheries management. ICES J. Mar. Sci. 74:1481–1495.

Greenland, S., S. J. Senn, K. J. Rothman, J. B. Carlin, C. Poole, S. N. Goodman, and D. G. Altman.
2016. Statistical tests, *P* values, confidence intervals, and power: a guide to misinterpretations. Eur. J. Epidemiol. 31:337–350.

Hilborn, R., J. M. Orensanz, and A. M. Parma.
2005. Institutions, incentives and the future of fisheries. Philos. Trans. R. Soc. Lond., B 360:47–57.

Karp, W. A., M. Breen, L. Borges, M. Fitzpatrick, S. J. Kennelly, J. Kolding, K. N. Nielsen, J. R. Viðarsson, L. Cocas, and D. Leadbitter.
2019. Strategies used throughout the world to manage fisheries discards—lessons for implementation of the EU landing obligation. *In* The European landing obligation: reducing discards in complex, multi-species and multi-jurisdictional fisheries (S. Uhlmann, C. Ulrich, and S. J. Kennelly, eds.), p. 3–26. Springer, Cham, Switzerland.

Lewis, S. G., and M. Boyle.
2017. The expanding role of traceability in seafood: tools and key initiatives. J. Food Sci. 82(S1):A13–A21.

Lewison, R. L., L. B. Crowder, A. J. Read, and S. A. Freeman.
2004. Understanding the impacts of fisheries bycatch on marine megafauna. Trends Ecol. Evol. 19:598–604.

Magnuson–Stevens Fishery Conservation and Management Reauthorization Act of 2006. 16 U.S.C. 1801–1891d (2018). [Available from website.]

Marine Mammal Protection Act. 16 U.S.C. 1361–1421 (2018). [Available from website.]

Melvin, E. F., K. S. Dietrich, R. M. Suryan, and S. M. Fitzgerald.
2019. Lessons from seabird conservation in Alaskan longline fisheries. Conserv. Biol. 33:842–852.

Miller, T. J., J. R. Skalski, and J. N. Ianelli.
2007. Optimizing a stratified sampling design when faced with multiple objectives. ICES J. Mar. Sci. 64:97–109.

Moore, J. E., B. P. Wallace, R. L. Lewison, R. Žydelis, T. M. Cox, and L. B. Crowder.
2009. A review of marine mammal, sea turtle and seabird bycatch in USA fisheries and the role of policy in shaping management. Mar. Policy 33:435–451.

NMFS (National Marine Fisheries Service).
2004. Evaluating bycatch: a national approach to standardized bycatch monitoring programs. NOAA Tech. Memo. NMFS-F/SPO-66, 108 p.

NRC (National Research Council).
1998. Improving fish stock assessments, 177 p. Natl. Academy Press, Washington, DC.

O'Keefe, C. E., S. X. Cadrin, and K. D. E. Stokesbury.
2014. Evaluating effectiveness of time/area closures, quotas/caps, and fleet communications to reduce fisheries bycatch. ICES J. Mar. Sci. 71:1286–1297.

Palmer, M. C., P. Hersey, H. Marotta, G. R. Shield, and S. B. Cierpich.
2016. The design and performance of an automated observer deployment system for the northeastern United States groundfish fishery. Fish. Res. 179:33–46.

Porter, R. D.
2010. Fisheries observers as enforcement assets: lessons from the North Pacific. Mar. Policy 34:583–589.

Stock, B. C., E. J. Ward, J. T. Thorson, J. E. Jannot, and B. X. Semmens.
2019. The utility of spatial model-based estimators of unobserved bycatch. ICES J. Mar. Sci. 76:255–267.

Roberson, L. A., J. J. Kiszka, and J. E. M. Watson.
2018. Need to address gaps in global fisheries observation. Conserv. Biol. 33:966–968.

Sullivan, J., and C. Faunce.
2018. Alternative sampling designs for the 2018 annual deployment plan of the North Pacific Observer Program. NOAA Tech. Memo. NMFS-AFSC-364, 30 p.

Sun, C.-H. J., and L. Fine.
2016. A cost-effective discards-proportional at-sea monitoring allocation scheme for the groundfish fishery in New England. Mar. Policy 66:75–82.

Sutinen, J. G.
1999. What works well and why: evidence from fishery-management experiences in OECD countries. ICES J. Mar. Sci. 56:1051–1058.

Thompson, S. K.
2012. Sampling, 3rd ed., 472 p. John Wiley and Sons Inc., Hoboken, NJ.

Ulrich, C., D. C. K. Wilson, J. R. Nielsen, F. Bastardie, S. A. Reeves, B. S. Andersen, and O. R. Eigaard.
2012. Challenges and opportunities for fleet- and métier-based approaches for fisheries management under the European Common Fishery Policy. Ocean Coast. Manage. 70:38–47.

van Helvoort, G.
1986. Observer program operations manual. FAO Fish. Tech. Pap. 275, 207 p. FAO Rome.

Vølstad, J. H., P. S. Afonso, A. P. Baloi, N. de Premegi, J. Meisfjord, and M. Cardinale.
2014. Probability-based survey to monitor catch and effort in coastal small-scale fisheries. Fish. Res. 151:39–46.

Wigley, S. E., and C. Tholke.
2018. 2018 discard estimation, precision, and sample size analyses for 14 federally managed species groups in the waters off the northeastern United States. NOAA Tech. Memo. NMFS-NE-243, 182 p.

Zollett, E. A., R. J. Trumble, J. H. Swasey, and S. B. Stebbins.
2015. Guiding principles for development of effective commercial fishery monitoring programs. Fisheries 40:20–25.

Fishery Bulletin

Guidelines for authors

Contributions published in *Fishery Bulletin* describe original research in marine fishery science, fishery engineering and economics, and marine environmental and ecological sciences (including modeling). Preference will be given to manuscripts that examine processes and underlying patterns. Descriptive reports, surveys, and observational papers may occasionally be published but should appeal to an audience outside the locale in which the study was conducted.

Although all contributions are subject to peer review, responsibility for the contents of papers rests upon the authors and not on the editor or publisher. *Submission of an article implies that the article is original and is not being considered for publication elsewhere.*

All submissions are subject to a double-blind review to remove the identity of author and reviewer during the review process.

Plagiarism and double publication are considered serious breaches of publication ethics. To verify the originality of the research in papers and to identify possible previous publication, manuscripts may be screened with plagiarism-detection software.

Manuscripts must be written in English; authors whose native language is not English are strongly advised to have their manuscripts checked by English-speaking colleagues before submission.

Once a paper has been accepted for publication, online publication takes approximately 2 weeks.

There is no cost for publication in *Fishery Bulletin*.

Types of manuscripts accepted by the journal

Articles generally range from 20 to 30 double-spaced typed pages (12-point font) and describe an original contribution to fisheries science, engineering, or economics. Tables and figures are not included in this page count, but the number of figures should not exceed 1 figure for every 4 pages of text. Articles contain the following divisions: abstract, introduction, methods, results, and discussion.

Short contributions are generally less than 15 double-spaced typed pages (12-point font) and, like articles, describe an original contribution to fisheries science. They follow the same format as that for articles: abstract, introduction, methods, results, and discussion, but the results and discussion sections may be combined. They are distinguished from full articles in that they report a noteworthy new observation or discovery—such as the first report of a new species, a unique finding, condition, or event that expands our knowledge of fisheries science, engineering, or economics—and do not require a lengthy discussion.

Companion articles should be submitted together and are published together as a scientific contribution. Both articles should address a closely related topic and may be articles that result from a workshop or conference.

Preparation of manuscript

Title page should include authors' full names, mailing addresses, and the senior author's email address.

Abstract should be limited to 200 words (one-half typed page), state the main scope of the research, and emphasize the authors' conclusions and relevant findings. Do not review the methods of the study or list the contents of the paper. Because abstracts are circulated by abstracting agencies, it is important that they represent the research clearly and concisely.

General text must be typed in 12-point Times New Roman font throughout. A brief introduction should convey the broad significance of the paper; the remainder of the paper should be divided into the following sections: Materials and methods, Results, Discussion, and Acknowledgments. Headings within each section must be short, reflect a logical sequence, and follow the rules of subdivision (i.e., there can be no subdivision without at least 2 subheadings). The entire text should be intelligible to interdisciplinary readers; therefore, all acronyms, abbreviations, and technical terms should be written out in full and defined the first time they are mentioned. Abbreviations should be used sparingly because they are not carried over to indexing databases and slow readability for those readers outside a discipline. They should never be used for the main subject (species, method) of a paper.

For general style, follow the U.S. Government Publishing Office *Style Manual* (2016, available at website) and *Scientific Style and Format: the CSE Manual for Authors, Editors, and Publishers* (2014, 8th ed.) published by the Council of Science Editors. For scientific nomenclature, use the current edition of the American Fisheries Society's *Common and Scientific Names of Fishes from the United States, Canada, and Mexico* and its companion volumes (*Crustaceans, Mollusks, Cnidaria and Ctenophora*, and *World Fishes Important to North Americans*). For species not found in the above mentioned AFS publications and for more recent changes in nomenclature, use the Integrated Taxonomic Information System (ITIS, available at website), or, secondarily, the California Academy of Sciences *Catalog of Fishes* (available at website) for species names not included in ITIS. Common (vernacular) names of species should be lowercase. Citations must be given for the identification of specimens. For example, "Fish species were identified according to Collette and

Klein-MacPhee (2002); sponges were identified according to Stone et al. (2011).”

Dates should be written as follows: 11 November 2018. Measurements should be expressed in metric units, for example, “58 metric tons (t);” if other units of measurement are used, please make this fact explicit to the reader. Use numerals, not words, to express whole and decimal numbers in the general text, tables, and figure captions (except at the beginning of a sentence). For example, “We considered 3 hypotheses. We collected 7 samples in this location.” Use American spelling. Refrain from using the shorthand slash (/), an ambiguous symbol, in the general text.

Cite all software, special equipment, and chemical solutions used in the study within parentheses in the general text, for example, “SAS, vers. 6.03 (SAS Institute Inc., Cary, NC).”

Word usage and grammar that may be useful are the following:

- *Aging*

  For our journal, the word *aging* is used to mean both age determination and the aging process (senescence). Authors should make clear which meaning is intended where ambiguity may arise.

- *Fish and fishes*

  The plural of the word fish (a collective noun that implies individuals without regard to species) is *fish*.
  Example: The *fish* were collected by trawl net.
  Example: The numbers of *fish* collected that season were less than the numbers from previous years.

  The plural for *fish species* is *fishes* (a contrived plural used by taxonomists to mean several or more *fish species*) or one can use *fish species* (which is preferred in this journal for clarity across disciplines).
  Example: The *fishes* of Puget Sound [biodiversity is implied] or
  Example: The *fish species* of Puget Sound [preferred plural for clarity across disciplines].

- *Crab and crabs, squid and squids, etc.*

  The plural of the word *crab* (i.e., many individuals without regard to species) is *crab*.
  Example: The crab were sorted by weight.
  Example: Many red king *crab* were dying [Many individuals of one species of crab.]

  The plural of *crab species* is *crabs* (a word used by taxonomists) or *crab species* (the latter is preferred in this journal for clarity).
  Example: These *crabs* were selected for treatment. [Different crab species are implied.]
  Example: These *crab species* were selected for treatment. [Preferred word choice for clarity of meaning.]
  Example: Snow *crabs* are found throughout the North Pacific Ocean and Bering Sea. [There are 2 species of snow crab and therefore the word *crabs* can be used here.]
  Example: *Two species* of snow *crab* are found throughout the North Pacific Ocean and Bering Sea. [Preferred usage for clarity.]
  Example: Three crabs were selected for treatment. [3 species of crab are implied.]
  Example: Three crab species were selected for treatment. [Preferred word choice for clarity.]

- *Fisherman and fisher*

  We use *fisherman* and *fishermen* in this journal not *fisher* and *fishers*. One can always use crew member, vessel operator, and angler (the latter for recreational fishing.

- *The definite article with common names of species*

  When the singular common name of a species represents the entire class or group to which it belongs, use the definite article.
  Example: Only one species of the genus *Salmo* is found in the Atlantic Ocean—*the* Atlantic salmon (*Salmo salar*).
  Example: The sonic emissions of *the* bottlenose dolphin are complex.

  For plural common names, this rule does not apply.
  Example: Chinook salmon are found throughout the Pacific Ocean.
  Example: Bottlenose dolphins are found in temperate and tropical waters.

- *Sex*

  For the meaning of male and female, use the word *sex*, not *gender*. Do not write “fish were sexed.” Write, “sex was determined.”

- *Participles*

  As adjectives, participles must modify a specific noun or pronoun.
  Example: Using mark-recapture methods, these scientists determined the size of the population. [Correct. The participle *using* modifies the word *scientists*.]
  Example: These scientists, based on the collected data, concluded that the mortality rate of these fish had increased. [Incorrect. The scientists were not based on the collected data.]
  Example: These scientists concluded, on the basis of collected data, that the mortality rate of these fish had increased. [Correct. The offending participle has been eliminated and an adverbial phrase modifies the verb *concluded*.]

Equations and mathematical symbols should be set from a standard mathematical program (MathType or Equation Editor). Equations formatted in LaTex are not acceptable. For mathematical symbols in the general text (α, χ^2, π, ±, etc.), use the symbols provided by the MS Word program and italicize all variables, except those variables represented by Greek letters and the superscript and subscript parts of variables and expressions. Do not use photo mode when creating these symbols in the general text, and do not cut and paste equations, letters, or symbols from a different software program.

Number equations (if there are more than one) for future reference by scientists; place the number within parentheses at the end of the first line of the equation.

Literature cited section comprises published works and those accepted for publication (in press) in peer-reviewed journals. Follow the name and year system for citation format in this section (i.e., citations should be listed alphabetically by the authors' last names, and then by year if there is more than one citation by the same author. A list of abbreviations for citing journal titles can be found on our website.

Authors are responsible for the accuracy and completeness of all citations. Literature citation format: Authors (last name, followed by initials for first name and, if given, middle name of first author; then list names of additional authors with initials before last names). Year. Title of article. Abbreviated title of the journal in which it was published. Always include either the range of page numbers (for a journal article) or a total number of pages (for a book or other type of publication). List a sequence of citations in the general text chronologically, for example, "(Smith, 1932: Green. 1947; Smith and Jones, 1985)." Avoid the use of multiple citations when a single citation sufficiently supports a statement; cite the work that first reported the information that supports a statement, not all of the subsequent works.

Acknowledgments should be no more than 6 lines of text. Only those who have contributed in an outstanding way should be acknowledged by name. For recognition of other persons or groups, use a general term, such as *crew*, *observers*, or *research coordinators*, and do not include names with these terms.

Digital object identifier (doi) code ensures that a publication has a permanent location online. A doi link (which may include a doi code) should be included at the end of citations of published literature. Authors are responsible for submitting accurate doi links. Faulty links will be deleted at the page-proof stage.

Footnotes are used for all documents that have not been formally peer reviewed and for observations and personal communications, but these types of references should be cited sparingly in manuscripts submitted to the journal.

All reference documents, administrative reports, internal reports, progress reports, project reports, contract reports, personal observations, personal communications, unpublished data, manuscripts in review, and council meeting notes are footnoted in 10-point font and placed at the bottom of the page on which they are first cited. Footnote format is the same as that for formal literature citations. A link to the online source (e.g., [Available from http://www... , accessed July 2017.]), or the mailing address of the agency or department holding the document, should be provided so that readers may obtain a copy of the document.

Tables are often overused in scientific papers; it is seldom necessary to present all the data associated with a study. Tables should not be excessive in size and must be cited in numerical order in the text. Headings should be short but ample enough to allow the table to be intelligible on its own.

All abbreviations and unusual symbols must be explained in the table legend. Other incidental comments may be footnoted with numeral footnote markers. Use asterisks only to indicate significance in statistical data. Do not put a table legend on a page separate from the table; place the legend above the table. *Do not submit tables in photo mode.*

- Note probability with a capital, italic P.
- Provide a zero before all decimal points for values less than one (e.g., 0.07).
- Round all values to 2 decimal points.
- Use a comma in numbers of 5 digits or more (e.g., 13,000 but 3000).

Figures must be cited in numerical order in the text. Graphics should aid in the comprehension of the text, but they should be limited to presenting patterns rather than raw data. The number of figures should not exceed 1 figure for every 4 pages of text. Place panel labels **A, B, C,** etc., within the upper-left area of graphs and photos. Avoid placing labels vertically.

Figure legends should explain all symbols and abbreviations seen in the figure and should be double spaced on a separate page at the end of the manuscript.

Line art and halftone figures should be saved at resolutions >600 dots per inch (dpi) and >300 dpi, respectively. Color is allowed in figures to show morphological differences among species (for species identification), to show stain reactions, to show gradations (such as those of temperature and salinity within maps), and to distinguish between numerous lines and symbols in graphs. Figures approved for color should be saved in CMYK format.

All figures must be submitted as PDF, TIFF, or EPS files.

- Capitalize only the first letter of the first word and proper nouns in all labels within figures.
- Do not use overly large font sizes in maps and for axis labels in graphs.

- Do not use bold fonts or bold lines in figures.
- Do not place outline rules around graphs.
- Place a north arrow and label degrees latitude and longitude (e.g., 170°E) in all maps.
- Use symbols, shadings, or patterns (not clip art) in maps and graphs.

Supplementary materials that are considered essential, but are too large or impractical for inclusion in a paper (e.g., metadata, figures, tables, videos, and websites), may be provided at the end of an article. These materials are subject to the editorial standards of the journal. A URL to the supplementary material and a brief explanation for including such material should be sent at the time of initial submission of the paper to the journal.

- **Metadata, figures, and tables** should be submitted in standard digital format (MS Word or PDF file) and should be cited in the general text, for example, as "... was determined (Suppl. Table 3, Suppl. Fig. 1)."
- **Websites** should be cited with a URL in the general text.
- **Videos** must not be larger than 30 MB to allow a swift technical response for viewing the video. Authors should consider whether a short video uniquely captures what text alone cannot capture for the understanding of a process or behavior under examination in the article. Supply an online link to the location of the video.

Copyright law does not apply to *Fishery Bulletin*, which falls within the public domain. However, if an author reproduces any part of an article from *Fishery Bulletin*, reference to source is considered correct form (e.g., Source: Fish. Bull. 97:105).

Failure to follow these guidelines and failure to correspond with editors in a timely manner will delay publication of a manuscript.

Submission of manuscript

Submit a manuscript online at the ScholarOne Manuscripts website for *Fishery Bulletin*. Commerce Department authors should submit papers under a completed NOAA Form 25-700. For further details on electronic submission, please contact the associate editor, Cara Mayo, at

cara.mayo@noaa.gov.

When requested, the text and tables should be submitted in MS Word format. Each figure should be sent as a separate PDF, TIFF, or EPS file. Send a copy of a figure in the original software if conversion to any of these formats yields a degraded version of the figure.

Questions? If you have questions regarding these guidelines, please contact the managing editor, Kathryn Dennis, at

kathryn.dennis@noaa.gov.

Questions regarding manuscripts under review should be addressed to Associate Editor Cara Mayo.

Please note that Sharyn Matriotti has retired after serving for 29 years as the managing editor of *Fishery Bulletin*.

Fishery Bulletin

Subscription form

Superintendent of Documents **Publications** Order Form

*5178

☐ YES, please send me the following publications:

____ Subscriptions to *Fishery Bulletin*
for $32.00 per year ($44.80 foreign)

The total cost of my order is $ ________ . Prices include regular domestic postage and handling and are subject to change.

(Company or Personal Name) (Please type or print)

(Additional address/attention line)

(Street address)

(City, State, ZIP Code)

(Daytime phone including area code)

(Purchase Order No.)

Charge your order. IT'S EASY!

VISA

MasterCard

Please Choose Method of Payment:

☐ Check payable to the Superintendent of Documents

☐ GPO Deposit Account ☐☐☐☐☐☐☐–☐

☐ VISA or MasterCard Account

☐☐☐☐☐☐☐☐☐☐☐☐☐☐☐☐☐☐☐☐

☐☐☐☐ (Credit card expiration date)

To fax your orders (202) 512-2104

(Authorizing Signature)

Mail to: Superintendent of Documents
P.O. Box 979050, St. Louis, Missouri 63197
Tel. no. (U.S. callers): 866-512-1800
Tel. no. (International callers): 1-202-512-1800

Thank you for your order!

Also available online at
http://bookstore.gpo.gov/actions/GetPublication.do?stocknumber=703-023-00000-2
email: ContactCenter@gpo.gov

SMITHSONIAN LIBRARIES
3 9088 01972 1844